Apprentissage spatial et planification de l'action dans un modèle de réseau neuronal inspiré du cortex préfrontal

Louis-Emmanuel Martinet

THÈSE DE DOCTORAT
DE L'UNIVERSITÉ PIERRE ET MARIE CURIE

Spécialité : Informatique

École doctorale ÉDITE

Présentée par
Louis-Emmanuel MARTINET

Pour obtenir le grade de
DOCTEUR
DE L'UNIVERSITÉ PIERRE ET MARIE CURIE

APPRENTISSAGE SPATIAL ET PLANIFICATION DE L'ACTION DANS UN MODÈLE DE RÉSEAU NEURONAL INSPIRÉ DU CORTEX PRÉFRONTAL

Soutenue le 28 octobre 2010 devant le jury composé de :

Rapporteurs :	Francesco BATTAGLIA	-	Université d'Amsterdam
	Ricardo CHAVARRIAGA	-	École Polytechnique Fédérale de Lausanne
Examinateurs :	Yves BURNOD	-	Institut des Systèmes Complexes
	Bruno GAS	-	Université Pierre et Marie Curie
	Bruno POUCET	-	Université de Provence
Directeur :	Angelo ARLEO	-	Université Pierre et Marie Curie
Invité :	Jean-Arcady MEYER	-	Université Pierre et Marie Curie

SPATIAL LEARNING AND ACTION PLANNING IN A PREFRONTAL CORTICAL NETWORK MODEL

Résumé (format long)

Introduction

Un nombre important d'expériences étudiant les bases neurales de la cognition spatiale chez le rongeur souligne le rôle majeur de la formation hippocampique (voir Arleo and Rondi-Reig, 2007 pour une revue). Cette région limbique est impliquée dans l'apprentissage spatial depuis que des neurones sélectifs à une position — nommés cellules de lieu hippocampiques (O'Keefe and Nadel, 1978) — ont été découverts au moyen d'enregistrements électrophysiologiques chez des rats se déplaçant librement. Ces neurones participent très certainement à l'encodage de représentations spatiales dans un système de coordonnées allocentriques (c'est-à-dire centrées sur le monde). Cependant deux autres composants sont nécessaires pour accomplir une navigation flexible (c'est-à-dire pour planifier des détours et/ou des raccourcis) : la représentation du but et la planification de séquences d'actions dirigées vers un objectif (Poucet et al., 2004). Il a été proposé que l'hippocampe encoderait des représentations topologiques (prenant en compte la connectivité entre les différentes positions de l'environnement) adaptées à l'apprentissage de séquences d'actions (voir Poucet et al., 2004). Cependant, d'autres études expérimentales suggèrent l'existence d'un système extra-hippocampique de planification de l'action partagé parmi de nombreuses régions (voir Knierim, 2006 pour une revue). Cette hypothèse postule une cognition spatiale distribuée dans laquelle *(i)* l'hippocampe prendrait part à la planification des actions en transmettant des représentations spatiales redondantes aux aires associatives supérieures, *(ii)* un réseau cortical élaborerait des représentations plus abstraites et compactes du contexte spatial (prenant en compte les informations de motivation, les contraintes cout de l'action / risque, et les séquences temporelles des réponses comportementales dirigées vers un but).

Le cortex préfrontal (CPF) pourrait jouer un rôle central dans la construction d'une carte cognitive et la planification d'actions, comme suggéré par des études lésionnelles (e.g., Granon and Poucet, 1995). Le CPF reçoit des projections directes depuis des structures sous-corticales (par exemple l'hippocampe, l'amygdale, et l'aire ventrale tegmentale), et des connexions indirectes depuis les ganglions de la base à travers les boucles baso-thalamo-corticales (Jay and Witter, 1991; Kita and Kitai, 1990; Thierry et al., 1973; Uylings et al., 2003). Ces projections fourniraient au CPF un contexte multidimensionnel allant au delà d'une représentation purement spatiale en incluant des entrées émotionnelles et motivationnelles, une modulation dépendante de la récompense, et des signaux associés aux actions (Aggleton, 1992; Schultz, 1998; Uylings et al., 2003). Le CPF semble donc bien adapté pour *(i)* traiter des informations spatiales multiples (Jung et al., 1998), *(ii)* encoder les valeurs motivationnelles associées aux évènements spatiaux-temporaires (Poucet et al., 2004), et *(iii)* prendre des décisions supramodales (Otani, 2003). En outre, le CPF pourrait être impliqué dans l'intégration des évènements dans le domaine temporel (Fuster, 2001), ce qui est pertinent pour l'organisation temporelle des les réponses comportementales, et pour l'encodage de mémoires rétrospectives et prospectives (Fuster, 2001).

Les cartes corticales sont formées par des circuits locaux répétitifs composés de différents neurones, les colonnes corticales (pour une revue voir Mountcastle, 1997). En résumé, les colonnes corticales, peuvent être divisées en six couches principales incluant: la couche I, contenant principalement des axones et des dendrites; la couche IV, recevant des entrées sensorielles depuis des structures sous-corticales; Les couches II-III, spécialisées dans les connexions cortico-corticales et la couche VI, envoyant ses sorties aux aires sous-corticales du cerveau. Les propriétés anatomo-fonctionnelles des colonnes corticales ont été largement examinées (Mountcastle, 1997, voir également Horton and Adams, 2005; Rakic, 2008 pour des discussions sur ce concept). Le CPF présente la même organisation (Gabbott and Bacon, 1996b; Gabbott et al., 2005). De plus des études neuroanatomiques ont indiqué que les populations de neurones formant les colonnes seraient divisées en plusieurs *minicolonnes*, composées d'une population neuronale fortement interconnectée (Buxhoeveden and Casanova, 2002). Cette organisation colonnaire permettrait un traitement efficace de l'information (Mountcastle, 1997).

Modélisation du cortex préfrontal pour la planification spatiale

Vue générale du modèle

L'approche présentée ici vise à relier l'organisation en colonne à la prise de décision à l'aide d'une architecture neuronale très simplifiée. L'hypothèse sous-jacente est que le réseau du CPF peut médier une éparsification de la représentation hippocampique des lieux (HP) pour encoder des cartes topologiques et servir à la planification d'actions orientées vers un but. Lors de l'exploration, les cellules de HP deviennent sélectives à des positions allocentriques grâce à l'intégration d'informations visuelles et d'intégration de chemin (voir Sheynikhovich et al., 2009). Le modèle exploite les caractéristiques anatomiques des projections excitatrices de l'hippocampe vers le CPF (Jay and Witter, 1991) pour transmettre la représentation redondante de l'espace d'état S depuis HP vers le réseau de colonnes du CPF, où une représentation éparse des couples état-action $S \times A$ est apprise (Figure 1A). Dans une colonne, chaque minicolonne devient sélective à une paire spécifique état-action $(s, a) \in S \times A$, où les actions $a \in A$ représentent les directions de mouvement allocentrique des transitions entre deux états $s, s' \in S$. Chaque colonne est donc composé d'un population de minicolonnes qui représentent l'ensemble des paires état-action $(s, a_1 \cdots a_N) \in S \times A$ effectuées par l'animal à un lieu s.

Encodage de cartes topologiques par un réseau de colonnes

Chaque colonne dans le modèle (Fig. 1B) a une structure très simplifiée composée de trois unités s, p, v et d'une population de minicolonnes, dont chacune est composée de deux unités de q et d. Ces unités représentent des populations de neurones pyramidaux des couches supragranulaires II-III (unités p, v, q) ou infragranulaires V-VI (unités s, d). Durant l'exploration, les neurones s deviennent sélectifs à des lieux et leur activité de population encode une représentation compacte de l'espace d'état. Dans chaque colonne, un neurone v code l'information de but associée à un état spécifique, alors que les neurones q codent la relation entre les actions et le but. Les neurones q et v rétropropagent un signal de but par l'intermédiaire du réseau cortical et leur décharge est corrélée avec la distance au

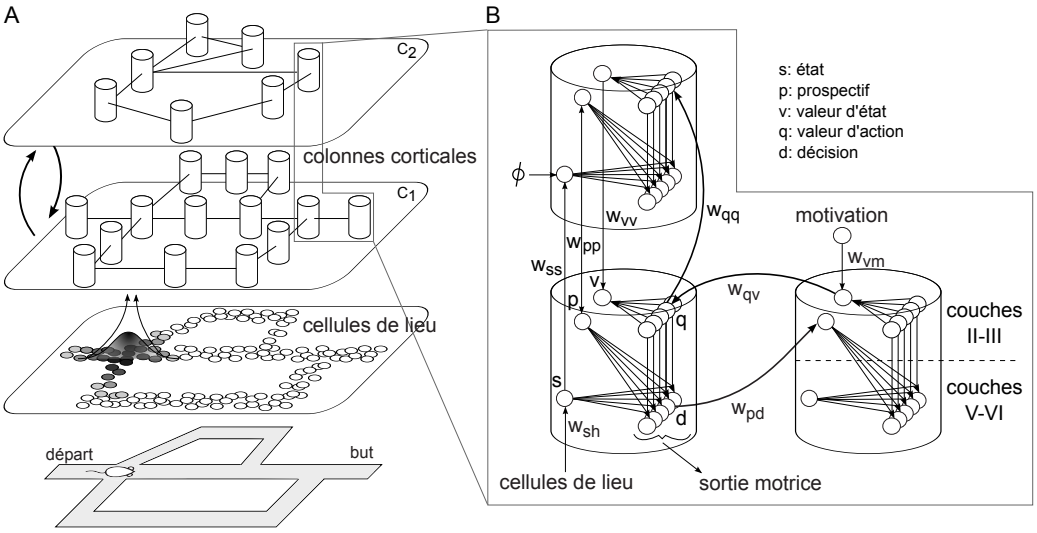

Figure 1: Vue générale de l'architecture du modèle (A) et de sa connectivité (B).

but. Les neurones p propage un signal antérograde codant le chemin sélectionné d'une position donnée vers le but. Les neurones d intègrent des informations spatiales et de récompense et entrent en compétition pour la sélection de la meilleur action locale. Leur activité déclenche une commande motrice (direction allocentrique de mouvement). La connectivité inter- et intra-colonne (Fig. 1B) implique des projections plastiques et non-plastiques, respectivement, dont les efficacités synaptiques sont modélisés par des matrices de poids $w \in [0, 1]$. Pendant l'exploration et la découverte de la topologie de l'environnement, les projections plastiques sont modifiées par un apprentissage non-supervisé Hebbien pour encoder soit des nouveaux états (e.g., w_{sh}) soit des associations antérogrades et rétrogrades entre états voisins (e.g., w_{pd} et w_{qv}).

Planification de la navigation par propagation de signaux lié à la récompense

Lors de l'exploration, des signaux motivationnels modulent l'activité des neurones v (Fig. 1B), ce qui permet à des colonnes spécifiques de devenir sélectives au but. Le signal de récompense transmis par les projections w^m simule une motivation physiologique possiblement induite par les neurones dopaminergiques de l'aire tegmentale ventrale (Schultz, 1998) ou de l'amygdale (Aggleton, 1992). Un

processus de diffusion d'activation inspiré par l'arbre d'appel de Burnod (1988) permet l'exploitation des informations topologiques pour déterminer les trajectoires optimales vers le but. Le signal de motivation suscite l'activité du neurone v dans la colonne correspondant à l'emplacement du but. Cette activité est alors retropropagée par le biais d'associations inverses médiée par les projections latérales w_{qv} (Fig 1B). Lorsque ce signal de but retropropagé atteint la colonne sélective pour la position actuelle, la coïncidence de l'activité de s et q déclenche la décharge des neurones d. L'activation de d, à son tour, entraîne la propagation d'un signal antérograde à travers les projections w_{pd} et codant le chemin orienté vers le but. Les décharges successives de neurones p et d permettent au signal de chemin de se propager vers l'avant jusqu'à la colonne de but. Un mécanisme compétitif (winner-take-all) sélectionne localement la meilleur action motrice $a \in A$ associée au neurone d le plus actif, et extrait les trajectoires vers le but.

Il convient de noter que les projections w_{qv} atténuent l'activité retropropagée : plus le nombre de relais synaptiques est petit, plus le signal de but reçu par les neurones q de la colonne correspondant à la position actuelle est fort. Ainsi, l'intensité du signal de but à un endroit donné est corrélé avec la distance au but. En d'autres termes, le réseau de colonnes encode une information métrique liée au but permettant de sélectionner le plus court chemin vers la récompense. Les animaux peuvent prendre des raccourcis vers un objectif à travers des régions non visitées de l'environnement, une capacité qui souvent associée à une cartographie métrique complexe (voir Trullier et al., 1997; Kubie and Fenton, 2009 pour des revues). La représentation apprise par le modèle encode suffisamment d'informations métriques pour déduire des raccourcis dans des situations simples semblables à celles testées avec des animaux (Chapuis et al., 1983; Poucet et al., 1983; Poucet, 1993; Etienne et al., 1998), en utilisant un mécanisme d'addition vectorielle (Etienne et al., 1998) des actions formant la trajectoire planifiée.

Traitements corticaux récurrents pour la cartographie topologique multi-échelle

Le modèle apprend des représentations hiérarchiques de l'espace d'état en utilisant des interactions récurrentes entre deux sous-populations de colonnes corticales (Figure 1). La première population C_1 reçoit et traite les entrées spatiales

directes de l'hippocampe. La deuxième population C_2 reçoit des informations d'état déjà transformées depuis les neurones $s \in C_1$, mais elle intègre également un signal proprioceptif ϕ utilisé pour encoder la probabilité de changements dans la direction égocentrique de locomotion. En conséquence, la sélectivité des neurones $s \in C_2$ est modulée par la présence de caractéristiques structurelles de l'environnement telles que les allées et les couloirs. La résolution spatiale de la représentation multi-échelle qui en résulte peut alors s'adapter à la complexité structurelle du labyrinthe. Le réseau de colonnes C_2, qui est appris de même similaire au réseau C_1, utilise également le mécanisme de diffusion d'activation afin de planifier des trajectoires orientées vers un but. Après apprentissage, les projections w_{vv} et w_{pp} permettent à C_2 de moduler l'activité des neurones $p, v \in C_1$ lors de la planification (Fig. 1B).

Comportement spatial du modèle

Protocoles expérimentaux

Tâche de détour de Tolman & Honzik

Le labyrinthe classique de Tolman & Honzik (Fig. 2A) se compose de trois couloirs étroits de différentes longueurs guidant les animaux d'un point de départ à une zone d'alimentation. L'expérience de Tolman & Honzik visaient à corroborer l'hypothèse que les rongeurs pourraient prédire les conséquences de trajectoires alternatives orientées vers un but en présence de couloirs bloqués dynamiquement. Le protocole expérimental débute par une période d'entrainement durant 168 essais (soit 14 jours avec 12 essais par jour), pendant laquelle les animaux simulés pouvaient explorer le labyrinthe afin d'élaborer des représentations topologiques et d'apprendre des politiques de navigation. Pendant le Jour 1, les sujets étaient autorisés à explorer librement le labyrinthe. Pendant les Jours 2 à 14, un bloc a été introduit à l'emplacement A (bloc A, Fig. 2A) pour induire un choix entre P2 et P3. Vient ensuite une période de test, durant 7 essais (Jour 15) avec un bloc à l'emplacement B obstruant la portion de chemin commune à P1 et P2 (Bloc B, Fig. 2A). Pour évaluer l'invariance de la performance du modèle par rapport à la taille de l'environnement, nous avons mis en œuvre le protocole expérimental ci-dessus pour deux échelles différentes du labyrinthe, 1:1 et 4:1.

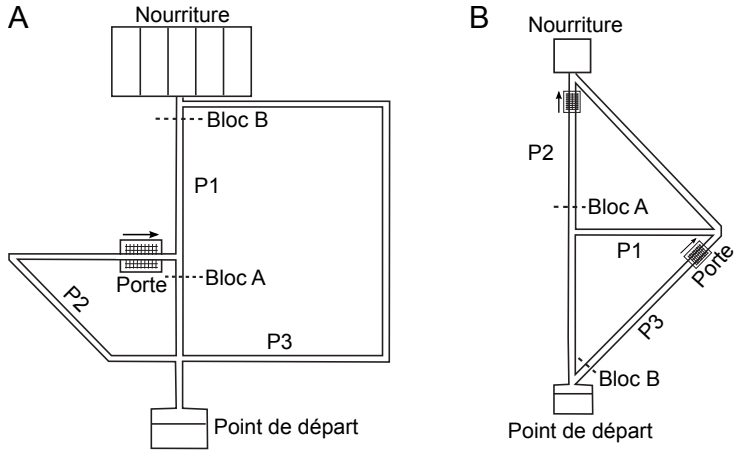

Figure 2: Tâches de navigation spatiale utilisées pour tester la capacité à l'inférence de détour (labyrinthe de Tolman & Honzik, A) et de raccourcis (B).

Tâche de navigation avec raccourcis

Les données expérimentales suggèrent que la sélection de chemin dépend de la longueur et de la directionnalité des trajectoires disponibles (Poucet, 1993). En outre, les animaux testés en présence d'un conflit entre longueur et directionnalité (par exemple avec un plus court chemin qui pointe moins directement vers le but) ont tendance à préférer le chemin plus court et moins direct lorsque le but est caché (Chapuis et al., 1983; Poucet et al., 1983). Le labyrinthe de la Figure 2B prend ces observations en considération. Il se compose de trois couloirs: P1 est le plus long chemin et ne comporte pas de raccourci; P2 implique un raccourci pointant directement vers le but; P3 est basé sur un raccourci indirecte, obligeant l'animal à se détourner du chemin apparemment la plus direct vers le but (la ligne droite du départ vers le but). Nous avons simulés deux séries d'expériences partageant le même protocole qui comprend deux phases: une période d'entrainement durant 6 essais, au cours de laquelle des rats simulées pouvaient passer uniquement par la voie P1 (i.e. les blocs A et B étaient tous deux présent, Fig. 2B), de sorte que P2 et P3 restent inexplorées; et une période de test durant 1 essai et visant à évaluer la façon dont les animaux simulés utiliseraient un raccourci nouvellement disponible. Dans une série d'expériences, les animaux simulés ont été autorisés à choisir entre P1 et P2 (i.e. raccourci direct, avec le bloc A enlevé), alors que dans une seconde série d'expériences, les animaux devaient choisir entre P1 et P3 (i.e. raccourci indirecte, avec le bloc B enlevé) .

Résultats

Tâche de détour de Tolman & Honzik

Nous avons d'abord examiné les réponses comportementales des $n = 40$ animaux simulés résolvant la version 1:1 de la tâche de Tolman & Honzik. le modèle a reproduit les observations comportementales présentées Tolman and Honzik (1930a).

Jour 1. Comme dans les résultats de Tolman & Honzik, le modèle a sélectionné le chemin le plus court P1 significativement plus que les chemins alternatifs P2 et P3 grâce à la carte spatiale apprise.

Jours 2-14. Le bloc A a forcé les animaux à mettre à jour leur représentation topologique pour planifier un détour. Conformément à Tolman & Honzik, nous avons observé un nombre de passages significativement plus important par le plus court détour P2 comparé à P3.

Jour 15. En accord avec les données de Tolman & Honzik, les animaux simulés ont agi selon l'hypothèse de l'"insight", i.e. ils ont préféré le chemin plus long mais valable P3 au chemin P2. Cette décision s'explique dans le modèle par le fait que, suite à l'ajout du bloc B, le signal retropropagé de but était bloqué dans le réseau cortical pour les chemins P1 et P2, entrainant le choix de P3.

Nous avons ensuite testé la robustesse des résultats ci-dessus par rapport à la taille de l'environnement. Nous avons utilisé une version à l'échelle 4:1 du labyrinthe de Tolman & Honzik et nous avons comparé les performances entre $n = 40$ animaux simulés avec des populations intactes C_1, C_2 (groupe "contrôle") et $n = 40$ animaux simulés sans population C_2 (groupe "sans C_2"). Ce dernier groupe n'a pas la propriété de codage multi-niveaux fournie par les dynamiques récurrentes entre C_1 et C_2. Le résultat principal est que, durant les Jours 2-14 et le jour de test Jour 15, le groupe sans C_2 n'a pas réussi à résoudre la tâche de détour, alors que les animaux du groupe contrôle ont fait face à la plus grande taille de l'environnement avec succès. Les meilleures performances des sujets témoins étaient dû au fait que la rétropropagation du signal du but dans le réseau cortical bénéficiait lors de la planification de la représentation topologique multi-échelle (et plus compacte) codée par la population C_2 et des interactions entre C_1 et C_2.

Tâche de navigation avec raccourcis

Dans deux série d'expériences, nous avons étudié les performances de navigation de $n = 40$ animaux lors de la résolution d'une tâche comportementale de raccourci. Au cours d'un unique essai de test, les animaux simulés de la première expérience ont eu l'occasion de prendre un raccourci *direct* (chemin P2 inexploré pendant la phase d'entrainement). Une fraction significative de rats simulés ont bien sélectionné P2 au lieu de P1 ($97,5\%$). Les animaux de la deuxième expérience ont été testés sur un unique essai au cours duquel le raccourci *indirect* P3 a été rendu accessible. La majorité des animaux simulés ont sélectionné P3 (95%). Ces résultats sont conformes aux résultats expérimentaux sur le comportement de navigation par raccourci (Chapuis et al., 1983; Poucet et al., 1983).

Des activités neuronales aux réponses fonctionnelles

Analyses statistiques

Nous avons analysé les décharges des neurones simulés en relation avec des données électrophysiologiques afin d'élucider le lien entre activité temporelle des cellules et comportement. Cela a été fait par : (i) la caractérisation des propriétés de sélectivité spatiale de cellules isolées; (ii) la comparaison de la redondance des codes spatiaux de population appris par des animaux simulés, (iii) la différenciation des propriétés de codage des neurones associés purement à la récompense (populations q et v) par rapport aux unités purement spatiales (population s); (iv) la quantification et la comparaison de la fiabilité des représentations spatiales neuronales en terme de contenu informatif — i.e. combien peut-on inférer au sujet de la position de l'animal ou de la phase particulière de la tâche courante en observant seulement les réponses de neurones ? En plus de relier nos résultats de simulation aux données expérimentales issues de la littérature, nous avons étudié la cohérence entre les réponses des neurones du modèle et celles d'un ensemble d'enregistrements électrophysiologiques du CPF médial de rats type Long-Evans résolvant une tâche de mémoire spatiale (voir Peyrache et al., 2009; Benchenane et al., 2010). L'analyse a examiné si les propriétés de codage des neurones du modèle pouvaient effectivement être observées dans le CPF au cours de l'apprentissage spatial.

Résultats

Codage spatial par des neurones isolés ou des populations

Analyse des champs récepteurs de neurones

Pour comprendre comment des neurones pris de manière isolée prennent part à l'encodage de lieux, nous avons comparé les activités sélective aux lieux de deux types d'unités du modèle : les cellules de lieux de l'hippocampe (HP) et les neurones corticaux $s \in C_1, C_2$. Nous avons analysé les patrons de décharge pendant que les animaux simulés résolvaient la version 4:1 de la tâche de Tolman & Honzik. La représentation codée par les unités $s \in C_1$ était du même ordre que l'organisation des champs de lieux des cellules de HP, tandis que l'activité des neurones $s \in C_2$ capturaient certaines propriétés structurelles de l'environnement (i.e. l'organisation en couloir). La taille moyenne du champ de lieux augmentaient considérablement pour les neurones de HP, à C_1 et à C_2 populations, en conformité avec les données expérimentales sur la taille des champs récepteurs des cellules de l'hippocampe et du CPF enregistrées chez des rats résolvant une tâche de navigation (Hok et al., 2005). Nous avons également caractérisé le traitement spatial en multi-étapes réalisé par le modèle en termes d'information mutuelle de Shannon entre réponses d'une unité donnée et l'emplacement spatial. L'activité des neurones $s \in C_2$ encodait, en moyenne, la plus grande quantité d'information spatiale, suivi par les neurones $s \in C_1$ et de HP. Cette relation est due au fait que plus le champ récepteur est petit, plus la région de l'espace d'entrée pour laquelle un neurone reste silencieux est grande, et donc moins peut être déduit des entrées en observant la variabilité de la décharge d'un neurone. Nous avons aussi comparé les réponses sélectives à un lieu des neurones $s \in C_1$ avec les patrons de décharge des cellules pyramidales enregistrées dans le CPF médian de rats effectuant une tâche de navigation. Les patrons réels et simulés sont compatibles entre eux en termes de forme et de ratio signal-bruit des profils de réponse. Ces résultats corroboraient l'hypothèse selon laquelle les neurones s du modèle, purement sélectifs à des lieux, pourraient trouver leur contrepartie biologique dans des populations du CPF réelles.

Analyse des propriétés d'encodage de lieux par population

Comme évoqué précédemment, nous avons modélisé les interactions entre l'hippocampe et le CPF pour produire des représentations spatiales compactes adaptées à la planification de la navigation. Le traitement multi-échelle implémenté a fourni une éparsification progressive du codage spatial par population. De manière consistante à des résultats expérimentaux présentés par Jung et al. (1998), nos unités corticales simulées encodaient des représentations spatiales moins redondant que les cellules de HP. Le taille des populations de neurones codant pour le labyrinthe de Tolman & Honzik a diminué de façon significative de HP à C_1, puis à C_2. Le nature plus éparse du code spatial cortical a été confirmée par la différence significative des densités spatiales des champs récepteurs. Finalement, nous avons mesuré le information mutuelle de Shannon entre les patrons de réponse des populations et lieux. Le code hautement redondant de HP avait le plus grand contenu d'informations spatiales. Bien que moins redondante, la population de neurones $s \in C_1$ encodait environ 85 % de la limite supérieure théorique, ce qui s'est avéré être adapté pour résoudre les tâches de comportement. Une perte importante d'information a été observé dans le code de la population des neurones $s \in C_2$. Ceci est cohérent avec le rôle fonctionnel du réseau cortical C_2, qui ne pourrait pas supporter la planification de la navigation seul, mais qui complète plutôt la représentation fournie par C_1 en encodant des caractéristiques de plus haut niveau de l'environnement.

Encodage de la distance au but

Outre la corrélation spatiale de l'activité des neurones s, le représentation corticale du modèle encode des informations dépendant de la récompense. Étant donné un emplacement dans le labyrinthe, plus courte était la longueur du chemin vers le but, plus grand était le taux de décharge moyen du neurone v appartenant à la colonne correspondant à cet emplacement. Cette propriété était pertinente pour le processus de décision guidant le comportement de navigation spatiale du modèle. Chaque neurone $v_i \in C_1$ avait une fréquence de décharge préférée f_i qui lui était propre, et corrélée à sa distance au but. L'ensemble des fréquences préférées f_i était uniformément répartis sur tout l'intervalle normalisé $[0, 1]$. Fait intéressant, lorsque nous avons analysé l'activité des cellules pyramidales du CPF

enregistrées, nous avons trouvé un sous-ensemble de neurones, sans corrélation spatiale, mais avec des fréquences de décharge préférées uniformément réparties. Finalement, nous avons mesuré l'information mutuelle I_t entre les phases de la tâche et les patrons de décharge des neurones v. Les neurones v fournissaient une quantité significative d'informations liées à la tâche, ce qui signifie que la phase du protocole pourrait être décodées de façon fiable en observant l'évolution dans le temps de leurs patrons de décharge.

Encodage de changements dans les contingences action-récompense

Nous avons étudié comment l'activité des neurones q et d du modèle contribuaient à la prise de décision. Rappelons que, après apprentissage, chaque minicolonne corticale $(q, d) \in C_{1,2}$ encodait une paire état-action spécifique (s, a). L'analyse présentée sur la figure 3 montre l'évolution temporelle de fréquence de décharge des unités q, d appartenant à la colonne codant pour la première intersection du labyrinthe de Tolman & Honzik au début de l'Essai 1, Jour 2 (i.e. avec le bloc A). Pendant le déplacement, l'animal simulé est arrivé au point d'intersection à $t \simeq 4$ s. En raison de la politique apprise pendant le Jour 1 (i.e. sans un bloc dans le labyrinthe), l'unité q_1 de la minicolonne associée à l'action menant à P1 déchargeait à cet instant avec le plus fort taux de décharge, suivie par l'unité q_2 de la minicolonne associée à P2, et enfin par q_3 liée à P3 (Figure 3B). Ainsi, les neurones correspondant $d_{1,2,3}$, qui combinent les entrées des $q_{1,2,3}$, respectivement, avec les activités sélective aux lieux des neurones s de la même colonne, déchargeaient selon le même classement à $t \simeq 4$ s (Figure 3C). En conséquence, l'action commandée par d_1 a été sélectionné et l'animal simulé a suivi P1. Toutefois, lorsque le bloc A a été rencontré à $t \simeq 5$ s, le modèle a mis à jour la représentation topologique, ce qui a entraîné un changement des contingences action-récompense (avec q_1 déchargeant moins fortement que q_2). Cette mise à jour d'activité est consistante avec des résultats montrant des changements soutenus des décharges, très sensibles à une modification des contingences de la récompense (Mulder et al., 2003; Rich and Shapiro, 2009). Lorsque l'animal s'est retrouvé de nouveau à l'intersection (à $t \simeq 7$ s), le neurone d_2 a déchargé avec la plus grande fréquence (Figure 3C) conduisant à la sélection de P2. La sélection de la meilleur action le jour de test (Jour 15) s'explique par le même principe.

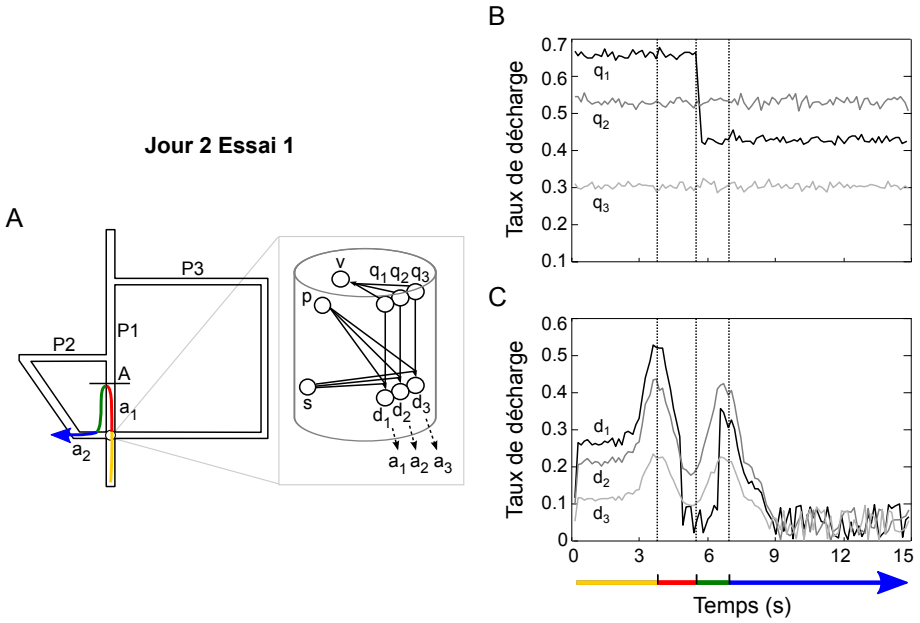

Figure 3: Analyse de l'évolution temporelle des changements de contingence action-récompense. **(A)** Exemple de trajectoire effectuée par les animaux simulés Les couleurs illustrent les actions distinctes. **(B,C)** Profiles temporels des taux de décharge de trois neurones q_1, q_2 et q_3 (resp. d_1, d_2 et d_3) appartenant à la colonne située à l'intersection et aux minicolonnes représentant les actions a_1, a_2 et a_3. Les lignes verticales en pointillés indiquent les évènements de prise de décision.

Encodage de séquences de lieux prospectifs

Nous avons analysé les champs récepteurs des unités p lorsque les animaux se déplaçaient de la position de départ vers le but. Contrairement aux champs récepteurs symétriques des neurones s, tous les neurones p avaient des profils de réponse asymétriques (i.e. avec la queue gauche de la distribution plus longue que la queue droite). L'asymétrie de ces réponses neuronales augmentaient quasi-linéairement avec le nombre de relais synaptiques formant une trajectoire planifiée mentalement. Lorsque nous avons analysé les données des enregistrements du CPF de rats, nous avons également trouvé un sous-ensemble de neurones avec des courbes de sélectivité asymétriques, dont l'asymétrie semblait être corrélée à la distance parcourue par l'animal. De plus, les neurones p (et non s) avaient une fréquence moyenne de décharge positivement corrélée à la distance parcourue vers le but. En accord avec cela, Jung et al. (1998) a fourni des preuves

expérimentales d'augmentations du taux de décharge neuronal lors de l'approche d'une récompense. Enfin, une propriété importante des neurones p du modèle est que leur décharges avaient tendance à anticiper dans le temps l'activité des neurones s. En d'autres termes, les neurones p encodaient une information prospective sur les lieux prédisant l'état suivant visité par l'animal, ce qui est compatible avec les données expérimentales sur les enregistrements du CPF rapportées Rainer et al. (1999).

Nous avons également étudié la nature de la prédiction fournie par l'activité des neurones p en relation avec les données expérimentales sur le codage neuronal de l'ordre sériel de séquences planifiées avant que les actions ne soient exécutées (Averbeck et al., 2002). Dans leur expérience, Averbeck et al. (2002) ont effectué des enregistrements simultanés des activités de neurones isolés du CPF chez des singes dessinant des séquences de lignes (i.e. des segments formant des formes abstraites). Chaque segment était associé à un patron distinct d'activité neuronale, et la force relative de ces patrons avant le dessin a été montrée comme prédisant l'ordre sériel de la séquence de segments effectivement dessinés par les singes. De manière consistante, nous avons constaté que la classement des fréquences de décharge des neurones p *avant* l'exécution effective d'une trajectoire planifiée était un bon prédicteur de l'ordre sériel des états sur le point d'être visité par l'animal simulé. Cette relation était vraie non seulement au temps $t = 0$ (c'est à dire au tout début d'une trajectoire), mais pour chaque temps t, ce qui signifie que le classement des taux de décharge des neurones p pourrait prédire à tout moment l'ordre de séquences d'états futurs.

Analyse comparative des patrons d'activité des populations de neurones préfrontales du modèle et expérimentales

Nous avons tout d'abord rassemblé les neurones non-silencieux s, v, p, q et d enregistrés dans la version 4:1 de la tâche de Tolman et Honzik. Nous avons caractérisé la décharge de chaque neurone en mesurant sa fréquence moyenne de décharge, son écart type, son asymétrie, son kurtosis au cours du temps, l'information spatiale par potentiel d'action et l'information mutuelle spatiale. Puis, nous avons effectué une analyse en composantes principales (ACP) sur l'espace multidimensionnel contenant les valeurs fournies par ces mesures pour chaque neurone. Nous avons également appliqué un algorithme de catégorisation

non-supervisé (méthode des k-moyennes, avec $k = 3$) pour partitionner la distribution des données. Fait intéressant, les neurones du modèle ayant différents rôles fonctionnels avaient tendance à occuper des régions distinctes de l'espace de l'ACP découpées automatiquement par la catégorisation. Par exemple, les neurones $v, q \in C_1, C_2$, dont la fonction dans le modèle est de propager les informations de but et encode la distance au but, se trouvaient dans le même groupe. Tous les neurones avec une activité sélective à un lieu de petite échelle, i.e. les neurones $s, p, d \in C_1$ (et aussi dans $p \in C_2$) ont été regroupés dans la même région. Enfin, les neurones $s, d \in C_2$, principalement impliqués dans la construction d'une carte spatiale et la planification à plus grande échelle ont également été séparés dans un groupe différent.

Nous avons effectué la même série d'analyses sur un ensemble de données de neurones du CPF médial enregistrés chez des rats en train de naviguer. Comme pour les données simulées, la méthode de catégorisation a identifié trois groupes principaux. Nous avons comparé les groupes du modèle et expérimentaux dans le but d'examiner si les données réelles et simulées appartenant aux mêmes groupes partageaient certaines caractéristiques de décharge. En termes d'information spatiale moyenne, nous avons trouvé des distributions similaires non homogènes pour le modèle et les données réelles. En particulier, un groupe des données expérimentales et du modèle encodaient un plus grand contenu d'information spatiale. Le groupe des données du modèle comportait surtout des activités issues de neurones ayant une sélectivité aux lieux $s, d, p \in C_2$. En observant les fréquences moyennes de décharge sur chaque groupe, nous avons aussi observé un groupe avec des activités réelles et du modèle avaient des fréquences significativement plus hautes que les autres. Le groupe modèle était principalement composé par des neurones $v, q \in C_1, C_2$ propageant des informations de récompense. Enfin, en comparant les valeurs absolue moyenne de l'asymétrie de champs récepteurs, nous avons trouvé des populations dans le modèle et expérimentales avec des champs asymétriques. Pris ensemble, Ces résultats indiquent que, dans l'ensemble de données expérimentales des enregistrements du CPF, des sous-populations de neurones existaient avec des propriétés distinctes de décharge, et que ces sous-populations pourraient être reliées à différents groupes fonctionnels prédits par le modèle.

Discussion

Nous avons présenté un modèle centré sur la planification de la navigation médiée par une population de colonnes corticales préfrontales. Lors de l'exploration d'un nouvel environnement, le modèle apprend une représentation topologique dans laquelle chaque lieu est codé par une colonne du néocortex et le renforcement des synapses entre les colonnes est utilisé pour représenter les liens topologiques entre les lieux. Lors de la planification de trajectoire vers le but, un mécanisme de diffusion d'activation produit une propagation de l'activité dans la population colonne menant à la sélection du plus court chemin vers le but. Nos résultats de simulation démontrent que le modèle peut reproduire le comportement des rongeurs précédemment attribué à la capacité des animaux à avoir un "insight" cognitive, une compréhension de la structure de l'environnement (Tolman and Honzik, 1930a). En outre, nous montrons que la planification spatiale dans notre modèle est invariante par rapport à la taille du labyrinthe. Cette propriété repose sur la capacité du modèle à encoder des cartes cognitives avec une résolution qui est adaptée à la structure de l'environnement (allées, par exemple). Une autre propriété du modèle est sa capacité à trouver des raccourcis à travers des parties inexplorées de l'environnement.

Au niveau neuronal, nous avons caractérisé les activités des neurones du modèle et comparé celles-ci aux données électrophysiologiques des neurones CPF réel. Notre analyse des réponses neuronales suggère comment l'interaction entre l'hippocampe et le cortex préfrontal modélisés peut mener à l'encodage d'informations multiples pertinentes pour la fonction de planification spatiale, y compris, par exemple, des corrélats liés à la distance au but. Le modèle fournit également un cadre fonctionnel pour l'interprétation de l'activité d'unités préfrontales observées durant l'exécution de tâches de mémoire spatiale (Watanabe, 1996; Jung et al., 1998; Tremblay and Schultz, 1999; Rainer et al., 1999; Averbeck et al., 2002; Mulder et al., 2003; Hok et al., 2005; Benchenane et al., 2010). D'un point de vue général, nos résultats sont conformes à l'hypothèse selon laquelle le contrôle cognitif découle de la maintenance active de patrons d'activité dans le CPF qui représentent les buts et les moyens pour les atteindre (Miller and Cohen, 2001).

Le modèle a deux limites en rapport avec la question de la représentation de but dans les CPF. La première est que le modèle prend des décisions basées sur

un signal de motivation seulement appétitif (i.e. la récompense au niveau du but). De toute évidence, d'autres variables que la taille de la récompense influent sur le processus de planification. Par exemple, il existe des résultats indiquant que les efforts physiques requis pour atteindre le but ou le retard dans la délivrance de la récompense influencent les décisions comportementales dépendant du CPF (Rudebeck et al., 2006). La deuxième limitation est que le modèle à l'heure actuelle ne peut gérer qu'un seul but et ne peut pas estimer les valeurs relatives de différents buts(Tremblay and Schultz, 1999). Afin de remédier à ces limitations, le mécanisme de diffusion d'activation dans le modèle peut être étendu pour propager plusieurs signaux motivationnels, les intensités desquels sont proportionnelles à leurs valeurs subjectives. Dans ce cas, un effort ou une récompense retardée peut être modélisée en ajustant les valeurs relatives des signaux de motivation à différents endroits dans le labyrinthe.

Une autre direction intéressante pour les travaux futurs est d'étudier l'encodage d'informations liées à la tâche dans le CPF au cours du sommeil. Bien qu'il soit probable que des informations sont transférées au cours de l'apprentissage de la tâche, la consolidation de la mémoire au cours du sommeil semble également jouer un rôle central (Peyrache et al., 2009). En particulier, des décharges intensives (sharp wave-ripple complexes) dans l'hippocampe semblent importants pour le transfert de souvenirs labiles de l'hippocampe vers le néocortex pour le stockage à long terme (Girardeau et al., 2009). Une question clé pour les approches de modélisation est de comprendre les propriétés computationnelles de ce mécanisme d'apprentissage.

Abstract

The interplay between hippocampus and prefrontal cortex (PFC) is fundamental to spatial cognition. Complementing hippocampal place coding, prefrontal representations provide more abstract and hierarchically organized memories suitable for decision making. We model a prefrontal network mediating distributed information processing for spatial learning and action planning. Specific connectivity and synaptic adaptation principles shape the recurrent dynamics of the network arranged in cortical minicolumns. We show how the PFC columnar organization is suitable for learning sparse topological-metrical representations from redundant hippocampal inputs. The recurrent nature of the network supports multilevel spatial processing, allowing structural features of the environment to be encoded. An activation-diffusion mechanism spreads the neural activity through the column population leading to trajectory planning. The model provides a functional framework for interpreting the activity of PFC neurons recorded during navigation tasks. We illustrate the link from single unit activity to behavioral responses. The results suggest plausible neural mechanisms subserving the cognitive "insight" capability originally attributed to rodents by Tolman & Honzik. Our time course analysis of neural responses shows how the interaction between hippocampus and PFC can yield the encoding of manifold information pertinent to spatial planning, including prospective coding and distance-to-goal correlates.

Keywords: hippocampus, navigation planning, prefrontal cortical minicolumns, reward-based learning, time course analysis.

Acknowledgments

Table of contents

Part I

INTRODUCTION

Chapter 1

Introduction

1.1 Motivation

Spatial cognition requires long-term neural representations of the spatiotemporal properties of the environment (O'Keefe and Nadel, 1978). These representations are encoded in terms of multimodal descriptions of the animal-environment interaction during active exploration. Exploiting these contextual representations (e.g. through reward-based learning) can produce goal-oriented behavior under different environmental conditions and across subsequent visits to the environment. The complexity of the learned neural representations has to be adapted to the complexity of the spatial task and, consequently, to the flexibility of the navigation strategies used to solve it (Trullier et al., 1997; Arleo and Rondi-Reig, 2007). Spatial navigation *planning* —defined here as the ability to mentally evaluate alternative sequences of actions to infer optimal trajectories to a goal— is among the most flexible navigation strategies (Arleo and Rondi-Reig, 2007). It can enable animals to solve hidden-goal tasks even in the presence of dynamically blocked pathways (e.g. *detour* navigation tasks, Tolman and Honzik, 1930a). Experimental and theoretical works have identified three main types of representations suitable for spatial navigation planning, namely route-based, topological, and metrical maps (Poucet, 1993; Trullier et al., 1997; Meyer and Filliat, 2003; Arleo and Rondi-Reig, 2007; Mallot and Basten, 2009). Route-based representations encode sequences of place-action-place associations independently from each other, which does not guarantee optimal goal-oriented behavior (e.g. in terms of capability of either finding the shortest pathway or solving detour tasks). Topo-

logical maps merge routes into a common goal-independent representation that can be understood as a graph whose nodes and edges encode spatial locations and their connectivity relations, respectively (Trullier et al., 1997). Topological maps provide compact representations that can generate coarse spatial codes suitable to support navigation planning in complex environments. Metrics-based maps go beyond pure topology in the sense they embed the metrical relations between environmental places and/or cues —i.e. their distances and angles— within an allocentric (i.e. world centered) reference frame (Poucet, 1993). The encoding of metric information favors the computation of novel pathways (e.g. shortcuts) even through unvisited regions of the environment. In contrast to the qualitative but operational space code provided by topological maps, metrical representations form more precise descriptions of the environment that are available only at specific locations until the environment has been extensively explored (Poucet, 1993). However, purely metric representations are prone to errors affecting distance and angle estimations (e.g. path integration, Etienne and Jeffery, 2004). Behavioral and neurophysiological data suggest the coexistence of multiple memory systems that, by being instrumental in the encoding of routes, topological maps and metrical information, cooperate to subserve goal-oriented navigation planning (White and McDonald, 2002).

In this work we propose a model of a spatial memory system that primarily learns topological maps. Our main attention is devoted to the following questions: *(i)* how can these representations be encoded by neural populations within the brain ? *(ii)* what can be inferred thanks to the model about the link between electrophysiological discharges recorded in the brain and behavior?

1.2 Roadmap of the dissertation

This thesis consists of two main parts. The first part (Chapters 2 and 3) reviews neurophysiological and behavioral data concerning the biological networks underlying navigation planning in the rat. In the second part (Chapters 4, 5, 6 and 7) we propose a neuromimetic model of spatial planning. Topics treated in each chapter are:

Chapter 2 reviews anatomical data concerning two main brain structures involved in spatial learning and planning, the hippocampus and the prefrontal cor-

tex. In particular, subdivisions as well as patterns of afferent and efferent connections are described for each structures. Additionally, we present the columnar organization found in the prefrontal cortex.

Chapter 3 reviews neurophysiological and behavioral data about the hippocampus and the prefrontal cortex to underline functional differences between these structures in spatial learning.

Chapter 4 presents a new model of rat planning behavior, with detailed description of its components and learning algorithms.

Chapter 5 examines results of computer simulations that tested model spatial performance in several behavioral tasks.

Chapter 6 analyses coding properties of the model neurons and their link with decision making, in relation with experimental data.

Chapter 7 provides a short descriptions theoretical models adressing navigation planning in the prefrontal cortex.

Chapter 8 discusses the overall results of the model and summarizes the contributions and possible future developments of this thesis.

Part II

NEURAL SUBSTRATES OF NAVIGATION PLANNING

Chapter 2

Anatomy of a distributed network underlying spatial cognition

Spatial cognition involves the ability of a navigating agent (be it an animal or an autonomous artefact) to acquire spatial knowledge (e.g., spatio-temporal relations between environmental cues or events), organize it properly, and employ it to adapt its motor response to the specific context (e.g., performing flexible goal-oriented behavior to solve a navigation task). Similarly to other high-level functions, spatial cognition involves parallel information processing mediated by a network of brain structures that interact to promote efficient spatial behavior (see Knierim, 2006; Arleo and Rondi-Reig, 2007 for a recent review; Dollé et al., 2010). In this chapter, we will discuss the anatomical properties of two important structures which are though to be involved in declarative spatial memory and high-level processing of spatial information, namely the hippocampus and the prefrontal cortex (with a focus on this latter structure). Other brain areas are also important for navigation. In particular, the basal ganglia are thought to mediate procedural learning and action selection (Redgrave et al., 1999; Khamassi, 2007); the amygdala is involved in the processing of emotional and motivational information (Aggleton, 1992); the motor cortices and the cerebellum encode motor-related representations (Georgopoulos et al., 1982; Ito, 2002); finally, the parietal cortex mediates visuo-motor transformations and egocentric spatial representations (Andersen, 1995; Andersen et al., 1997; Nitz, 2006).

2.1 The hippocampus

In this short review of hippocampal anatomical data we focus on connectivity between the hippocampus and other brain areas. See (Arleo, 2000; Hok, 2007; Alvernhe, 2010) for more detailed descriptions.

2.1.1 Subdivisions

The hippocampal formation includes the dentate gyrus (DG), the subiculum (SC) and the hippocampus proper (or cornu ammonis, CA) composed of four subfields CA1-CA4 (usually only CA1 and CA3 are considered), see Fig. 2.1A. The hippocampus occupies a large volume in rodent brains.

2.1.2 Connectivity

Hippocampal afferents

Two major types of input enter the hippocampal formation: *(i)* Inputs from neocortical areas converge through the entorhinal cortex via the perforant path. These signals carry information coming from most of the unimodal and multimodal associative areas. As a consequence, the hippocampal formation is the recipient of highly processed multimodal sensory information (Rolls, 1995). *(ii)* Inputs from subcortical areas reach the hippocampus via the fornix fiber bundle. Signals from the thalamus, the hypothalamus, the brainstem, and the amygdala, are though to convey arousal, emotional, and autonomic information (Burgess et al., 1999). The subcortical cholinergic and GABA-ergic inputs from the septal region modulate the ensemble hippocampal activity (Hasselmo and Bower, 1993).

Intrinsic hippocampal circuit

The highly processed information from neocortical areas reaches the entorhinal cortex (EC). Entorhinal cells, via the perforant path, project to DG granule cells, CA3/CA1 cells, and subicular cells (Fig. 2.1B). Furthermore, EC exhibits intrinsic recurrent connectivity. The dentate gyrus sends efferents to CA3 via the mossy fibers. Synaptic projections from DG to CA3 are very selective: each granule cell projects approximately onto 14 pyramidal cells only (Amaral, 1993). DG has also intrinsic projections: granule cells generate collateral synapses that terminate on

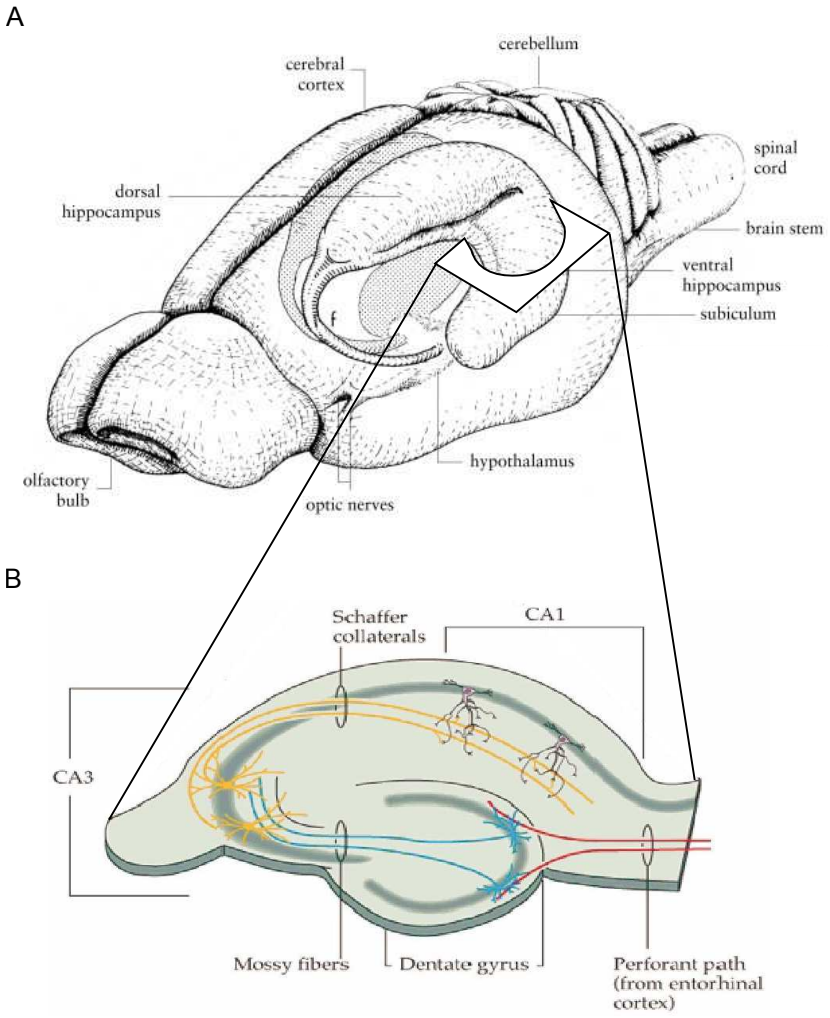

Figure 2.1: *Hippocampus of the rat from (Cheung and Cardinal, 2005).* **(A)** Position of the hippocampus within the brain and coronal sections. **(B)** Circuitry of the hippocampus. Transversal section.

the polymorphic DG region (Amaral and Witter, 1989). CA3 pyramidal cells form a recurrent network through the Shaffer collaterals, but the latter fiber bundle is also used to synapse CA1 and subicular cells. CA1 neurons send their output to entorhinal as well as subicular cells via the angular bundle (Amaral et al., 1991). Finally, SC projects onto the EC. The hippocampal circuit can be coarsely approximated by a feed-forward loop (Amaral and Witter, 1989): information enters the loop via EC, proceeds towards DG, then to CA3 and CA1, and finally arrives to SC which closes the loop by projecting to EC.

Hippocampal efferents

The SC forms the major output of the hippocampal formation (Amaral and Witter, 1989; Witter, 1993) (nevertheless, CA3 and CA1 regions also send an output directly to subcortical areas, e.g., the lateral septum; Swanson and Cowan, 1977). Until the mid-1970s it was thought that the hippocampal output was predominantly carried by the fornix. More recent studies have shown that an important pathway for the hippocampal outflow consists of the non-fornical projection to the deep layers of the entorhinal cortex (dEC). From dEC, information is sent to a variety of cortical areas (Witter, 1993; Insausti et al., 1997).

2.2 The prefrontal cortex

The prefrontal cortex (PFC) is a part of the frontal lobe, located in the anterior part of the mammal cortex. Uylings et al. (2003) proposed general criteria for the definition of the PFC and its comparison between two species, including its the cytoarchitectonic characteristics (Sec. 2.2.1), and the patterns and the density of afferent and efferent connections including the neuromodulator distribution (Sec. 2.2.3). The data presented in this section refer mainly to rats. However it is important to note that, with respect to all other cortical areas, PFC is particularly developed in primates and in humans and has come to represent nearly a third of the cortex (Brodmann, 1895).

2.2.1 Subdivisions

The rat PFC can be organized in medial, ventral and lateral (sulcal) parts. As shown on Fig. 2.2, the ventral and lateral parts are formed by the orbitofrontal cortex (OFC) and the agranular insular cortex (AIC). The medial part is composed the precentral cortex (PRC also called the frontal area 2 FR2 or agranular medial cortex AGC), the anterior cingulate cortex (ACC), the prelimbic cortex (PL) and the infralimbic cortex (IL) (Preuss, 1995; Paxinos and Watson, 1998; Uylings et al., 2003; Dalley et al., 2004; Vertes, 2006).

As shown in the next sections, the medial PFC of rats could be more generally divided in a dorsal part (PRC + dorsal ACC or PRC + ACC + dorsal PL) and a ventral part (ventral ACC + PL + IL or ventral PL + IL + medial OFC) (Vertes, 2006; Heidbreder and Groenewegen, 2003). The dorsal part could be equivalent to high level sensori-motor areas of the primate (frontal eye field, supplementary motor area and premotor area), whereas the ventral part could be similar to the primate areas involved in emotional, motivational and cognitive processing (orbital, cingulate and dorsolateral areas) (Condé et al., 1995; Vertes, 2006). More specifically, some authors suggest a strong homology between rat PL and primate dorsolateral PFC (Granon and Poucet, 2000).

2.2.2 Layered and columnar organization

Cortical layers.

The PFC share a cytoarchitectonic characteristic with other neocortical areas: various types of neurones compose its tissues, and are organized into layers parallel to the pial surface. Layer I mostly contains axons and dendrites. Layers II-III are called *supragranular* or *superficial* layers while layers V-VI are called *infragranular* or *deep* layers. The most prominent cytoarchitectonic feature of the *rat* prefrontal cortex is that it is composed exclusively of agranular cortical areas (i.e. without a layer IV). In primates, this layer receives the main sensory inputs, either directly from the thalamus or from columns of cortical areas involved in earlier stages of sensory processing (Mountcastle, 1997). We will see in Sec. 2.2.3 how the different layers are involved in afferent and efferent projections of the rat PFC, but a rather general property is that layers II/III project more strongly to other cortical areas while layers V/VI project more strongly to subcortical structures.

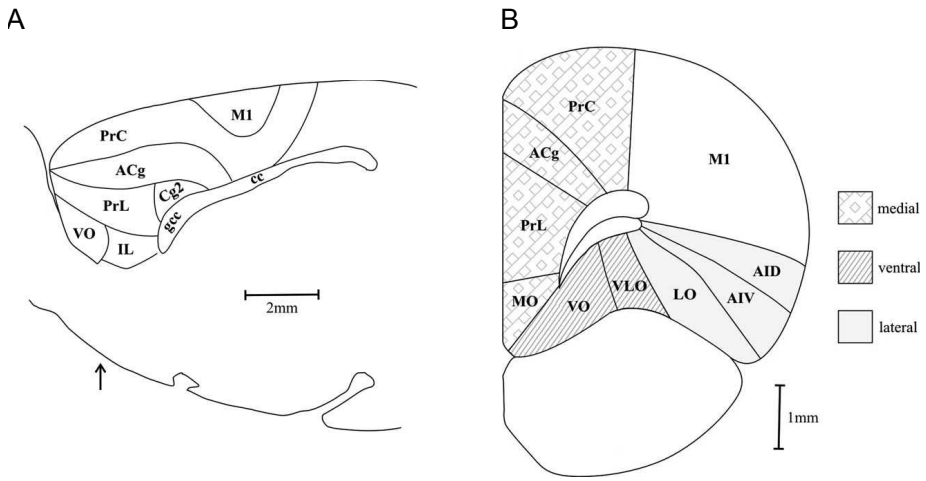

Figure 2.2: *Rat prefrontal cortex anatomy, from (Dalley et al., 2004).* **(A)** Lateral view, 0.9 mm from the midline. **(B)** Unilateral coronal section, approximately 3.5 mm forward of bregma (depicted by the arrow above). The different shadings represent the three major subdivisions of the prefrontal cortex (medial, ventral and lateral). Abbreviations: ACg, anterior cingulate cortex; AID, dorsal agranular insular cortex; AIV, ventral agranular insular cortex; cc, corpus callosum; Cg2, cingulate cortex area 2; gcc, genu of corpus callosum; IL, infralimbic cortex; LO, lateral orbital cortex; M1, primary motor area; MO, medial orbital cortex; PrL, prelimbic cortex; PrC, precentral cortex; VLO, ventrolateral orbital cortex; VO, ventral orbital cortex.

Thomson and Bannister (2003) reviewed the inter-laminar connections in adult mammalian neocortex: clear patterns are emerging from these studies, with 'forward' projections from layer IV to III and from III to V targeting both selected pyramidal cells and interneurons, while 'back' projections from layer V to III and from III to IV target only interneurons.

The composition and thickness of the layers differ according to the subparts of the PFC, and are progressively organized during development (Eden and Uylings, 1985). Fig. 2.3 illustrates the layered organization for three subparts (ACC, PL and IL) of the rat PFC (Gabbott et al., 1997). Gabbott et al. (1997) have performed a quantification of layer thickness and neuronal density for these three subparts (Fig. 2.4). To give a general idea, cumulated thickness for all layers varied from $\sim 1\,mm$ (IL) to $\sim 1.5\,mm$ (ACd). The total number of neurons under $1\,mm$ of cortex changed with the same gradient, from ~ 49000 neurons in IL (85.2 % of pyramidal cells vs. 14.8 % of inhibitory interneurons) to ~ 67000 neurons in ACd (82.8 % vs. 17.2 %).

General principle: functional columns

Lorente de No (1938) introduced the important idea of the "elementary cortical unit of operation". He considered the neocortex as consisting of small cylinders composed of vertical chains of neurons that crossed all cortical layers and that had specific afferent fibers as their axis. This idea formed the basis of the hypothesis of the columnar organization of the cerebral cortex that developed later, mainly after the works of Mountcastle, Hubel and Wiesel (for reviews see Hubel and Wiesel, 1977; Mountcastle, 1997; Buxhoeveden and Casanova, 2002; Goodhill and Carreira-Perpinan, 2002). This widely investigated hypothesis states that neurones in many cortical areas of the mammalian brain are arranged into functional columns (also called macrocolumns or modules) on the basis of their similar physiological response properties (Szentágothai, 1975; Eccles, 1981; Burnod, 1988; Vogt and Gabriel, 1993; Mountcastle, 2003). The existence of cortical columns was first reported by Mountcastle (1957), who observed chains of cortical neurones reacting to the same external stimuli simultaneously ("similarity" however, can be a difficult concept, especially outside the primary and early sensory cortices; Mountcastle, 2003). In the rat neocortex, columns are believed to be about $300 - 600\,\mu m$ wide and contain around 7500 neurons distributed non-uniformly

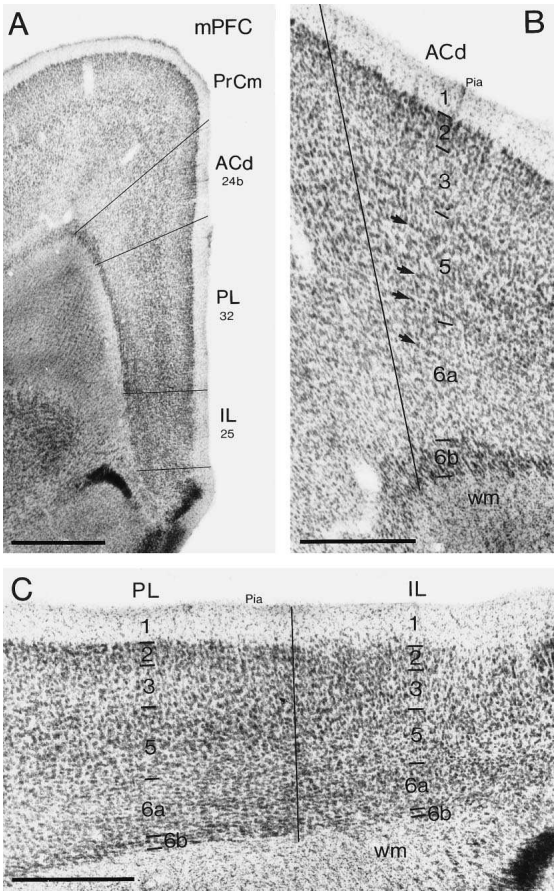

Figure 2.3: *Cytoarchitecture of rat mPFC, from (Gabbott et al., 1997).* **(A)** Coronal Nissl-stained section (13.2 mm anterior to bregma) showing the division of the rat medial PFC into dorsal ACC (ACd), PL, IL and PrCm. **(B)** Cytoarchitectural lamination of ACd. **(C)** Cytoarchitectural lamination of PL and IL cortices. White matter, wm. Calibration bars: A, $1000\,\mu m$; B, $500\,\mu m$; C,$500\,\mu m$.

across the cortical layers (Markram et al., 2004).

The columnar organization has been suggested to subserve efficient neocortical computation and information processing. For example, cortical columns have been compared to complex processing and distributing units that link a number of inputs to a number of outputs via overlapping internal processing chains (Mountcastle, 1997). A distributed system is a collection of processing units that are spatially separate and communicate by exchanging messages. A system is distributed if the message-transmission delay is a significant fraction of the time between single events in a processing unit. Given synaptic transmission times in the neocortex (1–5 ms) and the slow conduction velocity in cortico-cortical axons, this seems to fit. Some further and important properties of distributed systems are these (Mountcastle, 1997). *(i)* Signal flow through such a system may follow any of a number of pathways in the system. *(ii)* Action may be initiated at any of a number of nodal loci within a distributed system. *(iii)* Local lesions within such a system may degrade a function, but not eliminate it completely. *(iv)* Distributed systems are re-entrant systems, i.e. their nodes are open to both externally induced and internally generated signals.

The columnar organization is mostly related to the migration of neurons from the ventricular and subventricular zones into radial columns during development (Rakic, 1988). This radial migration has been suggested as a mechanism, known as the radial unit hypothesis (Rakic, 1988), by which the neocortex could expand enormously during evolution as a sheet of cells with a basically uniform thickness rather than increasing in size as a globe (reviewed in Rakic, 2002). However major issues regarding the basic nature, key features, and functional significance of the columnar organization remain unclear and often controversial (Rockland and Ichinohe, 2004; Horton and Adams, 2005). For example, Rakic (2008) stressed that the size, cell composition, synaptic organization, expression of signaling molecules, and function of various types of columns are dramatically different across the cortex, so that the general concept of column should be employed carefully. Moreover, studies such as (Jung et al., 2000) have suggested that response characteristics of neurons within the same cortical column are not as homogeneous as previously assumed, so that a balance between a redundant coding of information (which favors precision) and a heterogeneous coding (higher storage capacity) is maintain. Anatomically, another problem is that multiple column-

like structures can be recognized, at different spatial scales ranging from about $10\,\mu m$ to $400 - 1000\,\mu m$ (see Buxhoeveden and Casanova, 2002). The next section presents neuroanatomical findings that suggest that functional columns can be divided into small scale structures, closely related to an anatomical substrates, and often called structural minicolumns (or microcolumns).

Structural minicolumns

A common definition of the anatomical minicolumn is a basic unit, consisting of a narrow chain of neurons extending vertically across layers II-VI (Mountcastle, 1997, 2003). It is often described as having common inputs, common outputs, and as being rather uniform across cortical areas, although some cautions have been voiced against strong generalizations (Mountcastle, 1997; DeFelipe et al., 2002; Buxhoeveden and Casanova, 2002; Mountcastle, 2003; Rockland and Ichinohe, 2004; Rakic, 2008). Two main types of structural minicolumns can be found: one is of vertically oriented rows of cell bodies (Buxhoeveden and Casanova, 2002), the second is groups of neurons whose apical dendrites form bundles or clusters (also called pyramidal cell modules, Peters and Kara, 1987).

Vertical pyramidal cell rows. Vertically aligned rows of cell bodies can easily be discerned in Nissl-stained preparations of many cortical areas for many mammals (e.g. in the human PFC, see Fig. 2.5). The degree of verticality is highly variable across areas. Even in high-columnar areas like temporal cortex, cellular columns do not extend from layers II to VI, but rather consist of $15 - 20$ aligned cell bodies over a thickness of $300 - 500\,\mu m$. In human medial prefrontal cortex, stacks of $15-19$ soma have been reported to occur sporadically at different depths in layers III-VI (Gabbott, 2003).

Dendritic bundles. The fundamental structural subunits within a cortical module are thought to be the neurones and synaptic circuitry associated with a single cluster (bundle) of apical dendrites originating from pyramidal neurones (Peters and Kara, 1987; Rockland and Ichinohe, 2004). Particularly, pyramidal cell apical dendrites in layers II-V of the rat PL are not randomly distributed, but are organized into discrete radially aligned bundles (Fig. 2.6A-B; Gabbott and Bacon, 1996b). On Fig. 2.6C, the centers of clusters surrounding a central cluster have

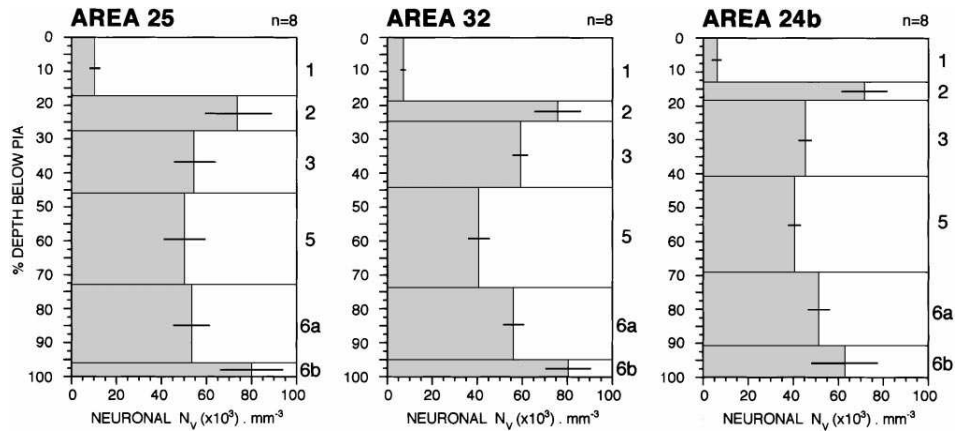

Figure 2.4: *Cortical depth distributions of laminar neuronal density N_V estimates in areas IL (25), PL (32) and ACd (24b) of rat mPFC, from (Gabbott et al., 1997).* The whole depth of the cortex is presented as 100% with laminar boundaries indicated at the corresponding percentage depths below the pial surface.

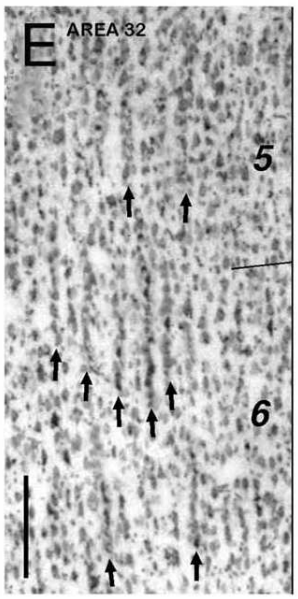

Figure 2.5: *Vertically organized stack of pyramidal cells in the dorsal ACC of human, from (Gabbott, 2003).* Nissl-stained cell bodies in layers 5 and 6. Note the long vertical alignment of the stacks. Readily apparent are the relatively somata-free regions between the columns of stacked cell bodies. Scale bar: $500\,\mu m$.

been linked together to indicate the predominant hexagonal packing of dendritic clusters. Additional groups of dendritic profiles occur between the recognized clusters (one example is shown encircled). This dendritic bundle organization can also be observed in monkey and human PFC (Gabbott and Bacon, 1996a; Gabbott, 2003).

The structural subunit of which a single dendritic bundle forms the central component could be conveniently modeled in the rat PL by an hexagon extending from white matter to pia through all layers of the cortex (Fig. 2.7A; Gabbott and Bacon, 1996b; Gabbott et al., 2005; see Fig.A.2 for a schematic representation of monkey minicolumns). In cross-section, the packing of minicolumns can be modeled ideally as a clustered hexagonal honeycomb lattice parallel to the pial surface (Fig. 2.7B), with a mean center-to-center distance between bundles of $45\,\mu m$, a mean surface area for each minicolumn of $1360\,\mu m^2$, and a minicolumn density of 735 minicolumns per mm^2 (Gabbott and Bacon, 1996b). Each minicolumn would contain about 63.5 pyramidal neurons (plus inhibitory interneurons) distributed over the six layers (Fig. 2.7C).

Functions of micro-circuits and inhibitory interneurons. Speculations about the functional capacity of dendritic bundles have centered on their ability to correlate or synchronize the activity between vertically aligned sets of pyramidal cells in the superficial and deep layers of the cortex in response to afferent input. For example, Rao et al. (1999) showed that, when recorded simultaneously at the same cortical site (about $20 - 50\,\mu m$ wide), the majority of neighboring neurons, whether inhibitory interneurons or pyramidal cells, displayed isodirectional tuning, i.e., they shared very similar tuning angles for the sensory and delay phases of the task (Rao et al., 1999; see also Constantinidis et al., 2001 for a cross-correlation study between pairs of neighboring neurons). These results support the interpretation that closely adjacent neurons within the same minicolumn may share a high proportion of their spatially tuned afferents (Shadlen and Newsome, 1998) and thus form a strong consensus in tuning preferences (a form of neural averaging) (Zohary et al., 1994). Besides, this suggests that interneurons are also involved at the first stages of processing afferent information from other brain regions, including cortex, thalamus, hippocampus, amygdala, VTA, and brainstem structures, possibly through the same monosynaptic projections that innervate the pyramidal cells (e.g., see Freund and Meskenaite, 1992; Vogt and Gabriel, 1993;

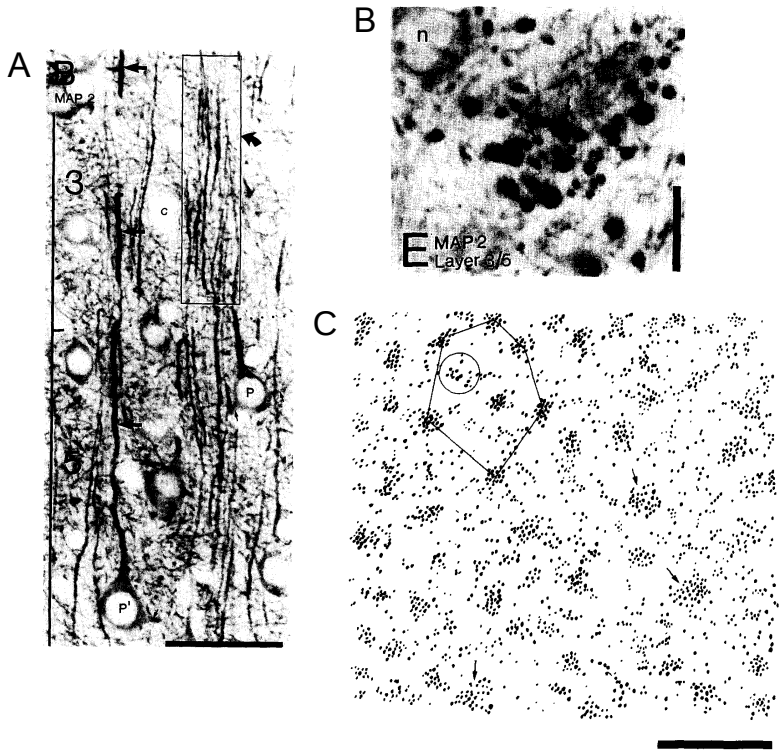

Figure 2.6: *Dendritic bundles in the rat PL, from (Gabbott and Bacon, 1996b).* **(A)** Micrograph of a section through layers 3 and 5. P and P' represent pyramidal neurones. Indicated is the clustering of dendrites ascending through the superficial layers of the cortex (boxed region in layer 3). c is a capillary. Scale bar: $50\,\mu m$. **(B)** Tangential section at the boundary between layer 3 and 5. Dendritic profiles of varying size aggregate to form a cluster. Scale bar: $10\,\mu m$. **(C)** Light microscope drawing showing the tangential distribution of dendritic bundles from the middle of layer 3. Several dendritic bundles are indicated (arrows). A line links centers of clusters surrounding a central cluster, and an example of additional dendritic group occurring between the recognized clusters is shown encircled. Scale bar: $100\,\mu m$.

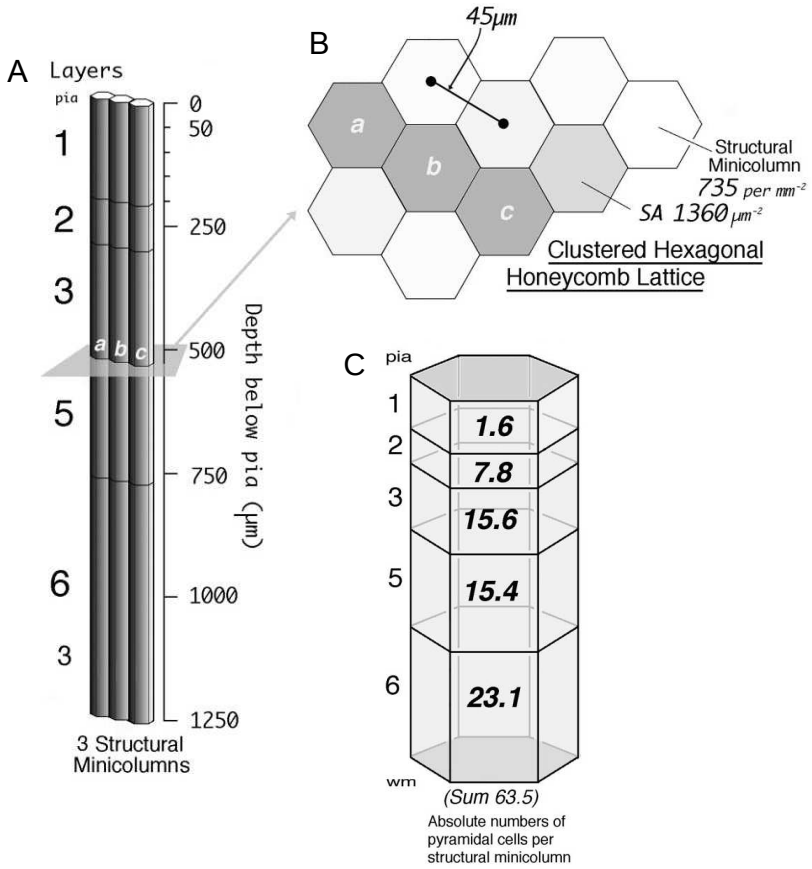

Figure 2.7: *Schematic representation of minicolumns in the rat PL, from (Gabbott et al., 2005).* **(A)** Three examples of structural minicolumns extending perpendicular to the pia through all cortical layers. **(B)** Cross-section representation of minicolumns ideally packed into a clustered "hexagonal" honeycomb lattice parallel with the pia. SA: surface area of each minicolumn (SA). **(C)** Approximate number of pyramidal neurons belonging to each layer of a minicolumn. The values are deducted from the volume of a minicolumn ($1360\,\mu m^2 \times 1250\,\mu m$) and the density of cell).

Sesack et al., 1995; Tierney et al., 2004).

GABAergic inhibitory interneurons play a central role in micro-circuits. Unlike pyramidal cells which project often to other far brain areas, inhibitory interneurons of the neocortex are strongly involved in the shaping of pyramidal cell responses belonging to the same minicolumn or to adjacent ones. That is why they are sometimes called "local circuit" neurons. Indeed they can control the balance between excitation and inhibition (Markram et al., 2004; Silberberg and Markram, 2007), the sharpness of the tuning of pyramidal cells (Rao et al., 2000) as well as the timing of their responses (Pouille and Scanziani, 2001; Constantinidis et al., 2002), which could support the synchronization of these pyramidal cells. This is possible because of the discharges properties of inhibitory interneurons such as larger and faster EPSPs, a smaller latency and a shorter action potential duration in interneurons versus pyramidal cells (Dégenètais et al., 2003; Tierney et al., 2004; Povysheva et al., 2006). As a consequence, it appears that nearby inhibitory neurons are more tightly synchronized than excitatory ones and account for much of the correlated discharges commonly observed in cortical networks (Constantinidis and Goldman-Rakic, 2002).

Inhibitory interneurons, which represent a part of 16% of pyramidal cell inputs, can have several type of connections with pyramidal cells (Markram et al., 2004): axonal connection, somatic connection and dendritic connection. Each of these types of connection have a different influence on the target neuron activity, respectively the timing of action potential, the gain summation of input currents, and the perturbation of other dendritic input currents and plasticity (Markram et al., 2004). In fact this depends on the type of interneurons, which are a heterogeneous group of cells whose repartition changes among cortical areas and among species (DeFelipe et al., 2002; Raghanti et al., 2010). In the rat PFC, several subtypes of GABAergic interneurons have been identified by the expression of defined calcium binding proteins. Kawaguchi and Kubota (1997) has classified them in three main groups according to their physiological firing patterns (see also Markram et al., 2004): *(i)* fast-spiking (basket and chandelier cells), *(ii)* late-spiking (neurogliaform cells) and *(iii)* regular-spiking and burst-spiking non-pyramidal cells (martinotti, double bouquet and arcade cells). Each cell subtype have typical morphological properties (e.g., shape of the dendritic tree and projection site on the target neurons; see Markram et al., 2004). For more details on

the density of interneuron subtypes in the dendritic bundles of the rat PFC, see (Gabbott et al., 1997).

Besides the inhibitory effect present within a minicolumn, inhibition can occur between minicolumns (Rao et al., 1999). Indeed, Thomson and Deuchars (1997) reported considerable inhibition between interneurons and pyramidal cells at distances of $50 - 250\,\mu m$. The differences found by Rao et al. (1999) in consensus of tuning between neighboring minicolumns may therefore provide the circuit basis for isodirectional inhibition, which serves to sharpen spatial tuning in a mechanism similar to that proposed for visual cortex (Kisvárday et al., 1994; Somers et al., 1995; Wörgötter and Koch, 1991). Finally, another inhibition could act at an even higher scale between set of minicolumns with different selectivity (cross-directional inhibition) and separated by about $400 - 800\,\mu m$ (Kisvárday et al., 1994). Rao et al. (1999) propose a simple representation of these multiple inhibitory effect (Fig. 2.8). Thus, inhibitory interneurons are an important component of columnar organization which govern local cortical microcircuitry and are fundamental for intra- and intercolumnar processing (Raghanti et al., 2010). Note that lateral interactions between minicolumns are not limited to inhibitory effects: pyramidal cells send also excitatory collaterals to adjacent and distant minicolumns (Mountcastle, 1997; Lewis et al., 2002).

2.2.3 Connectivity

"It is evident that each cortical neuron is the focus of input from many other neurons, and on the basis of the available data it is estimated that a single pyramidal cell in cortex receives its input from as many as 1,000 other excitatory neurons and as many as 75 inhibitory neurons" (Peters, 2002). We review here the main afferent and efferent connections of rat PFC neurons.

Intrinsic connections

The subparts of the PFC have strong interconnections which creates local recurrent circuits (Reep et al., 1996; Öngür and Price, 2000; Gabbott et al., 2003; Uylings et al., 2003; Heidbreder and Groenewegen, 2003). These connections are also topographically organized: ventral parts tend to be connected together, and dorsal areas with other dorsal areas (Heidbreder and Groenewegen, 2003).

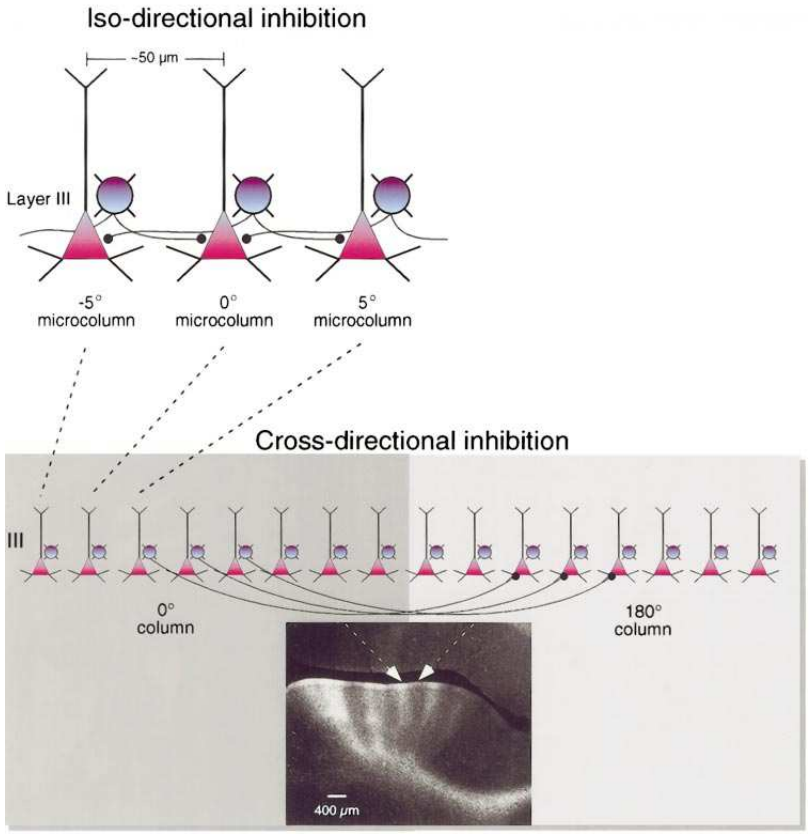

Figure 2.8: *Iso- and cross-directional inhibition in the PFC, from (Rao et al., 1999).* Hypothetical circuit demonstrating isodirectional tuning relationships between adjacent minicolumns with small differences ($\sim 5°$, top) in their directional preferences and cross-directional relationship between distant, functionally defined columns with a wide difference ($\sim 180°$, bottom) in their directional preference. The bulk of interactions is considered likely to take place in layer III, where a large proportion of horizontal connections and interneurons can be found. Bottom inset: autoradiographic visualization of the columnar organization of afferent input (corresponding to functional columns) to the principal sulcus of the monkey.

Cortico-cortical connections

"All major sensoria find some form of representation in the prefrontal cortex, however abstract or compounded" (Nauta, 1971). Indeed inputs from olfactory, gustatory, somatosensory and visual sensory areas have been reported in rats (Reep et al., 1996; Öngür and Price, 2000). Interestingly, neocortical areas involved in spatial processing such as the entorhinal, perirhinal and retrosplenial cortices send also connections to the PFC (Uylings et al., 2003). Particularly, the entorhinal cortex can exert a potent inhibition on PFC pyramidal cells (Valenti and Grace, 2009). The PFC sends in return connections to all these cortices, with its dorsal part more strongly connected with sensori-motor areas (Vertes, 2006; Heidbreder and Groenewegen, 2003). Layers II-III of the cortex are mainly responsible for these cortico-cortical connections to both adjacent and distant cortical zones.

Hypothalamus, brainstem and neuromodulation

By way of hypothalamic projections, the prefrontal cortex has an important influence on behavioral and autonomic functions. Medial prefrontal projections to the hypothalamus predominantly arise from the ventrally located cortical areas (Öngür and Price, 2000; Heidbreder and Groenewegen, 2003; Gabbott et al., 2005). The orbital and agranular insular prefrontal regions contribute to these projections, which are topographically organized. The PFC have also extensive connections with the brainstem, including the midbrain where the ventral tegmental area (VTA) and the substantia nigra compacta (SNc) can be found (Heidbreder and Groenewegen, 2003).

Connections between dopaminergic neurons and the PFC. VTA and SNc are the main dopaminergic inputs to the PFC. While the striatum is the major subcortical target for dopaminergic neurons, the PFC is one of the principal target in the neocortex. The whole PFC receives projections, but its ventral part is more innervated (Thierry et al., 1973). Again a topographical organization can be observed: the ventral part of the VTA projects to the dorsal PFC while the dorsal VTA is connected to the ventral PFC (Deutch, 1993). The dopaminergic projections are also organized according to the laminar structure of the PFC: SNc neurons have their terminal synapses in the superficial layers of the PFC (mainly the ACC) while VTA neurons target the deep layers (Heidbreder and Groenewegen, 2003).

Finally there is a difference between ventral and dorsal PFC for the processing of the dopamine. In the latter, dopaminergic transporters are denser, leading to a higher uptake capacity and a lower gradient of dopamine concentration. Compared to the striatum, the regulation of dopamine is much slower in the PFC (Cass and Gerhardt, 1995), which may indicate a difference in the temporal scale of the learning processes subserved by these two structures.

The PFC projects in turn excitatory glutamatergic connections to the VTA (Murase et al., 1993; Gabbott et al., 2005) and the SNc, so that the PFC may be able to exert a control over these neural population (Murase et al., 1993; Carr and Sesack, 2000; Gao et al., 2007). These projections originate mainly from the deep layers of the ventral PFC (Au-Young et al., 1999). Thus the PFC may control the release of DA in itself and in other brain structures.

Influence of dopaminergic neurons on the PFC. We will not discuss in details this complex influence, which is out of the scope of this thesis, but give some main ideas interesting to the general understanding of the PFC. Dopamine has been shown to modulate glutamatergic synaptic transmission and long-term changes in synaptic strength (Pennartz et al., 1994; Law-Tho et al., 1995; Otani et al., 1998; Laroche et al., 2000; Bao et al., 2001; Seamans and Yang, 2004). Dopamine transmission plays a prominent role in functions of the prefrontal cortex. For example, as clearly shown in the monkey and the rat, too much or too little dopamine may be detrimental for working memory, revealing the crucial role of dopamine transmission in prefrontal neuronal processes related to working memory (see Fig. A.4; Brozoski et al., 1979; Murphy et al., 1996; Zahrt et al., 1997; Williams and Goldman-Rakic, 1995).

DA modulates several ionic conductances along the somato-dendritic axis of pyramidal neurons and may thus contribute to the integration of segregated inputs (reviewed in Yang et al., 1999; Seamans and Yang, 2004). In addition, through its effect on local GABAergic interneurons, the mesocortical dopamine system can also indirectly modulate the excitability of pyramidal cells from their inputs and from the activation of recurrent collaterals of pyramidal neurons (Ferron et al., 1984; Pirot et al., 1992, 1996; Bandyopadhyay and Hablitz, 2007; Tierney et al., 2008). DA can influence neurons in the PFC through their D1 or D2 receptors (Yang and Seamans, 1996; Zheng et al., 1999; Seamans et al., 2001; Gorelova et al., 2002; Tseng and O'Donnell, 2004; Wang and Goldman-Rakic,

2004; Kröner et al., 2007; Tseng and O'Donnell, 2007). These receptors are activated respectively by a low concentration of DA and high concentration (Seamans and Yang, 2004). Thus the effect of DA are subtle, may maintain a balance between inhibition and excitation in the PFC (Seamans and Yang, 2004; Goto et al., 2007), and act at different time scales (Schultz, 2007; Lapish et al., 2007). It is also interesting to note that the information transfer between mesocortical neurons and the PFC can also be achieved by glutamatergic transmitters. This enables mesocortical neurons to have a fast influence of the PFC activity, compared to the slower effect of DA (Seamans and Yang, 2004).

Several roles has been attributed to the influence of DA over the PFC (see Cohen et al., 2002 for a review). Dopamine may modulate signal-to-noise ratio (i.e., the difference between basal neural discharges and stimulus-induced discharges) in PFC pyramidal cells. It may also maintain and update salient information in memory. The underlying assumption is that information storage in the PFC may be achieved by fixed-point attractor networks (a type of recurrent neural network whose population activity can have one stable attractor), and the DA may influence the stability of them to favor maintenance or updating of information (Seamans and Yang, 2004). According to (Phillips et al., 2004), the magnitude of dopamine release in the PFC may also be related to the accuracy of memory on a delayed response task. Goto and Grace (2008) suggest that DA may modulate the interaction between retrospective memory coming from the hippocampus and PFC prospective memory. In fact, dopamine effects may be different according to its release mode: tonic (slow release) or phasic (fast release) (Schultz, 2002). Indeed, phasic release has been implied in reward prediction, stimulus novelty coding or novel action discovery (Schultz, 1998, 2002; Redgrave and Gurney, 2006). Tonic release is related to the background dopamine concentration, and may be crucial for high-level functions such as working memory (Williams and Goldman-Rakic, 1995). A large number of models have been proposed to address many questions related to the influence of DA on PFC, such as the modulation of pyramidal and inhibitory neurons, the role in plasticity, the difference between phasic and tonic release, the active maintenance of information, decision making... (e.g. Ferron et al., 1984; Servan-Schreiber et al., 1990; Montague et al., 1996; Schultz et al., 1997; Suri and Schultz, 1999; Brown et al., 1999; Brunel and Wang, 2001; O'Reilly et al., 2002; Dreher et al., 2002; Tanaka, 2006; Braver et al., 1995, 1997, 1999, 2000;

Durstewitz et al., 1999, 2000a, 2000b, 2002, 2006; see also Cohen et al., 2002 for a review).

Other neuromodulatory inputs to the PFC. The PFC receives other monoaminergic and cholinergic neuromodulators from the brainstem. Serotonergic (5-HT) neurons from the raphe nuclei, noradrenergic (NA, also called norepinephrine) neurons from the locus coeruleus and cholinergic (ACh) neurons from the caudal part of the basal nucleus send direct projections to the PFC (Heidbreder and Groenewegen, 2003; Uylings et al., 2003). Similarly to the dopamine, a unique property of the PFC compared to other neocortical areas is to send in turn direct connections to these neural populations, mainly from its ventral part.

Serotonin has long been implicated in impulse choice (see Cardinal, 2006 for a review) and behavioral flexibility, such as reversal learning (reversal of stimulus-reward associations e.g., Clarke et al., 2004). The prefrontal noradrenergic system has been involved in novel action-outcome contingencies coding and attentional set-shifting (Dalley et al., 2004; McGaughy et al., 2008), the active maintenance of the information about a goal and the rules to achieve it during working memory task (Rossetti and Carboni, 2005) and the encoding of some aspects of uncertainty in the general sense of making predictions in a given context (Yu and Dayan, 2005). Acetylcholine has been associated with locomotor activity (Day et al., 1991), spatial working memory (Ragozzino and Kesner, 1998), attention and arousal (Sarter and Bruno, 1997) and the switch between memory systems during learning (Chang and Gold, 2003).

Striatum and thalamus

The PFC as a whole projects to the ventromedial part of the striatum, including the nucleus accumbens, the medial part of the caudate nucleus and the ventral part of the putamen (Sesack et al., 1989; Berendse et al., 1992; Öngür and Price, 2000; Heidbreder and Groenewegen, 2003; Voorn et al., 2004; Gabbott et al., 2005). Studies show that projections from the PFC to the striatum are topographically organized (Fig. 2.9). The ventral part of the PFC projects strongly to the shell of the nucleus accumbens and to a lesser extent to the medial caudate-putamen. The dorsal PFC sends connections to the core of the nucleus accumbens and a more dorsal part of the caudate nucleus. Lateral areas, such as the AIC, project

to a contiguous ventrolateral part of the striatum. Layers V/VI of the PL and IL project to the shell, whereas layer II only projects to the core (Ding et al., 2001). Moreover, another gradient of connections exists according to the depth of the PFC afferent synapses: PFC superficial layers project to the matrices of the striatum while the deep layers project to the patches (Gerfen, 1989).

In turn, the PFC does not receive direct connections from the striatum, but massive topographically-organized projections through the thalamus. More specifically, there is a gradient along the dorso-ventral areas of the PFC to the lateral-medial thalamus. The PFC has reciprocal connections with many nuclei of the thalamus, and particularly with the mediodorsal nucleus (Heidbreder and Groenewegen, 2003). We have already mentioned PFC-reuniens nuclei interactions. PFC connections to the thalamus originate generally from the layer VI, and the reciprocal projections from the medio dorsal nucleus target layer III.

In fact, as represented on Fig. 2.10, it is now well-established that the cerebral cortex and the basal ganglia are related through multisynaptic striato-pallido- and striato-nigro-thalamic loop circuits organized in parallel channels, also called "cortico-basal loops" (Alexander et al., 1986; Uylings et al., 2003; Haber, 2003; Heidbreder and Groenewegen, 2003). These loops are believed to be the neural basis of an important information transfer and integration as well as mnemonic processes such as stimulus-reward, stimulus-response, action-outcome association learning and response sequence learning (Uylings et al., 2003).

Amygdala

The amygdala is strongly connected to the PFC, via reciprocal connections (Heidbreder and Groenewegen, 2003). It sends synapses mainly to IL, the PL, the AIC and the OFC (Krettek and Price, 1977; Kita and Kitai, 1990). These connections originate with a higher density from the BLA and reach the PFC mainly in layers II and V (Bacon et al., 1996). Many neurons in the BLA, and to a lesser extent other amygdaloid nuclei send collaterals to both the prefrontal cortex and striatum (Mcdonald, 1991). Projections from the amygdala reach pyramidal cells as well as interneurons monosynaptically, which enables the amygdala to exert feedforward excitation and inhibition on the PFC (Bacon et al., 1996; Garcia et al., 1999; Gabbott et al., 2006).

In return the PFC projects with direct connections to the whole amygdala (Hei-

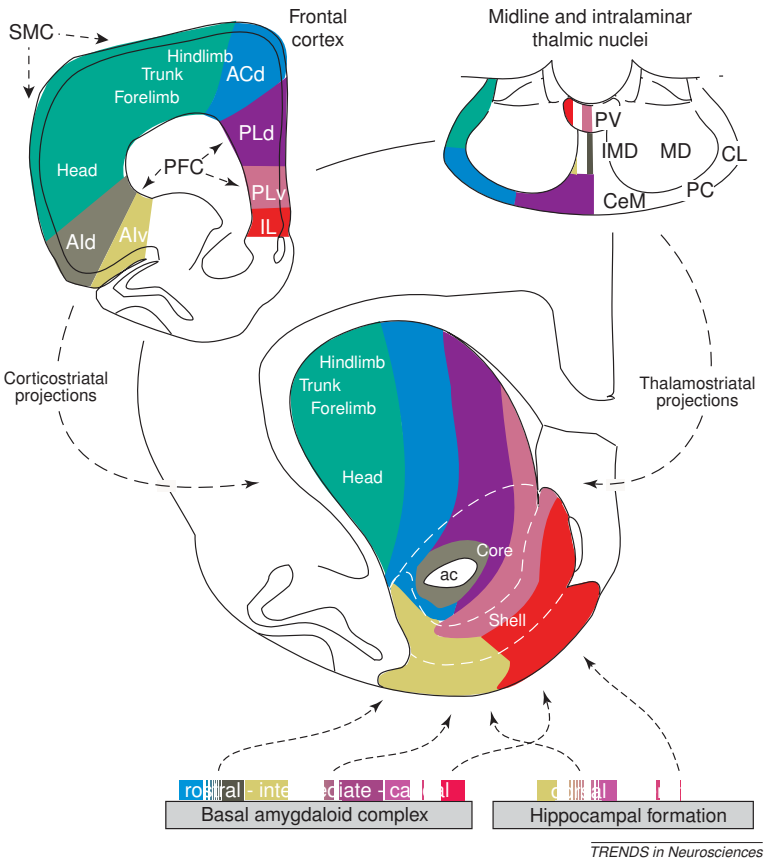

Figure 2.9: *Cortical and thalamic inputs to the striatum distributed in dorsomedial-to-ventrolateral zones from (Voorn et al., 2004).* The topographical arrangement of striatal afferents originating in the frontal cortex (upper left), midline and intralaminar thalamic nuclei (upper right), basal amygdaloid complex (lower left) and hippocampal formation (lower right) are illustrated. Abbreviations: ac, anterior commissure; ACd, dorsal ACC; AId, dorsal AIC; AIv, ventral AIC; CeM, central medial thalamic nucleus; CL, central lateral thalamic nucleus; (I)MD, (inter)mediodorsal thalamic nucleus; PC, paracentral thalamic nucleus; PLd, dorsal PL; PLv, ventral PL; PV, paraventricular thalamic nucleus; SMC, sensorimotor cortex.

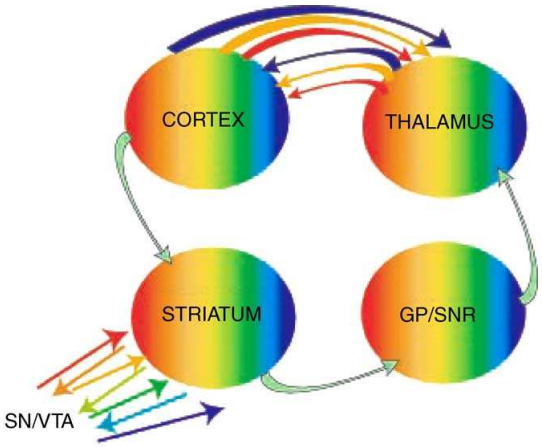

Figure 2.10: *Schematic illustrating two potential mechanisms for relaying and integrating information within the cortico-basal-ganglia circuitry, from (Haber, 2003).* Information from distinct cortical regions could be processed separately, and in parallel through functionally-related neurons (green arrows). Information from these distinct, parallel pathways could be integrated in two ways: (1) by spiraling connections between the midbrain dopamine cells and the striatum; and (2) via thalamo-cortico-thalamic projections.

dbreder and Groenewegen, 2003). Each subpart of the PFC tends to have a specific pattern of connectivity with amygdala nuclei (Mcdonald et al., 1996; Gabbott et al., 2005). Some indirect connections through the reuniens nuclei of the thalamus have also been spotted (Zhang and Bertram, 2002).

It should be noted that a particularly strong interaction exists between the BLA and the OFC (Holland and Gallagher, 2004). Indeed, both of these structures receive projections conveying high level sensory information. Within the BLA, these afferent connections overlap projections from the OFC, and conversely within the OFC.

Hippocampus

The interactions between the hippocampus and the prefrontal cortex are one of the important parts of our modeling work. Thus we will give more details about their properties.

Anatomical characteristics. Ventral CA1 and subiculum part of the hippocampal formation send dense monosynaptic projections to the PFC (Thierry et al., 2000). Swanson (1981) first demonstrated a direct pathway from the temporal field CA1 of the hippocampus to the IL. Then, it was shown by Ferino et al. (1987) that there was also a direct hippocampal projection to the PL originating mainly from the CA1 field and of the adjacent dorsal and ventral subiculum. Other studies revealed that this pathway innervates mainly the medial OFC and the PL (Jay et al., 1989; Jay and Witter, 1991; Condé et al., 1995), but also the AIC (Verwer et al., 1997) and with a small density the ACC. It is interesting to note that a large number of hippocampal neurons sending projections to the IL or to the AIC also have collaterals targeting the entorhinal cortex (Swanson, 1981) and the medial PFC (Verwer et al., 1997), respectively.

HP-PFC projection fibers first enter the alveus and course dorsally and rostrally through the fimbria/fornix. Then, these fibers continue in a rostroventral direction through the septum and the nucleus accumbens, enter the infralimbic area, and finally reach the PL/MO areas of the prefrontal cortex (Jay and Witter, 1991). Different patterns of connectivity can be observed between the ventral and the dorsal PL: in the former terminal arborizations are present in layers II to VI, whereas they are less dense and only present in layers V to VI in the dorsal part.

The HP projections are distributed in all layers of the medial OFC, with a slight preference for deep layers to layer II (Jay and Witter, 1991). The main neurotransmitter of the HP-PFC pathway is the glutamate excitatory amino acid which can activate AMPA and NMDA receptors (although PFC responses seem to result mainly from the activation of AMPA receptors) (Jay et al., 1992).

It should be noted that indirect but influent connections from the HP to the PFC (including medial and ventral OFC, ACC, PL, IL and AIC) through the reuniens nuclei of the thalamus have also been reported (Di Prisco and Vertes, 2006; Vertes, 2006; Vertes et al., 2006). These connections target the layers V/VI of the PFC. Finally, even if the majority of anatomical studies focus on the pathway between ventral HP and the PFC, recent electrophysiological data show that electrical stimulations of the posterior dorsal part of CA1 evoke monosynaptic responses within the PFC (Izaki et al., 2003; Kawashima et al., 2006), which tends to support the existence of a dorsal HP to PFC pathway.

In return, the PFC does not send direct projections to the HP. However, there are several indirect pathways available going through parahippocampal structures such as the entorhinal and the perirhinal cortex (Heidbreder and Groenewegen, 2003), and the reuniens nuclei of the midline thalamus (Vertes, 2006). Indeed, PL and IL send projections to the reuniens nuclei, which is a major hippocampal formation afferent. It is monosynaptically connected to CA1, subicular and entorhinal pyramidal cells and interneurons (Weel and Witter, 1996, 2000), and the CA1 field potential generated by its inputs is nearly as important as the CA3 one (Vertes, 2006). Finally, the reuniens nuclei neuron populations receiving inputs from the PFC are the one who project to the hippocampus (Vertes et al., 2007). Thus, it has been proposed that the symmetric connections between the HP, the reuniens nuclei and the PFC may be responsible to synchronize the HP and the PFC (Vertes, 2006; Vertes et al., 2007). It is interesting to note that for the primate, reciprocal connections between the HP and the dorsolateral PFC have also been exhibited (Goldman-Rakic et al., 1984), which support the homology between the rat ventral PFC and the primate dorsolateral PFC.

Electrophysiological properties of the HP-PFC pathway. The conduction time of HP-PFC connections is very short ($\sim$15 ms), with a conduction velocity of 0.6 m/s and a fiber refractory period of 2.3 $\pm$ 0.4 ms (Ferino et al., 1987; Dégenètais et al., 2003; Tierney et al., 2004). Single-cell extracellular recordings

of PFC neurons and electrical stimulation of the hippocampus were first used to determine the influence of the hippocampal formation on the PFC cortex in anesthetized rats (Laroche et al., 1990; Jay et al., 1992; Mulder et al., 1997). 42% of the recorded cells showed an excitatory response (i.e., a single action potential with a latency of 18 ms) often followed by a prolonged inhibition after a single-pulse stimulation of the hippocampus.

It was also demonstrated by intracellular recordings that the HP exerts a complex influence on the PFC pyramidal neurones. Indeed their activations consist of an EPSP-IPSP (excitatory postsynaptic potential - inhibitory postsynaptic potential) sequence (Thierry et al., 2000). Single-pulse stimulations of cells in the HP produced early EPSPs after 17,4 $\pm$ 7.5 ms in 89% of the recorded PFC neurons, followed by a prolonged phase of hyperpolarization (266 $\pm$ 139 ms). These early EPSPs caused action potential in 33% of cells. Late EPSPs were also observed in 35% of the neurons, probably generated by the activation of local excitatory networks (Thierry et al., 2000; Dégenètais et al., 2003).

The prolonged hyperpolarization observed in intracellular recordings was composed by a fast and a slow IPSP resulting from the activation of local inhibitory networks due to the activation of PFC recurrent collaterals or to the direct excitatory influence of HP over PFC interneurons (feedforward inhibition through monosynaptic projections) (Thierry et al., 2000; Gabbott et al., 2002; Tierney et al., 2004). This feedforward inhibition might be responsible for the pyramidal cell complex responses. A stimulation in the HP produces EPSPs in PFC pyramidal cells and at the same time in a larger pool of interneurons (Tierney et al., 2004). Thanks to the temporal properties of PFC inhibitory interneuron responses, such as a smaller latency (Dégenètais et al., 2003) and a shorter action potential duration (Tierney et al., 2004), these interneurons can exert an efficient control over the time window of EPSP summation in pyramidal cells. The pyramidal neurons would then have a role of coincident detector (König et al., 1996). Thus the feedforward inhibition may take part in the synchronization of pyramidal cell networks within the PFC and between the HP and the PFC in the theta band (Jones and Wilson, 2005a,b; Hyman et al., 2005; Siapas et al., 2005; Tsujimoto et al., 2006).

Combined influence of HP and amygdala on PFC. The amygdala, through its projections to the PFC and the striatum, is also partially involved in the cortico-

basal loops (Mcdonald, 1991; Heidbreder and Groenewegen, 2003). Interestingly, neurons in the hippocampal formation (including the entorhinal cortex) send axons at the same time to the PFC (PL area) and to the amygdala (BLA nuclei) (Ishikawa and Nakamura, 2006; McDonald and Mascagni, 1997). Moreover, BLA and HP project in the PL with overlapping synapses, which induces multimodal responses in PL pyramidal cells: coincident HP and amygdala inputs produced an increase of discharge, whereas temporally disjoint inputs (e.g. 20-40 msec) generated an inhibitory effect (Ishikawa and Nakamura, 2003). Taken together, all these data suggest a strong interaction between the HP, the amygdala and the PFC. The latter may integrate motivational or emotional information from the amygdala with contextual information from the HP within a short time windows (coincident detection).

Modulation of the HP-PFC pathway through the striatum and dopamine neurons. One particular aspect of these loops is to be able to modulate the HP-PFC pathway (Fig. 2.11; Thierry et al., 2000). Via the "core" of the nucleus accumbens, to the substantia nigra pars reticulata projections, to the thalamus and then to the PFC, the PFC can modulate the excitability of its neurons (Fig. 2.11A). Interestingly, the CA1/subiculum sends an excitatory input to PL/MO neurons identified as projecting to the "core" of the nucleus accumbens. This hippocampal excitatory influence on PL/MO neurons innervating the "core" could thus lead to an activation of the related basal ganglia-thalamo-cortical loop circuits, which in turn modulate the excitability of prefrontal neurons and, consequently, the influence of the direct hippocampo-prefrontal pathway. The CA1/subiculum may also modulate the excitability of prefrontal cortical neurons through the indirect "shell"-ventral palladium medial-thalamocortical circuit (Fig. 2.11B).

Through direct and indirect pathways, the prefrontal cortex and the hippocampus may modulate the activity of mesencephalic ascending dopaminergic systems (Fig. 2.11B; Thierry et al., 2000). Through its direct excitatory inputs to dopamine cells in the VTA, the prefrontal cortex can contribute to the activation of some dopaminergic ascending neurons and therefore to the level of dopaminergic transmission in their target structures. The VTA/SNC complex does not receive a direct input from the CA1/subiculum; however, via the hippocampal projections to the "shell," the CA1/subiculum can indirectly modulate the activity of ascending dopaminergic neurons. In turn, dopamine transmission in the prefrontal cortex

interferes with hippocampal inputs (Thierry et al., 2000). Studies have shown that dopamine and hippocampal terminals are frequently in direct apposition to one another in the PFC, although they do not establish synaptic contacts onto common dendritic spines (Carr and Sesack, 1996). A functional interaction between the mesocortical dopamine system and hippocampal inputs has been shown, using an electrophysiological approach: a blockade of excitatory responses evoked in prefrontal neurons by hippocampal stimulation is observed following activation of the mesocortical dopamine system (Jay et al., 1995b).

In conclusion, the existence of direct connections between the hippocampus, the prefrontal cortex, and the nucleus accumbens, as well as the existence of reentrant circuits involving the nucleus accumbens and directed to the prefrontal cortex, suggest that these structures operate as an integrated unit. Dopamine ascending systems which innervate these structures may modulate or "gate" information processing at different levels of these circuits. In particular, it has been shown that tonic and phasic DA release selectively modulates hippocampal and prefrontal cortical inputs in the striatum through D1 and D2 receptors (Goto and Grace, 2005). Moreover, Goto and Grace (2008) showed that, depending on the dopamine receptors activation, PFC either incorporates retrospective information processed by the hippocampus (D1 activation) or processes its own information to effect preparation of future actions (D2 activation).

Plasticity and neuromodulation of the HP-PFC pathway. It is known now that hippocampal to prefrontal cortex synapses are modifiable synapses and can express different forms of plasticity, including long-term potentiation (LTP) and long-term depression (LTD) (see Laroche et al., 2000 for a review, see also Otani, 2003 for LTP/LTD induction in PFC slices in vitro). The first evidence for long-lasting neuronal plasticity of hippocampal to prefrontal cortex synapses came from studies showing that high-frequency tetanic stimulation of the hippocampus in the anesthetized rat induces a rapid and stable long-term potentiation (LTP) of the stimulated synapses in the prelimbic cortex (Laroche et al., 1990). In the awake, freely moving rat, LTP at the hippocampal to prelimbic cortex synapse results in an enduring increase in synaptic strength which persists for several days (Jay et al., 1996). In terms of the mechanisms of induction, the activation of the NMDA receptor is required for the induction of LTP in the hippocampo-prefrontal cortex pathway (Jay et al., 1995a). Additionally Dégenètais et al. (2003) showed

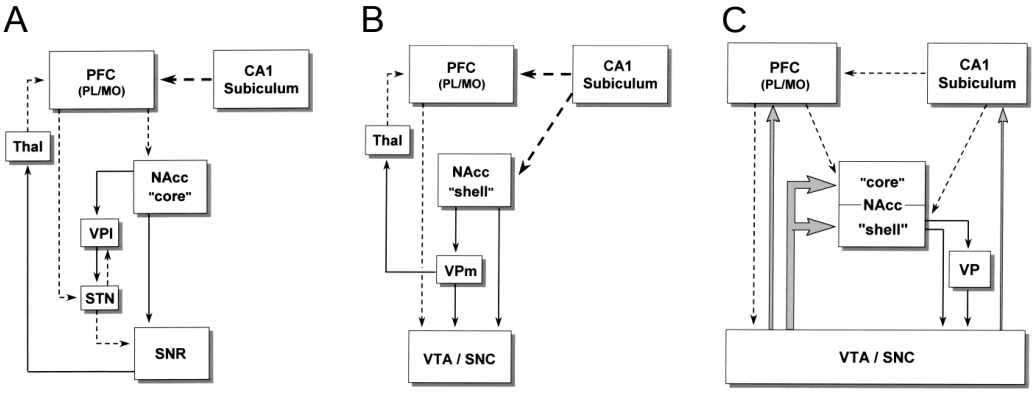

Figure 2.11: *Schematic representation of the relationships between the hippocampus, the prefrontal cortex, the nucleus accumbens, the thalamus, the dopamine neurons of the ventral tegmental area/substantia nigra complex from (Thierry et al., 2000).* **(A)** Prefrontal cortex-"core" and related basal ganglia circuits. **(B)** CA1/subiculum-"shell" and related circuits. **(C)** Dopaminergic circuits. Broken and solid lines represent glutamatergic and GABAergic pathways, respectively. Grey lines represent the dopaminergic pathways. NAcc, nucleus accumbens; PL/ MO, prelimbic/medial orbital areas; SNC, substantia nigra pars compacta; SNR, substantia nigra pars reticulata; STN, subthalamic nucleus; Thal, thalamus; VP(m/l), ventral pallidum (medial/lateral); VTA, ventral tegmental area.

tetanic stimulation of the hippocampus produced long-term potentiation of the monosynaptic EPSPs as well as IPSPs.

The mechanisms that lead to this plasticity are complexes because they involve the emotional state of the animal (e.g., its stress level; Jay et al., 2004) and neuromodulatory effects (e.g., dopamine; (Laroche et al., 2000; Jay et al., 2004). Indeed, Gurden et al. (1999) showed that the integrity of the mesocortical dopaminergic system was important for long-term potentiation to occur in the hippocampal-prefrontal cortex pathway (with a particular role of phasic dopamine release). In a second experiment, these authors also demonstrated that D1 but not D2 receptors are crucial for the DA control of the NMDA receptor-mediated synaptic plasticity for the HP-PFC pathway (Gurden et al., 2000). The complex aspect of dopamine modulation of plasticity was studied within PFC slice preparations: high-frequency stimulations of layer V pyramidal cells, which did not induced synaptic changes alone (Otani et al., 1998), induced LTD if dopamine was introduced at the same time as the stimulation, but LTP if dopamine was pre-introduced 12-40 min before (Matsuda et al., 2006) (see also Fig. A.4A about the influence of DA concentration on LTD/LTP). It is important to note that, in spite of its strong influence, dopamine is not the only neuromodulator involved in HP-PFC pathway plasticity: for example serotonin has also been pointed out (Ohashi et al., 2002).

Summary

The PFC receives a vast range of information through its cortical and subcortical connections. In particular, it is interesting to note the variety and density of neuromodulator afferents, which may be implied strongly in the PFC processing (Cardinal, 2006; Doya, 2008). The dorsal part of the PFC receives projections mainly from sensorimotor and association cortical areas, whereas the ventral part is more connected with limbic structures. There is not an abrupt transition in the ventral/dorsal organization, and for example, Condé et al. (1995) suggested that the ACC may be an intermediate between the PL and the Fr2. Among the subpart of the PFC, the PL seems really important because of the high variety of its afferents, which is summarized by Vertes (2006) as the “PL circuit”: this brain area is ideally situated to integrate past and current contextual information (hippocampus), their related emotional and reward values (BLA/MD/VTA) so that the

best decision can be made. A columnar view of afferent and efferent projections is presented on Fig. 2.12 (see also A.3 for efferent projections). Afferent connections tend to reach supragranular as well as infragranular layers. However, efferent projections to subcortical structures appear stronger from the deep layers.

2.3 Conclusion

The high variety of afferents to both the hippocampus and the prefrontal cortex indicates that these brain structures have an important integrative function. In particular, the anatomo-functional properties of the PFC seem appropriate to encode multimodal contextual memories that are not merely based on spatial correlates. The PFC receives direct projections from sub-cortical structures (e.g., the hippocampus, Jay and Witter, 1991; the thalamus, Vertes, 2006; the amygdala, Kita and Kitai, 1990; and the ventral tegmental area, Thierry et al., 1973), and indirect connections from the basal ganglia through the basal ganglia - thalamocortical loops (Uylings et al., 2003). These projections convey multidimensional information onto the PFC, including (but not limited to) emotional and motivational inputs (Aggleton, 1992), reward-dependent modulation (Schultz, 1998), and action-related signals (Uylings et al., 2003). The PFC seems then well suited to process manifold spatial information.

The presence of loops of connectivity within these structures and with other brain area suggests that their processing should be highly dynamical, thus integrating a temporal component. It should be noted that each subparts of the hippocampus and of the prefrontal cortex has different afferent and efferent connectivity patterns, which may underlie a functional or sensory segregation. A neural pathway that may be important for spatial cognition is the direct projections from the hippocampus to the prefrontal cortex. These connections may convey spatial or contextual information between the structures. Finally, a columnar organization of the PFC, similarly to other neocortical areas, can subserve important cortical computations. The model presented in Part III accounts for some of these properties: direct projections from the hippocampus to the prefrontal cortex conveying spatial information, integration of a motivational signal within the PFC (which may come from the amygdala or dopaminergic neurons, for example) and a columnar organization subserving spatial learning and planning processes.

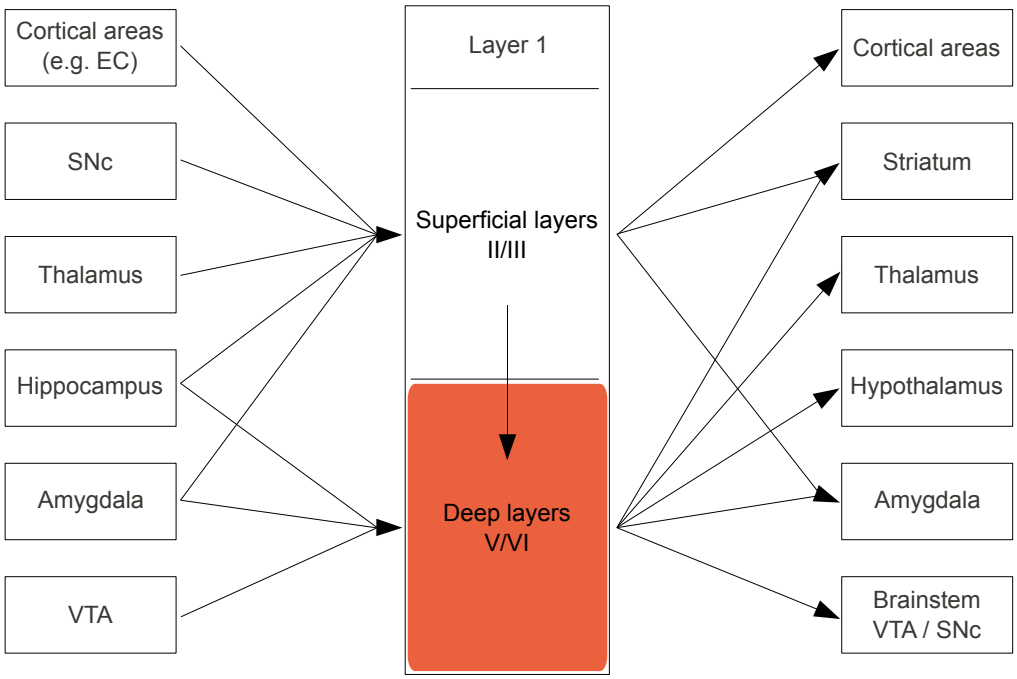

Figure 2.12: *Summary of afferent and efferent connections of a PFC minicolumn.* Arrows represent excitatory projections. Note that only a relevant subset of connections is represented on this figure. Moreover subparts of the PFC (in particular ventral and dorsal parts) have slightly different patterns of afferent and efferent connections, which is not showed here.

In the next chapter we review neurophysiological and behavioral data about the hippocampus and the prefrontal cortex to underline functional differences between these structures in spatial learning.

Chapter 3

Role of hippocampus and prefrontal cortex in navigation planning

Spatial navigation planning involves at least two main components (Poucet et al., 2004). The two first important abilities are to be able to represent places visited by the animal as well as one or more goals. The third component can be defined as the temporal organization of the behavior. In this chapter, we will discuss some potential similarities and differences of hippocampal and prefrontal involvements for these functions. Data from electrophysiological recordings, brain imageries and anatomical lesions will be used to illustrate our review. Some data presented in this chapter will also be related to human and non-human primates. Indeed, hippocampus and prefrontal have been studied for a long time in these species, and because of the plausible functional homologies between primates and rats, it can thus help to clarify our discussion (Burgess et al., 2002; Granon and Poucet, 2000; Brown and Bowman, 2002; Uylings et al., 2003; Heidbreder and Groenewegen, 2003).

3.1 Representation of places and goals

3.1.1 Spatial representation

Hippocampal place cells

An extensive body of experimental work has investigated the neural bases of spatial learning capabilities. In particular, extracellular single-cell recordings have

largely focused on the properties of pyramidal neurones in the hippocampal formation, that we review in this section. This limbic region has been thought to mediate spatial memory functions ever since location-sensitive cells, called *place cells*, were found in the hippocampus of freely moving rats (O'Keefe and Dostrovsky, 1971; see also place cell recordings in humans Ekstrom et al., 2003). A typical hippocampal place cell discharges strongly when the animal crosses a cell-specific region of the environment, the *place field* of the cell, and is usually silent elsewhere in the environment (Morris et al., 1982) (Fig. 3.1). The place cell population represents a large part of the hippocampal cells, estimated between 40 and 70 % over 1000000 neurons (Muller et al., 2001). These place cells can be found in the CA1 and CA3 subfields of the dorsal hippocampus (O'Keefe and Dostrovsky, 1971), as well as the ventral hippocampus (even if the spatial selectivity is coarser there, Poucet et al., 1994; Jung et al., 1994).

Place field properties. Several important properties of place fields can be pointed out (see Arleo and Gerstner, 2000; Hok, 2007; Alvernhe, 2010 for more details). In a small and simple open field environment, a typical place field can be approximated by a two-dimensional single-peak Gaussian surface (Muller et al., 1991; Burgess et al., 1999). However, cells encoding peripheral locations show crescent-shaped fields hugging the arena walls (Muller et al., 1987). Place cells may also exhibit multi-peak fields within a single environment (O'Keefe and Conway, 1978), particularly in larger scale environments (Fenton et al., 2008; Henriksen et al., 2009). Kjelstrup et al. (2008) have recently shown a scale gradient of place fields when recording pyramidal neurones along the dorso-ventral axis of the hippocampus (the size of place fields varied from 50 cm to 10 m when rats were moving on an 18 m linear track). This gradient property may support the representation of spatial contexts at different scales, to adapt the spatial code to the size and/or the complexity of the environment.

As the animal experiences several times a route, CA1 cells tend to asymmetrically expand their (initially symmetric) field and to shift their field center backwards with respect to the rat's direction of motion (Mehta et al., 1997; Mehta, 2000). Such an asymmetric expansion property does not persist across different environments and across different sessions in the same apparatus. Additionally, whereas place cells have non-directional place fields (i.e., their firing activity does not depend on head direction) when the animal randomly moves over two-

dimensional open environments, they may have directional place fields when the rat moves along fixed trajectories along a corridor or in an openfield (e.g., Muller et al., 1994; Markus et al., 1995). Finally, establishing a place field representation in a novel environment takes a relatively short time from a few minutes to 30 minutes (Austin et al., 1993; Wilson and McNaughton, 1993), with a difference between CA1 and CA3 place cells (Lee et al., 2004).

A dense population code. It is important to note that hippocampal spatial code is a population code. Place fields are generally a few times larger than the animal's size (Burgess et al., 1999), which do not provide a precise single-cell coding. Also, the activity of individual place cells can be extremely variable from one run through the firing field to another, a phenomenon referred to as *overdispersion* (Fenton and Muller, 1998). However, the proportion of active and location-selective pyramidal cells in the CA1 subfield in a given environment is very large, about $30-40$ % (Wilson and McNaughton, 1993). This results in highly overlapping place fields, uniformly distributed over the environment (O'Keefe and Conway, 1978; Thompson and Best, 1989), which is usually referred to as a *dense* spatial representation (Willmore and Tolhurst, 2001). As a consequence, accurate space decoding may be achieved by taking into account the ensemble, rather than single-cell, firing activity (Muller et al., 1987; Wilson and McNaughton, 1993; Brown et al., 1998). Two properties of the place cell population are also interesting to mention. First place cells are not topographically organized: two cells coding for neighboring locations do not seem to be anatomically adjacent (O'Keefe and Conway, 1978; Thompson and Best, 1989). Second the spatial relationships between place cells are not preserved across environments: two cells coding for neighboring locations in one environment may not code for neighboring locations in another environment (O'Keefe and Conway, 1978; Thompson and Best, 1989).

A temporal code: theta rhythm and phase precession. The hippocampal electroencephalogram (EEG) exhibits a characteristic pattern depending on the animal's ongoing behavior. During locomotor activity (e.g., walking, running, swimming, jumping), exploration, strong attentional demand or paradoxical sleep (also called REM sleep, rapid eye movement sleep), the hippocampus is timed by a regular sinusoidal signal of $7-12\,Hz$ termed *theta rhythm* (Green and Arduini, 1954; Vanderwolf, 1969; Jouvet, 1969; Whishaw, 1972; Fox et al., 1986; O'Keefe and

Recce, 1993; Skaggs et al., 1996; Buzsáki, 1996). Colgin and Moser (2009) suggest that there may be multiple sources for this theta rhythm: locomotion-induced rhythm may originate from intrahippocampal networks, whereas rhythm observed during resting states may be initiated by the septum. Moreover, the frequency of the theta rhythm varies increases with the speed of the animal (Slawińska and Kasicki, 1998; Maurer et al., 2005).

The theta oscillation can be described as a cycle, with a phase varying during time between 0° and 360°. There exists a phase correlation between the theta rhythm and hippocampal place cell firing (O'Keefe and Recce, 1993; Skaggs et al., 1996). As the animal goes through the place field of a neuron on a linear path, the theta phase at which the neuron discharges shifts systematically: every time the rat enters the field, the neuron starts firing at the same phase late in the theta period. Then, as the animal runs through the field, the neuron tends to fire earlier and earlier in the theta cycle. This phase shift phenomenon is termed *phase precession*. Such a temporal firing property of a place cell provides more information than the solely firing rate: measuring the phase allows to estimate the position of the animal inside the place field of a cell (e.g., Jensen and Lisman, 2000). More precisely, in an open environment, the spiking activity during the early phase of the theta cycle seems to code for the position of the animal, while firings during the late phase represent the direction of travel of the current trajectory (not all available trajectories) (Huxter et al., 2008).

Main determinants of place cells activity. In order to understand the hippocampal place code, a large number of studies have described the relation between changes in the environment and potential changes in place cell activities (e.g., change of location, appearance or disappearance of place fields), a phenomenon called "remapping" (Muller et al., 1987). Remapping may take place between and within sessions in a given environment whenever the animal perceives a world which is no longer congruous with its internal spatial code (Knierim et al., 1995). We summarize here the main determinants of place cells activity (see Arleo and Gerstner, 2000; Hok, 2007; Alvernhe, 2010 for reviews). Hippocampal place fields strongly depend on distal visual cues (O'Keefe and Conway, 1978) but to a lower extent on local landmarks (Cressant et al., 1997; Lenck-Santini et al., 2005). Also, the more stable an allothetic cue is perceived by the animal, the higher its influence upon place cell dynamics (Knierim et al., 1995). The geome-

try of an environment, such as its scale (Muller and Kubie, 1987; Kjelstrup et al., 2008) and its shape (O'Keefe and Burgess, 1996), seems to influence hippocampal place cell activity directly. Despite their dependence on allothetic signals, place cells exhibit clean location selectivity even when external cues are absent (e.g. in darkness, Quirk et al., 1990) or ambiguous (e.g. symmetric environment, Sharp et al., 1990). This suggests that hippocampal cells are also influenced by idiothetic movement-related signals, such as vestibular as well as optical flow signals (Sharp et al., 1995). An interesting experience-dependent property is that place fields are influenced after learning by the introduction or removal of a barrier into the arena (Muller and Kubie, 1987; Rivard et al., 2004; Alvernhe et al., 2008, 2010). However, the influence of the barrier vanishes whenever its height is such that the animal's motion is not affected. This suggests that locomotion-related information is relevant for establishing and maintaining place fields.

Grid and head direction cells. It should be noted that place cells are not the only examples of neurons with particular discharges properties related to the spatial memory. Recent electrophysiological findings have brought evidence for a key contribution of the entorhinal cortex (within the hippocampal formation) to the spatial memory function (Hafting et al., 2005). Indeed, neurones in the medial entorhinal cortex have been found that exhibit spatially-selective discharges with multiple receptive fields (in contrast to most place cells) that cover the environment with regularly spaced hexagonal patterns. It has been suggested that these neurones, termed *grid cells*, could mediate the encoding of metric spatial information necessary for the path integration process (see McNaughton et al., 2006 for a review). Complementing the allocentric place responses of hippocampal neurones, *head direction cells* provide an allocentric representation of the orientation of the animal (see Wiener and Taube, 2005 for a review). The discharge of these neurones is highly correlated with the direction of the head of the animal in the azimuthal plane, regardless of the orientation of the head relative to the body, of the animal's ongoing behaviour and of its spatial location. Each head direction cell is selective for one specific 'preferred' direction, and the preferred directions of a population of head direction cells tend to be evenly distributed over 360 degrees.

A spatial code in the PFC?

Based on the anatomical evidence of projections from the HP to the PFC, researchers looked for neurons in the PFC whose discharges were correlated with the position of the animals. This gave rise to contrasted results. During random foraging behavior, these kind of discharges were hardly recorded (Poucet, 1997; Gemmell et al., 2002). Instead PFC neuron discharges were more correlated with food-searching or exploratory behavior. However, other studies described some place cell-like activities during navigation task (Jung et al., 1998; Pratt and Mizumori, 2001). More recently, Hok et al. (2005) recorded jointly neurons of the hippocampus and the prefrontal cortex of navigating rats (Fig. 3.2). They showed that hippocampal and prefrontal location-selective neurons had different distributions of place fields over the environment (homogeneous versus goal-centered distributions), and different sizes of place fields (smaller versus larger). These authors concluded that both hippocampus and prefrontal cortex may be involved in the representation of different spatial maps with small and coarser granularity, respectively. Several reasons may explain the lesser spatial selectivity of PFC neurons. The highly integrative function of this area (see its connectivity, Chap. 2.2.3, and the other electrophysiological recordings described in this chapter) may mask the spatial aspect of PFC neuron discharges. Another explanation could be that the PFC is involved in spatial coding in function of the requirement of the task: for example random search of food may not require a complex spatial representation.

3.1.2 Goal representation

Influence of goals on hippocampal place cell activities

The influence of goals on place cell activities remains controversial. When the animal switches from a random search of food to a goal-directed search in the same environment, approximately one third of the place fields move, appear, disappear, or acquire a new directionality (Markus et al., 1995). Several explanations are possible, one of which is that the position of goals influences the activity of place cells. Indeed, areas associated with fixed goals in a familiar environment are overrepresented by CA1 place cells (Breese et al., 1989; Hollup et al., 2001b). Similarly, in a radial maze task, some place cells stop discharging when visiting an arm for the second time (i.e. the food has already been eaten) (Hölscher et al.,

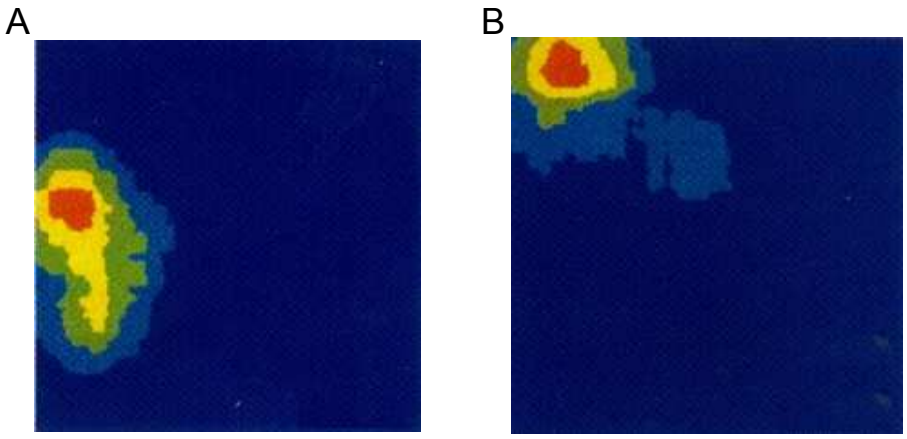

Figure 3.1: *Hippocampal place fields.* Two samples of CA3 (A) and CA1 (B) place fields recorded from a freely-moving rat in a square arena. The red region indicates the area in which the cell is maximally responding. By contrast, when the animal is visiting a dark-blue region, the cell remains silent. Adapted from (O'Keefe and Burgess, 1996).

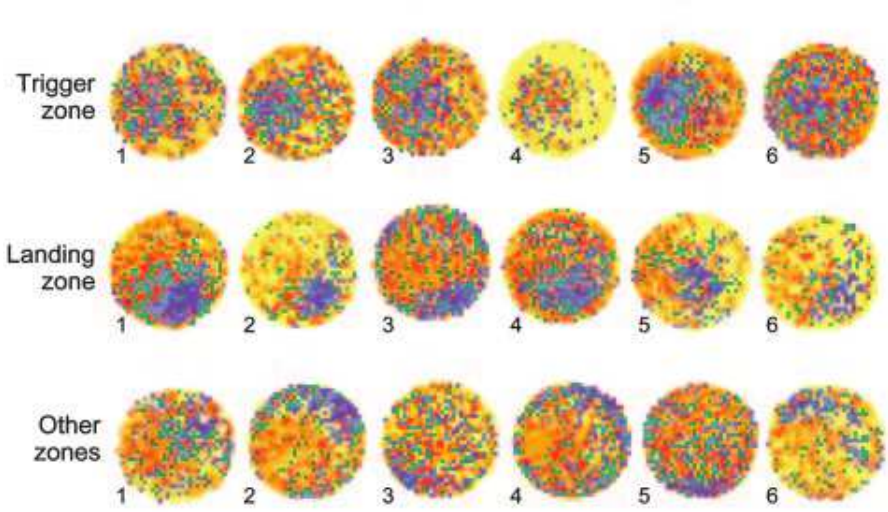

Figure 3.2: *Firing rate maps* of representative PFC cells with fields in trigger zone (where the animal waits for food, top row), landing zone (where the food falls, middle row), or other zones (bottom row). Each firing rate map was built by using the data from the entire recording session. In all maps, yellow indicates no firing and blue indicates maximum firing. The environment is a cylinder with a diameter of 76 cm. Adapted from (Hok et al., 2005).

2003). Changes in electrophysiological discharges related to the goal could be observed for about 10 to 20 % of recorded place cells.

However, other authors find no change in place cell activities following a goal shifting (Speakman and O'Keefe, 1990; Trullier et al., 1999; Lenck-Santini et al., 2001b) or a modulation of the goal value (Tabuchi et al., 2003). The reasons for these differences between studies are not well understood. Similarly, Hok et al. (2007) found no accumulation of place fields near the goal position in a spatial navigation task (see also Lenck-Santini et al., 2001a). However they observed for some cells a secondary extra-field activity at the goal site. This activity was associated with a slow theta rhythm, and not with sharp-waves/ripples events during which it is known that reactivation of sequences of place cells occur (see Sec. 3.2.2).

Goal coding in the PFC

The most consistent behavioral correlate identified for prefrontal cortex neurons was reward-related discharge. Similar to amygdala neurons, prefrontal neurons changed firing rates in anticipation of encounters with rewards of different magnitudes (Pratt and Mizumori, 2001, see also Watanabe, 1996 for primates). Neurons are also selective for the type of reward the animal receives (Miyazaki et al., 2004), and for a switch in action-outcome contingencies (Mulder et al., 2003; Kargo et al., 2007). As already mentioned, Hok et al. (2005) showed that a substantial proportion of PFC cells had place fields. In fact, the distribution of place fields was not homogeneous: goal locations were overrepresented. Because such locations were spatially dissociated from rewards in their protocol, they suggested that PFC neurons might be responsible for encoding the rat's goals (see also Feierstein et al., 2006).

These studies mainly targeted the PL and IL of the PFC. Even if it is still subject to debate, the different subparts of the PFC may be involved in different reward-related representations. In particular, the OFC may be responsible to encode the incentive value (a subjective value based on the internal states of the animal) of the reward in a common currency independent from its position, physical characteristics and related actions so that it can be compared with other rewards or to encode the amount of time before reward presentation reflecting the discounted value of the delayed reward (e.g. for data on primates see Tremblay

and Schultz, 1999; Roesch et al., 2006; Padoa-Schioppa and Assad, 2006). The ACC may represent action values in relation to the goal, the uncertainty of the reinforcement, the history of obtained rewards or prediction errors about the reward (see Rushworth et al., 2007; Rushworth, 2008 for reviews).

3.1.3 Hippocampo-frontal electrophysiological interactions

Influence of the hippocampus on prefrontal neurons

Neurons in the prefrontal cortex present a spatial-selective activity, when the animal is engaged in a navigation task. However the nature and the origins of this activity remain unclear. Anatomical evidence suggests a contribution of the hippocampus (see Sec. 2.2.3). To test this hypothesis, Burton et al. (2009) recorded PFC neuron activity in normal and hippocampal rats (lesion of the ventral hippocampus after learning) while the animals had to perform a navigation task. An important result is that neurons in the prefrontal cortex of lesioned animals still show a spatial-selective activity, and that this activity is present regardless of the position of the goal in the environment. Two main explanations can be proposed. It is possible that spatial-selective activity of prefrontal neurons originates from subicular afferents, consistently with the noisy spatial selectivity found in subicular neurons (Sharp and Green, 1994). The prefrontal spatial selectivity may also come from cortico-cortical afferents reinforced during learning and consolidation, leading to a weaker dependence on hippocampal inputs (see Sec. 3.3.4).

Several experimental works studied the timing relationships between neuronal activity in the prefrontal cortex and the hippocampal theta rhythm, showing that prefrontal neurons were phase locked to the hippocampal theta rhythm (Siapas et al., 2005; Hyman et al., 2005; Jones and Wilson, 2005b). In a spatial alternation task, Jones and Wilson (2005b) show an increase in phase coherence in the theta band of prefrontal and hippocampal local field potentials. This phenomenon appears to be present primarily when the animal must choose the correct arm to visit while it is in the central segment. Another result from the same experience shows that this phase coherence is accompanied by a phase precession of the prefrontal neuron activity in relation to the hippocampal theta rhythm (Jones and Wilson, 2005a). Besides the fact that this is an important result showing the existence of a phase precession outside the hippocampal formation, this phenomenon appears

only when the animal is at the end of the central segment, i.e. when it must make a choice to select the correct arm to visit. More recently, Benchenane et al. (2010) showed several effects of learning on theta oscillation coherence between HP and PFC, and on the reorganization of spike timing in PFC neurons. The functions of these synchronized activity remain to be fully elucidated, but it is suggested that phase synchronization could be a candidate for large-scale integration between brain areas, enabling the emergence of coherent behavior and cognition (Varela et al., 2001).

Influence of the prefrontal cortex on hippocampal place cells

An important issue is to understand to what extent the PFC exert a control on HP place cells. Kyd and Bilkey (2003) recorded the activity of hippocampal place cells of PFC lesioned rats, while the animals were randomly searching for food in their environment. Place cells recorded from prefrontal animals exhibited an increased information content and a lower overall firing rate compared to control animals. Place fields did not seem to have different sizes in lesioned rats, but were unstable over time. In a subsequent study (Kyd and Bilkey, 2005), these authors failed to find the same modulation of hippocampal activity. Nevertheless, it appears that electrophysiological characteristics of action potentials were altered: amplitude and width of these potentials were higher in injured animals, and there were a greater proportion of neurons discharging in bursts. In a second experiment of the same study, modulations observed following lesions of the PFC did not cause the same effects. In spite of the variability of these results, the authors identified a general trend for the implications of PFC lesions on hippocampal representation, a hypersensitivity of place cell activity in response to environmental proximal changes, that may be seen as a lack of attention control. More recently, Hok (2007) re-examined the PFC influence on HP cells. The inactivation of PFC caused an overall increase of hippocampal network activity. The modulation of place cell activity was related to an increase of the maximum intra-field firing frequency (i.e. the alteration was highly spatially focused). Place field size was increased, but the information content remained unchanged. Moreover, the extra-field goal-related activity recorded at the goal position (Hok et al., 2007) was not changed, indicating that the hippocampus received goal information from other afferents.

3.2 Retrospective and prospective coding, sequence representation

The third component of an affective planning system is the ability to predict the consequence of its actions in order to evaluate the possible alternatives. This involves past as well as possible future experiences. Hence, we present here data related to retrospective coding (i.e. neural discharges influenced by past events and actions) and prospective coding (i.e. neural discharges influenced by future events and actions). Then we describe correlates of sequence representations, which could be used to organize retrospective and prospective events.

3.2.1 Retrospective and prospective coding

Hippocampal place cells

The influence of the past or the future on place cell activity is visible in spatial alternation tasks (in which the goal position alternates between trials or between blocks of trials). In these experiments, CA1 place cells can indeed discharge at different frequencies and / or positions on the same section of the maze, depending on where the animal comes (retrospective coding) and / or according to where it goes (prospective coding) (Frank et al., 2000; Wood et al., 2000; Ferbinteanu and Shapiro, 2003; Bower et al., 2005; Dayawansa et al., 2006; Lee et al., 2006; Shapiro and Ferbinteanu, 2006; Ainge et al., 2007). Prospective or retrospective coding would affect one to two thirds of recorded place cells, and could be expressed simultaneously in the population.

However, the retrospective and prospective coding are hard to study. The content of these prospective / retrospective codes is still under debate: is it only composed by the start points and / or the goals? Does it encode trajectories ? Moreover, these codes can not be recorded everywhere in a maze. For example, when a pause is imposed to the animal at a given position (before an intersection or in a running wheel), these differential codes can only be recorded at this position (Ainge et al., 2007; Pastalkova et al., 2008). Also, prospective / retrospective codes can not be recorded in every protocols, e.g. in random exploration tasks (Smith and Mizumori, 2006) and in an alternation task with a unique goal at a fixed position (Lenck-Santini et al., 2001b; Bower et al., 2005). Finally, the main

studies have recorded CA1 neurons, hence little is known about similar discharge properties for CA3 neurons.

Prefrontal neurons

The discovery that a large number of prefrontal cortex neurons increase their rate of firing preferentially during the delay period in a variety of delay tasks, that they display sustained discharges during the length of the delay (except in the absence of a mnemonic load), and that failure of these neurons to maintain their activity during the delay is associated with errors in performance, has formed the basis of a neurobiological theory of *working memory* where the delay-related firing of cortical neurons is an essential mechanism for holding information on line for the time necessary to organize behavior (e.g. Batuev et al., 1990 for rats; Fuster and Alexander, 1971 for primates; see reviews in (Fuster, 1993, 1984, 2001; Goldman-Rakic, 1987)). We will not discuss here the vast literature about delay activity in the PFC, but only the fact that this activity may be related to a retrospective and / or prospective coding. To test this hypothesis, Baeg et al. (2003) have recorded simultaneously prefrontal neurons in rats solving a spatial alternation task in 8-shaped maze. Their recordings show that both retrospective and prospective coding could be observed within the prefrontal neural population. The strength of these codes was more and more important as rats learned the task: the correlation of neural discharges with past and future goals increased as well as the size of the area where these differential codings could be recorded. These results are consistent with other studies that suggested transformation from retrospective to prospective coding across the delay period in primate PFC (Rainer et al., 1999; Hoshi et al., 2000; Takeda and Funahashi, 2002).

3.2.2 Representation of sequences

Hippocampal place cells

Phase precession and sequence coding. An important consequence of the phase precession phenomenon is that cells with spatially neighboring place fields will fire at close phases of the theta cycle. When the animal is about to exit the place field of a cell and at the same time is entering an overlapping place field of a second cell, the first cell will fire few milliseconds before the second cell. Thus,

the sequence of place fields crossed by the animal can lead, within each theta cycle, to an orderly and sequential activation of place cells associated with these fields (Dragoi and Buzsáki, 2006; Foster and Wilson, 2007; Lisman and Redish, 2009). Theoretical studies have suggested that phase precession and sequential activation of place cells could be explained by the potentiation of asymmetric connexions between sequentially visited place cells (Jensen and Lisman, 1996; Tsodyks et al., 1996). However they are challenged by the fact that NMDA receptor blockade does not abolish phase precession (Ekstrom et al., 2001). Maurer and McNaughton (2007) have proposed that this hippocampal phase precession may be caused mainly by entorhinal afferent connexions (as suggested by O'Keefe and Recce 1993), plus an amplification through synaptic potentiation between place cells.

Usually, phase precession affects place cells activated by the presence of the animal in their firing field (or near the center of their field). However, Johnson and Redish (2007) observed place cell activations (and phase precession) outside of their firing fields, particularly when the animal makes micro-choices by orienting its head to the different possible pathways. The authors also showed that the sequence of activated place cells was correlated with the direction of the animal's head (and so with the prediction of places that can be visited in close future), but does not predict the final choice of the animal. This is consistent with extra-field sequential activities recorded in place cells of rats running in a wheel at the decision point of a maze (Pastalkova et al., 2008). These sequences of activations are one more example of activation of place cells outside their firing fields, in addition to goal-related activations (see Sec. 3.1.2).

Sharp waves/ripples et sequence reactivations. During sleep, or during some waking states, the hippocampal EEG shows a pattern of irregular slow waves. This pattern is occasionally interrupted by large oscillations called sharp waves (Buzsáki, 1986). These events are associated with bursts of spike activity, lasting 50–120 msec, in pyramidal cells of CA3 and CA1. They are also associated with short-lasting high-frequency EEG oscillations called *ripples*, with frequencies in the range 150–200 Hz in rats. Sharp waves/ripples (SWRs) are most frequent during sleep, when they occur at an average rate around 1 per second (in rats), but in a very irregular temporal pattern. SWRs can be observed during waking states, when the animal is still or not exploring (grooming, eating or drinking).

Some SWRs have also been recorded during exploratory activity in an open field, interrupting the theta rhythm (O'Neill et al., 2006; Csicsvari et al., 2007).

As during theta oscillations, sequences of activation of place cells, called *re-activations* or *replays*, appear during SWRs, but in a compressed manner (15-20 times faster than the average actual speed of animals), during slow wave sleep (Wilson and McNaughton, 1994; Skaggs and McNaughton, 1996; Lee and Wilson, 2002; O'Neill et al., 2008) or awake states (Foster and Wilson, 2006; O'Neill et al., 2006; Csicsvari et al., 2007; Diba and Buzsáki, 2007; Davidson et al., 2009; Karlsson and Frank, 2009; Gupta et al., 2010). Moreover, the sequences of activation of place cells occurring during SWRs can be replayed in reverse order (*reverse replay*) or in the same order as actually experienced (*forward replay*). Reverse replays have been observed only during wakefulness, while forward replays have been observed during slow wave sleep and or wakefulness (Skaggs and McNaughton, 1996; Lee and Wilson, 2002; Foster and Wilson, 2006; Diba and Buzsáki, 2007). Note that temporally structured replay of awake hippocampal ensemble activity has also been recorded during rapid eye movement sleep, with the particular property that the sequences were not compressed (Louie and Wilson, 2001).

Reactivations (reverse or forward) may represent trajectories towards or away from the current position of the awake and still animal (Davidson et al., 2009; Gupta et al., 2010). Davidson et al. (2009) also showed that the reactivated sequences can be long (corresponding to distances over 10 meters in their experiment). In that case, the sequences may be replayed through several successive SWRs instead of a single SWR. During exploratory behaviors however, it seems that the reactivation is limited to place cells activated by the presence of the animal in their firing fields (O'Neill et al., 2006; Csicsvari et al., 2007).

Studies show that cells representing areas associated with reward tend to be reactivated during SWRs more often than other cell (Singer and Frank, 2009). Some authors also show that the more frequently coactivated are place cells during exploration, the more they will be co-active during the subsequent SWRs, especially in a new environment or context (Foster and Wilson, 2006; O'Neill et al., 2008). Other authors show instead that, in familiar surroundings, place cells whose place fields were sampled more often by animals are not reactivated more often than others during awake SWRs (Gupta et al., 2010). In fact, these different

results suggest that the phenomenon of reactivation during SWRs is adapted to the mnemonic needs of the animal, according to the task, the degree of novelty, the experience, the attentional demand, ... Finally, it is important to note that, at least in some cases, reactivation of sequences never experienced by the animal seem to occur (Gupta et al., 2010). If this last result, which has been observed to date in only one rat, was confirmed in future studies, it would show that the nervous system of rats (and in particular the hippocampus) can actually infer new paths, consistently with the theory of cognitive maps (Tolman, 1948; O'Keefe and Nadel, 1978), and in agreement with the predictions of the model of Molter et al. (2007).

Prefrontal neurons

Sequence coding by prefrontal neuron activity has been less studied for rats. The characteristic delay activity of PFC neurons (Batuev et al., 1990; Baeg et al., 2003) has been seen as a support to link temporally separated events into behavioral sequences, similarly to primates (Fuster, 2001). Consistently, forward replays of recent memory sequences were recorded in prefrontal cortex during sleep (Euston et al., 2007). Using an experimental procedure similar to Bower et al. (2005), Euston and McNaughton (2006) tried to invalidate this sequence coding hypothesis. All observed modulations of activity during their sequential task could merely be explained by behavioral variability instead of sequence representation. It is possible that the complexity of the task was not sufficient to involve an active contribution of the PFC, but this experiment indicates that the role of rat PFC neuronal activity in sequence coding has still to be clearly demonstrated. The remaining part of this section will be dedicated to prefrontal neuron discharges in primate, because of the higher number of available studies.

Prefrontal cortical neurons show correlates with the temporal organization of action sequences (Procyk et al., 2000; Tanji and Hoshi, 2001; Averbeck et al., 2002; Mushiake et al., 2006; Shima et al., 2007). Several types of information can be encoded by single neurons, from the simple position of an action in the sequence (Averbeck et al., 2003a), to a whole sequence (Averbeck et al., 2006) and to an abstract category of sequences (e.g. given two actions A and B, AABA = BBAB = twice the same action then the other action then the first action) (Shima et al., 2007). Fujii and Graybiel (2003) have shown that macaques prefrontal

neurons exhibited a phasic activity at the beginning and at the end of the execution of a motor sequence, which could be seen as markers indicating the boundaries of a sequence.

Using a task of shape drawing requiring a sequence of movements (several segments needed to be drawn to form different objects such as a triangle, a square...), Averbeck et al. (2002) have showed that during the delay before the execution, the rank of the representation strength of a segment within the PFC population of neurons predicted the serial position of the segment in the motor sequence actually executed. In his theory of serial order in behavior, Lashley (1951) proposed that the neural representation of all serial elements should exist before acting starts. The results of Averbeck et al. (2002) are consistent with this proposal, particularly because errors in segment drawing was more likely to occur when the representations strength of a segment was weak. In two additional studies, the authors analyzed the contribution of single neurons and neural population to sequence coding (Averbeck et al., 2003a,b). Single neurons could encode the position of a segment, simultaneously with other characteristics such as the drawn shape, the length of the segment, ... (Averbeck et al., 2003a). Moreover, they showed that this code was distributed among the recorded population, with each neuron being broadly tuned to a preferred segment and similar ones (Averbeck et al., 2003b). Finally, the neural activity dynamically tracked the monkeys' uncertainty about the correct sequence of actions (Averbeck et al., 2006), and regardless of whether information was remembered correctly or incorrectly, the prefrontal activity veridically reflected the animal's action plan (Averbeck and Lee, 2007).

Prefrontal neuronal activity was also examined in primate performing a task of path planning in a virtual maze simulated on a computer (Saito et al., 2005). During the delay period after the goal presentation, two types of activities have been identified: one representing the next targeted position in the maze, whereas the other represented the position of the final goal. It is important to note that none of these activities reflected motor responses, which would suggest a role of PFC in sequential behavior organization directed toward a goal, rather than in the sensorimotor transformations. In a subsequent study, Mushiake et al. (2006) extended their results: PFC neurons reflected each position to be visited (not just the first and last position), but not the arm movements controlling the position

on the screen (as opposed to the activity of neurons in primary motor cortex) supporting the role of PFC in planning future events. The authors proposed that the monkeys were engaged in planning the sequence of positions in a retrograde order (starting from the last motion to capture the goal), in conjunction with a sequence planning with an anterograde order (Mushiake et al., 2006).

3.3 Relations to navigation planning behavior

Hippocampus and prefrontal cortex are both involved in numerous functions subserving behavior. Here we focus on their functional involvement in planning-related processes, i.e. spatial and goal-related processing, temporal organization of behavior, cost-benefit decision making, and the influence of memory consolidation on the HP-PFC pathway function. More general consideration will be discussed in the concluding section of this chapter (Sec. 3.4).

3.3.1 Spatial and goal-related processing

It is tempting to propose that hippocampal *place cells* form a spatial representation in allocentric (i.e., world centered) coordinates, thus providing a cognitive map to support flexible navigation (O'Keefe and Nadel, 1978). In accordance, lesion data studies have indicated that the hippocampal formation seemed necessary for spatial navigation (see Poucet, 1993; Poucet and Benhamou, 1997 for reviews), for example in the classical task of the Morris water maze (Morris et al., 1982, 1990; Sutherland et al., 1983; Sutherland and Rodriguez, 1989; Eichenbaum et al., 1990; Whishaw and Jarrard, 1995; Bannerman et al., 1999; Steele and Morris, 1999) and in tasks based on the localization according to the geometrical organization of beacons or walls (McGregor et al., 2004; Rondi-Reig et al., 2006). Moreover, Hollup et al. (2001a) showed that an intact hippocampus was necessary to recognize the goal location, indicating that this structure is involved in the distributed network of brain structures coding for the goal.

It seems also that spatial processing are more related to the dorsal hippocampus than to the ventral, which may be also involved in the resolution of conflicts based on fear or anxiety (Moser et al., 1993; Hock and Bunsey, 1998; Bannerman et al., 1999; Trivedi and Coover, 2004). Moreover, selective lesions have targeted subfields (dentate gyrus, CA1, CA3) of the hippocampus to gain insights

on their relative contribution in fast learning, pattern completion and separation... (e.g., Gilbert et al., 2001; Nakazawa et al., 2003; Gold and Kesner, 2005; see also Alvernhe, 2010 for a short review).

On the other hand, the involvement of the PFC in spatial coding seems to depend on the requirements and the complexity of the task. Lesion studies tend to corroborate this hypothesis. Rats with PFC lesions are neither impaired in spatial learning of a simple navigation task (De Bruin et al., 1994; Granon and Poucet, 1995; Ragozzino et al., 1999; Delatour and Gisquet-Verrier, 2000), nor in spatial discrimination (Hannesson et al., 2004). However, permanent prefrontal cortical lesions in rats result in reliable deficits on tasks that require the flexible use of location information related to the current position or the goal position (Poucet and Herrmann, 1990; Granon et al., 1996; Gemmell and O'Mara, 1999). Thus, the PFC seems to be involved in spatial tasks only if complex cognitive processing are needed. For example, Granon and Poucet (1995) have showed that frontal animals are impaired only for the most complex version of a navigation task in a morris water maze, when animals have to reach a platform from four different starting points. Functional dissociations should also be made between subparts of the PFC. Heidbreder and Groenewegen (2003) reviewed evidence for a dissociation between ventral and dorsal PFC for spatial processing. For example, the dorsal PFC seems more involved in the egocentric component of spatial learning (Kesner et al., 1989; King and Corwin, 1992; De Bruin et al., 1997), while lesions of the ventral PFC produces deficits in allocentric but not egocentric spatial tasks (Corwin et al., 1994).

In humans, damages to the medial temporal lobe (and in particular to the hippocampus, e.g. bilateral temporal lobectomy patient H.M. or degenerative temporal lobe pathologies such as Alzheimer's disease) produce anterograde and retrograde memory deficits that tend to impair, among others, the ability to learn spatial navigation tasks (Eichenbaum, 2001). Neuroimaging experiments have provided support for this hippocampal function, showing for example that the right hippocampus appeared particularly involved in memory for locations within an environment (see Burgess et al., 2002 for a review). More recent neuroimaging studies provide new perspectives for the understanding of the global network interacting to promote spatial navigation (e.g., Spiers and Maguire, 2006, 2007a,b; Spiers, 2008). These authors used an accurate virtual reality environment repre-

senting the London city, where taxi drivers had to take customers to the destination of their choices. Imaging results revealed complex dynamics comprising focal and distributed, transient and sustained brain activity across several brain areas including the hippocampus and the prefrontal cortex (Spiers and Maguire, 2006). One important finding was the important involvement of the PFC in goal representation, in particular the distance to the goal (Spiers and Maguire, 2007a; Spiers, 2008). Recent data from a patient with PFC lesion strongly support this role (Ciaramelli, 2008).

3.3.2 Temporal organization of behavior

The rat hippocampal formation would participate to the learning or recall of sequences of spatio-motor responses (Rondi-Reig et al., 2006), non-spatial sequences (Rondi-Reig et al., 2001; Kesner et al., 2002; Fortin et al., 2002; Agster et al., 2002), and would be particularly necessary when a delay is imposed between the presentations of information to be linked (Huerta et al., 2000; Lee and Kesner, 2003; Lee et al., 2005; Farovik et al., 2010).

In humans, monkeys and rats, prefrontal damage results in impaired temporal structuring (i.e. sequencing) of information and mediation of prospective codes – that is, in the use of past experiences to set up expectancies and anticipations (e.g., Semmes et al., 1963; Pohl, 1973; Petrides and Milner, 1982; Kesner and Holbrook, 1987; Kesner, 1989; Shallice and Burgess, 1991; Mogensen and Holm, 1994; Granon and Poucet, 1995; Chiba et al., 1997; Hannesson et al., 2004; Gisquet-Verrier and Delatour, 2006). This in turn results in a reduced ability to plan complex sequences of behavior as a result of a failure to bridge temporally specific actions (Granon and Poucet, 1995; Fuster, 2001). Note that a ventral-dorsal PFC dissociation has been proposed for this function (see Heidbreder and Groenewegen, 2003 for a review).

Thanks to their driving task in a virtual environment, Spiers and Maguire (2006, 2007b) provide also further neuroimaging details on the distributed network mediating spatial route planning. Both hippocampus and prefrontal cortex were activated during route planning following a journey request from a customer. Interestingly, when subjects spontaneously decided to alter their route during navigation (e.g. because of blocked road), the hippocampus did not activate, but the prefrontal cortex was engaged. In fact, the hippocampus was not significantly

more active during any other aspect of navigation besides customer-driven route planning to new destinations, which is a very specific and temporally discrete role for the human hippocampus in real-world navigation. This result is consistent with the view that during goal-specified route planning, the hippocampus activates, or retrieves from elsewhere, the information relating to the relevant region of space to be navigated from a stored cognitive map of the environment. Throughout the subsequent navigation, the relevant allocentric spatial information is available to the hippocampus and other neural structures such as the PFC, and no increased processing demands are made of the hippocampus. Then, during spontaneous re-planning, the PFC uses the retrieved spatial information to organize the behavior in order to cope with the unpredicted events.

3.3.3 Cost-benefit decision making

As has been appreciated for many years in other behavioral sciences such as behavioral ecology and economics, animals, including humans, do not just make decisions and select actions on the basis of an expected reward but also weigh up the potential costs of the different courses of action that might be pursued (Stephens and Krebs, 1986). Such costs may involve the investment of time or effort, a willingness to tolerate a risk that a reward may not be forthcoming or to endure pain in the pursuit of a goal. This diminution of the value of a reward by the cost incurred to achieve it is known as discounting and has been shown consistently to influence the way in which animals and humans make choices (Stephens and Krebs, 1986). If we assume that the basic machinery of motivation is designed to bias animals towards courses of action that result in more certain, easily obtained and immediate reward, then the question arises of what mechanisms exist to resist such temptation when more taxing options may result in greater overall utility.

Using a cost-benefit T-maze paradigm, Walton et al. (2002) demonstrated that medial frontal cortex is essential for allowing an animal to put in extra work for greater reward (see Fig. 3.3A). Rats chose between investing effort by surmounting a large barrier to obtain a high reward (HR) or selecting a low reward (LR) which did not incur any additional response cost. Following lesions of this region, animals became profoundly cost averse, switching from selecting to climb the barrier for the HR on the majority of trials pre-surgery to choosing the more easily obtained LR option on almost all occasions. However, when the response

costs were equated by adding an identical barrier into the LR arm, meaning that the rats were now required to put in the same amount of effort to obtain either size of reward, all animals returned to choosing the HR. This implies that the deficit was not caused by any gross motor deficits or spatial impairments, but is instead primarily one concerned with making optimal decisions. Subsequent experiments have localized this effect to the ACC, not to the adjacent prelimbic cortex nor the OFC (Walton et al., 2003; Rudebeck et al., 2006). Interestingly, disruption of the amygdala-ACC pathway lead to the same pattern of behavior, suggesting that extended interconnected frontal-subcortical circuits are required in order to compare cost and benefit (Floresco and Ghods-Sharifi, 2007).

While OFC lesions did not make animals cost averse on the T-maze barrier task, several neuropsychological studies in humans and animals have implicated the OFC in mediating certain types of cost-benefit decision making, in particular in aspects of impulsivity and foresight (see Wallis, 2007 for a review). However, the results from studies of delay-based decision making in humans and rodents are similarly conflicting, with some showing an increase in impulsive choices following OFC lesions and other the opposite effect (see Dalley et al., 2004 for a review). All of these studies were performed in operant boxes, making tricky direct comparison with the effort-based decision making findings in the T-maze. To investigate this inconsistency, Rudebeck et al. (2006) also tested animals with lesions of the OFC on a T-maze *delay*-based decision making task where they could choose between a delayed HR or an immediately available LR option (see Fig. 3.3B). Prior to surgery, all animals preferred to wait for the HR. However, post-operatively, in contrast to the animals with ACC lesions, the OFC-lesioned rats became cost-averse, switching to the immediate LR option on the majority of trials. This was not caused by a general hyperactivity as the same animals showed no increase in spontaneous locomotor activity. Moreover, as with the ACC-lesioned animals on the T-maze barrier task, when the costs were equated by requiring the animals to wait for an identical amount of time for both the HR and LR options, the OFC group returned to choosing the HR. This again implies that the increase in impulsive choices was a consequence of an alteration in the way the costs and benefits of the options were processed rather than being a simple impairment in spatial or reward magnitude processing.

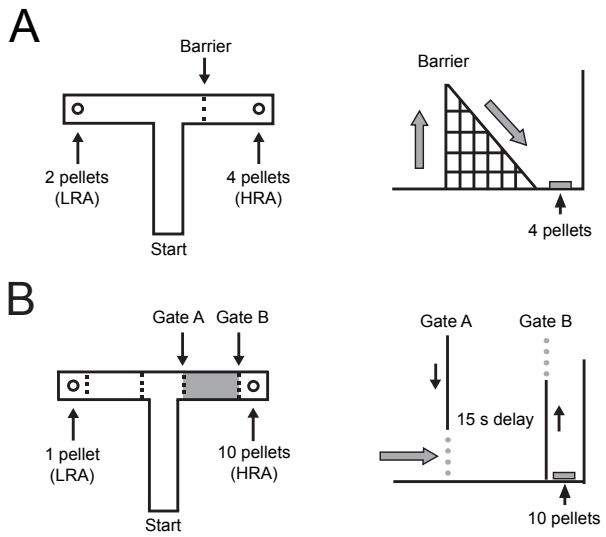

Figure 3.3: *Experimental apparatus from (Rudebeck et al., 2006).* **(A)** Effort-based decision-making test apparatus. Rats were placed in the start arm of the T-maze and allowed to choose between the two goal arms. If rats chose the HRA containing the wire mesh barrier, they had to climb over it to receive four food pellets. Choosing the LRA meant they could obtain two food pellets without climbing a barrier. The same task was used by Walton et al. (2002). **(B)** Delay-based decision-making apparatus. Rats were placed in the start arm and chose between the two goal arms. When rats entered one of the goal arms, Gate A was immediately inserted, keeping the rat in the goal arm. Gate B was then retracted after the required delay. Selecting the HRA initially led to ten food pellets after 15 s, whereas the LRA led to only one food pellet immediately.

3.3.4 Hippocampo-frontal functional interactions and memory consolidation

Hippocampo-frontal functional interactions

Although few studies have specifically addressed the issue of the role of the hippocampo-prefrontal cortex pathway, Floresco et al. (1997) showed that disconnection lesions produced by transient inactivation of the ventral CA1/subiculum and the contralateral prelimbic cortex produce a selective impairment of performance in the test phase of a spatial delayed nonmatching to position task in the radial-arm maze. A similar impairment was observed with bilateral inactivation of the CA1/subicular region, or the prelimbic cortex (Seamans et al., 1995). These data have strong implications that the hippocampal-prefrontal cortex connection is involved in a process through which recently acquired spatial information encoded in the hippocampus is used to organize responses in a prospective manner in the prefrontal cortex (Floresco et al., 1997), a conclusion that has also been reached after detailed analysis of the effects of prefrontal lesions in a variety of learning tasks (Delatour and Gisquet-Verrier, 1999; Gemmell and O'Mara, 1999). In a subsequent study, Seamans et al. (1998) showed that blockade of D1 receptors in the PFC resulted in the same behavioral patterns, indicating an important functional role of dopamine for the hippocampo-frontal pathway. Consistently, Goto and Grace (2008) recently showed that, depending on the dopamine receptors activation, PFC either incorporates retrospective information processed by the hippocampus or processes its own information to effect preparation of future actions.

The finding that synaptic depression of hippocampal-prefrontal cortex pathway occurs during the delay period of a delayed nonmatching-to-position task, and that the progress in learning is associated with the establishment of long-term depression (Burette et al., 2000), have intriguing implications for the concept of how cortical networks subserve the planning of responses. Depression of synaptic transmission observed during the spatial working memory task is functionally equivalent to a reduction in the potency of synaptic drive exerted by hippocampal inputs on prefrontal cortex neurons. A background reduction in synaptic efficacy between the hippocampus and the prefrontal cortex may in fact be a means for increasing signal-to-noise ratio for the transmission of pertinent signals, in particular

information stored in memory for example by low-resolution spatial information originating from neurons in the ventral hippocampus (Jung et al., 1994), and this could be mediated by potentiation of a subset of the population of input synapses against a background of reduced synaptic transmission.

Memory consolidation

Current theories concerning memory suggest that memories are initially encoded quickly in the hippocampus, as a simultaneous indexing of the different brain regions representing the lived experience (McClelland et al., 1995). Among these theories, the *classical theory of consolidation* suggests that the hippocampus transfers this learning progressively to the neocortex (including the PFC), by facilitating the development of some cortico-cortical connections (Marr, 1971; Squire et al., 1993; McClelland et al., 1995; Frankland and Bontempi, 2005). Once "copied" in the neocortex, the information would be less sensitive to hippocampal damage or neglect. Another theory, known as *multiple traces* suggests that the hippocampus and the neocortex do not underlie the same forms of memory, the former encoding *episodic* or *contextual* memory and the latter *schematic* or *semantic* memory (Nadel and Moscovitch, 2001; Moscovitch et al., 2006). Inspired by the two previous theories, the theory of mnemonic transformations suggests that episodic memory is always hippocampal-dependent, and that semantic / schematic memory results from a transformation of hippocampal episodic memory during its transfer to the neocortex (Winocur et al., 2010a). The theory of transformation proposes, unlike the classical theory of consolidation, that the same experience can be encoded simultaneously in both memory forms (episodic and semantic). The authors also suggest that a person may use one or other of these representations, and that this choice depends on a flexible mechanism potentially involving the PFC and the ACC (Frankland and Bontempi, 2005; Winocur et al., 2010a).

When it comes to information useful for navigation, such as topological representations, it becomes more difficult to distinguish between episodic (or contextual) memory and semantic (or conceptual, schematic) memory. Winocur et al. (2010b) lesioned partially the hippocampus of rats several weeks after they learned to navigate in a complex environment containing different goals at fixed positions. The lesioned animals continues to use distal information to find the

goals, but were impaired to find the best alternative route leading to the goal when a blocks was introduced in the maze.

The slow-wave sleep (see Sec. 3.2.2) would have an important role in exchange of information between hippocampus and neocortex (Marr, 1971; Buzsáki, 1986; McClelland et al., 1995), by replaying the neural patterns concerning previously acquired information (Wilson and McNaughton, 1994; Euston et al., 2007; O'Neill et al., 2008; Peyrache et al., 2009). This replay would induce a change in the neural substrate of memory traces and take part to memory consolidation. Consistently, animal performance drop during recall in hippocampo-dependent tasks if SWRs are blocked by electrical stimulation during the consolidation phase (after training) (Girardeau et al., 2009), suggesting that SWRs are likely vectors for hippocampal-neocortical information exchange (Buzsáki, 1989). Among the cortical areas, the PFC is often implicated in long-term memory consolidation (Frankland and Bontempi, 2005), particularly for hippocampal-dependent spatial and contextual information.

3.4 Conclusion

In this concluding section, we present our working hypotheses about the respective roles of the hippocampus and the prefrontal cortex in navigation planning. The model described in the next part is based on these hypotheses.

Hippocampal spatial-selective place/grid/head-direction cells are crucial components of the neural system subserving the spatial learning function. The spatially selective responses of hippocampal neurones might result from the projection of contextual (relational) memories onto the two-dimensional locomotion space of the animal. Therefore, several authors have postulated a role for the hippocampal formation in a larger class of memories, namely episodic memory, encoding context-dependent experienced events (e.g., Burgess et al., 2002; Fortin et al., 2002). However place cells spatial selectivity remains one of the main characteristics of the hippocampal code, and is a convenient paradigm to understand the role of the hippocampus in the learning of a cognitive representation (Poucet et al., 2004).

In order to perform flexible goal-directed navigation (e.g., to plan alternative pathways and/or shortcuts) two others mechanisms are necessary: goal representa-

tion, and reward-dependent navigation planning (Poucet et al., 2004). The encoding of a goal representation in the hippocampus is still under debate, because of conflicting evidence (e.g. Speakman and O'Keefe, 1990; Hok, 2007). Moreover, very few electrophysiological studies investigate the encoding of a topological map within the hippocampus, subserving spatial planning (e.g. Alvernhe et al., 2008, 2010). Phase precession, replay of experienced trajectories and recurrent dynamics generated by the CA3 collaterals may support the learning of behavioral sequences (i.e. routes), but it is not know whether these routes could be integrated into a topological map within the hippocampus (see Poucet et al., 2004 for a short review of hippocampal models based on this idea; Muller et al., 1996). On the other hand, the hippocampal space code is likely to be highly redundant and distributed (Wilson and McNaughton, 1993), which does not seem adequate for compact topological representations of highly-dimensional spatial contexts.

Our work relies on the hypothesis of a distributed spatial cognition system in which the hippocampal formation would contribute to navigation planning by conveying redundant spatial representations to higher associative areas, and a cortical network would elaborate more compact representations of the spatial context — accounting for motivation-dependent memories, action cost/risk constraints, and temporal sequences of goal-directed behavioral responses (Knierim, 2006; Spiers and Maguire, 2007b).

Among the cortical areas involved in map building and action planning, the prefrontal cortex is likely to play a central role. Indeed, prefrontal cortical neurons show correlates with the temporal organization of action sequence, as well as with the motivational values associated to spatiotemporal events (e.g. Averbeck et al., 2002; Hok et al., 2005). Anatomical PFC lesion and imagery studies support the general view that prefrontal cortex is responsible for the encoding retrospective and prospective memories, for the temporal organization of the behavior and more generally for cognitive control, that is to say, the ability to coordinate thoughts and actions in relation with internal goals (Miller and Cohen, 2001; Fuster, 2001; Koechlin et al., 2003).

How may location, goal and topological information be represented in a prefrontal neural population? How can this information be exploited to plan action sequences? These questions are addressed in the next chapter describing our model.

Part III

MODELING THE ROLE OF THE PREFRONTAL CORTEX FOR SPATIAL PLANNING

Chapter 4

A cortical column model for spatial learning and navigation planning

In this chapter, we introduce our model of spatial navigation planning based on the columnar organization of the PFC. The first four sections present an overview of the main bases of the main (topological learning, planning and multilevel mapping). The last section gives a lot of equations describing in details the internal mechanisms of the model.

4.1 Overview of the model

Figure 4.1A shows an overview of the model architecture based on the notion of cortical column organization. Cortical maps consist of local circuits —i.e. the cortical columns (Mountcastle, 1957)— that share common features in sensory, motor and associative areas, and thus reflect the modular nature of cortical organization and function (Mountcastle, 1997). Cortical columns can be divided in six main layers including: layer I, which mostly contains axons and dendrites; layers II-III, called *supragranular* layers, which are specialized in cortico-cortical connections to both adjacent and distant cortical zones; layer IV[1], which receives sensory inputs from sub-cortical structures (mainly the thalamus) or from columns of cortical areas involved in earlier stages of sensory processing; and layers V-VI, called *infragranular* layers, which send outputs to sub-cortical brain areas (e.g. to

[1] According to the cytoarchitectonic properties of the rat medial PFC (Uylings et al., 2003), no layer IV is considered in the model columns.

the striatum and the thalamus) regulating the ascending information flow through feedback connections. Neuroanatomical findings (see Mountcastle, 1997 for a review; see Gabbott and Bacon, 1996b; Gabbott et al., 2005 for anatomical data on rat PFC) suggest that columns can be further divided into several *minicolumns*, each of which consists of a population of interconnected neurons (Buxhoeveden and Casanova, 2002). Thus, a column can be seen as an ensemble of interrelated minicolumns receiving inputs from cortical and sub-cortical areas. It processes these afferent signals and projects the responses both within and outside the cortical network. This twofold columnar organization has been suggested to subserve efficient computation and information processing (Burnod, 1988; Mountcastle, 1997). Several models have been proposed to study the cortical columnar architecture, from early theories on cortical organization (Szentágothai, 1975; Eccles, 1981; Burnod, 1991) to recent computational approaches (e.g. the blue brain project; Markram, 2006). These models either provide a detailed description of the intrinsic organization of the column in relation to cythological properties and cell differentiation or focus on purely functional aspects of columnar operations.

The approach presented here attempts to relate the columnar organization to decision making and behavioral responses using a highly simplified neural architecture which does not account for cell diversity and biophysical properties of PFC neurons. As aforementioned, the underlying hypothesis is that the PFC network may mediate a sparsification of the hippocampal place (HP) representation to encode topological maps and subserve goal-directed action planning. As the simulated animal explores the environment, model HP cells become selective to allocentric positions through the integration of visual cues and path integration information (it is out of the scope of this paper to describe the HP cell model, see Arleo and Gerstner 2000; Arleo et al. 2004; Sheynikhovich et al. 2009 for detailed accounts). The model exploits the anatomical excitatory projections from hippocampus to PFC (Jay and Witter, 1991) to convey the redundant HP state-space representation S to the columnar PFC network, where a sparse state-action code $S \times A$ is learned. Within a column, each minicolumn becomes selective to a specific state-action pair $(s, a) \in S \times A$, with actions $a \in A$ representing allocentric motion directions to perform transitions between two states $s, s' \in S$. Each column is thus composed by a population of minicolumns that represent all the state-action pairs $(s, a_1 \cdots a_N) \in S \times A$ experienced by the animal at a location

s. This architecture is consistent with data showing that minicolumns inside a column have similar selectivity properties (Rao et al., 1999) and that some PFC units encode purely cue information while others respond to cue-response associations (Asaad et al., 1998).

The model employs the excitatory collaterals between minicolumns (Mountcastle, 1997; Lewis et al., 2002) to learn multilevel topological representations. Egocentric self-motion information (provided by proprioceptive inputs) biases the selectivity properties of a subpopulation of columns to capture morphological regularities of the environment. Unsupervised learning also modulates the recurrent projections between minicolumns to form forward and reverse associations between states. During planning, the spreading of a reward signal from the column selective for the goal through the entire network mediates the retrieval of goal-directed pathways. Then, a local competition between minicolumns allows the most appropriate goal-directed action to be inferred.

The following sections provide a functional description of the model columnar structure, connectivity and input-output functional properties. A more comprehensive account –including equations, parameter settings and explanatory figures– can be found in Supplementary Material Sec. 4.5.

4.2 Encoding topological maps by a network of columns

Every column in the model (Fig. 4.1B) has a highly simplified structure consisting of three units s, p, v and of a population of minicolumns, each of which is composed of two units q and d. The activity of each of these units (see Sec. 4.5) represents the mean firing rate of a population of pyramidal neurons either in supragranular layers II-III (p, v, q units) or in infragranular layers V-VI (s, d units).

As exploration proceeds, neurons s become selective to spatial locations and their population activity encodes compact state-space representations. Within each column one neuron v encodes goal information related to a specific state, whereas neurons q encode the relation between actions and goal. Neurones q and v back-propagate the goal signal through the cortical network and their discharge correlates to the distance to the goal. Neurones p forward-propagate the selected path signal (i.e. the planned trajectory) from a given position towards the goal.

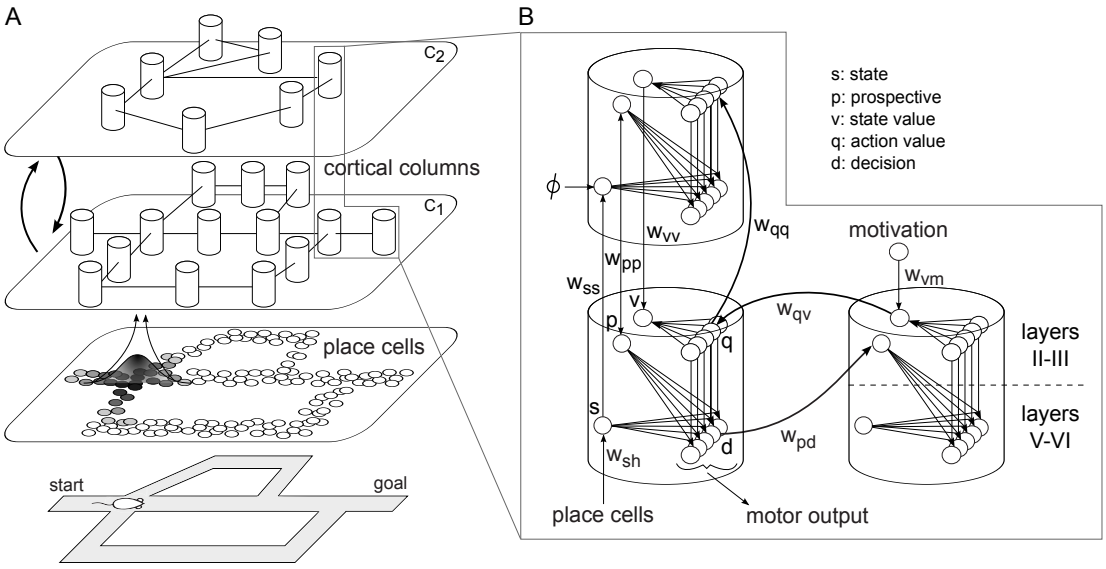

Figure 4.1: *Overview of the model architecture and connectivity.* **(A)** Model hippocampal place (HP) cells are selective to allocentrically-encoded positions. The prefrontal cortex (PFC) columnar network takes HP cell activities as input to learn a sparse state-action code $S \times A$ reflecting to topological organization of the environment. The model employs recurrent excitatory collaterals between minicolumns of two subpopulations (C_1 and C_2) to implement multilevel spatial processing capturing morphological regularities of the environment. **(B)** Each model column uses three units s, p, v and a population of minicolumns, each of which is composed of two units q and d. Neurons s receive inputs from HP cells through w_{sh} synapses to encode spatial locations. Forward and backward associations between locations are encoded by w_{pd} and w_{qv} connections, respectively, so that the minicolumn corresponding to the execution of an action in a given place is linked to the place visited after movement. The model uses a motivational signal conveyed by w_{vm} synapses to encode goal information. The population of neurons d projects to motor output, where ta winner-take-all competition takes place to select actions locally. Collateral projections between columns (w_{ss}, w_{pp}, w_{vv} and w_{qq}) together with a proprioceptive signal ϕ allow the model to implement multilevel spatial processing.

Neurones d integrate spatial and reward-related information and compete for local action selection. Their activity triggers a motor command tuned to a specific allocentric motion direction. Inter- and intra-column connectivity (Fig. 4.1B, see also Sec. 4.5) involves plastic and non-plastic projections, respectively, whose synaptic efficacies are modeled as scalar weight matrices $w \in [0, 1]$. Plastic synapses are randomly initialized to low efficacy values within $[0, 0.1]$, i.e. the cortical network starts with weak interconnectivity. As the simulated animal explores the environment, plastic projections are modified through unsupervised Hebbian learning to encode either states or forward and reverse associations between adjacent states (i.e. environment topology). For instance, whenever the simulated rat moves from one place to another, collateral projections w_{pd} and w_{qv} (Fig. 4.1B) are updated to reflect to connectedness between the two places.

4.3 Spatial planning through propagation of reward-dependent signals

The simulated animal behaves to either improve its representation or follow known goal-directed pathways (see Sec. 4.5). This exploration-exploitation trade off is governed by a simple stochastic policy (Arleo et al., 2004). During exploration, motivation-dependent signals modulate the activity of neurons v in layer II-III of the model (Fig. 4.1B), which allows specific columns to become selective to reward states. The reward-related signal transmitted by w^m projections simulates a physiological drive mediated by either dopaminergic neurons in the ventral tegmental area (Schultz, 1998) or the amygdala (Aggleton, 1992), both sending synapses to the prefrontal cortex (Uylings et al., 2003). An activation diffusion process (Burnod, 1991) supports the exploitation of topological information to retrieve optimal trajectories to the goal. The motivation signal elicits the activity of the v neuron in the column corresponding to the goal location. This reward-based activity is then back-propagated through reverse associations mediated by the lateral projections w_{qv} (Fig. 4.1B). When the back-propagated goal signal reaches the column selective for the current position, the coincidence of s and q activity triggers the discharge of neurons d. The d activation, in turns, activates the forward propagation of a goal-directed signal through projections w_{pd}. Since q neurons are already active, successive discharges of d and p neurons allow the

path signal to spread forward to the goal column. A competitive winner-take-all scheme, which locally selects the motor action $a \in A$ associated to the most active neuron d, reads out goal-directed trajectories.

It is worth mentioning that projections w_{qv} attenuate the back-propagating activity such that the smaller is the number of synaptic relays, the stronger is the goal signal received by the q neurons of the column corresponding to the current location. Thus, the activation diffusion mechanism produces an exponential decrease of the intensity of the goal signal that propagates along the network of columns. Since the receptive fields of the model columns tend to be evenly distributed over the environment, the intensity of the goal signal at a given place does correlate with the distance to the rewarding location. In other words, the columnar network encodes goal-related metrical information allowing the shortest pathway to the target to be selected. Animals can take shortcuts to a goal through inexperienced regions of the environment, an ability that has often been associated to complex metrical mapping (see Trullier et al., 1997; Kubie and Fenton, 2009 for reviews). The representation learned by the columnar network model encodes enough metrical information to infer shortcuts in simple situations similar to those tested with animals (Chapuis et al., 1983; Poucet et al., 1983; Poucet, 1993; Etienne et al., 1998). In the model, vector addition (Etienne et al., 1998) is approximated by means of a simple readout mechanism that sums the allocentric motion directions encoded by the actions of a planned trajectory (Sec. 4.5).

4.4 Recurrent cortical processing for multilevel topological mapping

The model can learn hierarchical state-space representations by employing recurrent projections between columns (Mountcastle, 1997; Lewis et al., 2002). As shown in Figure 4.1 (but see Sec. 4.5 for more details), this multistage processing can simply be understood in terms of the interaction between two subpopulations of cortical columns. The first population C_1 receives and processes direct spatial inputs from the hippocampus. The second population C_2 receives already-processed state information from neurons $s \in C_1$, but it also integrates a putative proprioceptive signal ϕ used to encode the probability of steady changes in egocentric locomotion direction. For instance, the signal ϕ may indicate a high

probability of turning by 90° at a given location. Since the activity of neurons s in the population C_2 integrates state-related information and motion direction changes, their selectivity is modulated by the presence of structural features of the environment such as alleys and corridors. The spatial resolution of the resultant multilevel representation can then adapt to the structural complexity of the maze.

The C_2 columnar network, which is learned similarly to the C_1 network, also supports the activation diffusion mechanism to plan goal-directed trajectories (Sec. 4.5). After learning, collateral projections w_{vv} and w_{pp} allow C_2 to modulate the activity of neurons $p, v \in C_1$ during planning (Fig. 4.1B).

4.5 Details: Columnar model, connectivity layout, and learning rules

4.5.1 Neuronal model

The elementary computational units of the model are firing-rate neurons i, whose mean discharge $r_i \in [0, 1]$ is given by:

$$r_i(t) = f\Big(V_i(t) \pm \eta\Big) \tag{4.1}$$

where $V_i(t)$ is the membrane potential at time t, f is the transfer function (when not specified $f_0(x) = x$), and η denotes random noise uniformly drawn from $[0, 0.1]$. The membrane potential V_i varies according to:

$$\tau_i \cdot \frac{dV_i(t)}{dt} = -V_i(t) + I_i(t) \tag{4.2}$$

where $\tau_i = 10$ ms is the membrane time constant, and $I_i(t)$ is the input synaptic drive. Eq. 4.2 is integrated by using a time step $\Delta_t = 1$ ms. For a given neuron i receiving inputs from an afferent population J, the synaptic drive $I_i(t)$ is taken as:

$$I_i(t) = \max_{j \in J} \{w_{ij} \cdot r_j(t)\} \tag{4.3}$$

where $w_{ij} \in [0, 1]$ indicates the synaptic weight of the projection from the presynpatic neuron j to the postsynaptic neuron i. See Riesenhuber and Poggio (1999) and Yu et al. (2002) for plausible neuronal implementations of $\max$ operators.

4.5.2 Column network connectivity

Every column of the model assembles three units s, p, v plus a population of mini-columns, each composed of two units q and d (Fig. 4.1B).

Intra-column connectivity layout

Neurons s, p respectively in layer V-VI and II-III, project onto units d of layer V-VI by means of one-to-all non-plastic synapses. Each neuron q in layer II-III sends a constant one-to-one projection to the corresponding d neuron in the same minicolumn. Each neuron v in layer II-III receives all-to-one projections from neurons q in layer II-III of the column (Fig. 4.1B).

The activity of neurons s, p, v, q varies according to Eq. 4.3. The discharge of every neuron q induces a multiplicative effect on $s \rightarrow d$ and $p \rightarrow d$ synapses. The synaptic drive of a d neuron is taken as:

$$I_d(t) = \max\Big\{w_{ds} \cdot r_s(t)\ ,\ w_{dp} \cdot r_p(t)\Big\} \cdot w_{dq} \cdot r_q(t) \tag{4.4}$$

where $w_{ds} = w_{dp} = w_{dq} = K$ denote the weight matrices of $s \rightarrow d$, $p \rightarrow d$, and $q \rightarrow d$ synapses, respectively.

Inter-column connectivity layout and input-output of the network

Before learning, the connection patterns are general for all columns of the model. They are adapted during the learning process to specialize the network in two subpopulations C_1 and C_2 (Sec. 4.5.3). The model network relies on plastic connectivity and considers both sub-cortical projections and cortical collaterals (Fig. 4.1B):

- Neurons s of the model can receive three types of afferent information: *(i)* direct spatial inputs from hippocampal place (HP) cells via projections w_{sh}; *(ii)* indirect (pre-processed) state-related inputs from other cortical neurons s via collaterals w_{ss}; *(iii)* putative proprioceptive information ϕ encoding changes in motion direction (see below).

- Neurons p receive: *(i)* recurrent projections w_{pp} from other neurons p of the network; *(ii)* collaterals w_{pd} from neurons d of other PFC columns (used to encode forward associations between places).

- Neurons q receive: *(i)* recurrent projections w_{qq} from other neurons q of the network; *(ii)* collaterals w_{qv} from neurons v of the network (used to encode reverse place associations).

- Neurons v receive: *(i)* sub-cortical motivation-dependent signals via projections w_{vm} (used during learning to associate a column to a rewarding location); *(ii)* collaterals w_{vv} from other neurons v of the network.

- Infragranular neurons d form the outputs of the column and project to motor-related areas (Mountcastle, 1997). During exploration, each neuron d becomes selective to a specific (allocentric) motion direction.

4.5.3 Spatial learning: encoding topological representations

The cortical network starts with weak synaptic weights randomly initialized within $[0, 0.1]$. As exploration proceeds, all plastic projections w_{sh}, w_{qv}, w_{pd}, w_{ss}, w_{pp}, w_{qq}, w_{vm} and w_{vv} are learned to encode topological maps. As shown in Fig. 4.1A, the cortical network model performs a two-stage processing of state-related information. During spatial learning, a subpopulation C_1 of cortical columns becomes primarily selective to spatial inputs received directly from hippocampal place (HP) cells, whereas another subpopulation C_2 processes state-related inputs from recurrent projections from C_1. For sake of clarity, we first describe spatial learning at the level of C_1 columns and then at the more abstract level encoded by C_2.

State learning in C_1 population (w_{sh})

At each location visited by the animal at time t the cortical network is updated if-and-only-if the activity of neurons s of all existing columns is below threshold, that is:

$$\sum_{s \in C_1} \mathcal{H}\big(r_s(t) - \rho\big) = 0 \tag{4.5}$$

where $r_s \in [0, 1]$ is the firing rate of neuron $s \in C_1$, $\mathcal{H}$ is the Heaviside function (i.e., $\mathcal{H}(x) = 1$ if $x > 0$, $\mathcal{H}(x) = 0$ otherwise), and $\rho = 0.3$. If the novelty condition holds (Eq. 4.5), then a new column becomes selective to that location by potentiating the projections w_{sh} from all active place cells to the neuron s of

the column:

$$w_{sh} = \mathcal{H}\big(r_h(t) - \rho\big) \cdot r_h(t) \tag{4.6}$$

where $r_h(t)$ denotes the firing rates of place cells $h \in$ HP. If the location visited at time t is not novel (i.e. Eq. 4.5 does not hold), a winner-take-all scheme selects the most active neuron s of the cortical network and an unsupervised Hebbian learning rule regulates the strength of its hippocampal afferents w_{sh} according to:

$$\Delta w_{sh} = \alpha \cdot r_s(t) \cdot \big(r_h(t) - w_{sh}\big) \tag{4.7}$$

where $\alpha = 0.2$ is the learning rate.

State connectivity learning in C_1 population (w_{pd} and w_{qv})

The model exploits PFC excitatory collaterals (Mountcastle, 1997; Lewis et al., 2002) to encode the spatial connectivity between places. During exploration, projections w_{pd} and w_{qv} (Fig. 4.1B) are modified to learn forward and reverse place associations, respectively. Let $c, c' \in C_1$ denote the columns coding for the rat position before and after a state transition, respectively. One minicolumn, i.e. a pair of q and d neurons in c, becomes selective to this transition. In particular, the neuron d is associated to the locomotion orientation taken by the animal to perform the transition. The weight $w_{p'd}$ of the projection from $d \in c$ to $p' \in c'$ and the weight $w_{qv'}$ from $v' \in c'$ to $q \in c$ are modified according to the following LTP/LTD plasticity rule:

$$\Delta w_{p'd} = (1 - \lambda) \cdot (\beta_{LTP} - w_{p'd}) - \lambda \cdot \beta_{LTD} \cdot w_{p'd} \tag{4.8}$$

where $\beta_{LTP} = 0.9$, $\beta_{LTD} = 0.5$, and the term $(1 - \lambda)$ indicates whether the simulated animal succeeded or failed the transition from c to c' ($\lambda = 0$ or $\lambda = 1$, respectively). If, for example, a new obstacle prevents the simulated rat from achieving a previously learned transition from column c to c', then a depression of the synaptic efficacy $w_{p'd}$ occurs. Note that the learning rule defined by Eq. 4.8 leads to $w_{pd}, w_{vq} \in [0, \beta_{LTP}]$.

State learning in C_2 population (w_{ss}, w_{pp} and w_{vv})

The example of Figure 4.2 illustrates how the cortical network C_2 is established and interconnected to the population C_1 during spatial exploration. Recall that the activity of neurons $s_2 \in C_2$ is driven by both the collateral excitatory inputs from

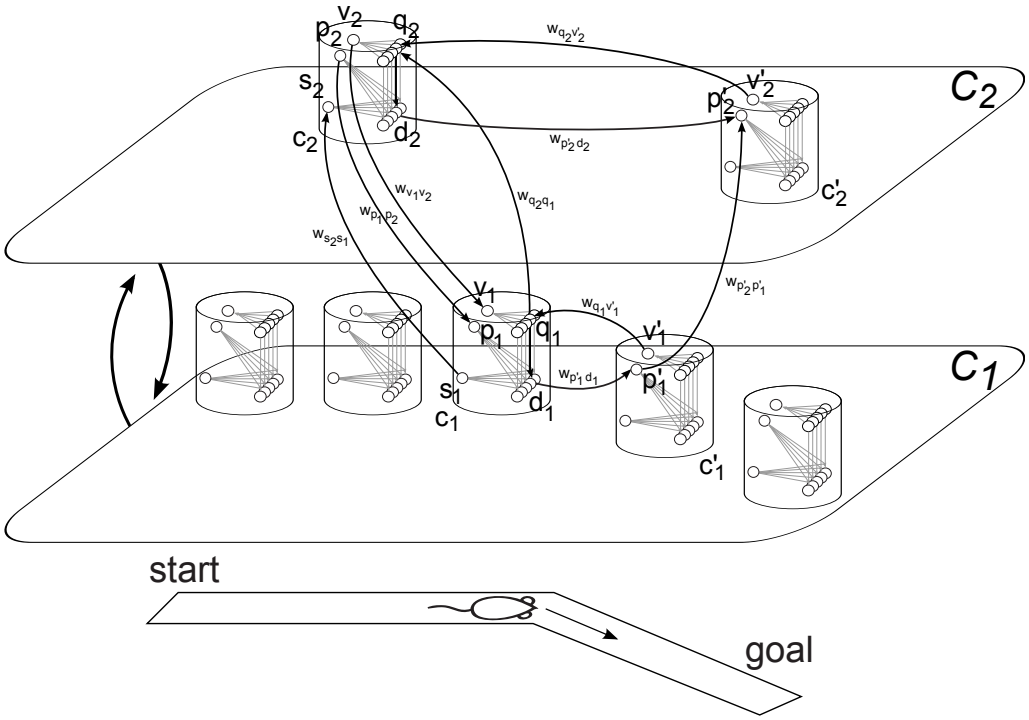

Figure 4.2: *Multilevel topological map learning in C_1 and C_2 populations.* Columns in C_1 and C_2 populations encode locations at different spatial resolutions. For instance, column $c_1 \in C_1$ corresponds to the end of the first alley, whereas $c_2 \in C_2$ encodes the entire alley before the turn. The model achieves multilevel state coding thanks to collateral projections $w_{s_2 s_1}$ between columns in C_1 and C_2. When a place transition occurs, lateral connections between columns selective for previous and next states are updated in C_1 population ($w_{p'_1 d_1}$ and $w_{q_1 v'_1}$), as well as in C_2 population ($w_{p'_2 d_2}$ and $w_{q_2 v'_2}$). These latter synaptic weights are modified thanks to the inputs conveyed by $w_{q_2 q_1}$ and $w_{p'_2 p'_1}$ projections so that the activity of $q_2 \in C_2$ will mirror the activity of $q_1 \in C_1$, whereas $p'_2 \in C_2$ will mirror $p'_1 \in C_1$. Finally, another set of collateral connections from C_2 to C_1 population ($w_{p_1 p_2}$ and $w_{v_1 v_2}$) enables columns in C_2 population to bias the activity in neurons p and v of C_1 population.

neurons $s_1 \in C_1$ and the modulatory effect of the putative proprioceptive signal ϕ. The latter encodes the probability that a steady and large change in locomotion direction occurs. For instance, $\phi \approx 1$ if the animal turns systematically by an angle greater than a threshold of 15° at a given location, whereas $\phi \approx 0$ if the animal goes approximately straight. The signal ϕ modulates the electroresponsiveness of neurons $s_2 \in C_2$. In the model, this modulation is implemented at the level of the transfer function of neurons s_2, which is taken as:

$$f(x) = x \cdot \gamma^{(1-\phi)} \tag{4.9}$$

with the constant parameter $\gamma = 1.1$. Note that $f(x)$ approximates the identity transfer function $f_0(x)$ when $\phi \approx 1$.

The network C_2 starts with weak connectivity and unsupervised learning modifies the synaptic weight distributions. The novelty condition to update the C_2 network is slightly different from Eq. 4.5 because it takes into account both the activity of units $s_2 \in C_2$ and the proprioceptive signal ϕ:

$$\phi(t) + \sum_{s_2 \in C_2} \mathcal{H}\big(r_{s_2}(t) - \rho\big) = 0 \tag{4.10}$$

If Eq. 4.10 holds, a new column of C_2 becomes interconnected to the most active column of the network C_1 as follows. Let $s_1 \in C_1$ be the most active unit when the novelty condition (Eq. 4.10) occurs, and let $s_2 \in C_2$ indicate the state neuron of the newly recruited column in C_2 (Figure 4.2). The $s_1 \rightarrow s_2$ projection is potentiated by:

$$w_{s_2 s_1} = \mathcal{H}\big(r_{s_1} - \rho\big) \cdot r_{s_1} \tag{4.11}$$

At each time step t, the following learning scheme shapes the interconnections between the most active column in C_1 and the most active column in the population C_2:

$$\Delta w_{s_2 s_1} = \eta \cdot r_{s_1} \cdot r_{s_2} \cdot \mathcal{H}\big(r_{s_1} - w_{s_2 s_1}\big) \cdot (1 - \phi) \tag{4.12}$$

$$\Delta w_{v_1 v_2} = 1 - w_{v_1 v_2} \tag{4.13}$$

$$\Delta w_{p_1 p_2} = 1 - w_{p_1 p_2} \tag{4.14}$$

whith $\eta = 0.6$. A consequence of this encoding scheme is that all C_1 columns that are sequentially activated when the simulated animal moves along a straight path (e.g. an alley) tend to be interconnected to the same column in C_2.

The activity of neurons $v_2, p_2 \in C_2$ influences the discharge of neurons $v_1, p_1 \in C_1$ through recurrent connections $w_{v_1v_2}, w_{p_1p_2}$, respectively. In the model, this is achieved by modulating the transfer function of units $v_1 \in C_1$ as follows (the same holds for the transfer function of units $p_1 \in C_1$):

$$f(x) = x \cdot \gamma^{\psi} \tag{4.15}$$

where γ is a constant factor set to 1.1 and $\psi = \mathcal{H}\big(\max_{v_2 \in C_2} \{w_{v_1v_2} \cdot r_{v_2}\}\big)$. The term ψ allows the activity of neurons $v_1, p_1 \in C_1$ to be enhanced in the presence of a discharge of neurons $v_2, p_2 \in C_2$, respectively. By contrast, $f(x)$ reduces to $f_0(x)$ when no activity from $v_2, p_2 \in C_2$ occurs.

State connectivity learning in C_2 population (w_{pd}, w_{qv}, w_{pp} and w_{qq})

After learning, transitions in the C_2 state-space representation are likely to map steady discontinuities in the environment structure (e.g. a L-turn in an alley of a maze). The example of Figure 4.2 shows how recurrent projections w_{qv}, w_{pd}, w_{pp}, and w_{qq} are updated when a state transition occurs in the C_2 representation:

- Let $c_2, c_2' \in C_2$ be the columns encoding the states before and after a transition, respectively.
- Let $(q_2, d_2) \in c_2$ be the minicolumn selective for the $c_2 \rightarrow c_2'$ transition.
- Let c_1, c_1' be the columns of C_1 that are active before and after the transition, respectively.
- Let $(q_1, d_1) \in c_1$ be the minicolumn selective for the $c_1 \rightarrow c_1'$ transition.

At each time step t the interconnectivity between these units is updated according to:

$$\Delta w_{p_2'd_2} = \frac{w_{p_2'p_1'} \cdot r_{p_1'}}{r_{d_2}} - w_{p_2'd_2} \tag{4.16}$$

$$\Delta w_{q_2v_2'} = \frac{w_{q_2q_1} \cdot r_{q_1}}{r_{v_2'}} - w_{q_2v_2'} \tag{4.17}$$

$$\Delta w_{p_2'p_1'} = 1 - w_{p_2'p_1'} \tag{4.18}$$

$$\Delta w_{q_2q_1} = 1 - w_{q_2q_1} \tag{4.19}$$

This mechanism allows the C_2 network to adapt its topology while accounting for the goal-distance information encoded by neurons C_1. Neuron $q_2 \in C_2$ will mirror the activity of $q_1 \in C_1$, whereas $p'_2 \in C_2$ will mirror $p'_1 \in C_1$. As a consequence, the information propagated at the level of the C_1 network will also be available in C_2. Thus, planning (see below) can be consistently achieved in parallel by C_1 and C_2 based on a bidirectional flow of information between these two cortical populations.

4.5.4 Exploiting the topological representation for planning

Figure 4.3 illustrates a simple example of activation diffusion process mediated by the columnar network model during planning. A putative motivation signal first elicits the activity of neurons v in the columns of C_1 and C_2 associated to the goal location (Figure 4.3A). The reward-based activity of neurons v is then back-propagated through the reverse state associations encoded by collaterals $w_{vq} \in C_1, C_2$. Each synaptic relay along the neural pathway formed by w_{vq} projections attenuates the back-propagating activity ($w_{vq} < 1$). Thus, the activation diffusion mechanism produces an exponential decrease of the intensity of the goal signal that propagates through the network of columns. It is worth noting that the recurrent dynamics induced by $w_{v_1v_2}$ and $w_{q_2q_1}$ increases the time constant of the exponentially decaying propagation (Eqs. 4.15 and 4.16). For example, after 10 synaptic relays the activity of a neuron $v \in C_1$ would be $r_v \approx 0.35$ without recurrent dynamics vs. $r_v \approx 0.9$ with the C_2 modulation (Figure 4.3B). Hence, the goal-dependent signal can spread over a larger number of columns before reaching the critical level of neuronal noise.

Since the receptive fields of C_1 columns tend to be evenly distributed, the intensity of the goal signal at a given place encodes the distance to the rewarding location. The learning rule implemented for collateral weights in C_2 (Eq. 4.16) allows this distance-to-goal coding property to be conserved at the level of the C_2 population.

The activity of d neurons integrates this reverse activity flow with the current state in both C_1 and C_2 populations (Eq. 4.4). In particular, the occurrence of the q input is a necessary condition for a neuron d to fire. In the presence of the q input, either the hippocampal signal relayed by the neuron s or the cortical input transmitted by neuron p is sufficient to trigger the discharge of a unit d (Eq. 4.4).

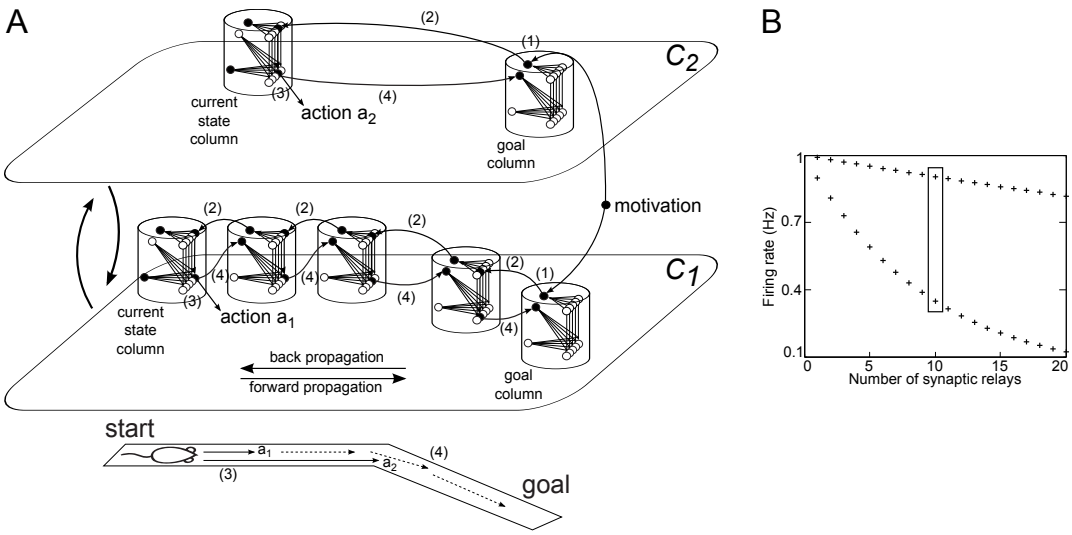

Figure 4.3: *Action planning through multilevel activation-diffusion of a goal signal*. **(A)** A motivation signal induces the activity of neurons v in the goal columns of C_1 and C_2 populations *(1)*. The goal information is then back-propagated through the reverse state associations encoded by neurons v and q in C_1 and C_2 *(2)*. When the back-propagated goal signal reaches the columns selective for the current position in both C_1 and C_2 populations, the coincidence of the state-related input conveyed by s neurons and the goal-related input transmitted by q neurons activates neurons d *(3)*. In turns, neurons d trigger the forward propagation of a pathway signal through the neurons p and d *(4)*. At each step of the forward propagation, the motor action associated to the most active neuron d can be selected (e.g. for the first planning step a_1 for C_1 population and a_2 for C_2 population) and the sequence of actions from the current position to the goal can be iteratively readout. **(B)** Effect of the top-down modulation exerted by the population C_2 upon the back-propagating activity at the level of neurons v in C_1. We plotted the relation between the number of synaptic relays connecting the columns that form the planned path from a given place to the goal and the firing rate of the neuron v belonging to the column representing that place. Each cross indicates the activity of one neuron v after a given number of synaptic relays. Without any modulation from the C_2 population (exponentially decreasing set of points), the activity of neurons v drops quickly to the noise level as the length of the planned path increases. With the C_2 modulation, the time constant of the decreasing function is much larger, leading to a better propagation in large environments.

When the back-propagated goal signal reaches the column selective for the current position, the coincidence of the state-related hippocampal input conveyed by s neurons and the goal-related input transmitted by q neurons activates the neuron d, which in turns triggers the forward propagation of a pathway signal through projections w_{pd}. The activity of d neurons also conveys distance-to-reward information (because d neurons are partially driven by q neurons). Thus, at each step of the forward propagation, the motor action associated to the most active neuron d can be selected and the sequence of actions from the current position to the goal can be iteratively readout (Figure 4.3A). This sequence of actions is also used to compute an overall direction between a given position and a target position. In the general case, vector addition sums the allocentric motion directions encoded by the actions (the distance traveled for each action is supposed to be unitary), which can be summarized by:

$$\theta = \arg\left(\sum_j r_j \cdot e^{i \cdot a_j}\right) = \arg\left(\sum_j e^{i \cdot a_j}\right) \tag{4.20}$$

where the complex term $r_j \cdot e^{i \cdot a_j}$ represents an action j of distance r_j and orientation a_j. In the particular case of a sequence with only two actions, this vector addition can be approximated thanks to Euler formula to provide an intuitive computation of the resultant orientation:

$$\theta = \arg\left(e^{i \cdot a_1} + e^{i \cdot a_2}\right) = \arg\left(2 \cdot \cos\left(\frac{a_1 - a_2}{2}\right) \cdot e^{i\frac{a_1 + a_2}{2}}\right) = \frac{a_1 + a_2}{2} \tag{4.21}$$

4.6 Conclusion

This chapter presented our model of the prefrontal cortex. It is based on the columnar organization of this structure and uses it to learn a joint space-action representation forming a topological map. A planning mechanism, called activation diffusion, is emploied to exploit this representation in order to plan detours and discover shortcuts. Two populations of columns encode two topological maps of the environment with different scales, to improve the flexibility of the model in large environments. Within each column, several neurons encode different types of information relevant for planning such as spatial and goal-related information.

The next chapter examines results of computer simulations that tested model spatial performance in several behavioral tasks.

Chapter 5

Spatial behavior of the model

This chapter demonstrate the ability of the model to learn topological representations and plan goal-oriented trajectories. Performances of the simulated animals were measured in a detour and a shortcut navigation task.

5.1 Methods

We considered two navigation tasks: the Tolman & Honzik's *detour* task and a novel *shortcut* task. In both cases, the behavioral responses of simulated rats are constraint by intersecting alleys, which, in contrast to open field mazes, generate clear decision points and permit dynamic blocking of goal-directed pathways.

5.1.1 Tolman & Honzik's detour task

The classical Tolman & Honzik's maze (Fig. 5.1A) consisted of three narrow alleys of different lengths (Paths 1, 2, and 3) guiding the animals from a starting location to a feeder location. Tolman & Honzik's experiment aimed at corroborating the hypothesis that rodents, while undergoing a navigation task, can predict the outcomes of alternative goal-directed trajectories in the presence of dynamically blocked pathways. We ran a series of numerical simulations to emulate the experimental protocol originally designed by Tolman & Honzik:

Training period. It lasted 168 trials (that correspond to 14 days with 12 trials per day), during which the simulated animals could explore the maze to elaborate topological representations and learn navigation policies. Simulated rats moved

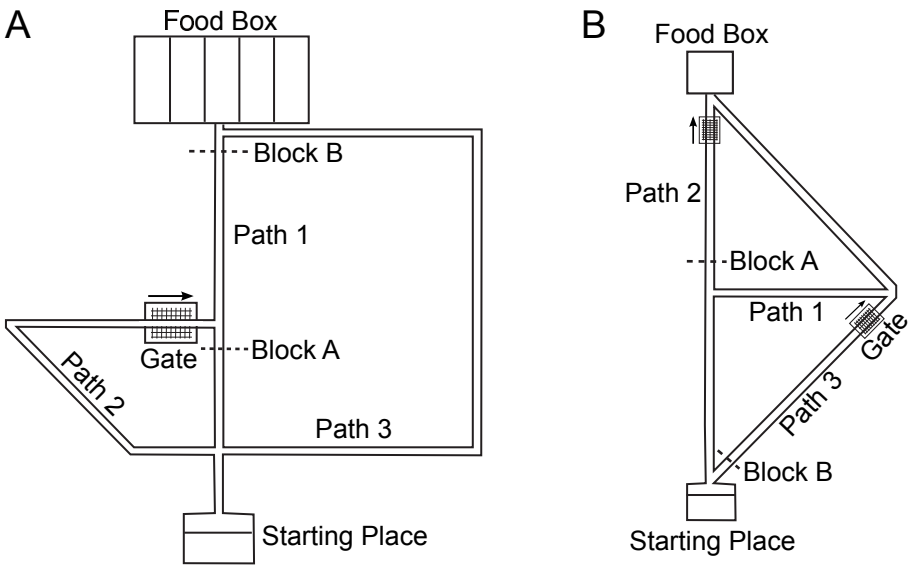

Figure 5.1: *Spatial navigation tasks used to test the capability of infering detours and shortcuts.* **(A)** The Tolman & Honzik's maze (adapted from Tolman and Honzik, 1930a) consists of three pathways (Path 1, Path 2 and Path 3) with different lengths. The original maze fits approximately within a rectangle of 1.20 x 1.55 m. Two blocks can be introduced to prevent animals from navigating through Path 1 (Block A) or both Path 1 and Path 2 (Block B). The gate near the second intersection prevents rats from going from right to left. **(B)** The shortcut maze includes a main pathway P1, plus one direct shortcut (Path 2) and one indirect shortcut (Path3). Two blocks A and B are present at the beginning of the task, and can selectively be removed to test the ability to find direct vs. indirect shortcuts.

at a speed of 15 cm/s. In the following, we refer to 12 training trials as a "day" of simulation.

- *Day 1*. A series of 3 *forced runs* was carried out in which the simulated rats were forced to go through P1, P2, and P3 successively. Then, during the remaining 9 trials, the subjects were allowed to explore the maze freely. At the end of Day 1, a preference for P1 was expected to be already established (Tolman and Honzik, 1930a).

- *Day 2 to 14*. On each trial, a block was introduced at location A (Block A, Fig. 5.1A) to induce a choice between P2 and P3. Entrances to P2 and P3 were also blocked in order to force the animals to go first to Block A. When the simulated rats reached block A and returned back to the first intersection, doors were removed and subjects had to decide between P2 and P3. Every day, 10 runs with a block at A were mixed with 2 non-successive free runs to maintain the preference for P1.

Probe test. It lasted 7 trials (Day 15) with a block at location B (Block B, Fig. 5.1A) to interrupt the portion of pathway shared by P1 and P2. Animals were forced to decide between P2 and P3 when returning to the first intersection point. Both training and probe trials ended when the simulated animal reached the goal, i.e. when it crossed the entrance to the food box.

Multiple maze sizes. To assess the invariance of the model performance with respect to the size of the environment, we implemented the above experimental protocol for two different maze scales, 1:1 and 4:1. We took the dimensions of the simulated mazes so as to maintain the proportions of Tolman & Honzik's setup.

Behavioral analysis. We employed a population of 40 simulated rats for each experimental protocol. We quantified the statistical significance of the results by means of an ANOVA analysis ($P < 0.001$ was considered significant).

5.1.2 Shortcut navigation task

Experimental evidence suggests that path selection depends on both the length and the directionality of the available trajectories (Poucet, 1993). In addition, animals tested in the presence of a conflict between length and directionality properties (e.g. with the shorter path being less direct to the goal and vice versa) tend to prefer the shorter, yet less direct, path when the goal is hidden (Chapuis et al., 1983;

Poucet et al., 1983). The maze shown in Figure 5.1B takes these observations into account. It consists of three pathways: P1 is the longest path and does not involve any shortcut; P2 involves of a direct shortcut pointing toward the goal; P3 is based on an indirect shortcut, forcing the animal to divert from the apparently most direct way to the goal (the straight line from start to goal). We simulated two set of experiments sharing the same protocol consisting of two phases:

Training period. It lasted 6 trials, during which the simulated rats were enabled to go through pathway P1 only (i.e. blocks A and B were both present, Fig. 5.1B), so that P2 and P3 sub-pathways remained unexplored.

Probe test. It lasted 1 trial and it aimed at testing how simulated animals would use a newly available shortcut. In one set of experiment, simulated animals were allowed to choose between P1 and P2 (i.e. direct shortcut, with block A removed), whereas in a second experiment animals had to choose between P1 and P3 (i.e. indirect shortcut, with block B removed).

Behavioral analysis. We employed two populations of 40 simulated rats each for this protocol (one for the direct shortcut test and the other for the indirect shortcut test). We used a χ^2 test to assess the statistical significance of results ($P < 0.001$ was considered significant).

For all these experiments we used a robotic software called *webots*, which enables the generate a 3D environment where the simulated animals could move in a physically realistic way.

5.2 Results

5.2.1 Tolman & Honzik's detour task

We first examined the behavioral responses of $n = 40$ simulated animals solving the 1:1 version of Tolman & Honzik's task (see Sec. 5.1.1 and Figure 5.1A for details on the experimental apparatus and protocol). The qualitative and quantitative results shown on Figures 5.2A and B, respectively, demonstrate that the model reproduced the behavioral observations originally reported by Tolman and Honzik (1930a).

Day 1. During the first 12 training trials the simulated animals learned the topology of the maze and planned their navigation trajectories in the absence of blocks A and B. Similar to Tolman & Honzik's findings, the model selected the short-

est pathway P1 significantly more than alternative paths P2 and P3 (ANOVA, $P < 0.0001$; Figures 5.2A,B, left column).

Days 2-14. During the following 156 training trials, a block at location A forced the animals to update their topological maps dynamically, and plan a detour to the goal. The results reported by Tolman & Honzik provided strong evidence for a preference for the shortest *detour* path P2. Consistently, we observed a significantly larger number of transits through P2 compared to P3 (ANOVA, $P < 0.0001$; Figures 5.2A,B, central column).

Day 15. The simulated protocol included 7 probe trials during which the block A was removed whereas a block at location B was added. This manipulation aimed at testing the "insight" working hypothesis: after a first run through the shortest path P1 and after having encountered the unexpected block B, will animals try P2 (wrong behavior) or will they go directly through P3 (correct behavior)? In agreement with Tolman & Honzik's findings, simulated animals behaved as predicted by the insight hypothesis, i.e. they tended to select the longer but effective P3 significantly more often than P2 (ANOVA, $P < 0.0001$; see Figures 5.2A,B, right column). The patterns of path selection during this task is explained by the ability of the model to choose shortest paths. When a block is added into the environment, the goal propagation signal is also blocked at the level of the column network, and hence the simulated animals choose the shortest *unblocked* pathways.

We then tested the robustness of the above behavioral results with respect to the size of the environment. We considered a 4:1 scaled version of Tolman & Honzik's maze and we compared the performances of $n = 40$ simulated animals with intact C_1, C_2 populations ("control" group) against those of $n = 40$ simulated animals lacking the C_2 cortical population ("no C_2" group). The latter group did not have the multilevel encoding property provided by the C_1-C_2 recurrent dynamics, (Sec. 4.4). Figure 5.2C compares the average path selection responses of the two simulated groups across the different phases of the protocol. During *Day 1* (i.e. no blocks in the maze) both groups selected the shortest path P1 significantly more often (ANOVA, $P < 0.0001$; Figure 5.2C left). However, the action selection policy of subjects without C_2 began to suffer from mistakes due to the enlarged environment, as suggested by lower median value corresponding to P1. During *Days 2-14* (with block A), the group without C_2 did not succeed in solving the *detour* task, because no significant preference was observed between

P2 (shortest pathway) and P3 (ANOVA, $P > 0.001$; Figure 5.2C center). By contrast, control animals coped with the larger environmental size successfully (i.e. P2 was selected significantly more often than P3, ANOVA, $P < 0.0001$). During the probe trials of *Day 15* (with a block at B but not at A), the group without C_2 was impaired in discriminating between P2 and P3 (ANOVA, $P < 0.6756$; Figure 5.2C right), whereas control subjects behaved accordingly to the insight hypothesis (i.e. they selected the longer but effective P3 significantly more than P2; ANOVA, $P < 0.0001$). The better performances of control subjects were due to the fact that back-propagating the goal signal through the cortical network benefited from the higher-level representation encoded by the C_2 population and from the C_1-C_2 interaction during planning (see Sec. 4.5.4, Figure 4.3). Indeed, an intact C_2 population allowed the goal signal to decay with a slower rate compared to C_1, due to the smaller number of intermediate columns in C_2 (i.e. planning could benefit from a more compact topological representation).

5.2.2 Shortcut navigation task

In two set of experiments, we studied the navigation performance of $n = 40$ animals when solving the shortcut behavioral task (Figure 5.3; see also Sec. 5.1.2 for details on setup and protocol). Simulated animals in both experiments underwent a training period during which they could explore the pathway P1 only (both block A and B were present). During a single-trial probe test of the first experiment, simulated animals had the opportunity to take a *direct* shortcut (pathway P2 unexplored during training, with no block A) to the goal. Figures 5.3A,B (left column) show that a significant fraction of simulated rats selected P2 instead of P1 (97.5%, χ^2 test: $P < 0.0001$). The animals of the second experiment were tested on a single-trial probe test in which the *indirect* shortcut P3 was made available by removing block B. A majority of simulated animals selected P3 (95%, χ^2 test: $P < 0.0001$; Figures 5.3A,B right column). These results are consistent to experimental findings on shortcut navigation behavior by Chapuis et al. (1983) and Poucet et al. (1983).

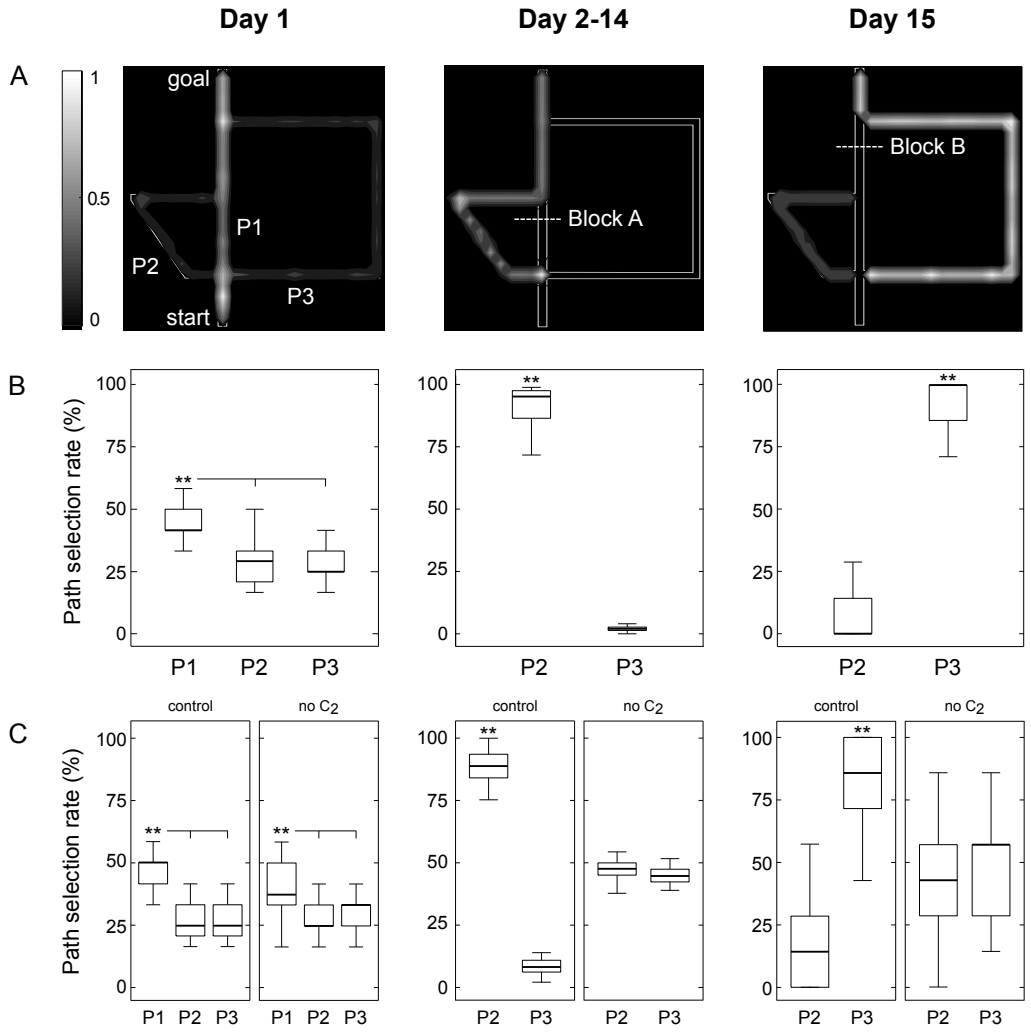

Figure 5.2: *Spatial behavior performance in the Tolman & Honzik's detour task. Simulation results.* Day 1: left column; Day 2-14: central column; Day 15: right column. **(A)** Occupancy grids representing path selection results qualitatively. **(B)** Mean path selection rate (averaged over 40 simulated animals) in the 1:1 scale version of the maze. Note that similar to Tolman and Honzik (1930a) we ignored P1 in Day 2-14 and Day 15 analyses because blocked. **(C)** Performance of "control" vs. "no C_2" animals in the 4:1 version of Tolman & Honzik's maze.

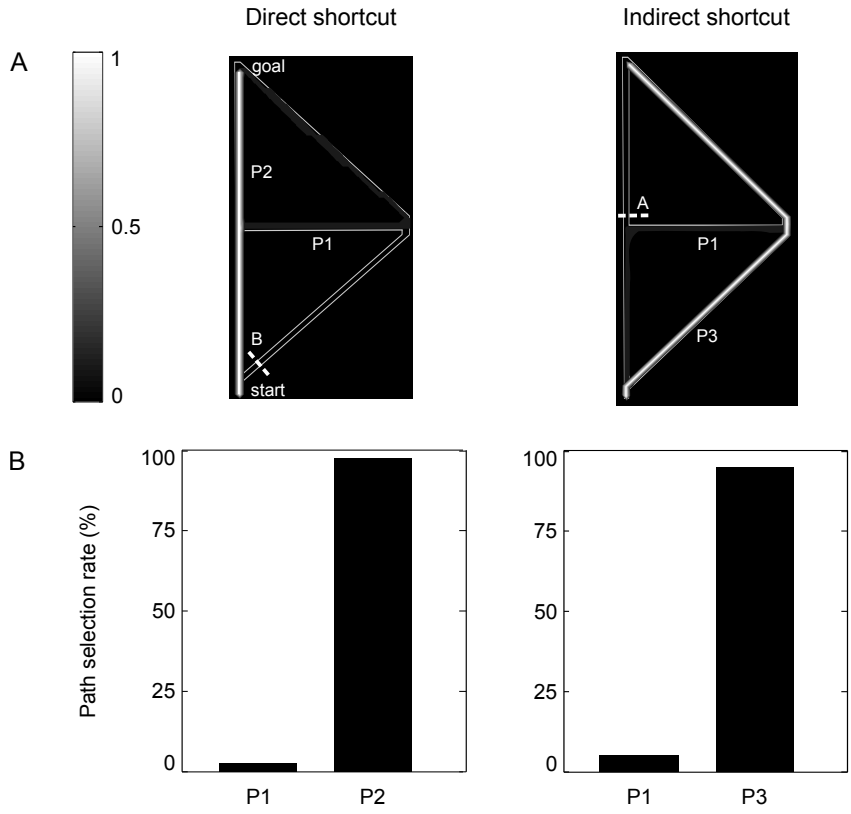

Figure 5.3: *Spatial behavior performance in the shortcut navigation tasks. Simulation results*. Direct shortcut experiment: left column; indirect shortcut experiment: right column. **(A)** Occupancy grids representing path selection policies qualitatively. **(B)** Mean path selection rates averaged over 40 subjects.

5.3 Conclusion

We presented a model focusing on navigation planning mediated by a population of prefrontal cortical columns. During exploration of a new environment, the model learns a topological representation in which each place is encoded by a neocortical column and strengthening of synapses between columns is used to represent topological links between places. During goal-oriented trajectory planning, an activation diffusion mechanism produces a spread of activity in the column population leading to selection of the shortest path to the goal. Our simulation results demonstrate that the model can reproduce rodent behavior previously attributed to the animals' ability to experience a cognitive "insight" about the structure of the environment (Tolman and Honzik, 1930a). Moreover, we show that spatial planning in our model is invariant with respect to the size of the maze. This property relies on the ability of the model to encode cognitive maps with a resolution that fits the structure of the environment (e.g. alleys). Another property of the model is its ability to find shortcuts through unexplored portions of the environment.

How does the cortical column population subserve spatial learning and navigation planning? In the next chapter, we analyse coding properties of the model neurons and their link with decision making, in relation with experimental data.

Chapter 6

From neural activities to functional responses

We analyzed the activity patterns of simulated neurons in relationship to electrophysiological data. This study aimed at elucidating the link between cell activity and behavior and it stressed the importance of relating the time course profile of single cell discharges to decision-related behavioral responses. This was done by: (i) characterizing the spatial selectivity properties of single cell types; (ii) comparing the density —and other correlated measures such as sparseness and redundancy— of the spatial population codes learned by simulated animals (we recall that one of the aims of the cortical column model was to build spatial codes less redundant than hippocampal place field representations); (iii) differentiating the coding properties of purely reward-related neurons (q and v populations) vs. purely spatial units (s population); (iv) quantifying and comparing the reliability of neural spatial representations (both at level of single cell and population code) in terms of information content —i.e. how much can we infer about either the animal's position or a particular phase of the task by observing neural responses only?

Besides relating our simulation results to literature experimental data, we studied the consistency between model neural responses and a set of PFC electrophysiological recordings from navigating rats. In these experiments —carried out at S.I. Wiener's laboratory; see detailed methods in Peyrache et al. (2009); Benchenane et al. (2010)— extracellular recordings were performed from medial PFC pyramidal cells of Long-Evans rats solving a spatial memory task. The analysis presented

here investigated whether the coding properties of all types of neurons in the cortical network model could actually be observed in the PFC during spatial learning.

6.1 Methods

In order to quantify spatial-related correlates of neural activity, the continuous two-dimensional input space was discretized by a grid of 5 x 5 cm square regions (pixels). Let S denote the set of stimuli, i.e. the set of locations s visited by the simulated animal while solving the task.

Place field area. For each neuron, the mean firing rate associated to each pixel s was computed by dividing the spike count associated to s by the time spent by animal in s. The size of a receptive (place) field was then taken as the number of adjacent pixels with a firing rate above the grand mean rate —i.e. total spike count divided by the total time spent moving in the maze— plus the standard deviation (similarly to Muller et al., 1987; Hok et al., 2005).

Spatial density of receptive fields. To assess the redundancy level of a spatial code —i.e. the average number of units encoding a spatial location $s \in S$— the following density measure was used:

$$D_S = \left\langle \sum_{j \in J} \mathcal{H}\Big(r_j(s) - \eta\Big) \right\rangle_{s \in S} \tag{6.1}$$

where $r_j(s)$ is the response of a neuron $j \in J$ when the animal is visiting the location $s \in S$, η denotes the noise level activity, and $\mathcal{H}$ is the Heaviside function.

Sparseness and shape of the spatial code. The *kurtosis* function —i.e. the normalized fourth central moment of a probability distribution and estimates its degree of peakedness— was applied to quantify the sparseness across the neural population and across time (for single neurons) (Willmore and Tolhurst, 2001).

Population kurtosis:

$$K_P(s) = \left\langle \left[\frac{r_j(s) - \bar{r}_J(s)}{\sigma_J(s)} \right]^4 \right\rangle_{j \in J} - 3 \tag{6.2}$$

with $\bar{r}_J(s)$ and $\sigma_J(s)$ representing the mean and the standard deviation of the population activity distribution for a given stimulus s, respectively, was used to estimate how many neurons j in a population J were, on average, simultaneously responding to a stimulus s.

Single cell lifetime kurtosis:

$$K_L(j) = \left\langle \left[\frac{r_j(s) - \bar{r}_j}{\sigma_j} \right]^4 \right\rangle_{s \in S} - 3 \tag{6.3}$$

with $\bar{r}_j$ and σ_j being the mean and the standard deviation of the cell response r_j to the set of stimuli S, respectively, was employed to assess how rarely over time a neuron j responded to stimuli S.

Single cell skewness: In order to quantify the degree of asymmetry of spatial receptive fields, we used the skewness measure, defined as the third moment of the place field firing rate distribution (Mehta, 2000). Given a random variable X_j with N samples whose distribution matches the shape of the receptive field of the cell j, the skewness $S_k(j)$ is:

$$S_k(j) = \left\langle \left[\frac{X_j(i) - \bar{X}_j}{\sigma_{X_j}} \right]^3 \right\rangle_{i \in N} \tag{6.4}$$

Spatial information content of the spatial code. An information theoretical analysis quantified how much information the neural responses $r \in R$ conveyed about spatial locations $s \in S$. *Shannon mutual information* $\mathrm{I}(R;S)$ (Shannon, 1948; Bialek et al., 1991) between neural responses R and spatial locations S was computed:

$$I(R;S) = \sum_{s \in S} p(s) \sum_{r \in R} p(r|s) \cdot \log_2 \left(\frac{p(r|s)}{p(r)} \right) = \sum_{s \in S} p(s) \cdot I(R;s) \tag{6.5}$$

where $p(r|s)$ indicates the conditional probability of recording a response r while having the simulated rat visiting a region s; $p(s)$ the a priori probability computed as the ratio between time spent at place s and the total time; $p(r) = \sum_{s \in S} p(s) \cdot p(r|s)$ the marginal probability of observing a neural response r; and $I(R;s)$ is the *stimulus-specific surprise* (DeWeese and Meister, 1999; Bezzi et al., 2001). The continuous output space of a neuron $R = [0,1]$ was discretized via a binning

procedure (bin-width equal to 0.1). A correcting term C was subtracted to mutual information to limit the sampling bias (Panzeri and Treves, 1996):

$$C = \frac{\sum_s R_s^+ - R^+ - (|S| - 1)}{2N\, ln(2)} \tag{6.6}$$

where $R_s^+ = \sum_{r \in R} \mathcal{H}(p(r|s))$ denotes the number of response bins in which the occupancy probability $p(r|s) > 0$; $R^+ = \sum_{r \in R} \mathcal{H}(p(r))$ denotes the number of response bins where $p(r) > 0$; $|S|$ is the number of stimuli; N is the number of stimulus-response pairs (s, r).

While the kurtosis measures the shape of a response distribution, the mutual information quantifies the reliability of the neural spatial representation in terms of decoding efficacy. Mutual information was computed considering both the responses of single units j, $I_j(R; S)$, and the neural population responses, $I_{pop}(R; S)$. The ratio:

$$I^*(R; S) = \frac{I_{pop}(R; S)}{\sum_{j \in J} I_j(R; S)} \tag{6.7}$$

was used to measure the "information sparseness" of a population code, or, conversely, the redundancy level of the spatial information content of a neural code.

Finally, for a given neuron j, the Pearson correlation coefficient $PC(j)$ between the firing rate r_j and the stimulus-specific surprise $I_j(R; s)$, was computed to measure the degree of localization of the spatial code (Bezzi et al., 2001):

$$PC(j) = \frac{\left\langle \left(I_j(R; s) - \bar{I}_j\right) \cdot \left(r_j(s) - \bar{r}_j\right) \right\rangle_{s \in S}}{\sigma_{I_j} \cdot \sigma_j} \tag{6.8}$$

with $\bar{I}_j$ and σ_{I_j} being, respectively, the mean and the standard deviation of the stimulus-specific surprise of neuron j for the set of stimuli S.

Mutual information measures the mean information content over the whole environment, but it does not quantifies the specificity of the neuronal discharges. Thus, we employed an additional measure, namely the information per spike I_{spike} (Skaggs et al., 1993) defined for a neuron j as:

$$I_{spike}(j) = \sum_{s \in S} \frac{r_j(s)}{\bar{r}_j} \cdot \log_2 \left(\frac{r_j(s)}{\bar{r}_j} \right) \cdot p(s) \tag{6.9}$$

Behavioral relevance of neural responses. We estimated the mutual information $I_t(R; F)$ between task-related information (the phase $f \in F$ of the protocol, e.g.

"Day 1", "Day 2-14" or "Day 15" period) and the firing activity $r \in R$ of a given neural population:

$$I_t(R;F) = \sum_{f \in F} \sum_{r \in R} p(r,f) \ \log_2 \left(\frac{p(r,f)}{p(r)\ p(f)} \right) \tag{6.10}$$

where $p(r,f)$ is the joint probability of observing a population response r when solving the phase f of the protocol; $p(f)$ indicates the a priori probability computed as the ratio between the length of phase f and the total length of the protocol; and $p(r) = \sum_{f \in F} p(r,f)$ is the marginal probability of observing the response $r \in R$.

6.2 Results

Here we demonstrate how the modeled neural processes can be interpreted as elements of a functional network mediating spatial learning and decision making. We show that the neural activity patterns of all types of neurons in the cortical model are biologically plausible in the light of PFC electrophysiological data (Watanabe, 1996; Jung et al., 1998; Rainer et al., 1999; Tremblay and Schultz, 1999; Miller and Cohen, 2001; Averbeck et al., 2002; Mulder et al., 2003; Hok et al., 2005; Peyrache et al., 2009; Benchenane et al., 2010).

6.2.1 Single cell and population place codes

Analysis of single cell receptive fields

To understand how single neurons took part to place coding, we compared the location-selective activities of two types of units of the model: hippocampal place (HP) cells and cortical neurons $s \in C_1, C_2$ (Figure 4.1). We analyzed their discharge patterns while simulated animals were solving the 4:1 version of the Tolman & Honzik's task. Figure 6.1A displays some samples of receptive fields recorded from each of these populations. The representation encoded by units $s \in C_1$ was in register with the place field organization of HP cells (left and center panels), whereas the activity of neurons $s \in C_2$ (right panel) captured some structural properties of the environment (i.e. alley organization). As quantified on Figure 6.1B, the mean size of place fields increased significantly as spatial information was subsequently processed by HP, C_1 and C_2 populations (ANOVA,

$P < 0.0001$; see also Figure 6.3A for results based on a kurtosis analysis). These findings are consistent to experimental data on the sizes of receptive fields of hippocampal and PFC cells recorded from rats solving a navigational task (Hok et al., 2005).

We also characterized the multistage spatial processing of the model in terms of Shannon mutual information between single unit responses and spatial locations. As shown on Figure 6.1C, the activity of neurons $s \in C_2$ encoded, on average, the largest amount of spatial information, followed by neurons $s \in C_1$ and HP cells (ANOVA, $P < 0.0001$). This relationship was due the fact that the smaller the receptive field is, the larger is the region of the input space for which a neuron remained silent, and then the lesser can be inferred about the entire input set by observing the variability of the neuron discharge. This result was based on the computation of the total amount of information, averaged over all positions. Other authors characterized the spatial locations where cells are most informative, such as the spatial coherence, which estimates the local smoothness of receptive fields (Hok et al., 2005), or the local information, which is a well-behaved measure of a location-specific information (Skaggs et al., 1993; Bezzi et al., 2001).

We also compared the location-selective responses of single neurons $s \in C_1$ with the discharge patterns of pyramidal cells recorded from the medial PFC of navigating rats (see Materials and Methods Sec. 6.1). Figure 6.1D shows three examples of experimental (top) and simulated (bottom) receptive fields evenly distributed on a linear alley. Real and simulated patterns are consistent to each other in terms of both shape and signal-to-noise ratio of the response profiles. These results corroborated the hypothesis that purely location-selective neurons s of the model might find their biological counterpart in real PFC populations.

Analysis of population place coding properties

As aforementioned, we modeled the interplay between hippocampus and PFC to produce compact space codes suitable to support navigation planning. Figure 6.2 shows how the implemented multistage processing (including the C_1-C_2 recurrent dynamics) provided a progressive sparsification of the population place code. Figure 6.2A qualitatively compares three examples of distributions of receptive field centers of HP and $s \in C_1, C_2$ neural populations (left, center and right, respectively). Consistently to experimental findings reported by Jung et al. (1998),

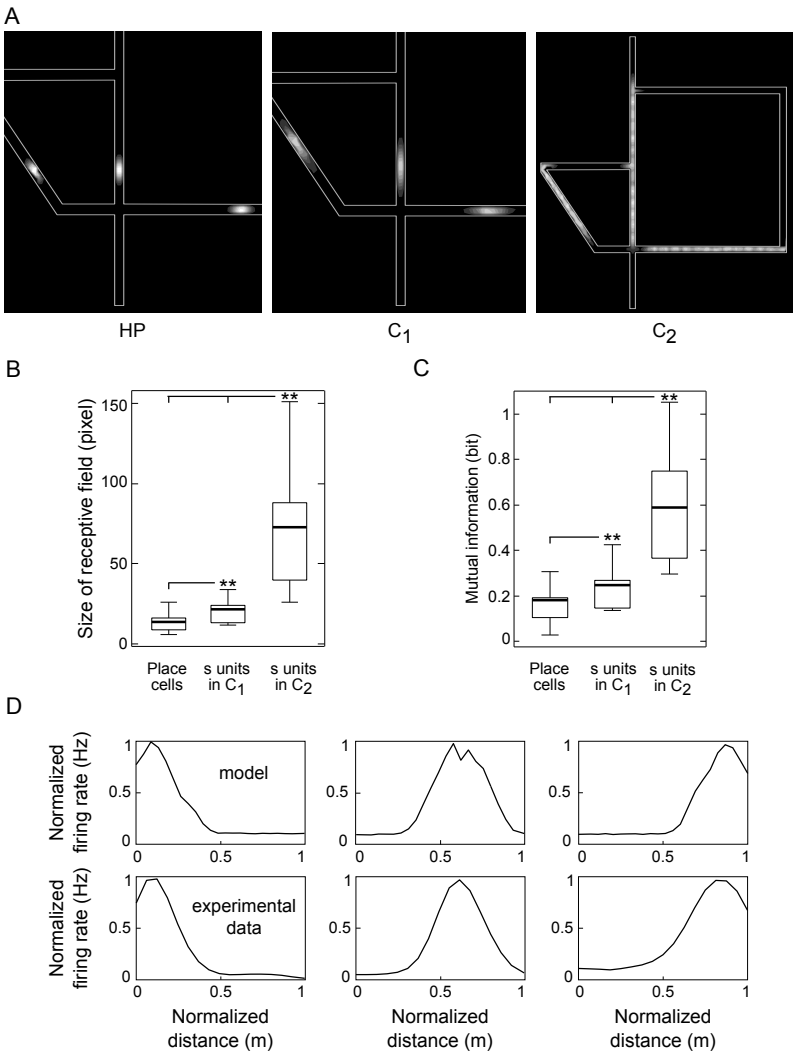

Figure 6.1: *Single cell response analysis. Simulation results and relation to electrophysiological PFC recordings.* **(A)** Examples of receptive fields of model hippocampal place (HP) cells (left), cortical neurons s in C_1 (center) and s in C_2 (right) when the simulated animals were solving the 4:1 version of Tolman & Honzik's maze. White regions denote large firing rates whereas black regions correspond to silent activity. **(B)** Mean size of the receptive fields for each neural population, measured in pixels (i.e. 5 x 5 cm square regions). **(C)** Mutual information between single unit responses and spatial input for each population. **(D)** Location-selective responses of model single neurons $s \in C_1$ functions of the normalized distance traveled along a section of the linearized trajectory P3 (top row) and medial PFC pyramidal cells recorded from navigating rats (bottom row).

our simulated cortical units produced less redundant place representations than HP cells. The size of neural populations encoding the Tolman & Honzik's maze decreased significantly from HP to C_1 and then to C_2 (ANOVA, $P < 0.0001$; Figure 6.2B). The sparser nature of cortical place codes was confirmed by the significant difference between spatial densities of receptive fields (Figure 6.2C; see also Figures 6.3B,C for the results of population kurtosis and information sparseness analyses, respectively).

Finally, we measured the Shannon mutual information between population response patterns and spatial locations. The highly redundant HP code had the largest spatial information content (ANOVA, $P < 0.0001$; Figure 6.2D). Yet, although less redundant, the population of neurons $s \in C_1$ encoded about 85% of the theoretical upper bound, which proved to be suitable for solving the behavioral tasks. A significant loss of information content was observed for the population code implemented by neurons $s \in C_2$. This is consistent with the functional role of the C_2 cortical network, which could not support navigation planning alone, but it rather complemented the C_1 representation by encoding higher level features of the environment.

6.2.2 Goal distance coding

Besides the spatial correlates of s neurons' activity, the model cortical representation encoded reward-dependent information. Figure 6.4A shows the correlation between the firing rate of units $v \in C_1$ and the shortest distance-to-goal. The diagram shows that, given a location in the maze, the smaller the length of the shortest goal-directed pathway was, the larger was the mean discharge of the v neuron belonging to the column corresponding to that location. This property was relevant to the decision making process determining the spatial navigation behavior reported in Sec. 5.2. When the exponentially decaying frequency of v units reached the basal neural noise level, the action selection policy reduced to random search (see the performance of *"no C_2"* simulated animals on Figure 5.2C, central and right panels). The distance-to-goal coding property of v neurons called upon their selective responses in the frequency domain. The population spectral power of Figure 6.4B (top) demonstrates that each neuron $v_i \in C_1$ had a unique preferred discharge frequency f_i correlated to its distance-to-goal (Fig. 6.4A). Preferred frequencies f_i were uniformly distributed over the normal-

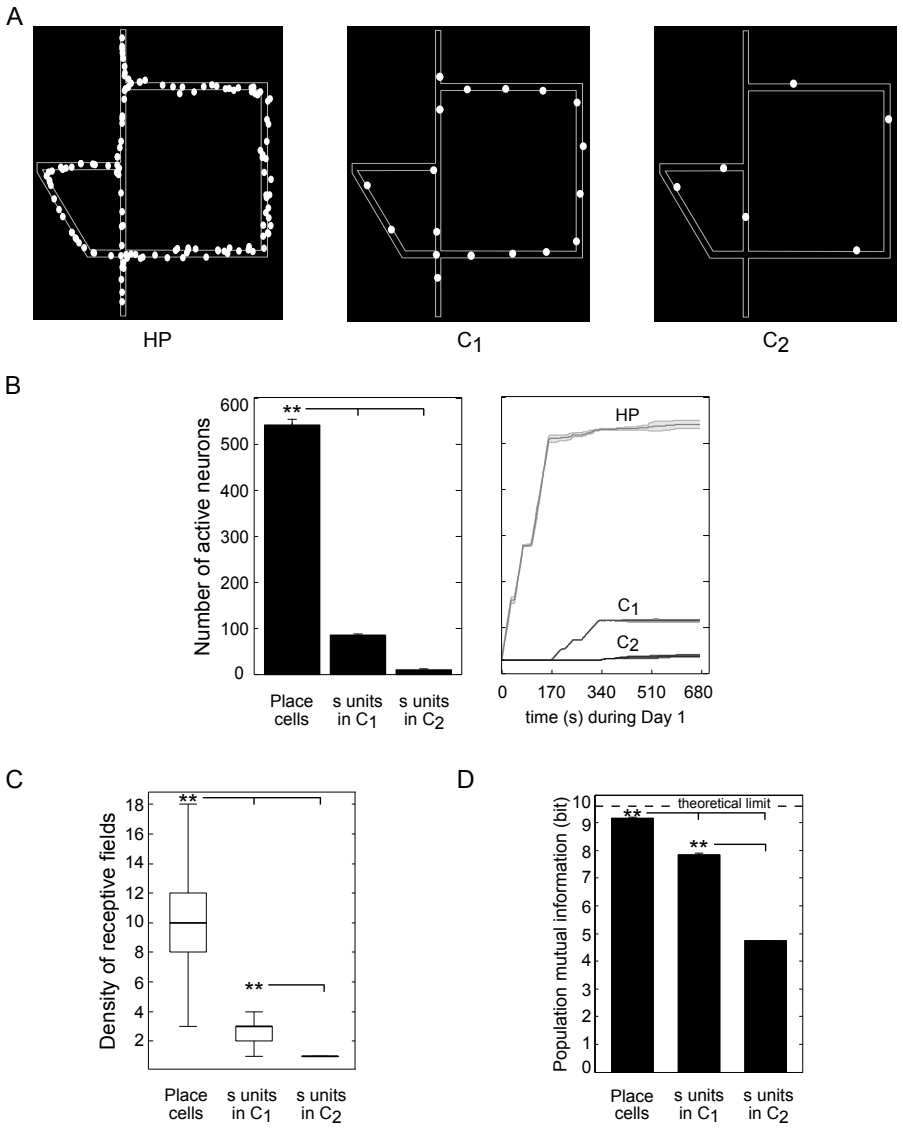

Figure 6.2: *Population place coding analysis. Simulation results.* **(A)** Examples of distributions of place field centroids for the populations of model HP cells (left), cortical neurons s in C_1 (center) and s in C_2 (right), when simulated rats were solving the 1:1 version of Tolman & Honzik's maze. **(B)** Mean number of active neurones (average over 40 animals) when learning the 4:1 Tolman & Honzik's maze (left). Evolution of the number of active neurons during the first 12 trials, i.e. Day 1 (right). **(C)** Mean spatial density (averaged over 40 animals) of receptive fields for each neural population. **(D)** Mutual information between population responses and spatial input states.

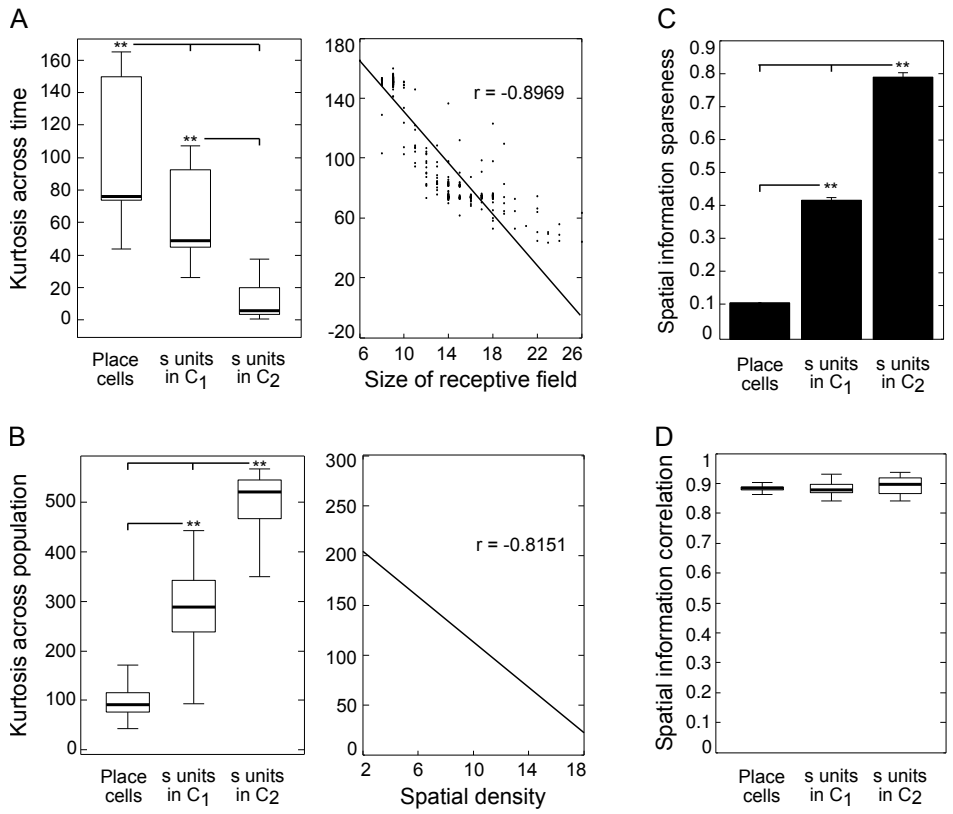

Figure 6.3: *Additional measures of the location selectivity property of neurons s in C_1 and neurons s in C_2.* **(A)** Left: sparseness of single cell responses as measured by their lifetime kurtosis. The larger the kurtosis is, the larger is the sparseness. Right: the size of the receptive field (see Fig. 6.1B) is anti-correlated to the lifetime kurtosis measure. **(B)** Left: sparseness of the population place code as measured by the population kurtosis function. Right: the density of receptive fields (see Fig. 6.2C) is anti-correlated to the population kurtosis measure. **(C)** The spatial information sparseness –computed as the ratio between population information and the sum of single cell information– demonstrates that the hippocampal place code is redundant in terms of spatial information content. By contrast, although loosing part of the spatial information, the cortical population achieves a better coding, maximizing the contribution of each unit to the population code, particularly for the C_2 population. **(D)** Spatial information Pearson correlation. Expectedly, the way spatial information is encoded by neurons firing rates is not different between the three populations: they all have their surprise information strongly correlated with the strength of the discharge activity.

ized range $[0, 1]$. Interestingly, when we analyzed the activity of PFC pyramidal cells recorded from navigating rats (see Sec. 6.1) we found a subset of neurons with no spatial correlate but with evenly distributed preferred discharge frequencies (see Figure 6.4B, bottom, for few examples). To summarize, in contrast to location-selective neurons s of the model, the activity of neurons v had characteristic discharge frequencies and encoded distance-to-reward information. During planning (i.e. the "mental" evaluation of multiple navigation trajectories), this property of v neurons allowed the value of each state to be assessed with respect to its relevance to goal-oriented behavior, consistently with PFC recordings showing reward-dependent activity patterns (Watanabe, 1996; Tremblay and Schultz, 1999).

Figure 6.4C shows how the activity of neuron v belonging to the column associated to the first intersection of Tolman's maze changed according to the task (phase of the protocol). Recall that the activity of neuron v was anticorrelated to the shortest distance to the goal among available pathways (Figure 6.4A). Thus, when at the end of Day 1 (i.e. Trial 12) the system learned to select the shortest path P1 (no block was present in the maze), neuron v exhibited the largest firing rate. When path P1 was blocked (e.g. Day 14 Trial 12), the length of the shortest available pathway (i.e. P2) increased, as indicated by the lower discharge rate of v. Finally, the distance to the goal was the largest when both P1 and P2 were blocked (e.g. Day 15 Trial 7). Consequently, the weakest activity of v corresponded to the available path P3. In order to quantify this coding property, we measured the mutual information I_t between the phases of the task and the discharge patterns of neurons v (we took neurons s as a control population). As shown in the inset of Fig. 6.4C, v neurons (unlike s neurons) provided a significant account of abstract task-related information, meaning that the phase of the protocol could be decoded reliably by observing the time course of their discharge patterns.

6.2.3 Coding of action-reward contingency changes

We studied how the activity of neurons q and d of the model contributed to decision-making. Recall that, after learning, each cortical minicolumn $(q, d) \in C_{1,2}$ encoded a specific state-action pair (s, a). The analysis reported on Figure 6.5 shows the time course of the firing rate of units q, d belonging to the column coding for the first intersection of Tolman & Honzik's maze. Figures 6.5 A,B,C focus

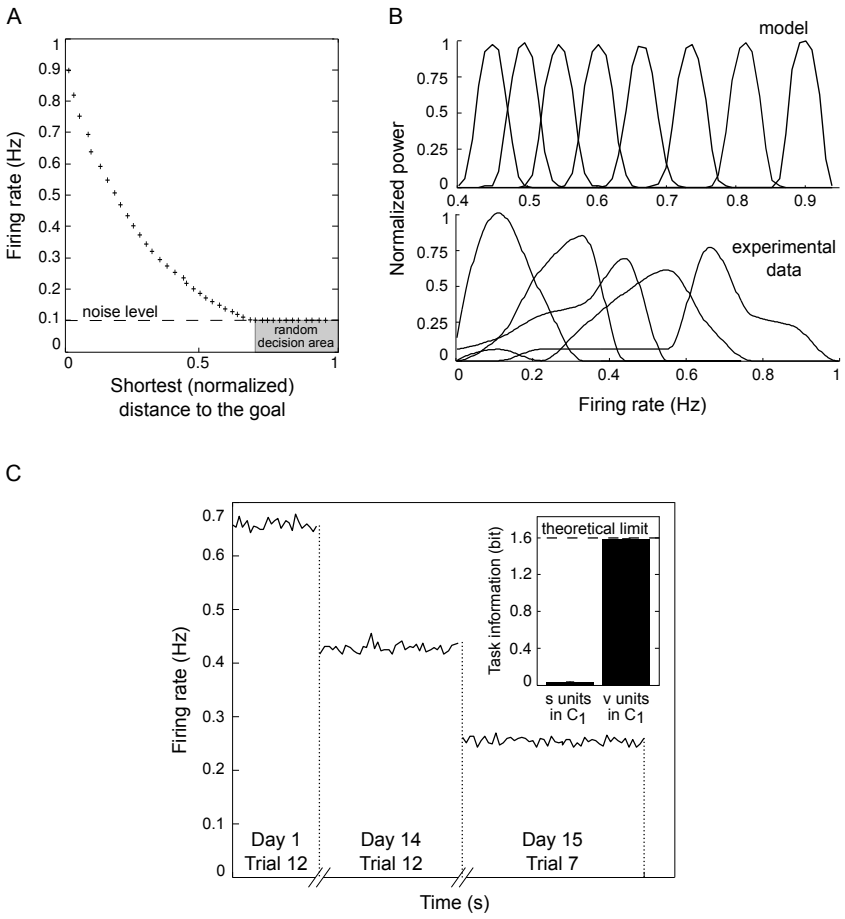

Figure 6.4: *Coding of distance-to-goal and task-related information. Simulation results and relation to experimental PFC recordings.* **(A)** Relation between the shortest distance of a place to the goal and the firing rate of the neuron v in C_1 belonging to the column representing that location. Each cross corresponds to one neuron v. Beyond a certain distance, the intensity of the back-propagated goal signal reaches the noise level. As a consequence, neurons v discharges become uncorrelated with the distance to the goal, and random decisions are made. **(B)** Frequency-selective responses of model single neurons $v \in C_1$ (top row) and of medial PFC pyramidal cells recorded from navigating rats (bottom row). **(C)** Relation between task-related information (Day 1 Trial 12: end of "no block" phase, Day 14 Trial 12: end of "block A" phase and Day 15 Trial 7: end of "block B" phase) and firing rate of the neuron v in C_1 belonging to the column representing the first intersection point. Inset: mutual information between the phase of the task and single unit responses of s in C_1 vs. v in C_1.

on the action selection process taking place at the beginning of Trial 1, Day 2 of training (i.e. with block A). During the outward journey, the simulated animal arrived at the intersection point at $t \simeq 4$ s. Due to the policy learned during Day 1 of training (i.e. without any block in the maze), at $t \simeq 4$ s the unit q_1 of the minicolumn associated to the action leading to P1 discharged with the largest firing rate, followed by unit q_2 of the minicolumn associated to P2, and finally by q_3 related to P3 (Figure 6.5B). Thus, corresponding neurons $d_{1,2,3}$, which combined inputs from $q_{1,2,3}$, respectively, with the location-selective activities of neurons s of the same column, discharged according to the same ranking at $t \simeq 4$ s (Figure 6.5C). As a consequence, the action driven by d_1 was selected and the simulated animal proceeded along P1. However, when block A was encountered at $t \simeq 5s$, the model updated the topological representation (see Sec. 4.5.3), which resulted in a change of action-reward contingencies (with q_1 firing rate dropping below that of q_2, meaning that the action leading to P2 from the intersection point was now better scored, Figure 6.5B). This activity update is consistent with findings showing sustained discharge changes highly sensitive to a switch in reward contingencies (Mulder et al., 2003; Rich and Shapiro, 2009). Thus, when during the backward journey the animal met again the intersection point (at $t \simeq 7$ s), neuron d_2 discharged with the largest frequency (Figure 6.5A, bottom) leading to the selection of P2.

Similarly, the analysis reported on Figures 6.5 D,E,F shows how the time course of the relative strengths of the activities of neurons $q_{1,2,3}$ and $d_{1,2,3}$ determined action selection at the beginning of the probe test, Trial 1, Day 15 (with block A removed and block B inserted). Notice the increased q_1 firing frequency at $t \simeq 6$ s reflecting the re-discovery of the transition blocked at A during Days 2-14 of training.

6.2.4 Coding of prospective place sequences

After a local decision was made (based on the competition between d neurons' discharges), collateral projections w_{pd} (Figures 4.1B and 4.3A) enabled the cortical network to forward propagate the selected state-action sequence. Figure 6.6 shows how the time course of p neurons' firing patterns subserved this propagation process. First, we analyzed the receptive fields of p units as the simulated animal proceeded from the starting position towards the goal. Figure 6.6A compares the

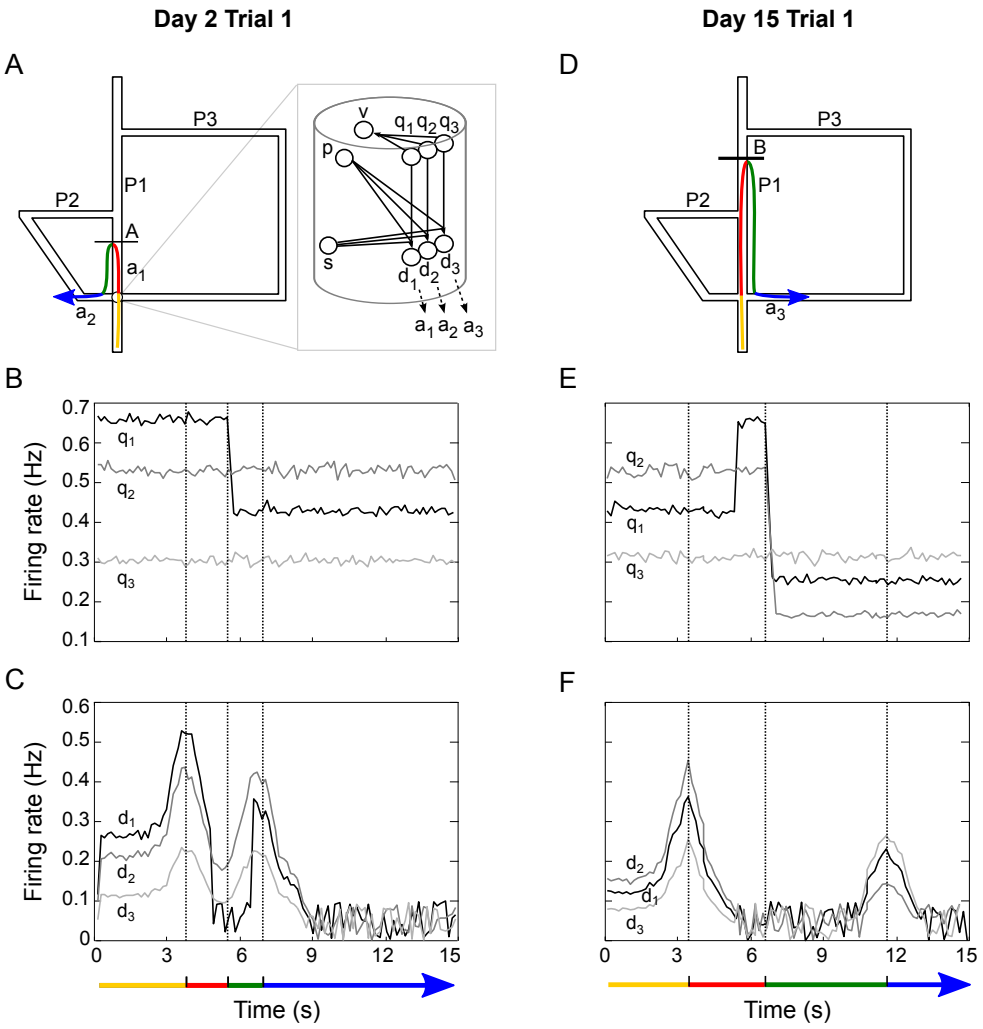

Figure 6.5: *Time course analysis of action-reward contingency changes. Simulation results.* Left column: Day 2 Trial 1 with block at A. Right column: Day 15 Trial 1 with block at B. **(A, D)** Examples of trajectories performed by simulated animals when encountering either block A or block B (distinct colors illustrate distinct actions). **(B, E)** Time course profile of firing rates of three neurons q_1, q_2 and q_3 belonging to the column encoding the first intersection (and, in particular, to the minicolumns representing the actions a_1, a_2 and a_3, respectively). Vertical dotted lines indicate decision-making events (according to colored arrows at the bottom). **(C, F)** Time course profile of neural activity of three neurons d_1, d_2 and d_3 belonging to the column representing the first intersection and to the minicolumns representing the actions a_1, a_2 and a_3, respectively.

activity profiles of neurons p and s belonging to the same columns (four different columns are considered in this example). In contrast to the symmetrical receptive fields of neurons s (see also Figure 6.1), all neurons p had asymmetric response profiles with negative skews (i.e. with the left tail of the distribution longer than the right tail). The skewness of these neural responses increased quasi-linearly with the number of synaptic relays forming a mentally planned trajectory (Figure 6.6A, top-right inset). When we analyzed PFC data recordings from navigating rats (see Materials and Methods, Sec. 6.1), we also found a subset of neurons with asymmetric tuning curves, whose negative skewness seemed to be correlated to the distance traveled by the animal (Figure 6.6B).

Another difference between neurons p and s of the model was that the peak discharge frequency of neurons s did not have any significant modulation, whereas all neurons p had mean peak firing rates positively correlated to the distance traveled towards the goal (Figure 6.6A). Accordingly, Jung et al. (1998) provided experimental evidence for increased neuronal firing rates during the approach to a reward. Finally, an important property of neurons p of the model is that their discharge tended to temporally anticipate the activity of neurons s (Figure 6.6A). In other words, p neurons encoded prospective place information predicting the next state visited by the animal. A cross-correlogram analysis showed that p neurons' activity anticipated the discharge of s neurons by a mean time delay $\tau \simeq 1.6$ s, std=± 0.6 s (given a constant velocity of $\simeq 15$ cm/s). The prospective coding property of neurons p is consistent with experimental findings on PFC recordings reported by Rainer et al. (1999).

We further studied the predicting nature of p neurons' activity in relationship to experimental data on neural encoding of the serial order of planned sequences before the action begins (Averbeck et al., 2002). In their experiment, Averbeck et al. (2002) performed simultaneous recordings of PFC single cell activities from monkeys drawing sequences of lines (i.e. segments forming abstract shapes). Each segment was associated to a distinct pattern of neural activity, and the relative strength of these patterns *prior* the actual drawing was shown to predict the serial order of the sequence of segments actually drawn by monkeys (Figure 6.6C left). Consistently, we found that the ranking of the discharge frequencies of p neurons *before* the actual execution of a planned trajectory was a good predictor of the serial order of the states to be visited by the simulated animal (Figure 6.6C

right). This relationship not only held at time $t = 0$ (i.e. at the very beginning of a trajectory), but for every time t, meaning that the ranking of p neurons' firing rates could predict the order of future state sequences at any moment.

6.2.5 Comparative analysis between model and experimental prefrontal population activity patterns

We studied to what extent the neural populations of the model (i.e. s, v, p, q and d neurons) could be quantitatively segregated on the basis of a set of statistical measures. We then compared the results to those obtained by applying the same clustering analysis to a population of neurons recorded from the medial PFC of navigating rats (see Materials and Methods Sec. 6.1).

We first gathered all non-silent simulated neurons recorded during the 4:1 version of Tolman & Honzik's task. All types of units (i.e. s, v, p, q, d) were pulled together in a data set. We characterized each neuron's discharge by measuring its mean firing rate, standard deviation, skewness, lifetime kurtosis, spatial information per spike and spatial mutual information. Then, we performed a principal component analysis (PCA) on the multidimensional space containing the values provided by these measures per each neuron (see Fig. 6.11A for details). Figure 6.7A shows the resulting data distribution in the space defined by the first three principal components. Interestingly, model neurons with different functional roles tended to occupy distinct regions of the PCA space. For instance, neurons $v, q \in C_1, C_2$, whose function in the model is to propagate goal information and code for the distance to the goal, were located within the same portion of the PCA space (blue and cyan crosses and circles). All neurons $s \in C_1$, which primarily code for spatial locations, were also clustered within the PCA space (red crosses). Neurons $p, d \in C_1$ (and also $p \in C_2$), responsible for forward signal propagation and local decision making, respectively, were aggregated within the same region (gray and black crosses, and black circles). Finally, neurons $s, d \in C_2$, mainly involved in high-level mapping and navigation planning, were also separated from other units in PCA space (gray and red circles).

Figures 6.7B, C, D display the mean values, averaged over each population $s, d, p, q, v \in C_1, C_2$ of the model, of three statistical measures (out of six) used to perform the PCA. These diagrams can help understanding the data point distribution of Figure 6.7A. When considering the mean spatial information per spike

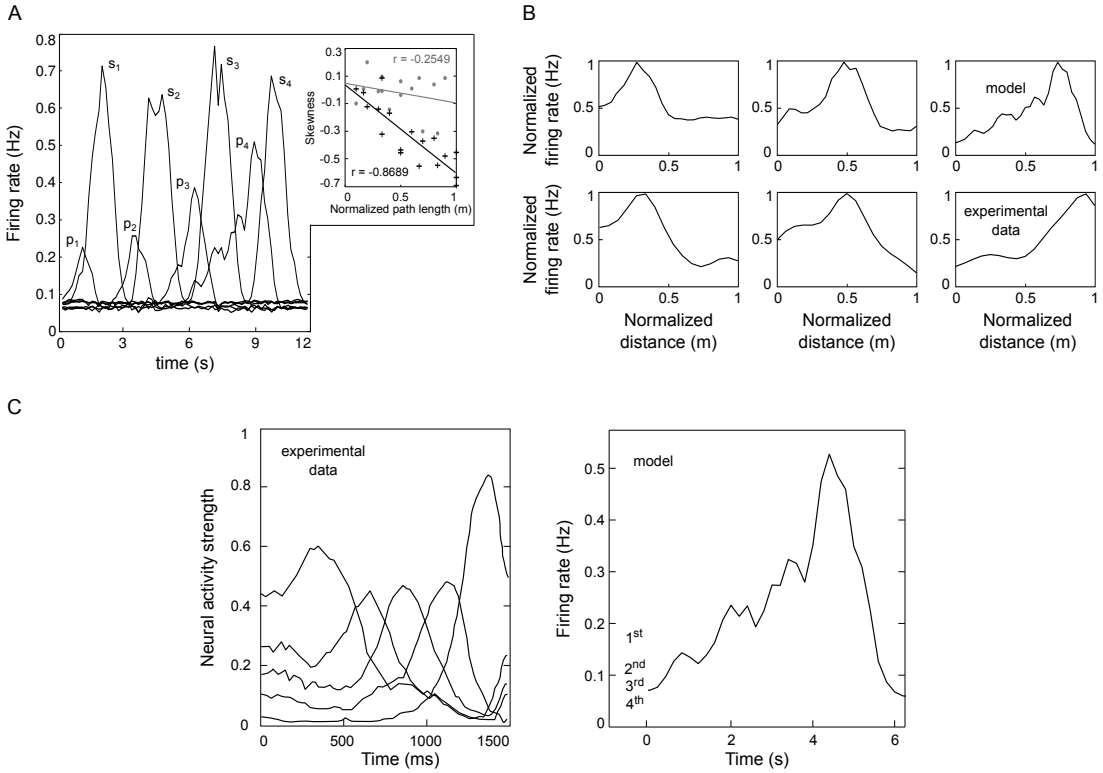

Figure 6.6: *Coding of prospective place sequences. Simulation results and relation to experimental PFC recordings.* **(A)** Comparison of time course shapes of the responses of four pairs of neurons s_i and p_i belonging to the same column ($i = 1 \cdots 4$). Inset: correlation between the position of a given column within a planned path (measured as the path length from the starting column to that given column) and the skewness of the time course profile of its neuron p activity (black crosses) or its neuron s activity (gray dots). **(B)** Asymmetric responses of model single neurons $p \in C_1$ (top row) and of pyramidal cells recorded from the PFC of navigating rats (bottom row). **(C)** Sequence order coding carried out by a population of monkey PFC neurons (left; data courtesy of Averbeck et al. 2002, copyright © by the National Academy of Sciences). Each curve denotes the strength of the neural activity encoding a specific segment of a planned drawing sequence (the peak of each curve corresponds to the time when the segment is actually being drawn). Similarly, a sequence order coding property was observed when recording neurons p in C_1 of the model (right). Each curve measures the activity of a neuron p belonging to a planned trajectory. The peaks of activity represent the times when places are actually visited.

(Fig. 6.7B), at least three groups could be observed: neurons whose activity had nearly no spatial correlate ($q, v \in C_1, C_2$), neurons conveying intermediate amounts of spatial information ($s, d, p \in C_1$ and $p \in C_2$), and neurons with larger spatial information values ($s, d \in C_2$). The mean firing rate parameter (Fig. 6.7C) allowed two distinct groups to be clearly identified: one with low average firing (neurons $s, p, d \in C_1, C_2$), and one with high firing rates (neurons $q, v \in C_1, C_2$). Together with Figure 6.7A, this diagram can help understanding why neurons $q, v \in C_1, C_2$, which had almost no spatial correlate and very high firing rates compared to other populations of the model, were well segregated within the same region of the PCA space (Fig. 6.7A, blue and cyan crosses and circles). Finally, when comparing the mean skewness values of all neural populations (Fig. 6.7D), neurons $d, p \in C_1$ and $p \in C_2$ were pulled apart, according to their distribution in the PCA space (Fig. 6.7A, gray and black crosses, and black circles). As a control analysis, we extended the data set used for the PCA by adding a population of neurons with random Poisson activities. As shown in supplementary Fig. 6.8, the population of Poisson neurons (light green data points) was well separated from all model neurons within the space defined by the first three principal components, suggesting that the variability of model discharge properties could not be merely explained by a random Poisson-like process.

We then applied an unsupervised clustering algorithm (k-means clustering method with $k = 3$) to partition the distribution of data points of Figure 6.7A, based on the discharge characteristics of model neurons. This blind clustering analysis (i.e. without any a priori knowledge on neural populations) allowed us to identify three main groups (Fig. 6.9A). The first cluster (blue data points) corresponded to non-spatial, reward-related neuronal activities (i.e. neurons $q, v \in C_1, C_2$). The second cluster (green points) represented location-selective activity (mainly from neurons $s, p, d \in C_1$, but also including some neurons $p \in C_2$). The third cluster (red data points) corresponded to location-selective activity of neurons in the cortical network C_2 (i.e. mainly $s, d, p \in C_2$). See supplementary Figure 6.10 for details on the composition of the three identified clusters.

We performed the same series of analyses on a dataset of medial PFC neurons recorded from navigating rats (see Materials and Methods, Sec. 6.1). We characterized every recorded activity according to the same set of statistical measures

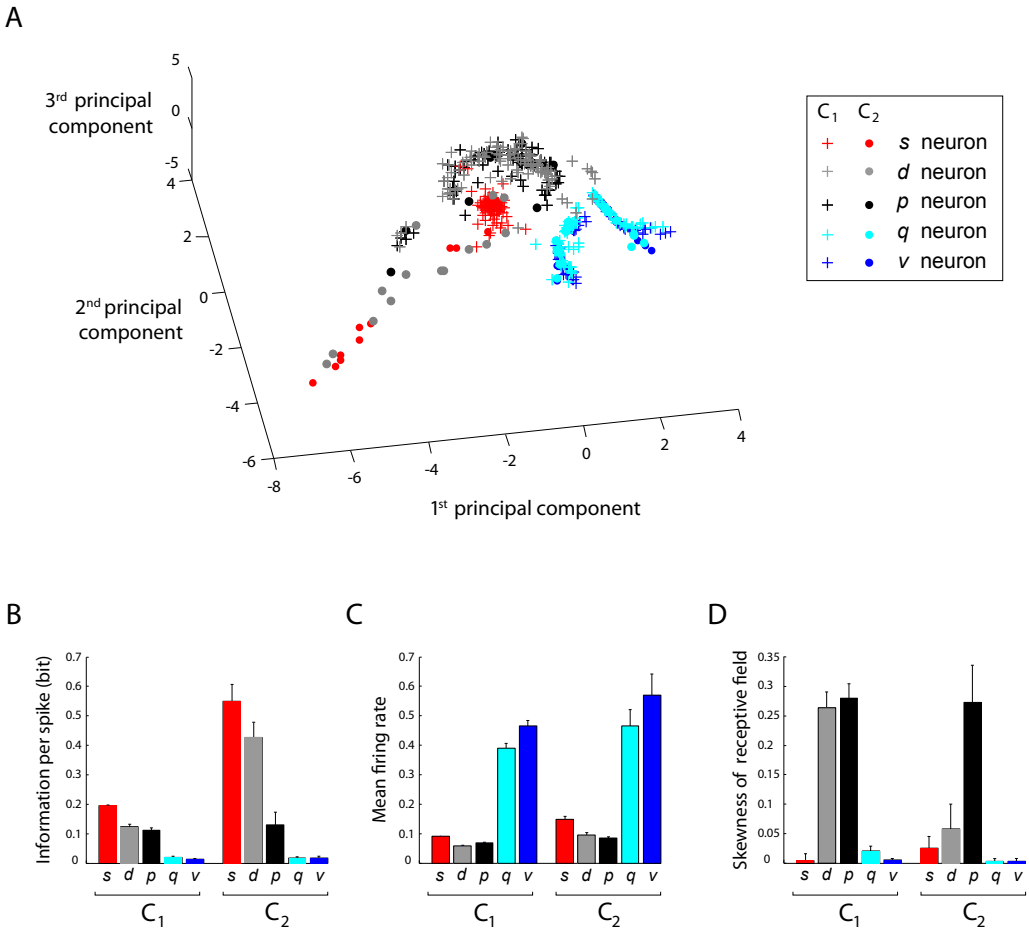

Figure 6.7: *Principal component analysis of simulated neuronal activities.* **(A)** Simulated neurons represented within the space defined by the first three principal components. **(B)** Spatial information per spike averaged over each neural population of the model. **(C)** Mean firing rate averaged over each neural population. **(D)** Mean absolute skewness average over each population. The color code is the same used in (A).

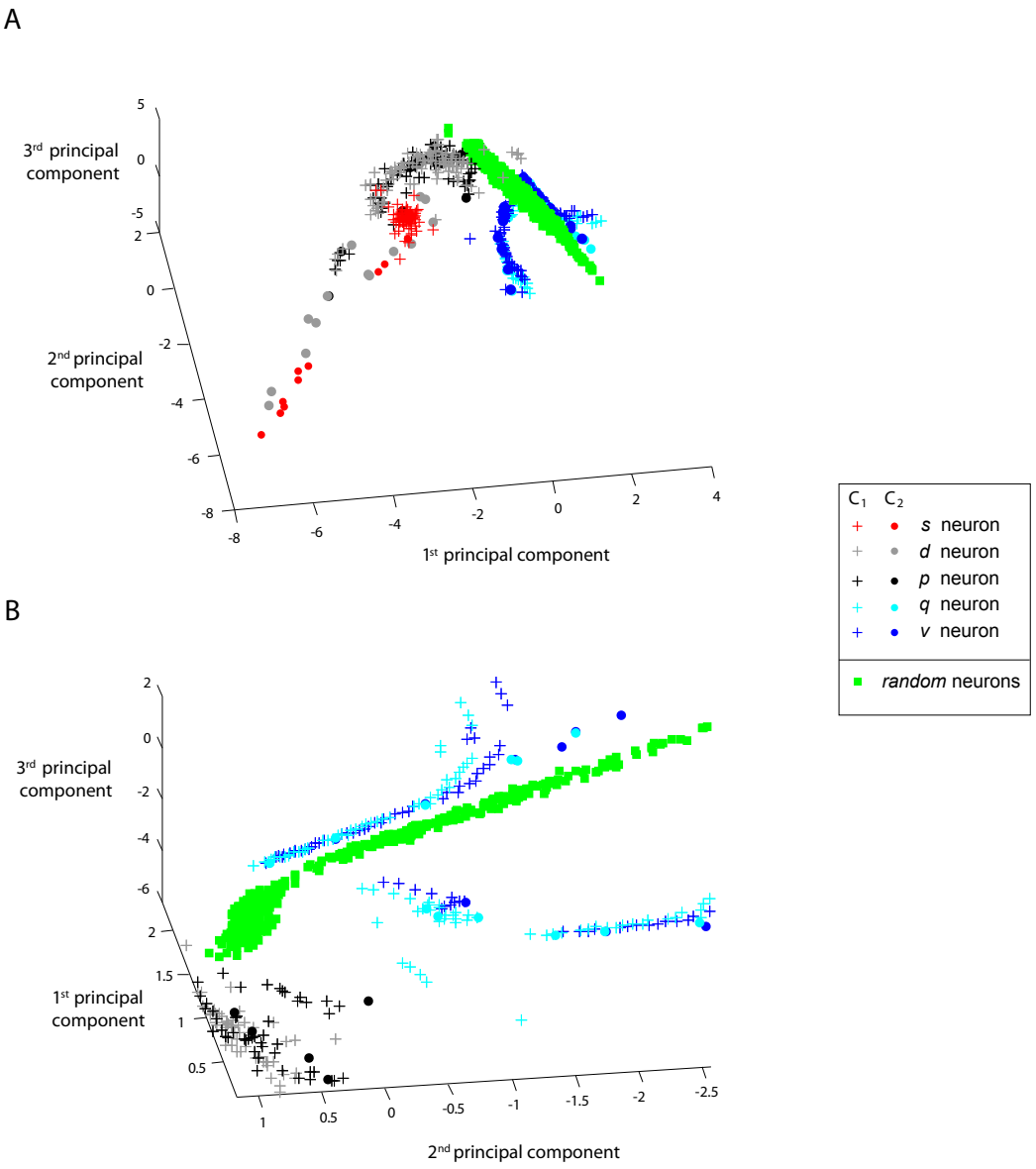

Figure 6.8: *Principal component analysis (PCA) of simulated neuronal activity.* Comparison between model and random population actvities. Two different views of the same three-dimensional PCA space are shown (A and B, respectively). The size of the original data set used for the analysis reported on Figure 10 was doubled by adding a population of Poisson neurons. The distribution of the mean firing rates over the original data set was fitted by the distribution of the mean firing rates computed over the population of Poisson neurons.

used for model neurons (i.e. mean firing rate, standard deviation, skewness, lifetime kurtosis, spatial information per spike and spatial mutual information). Then, we applied a PCA on the resulting high dimensional space containing, per each neuron, the resulting values of these measures (see Fig. 6.11B for details). Finally, we used the same unsupervised k-mean clustering algorithm to partition the data distribution in the space defined by the first three principal components. As for simulated data, the clustering method identified three main classes (Fig. 6.9; with red, green, and blue data points corresponding to three subsets of electrophysiologically recorded activities in the PFC). We then compared model and experimental clusters (Figs. 6.9C, D, E) in order to investigate whether real and simulated data points belonging to the same clusters shared some discharge characteristics. In terms of mean spatial information (Figs. 6.9C), we found similar non-homogeneous distributions between model and real clusters. Both red clusters encoded the largest spatial information content. Recall that the model red cluster mainly contained activities from location-selective neurons $s, d, p \in C_2$ (as quantified in supplementary Figure 6.10B). When looking at mean firing rates averaged over each cluster (Figs. 6.9D), we found that both real and simulated activities within the blue clusters had significantly larger frequencies than others. The model blue cluster was mainly composed by neurons $v, q \in C_1, C_2$ propagating reward-related information. Finally, when comparing the mean absolute values of the skewness of receptive fields (Figs. 6.9E), we found both model and experimental populations with asymetric fields (i.e. non-zero skewness). Model-wise, the red and green clusters (containing neurons $d, p \in C_1, C_2$, Figure 6.10B) had the largest mean skewness. Similarly, experimental red and green subpopulations had larger skewness values than the blue population. Taken together, these results indicated that, within the data set of experimental PFC recordings, subpopulations of neurons existed with distinct discharge properties, and that these subpopulations might be related to distinct functional groups predicted by the model.

6.3 Conclusion

On the neural level, we characterized the activities of model neurons and compared them to electrophysiological data from real PFC neurons. Our neural response analysis suggests how the interplay between the model hippocampus and

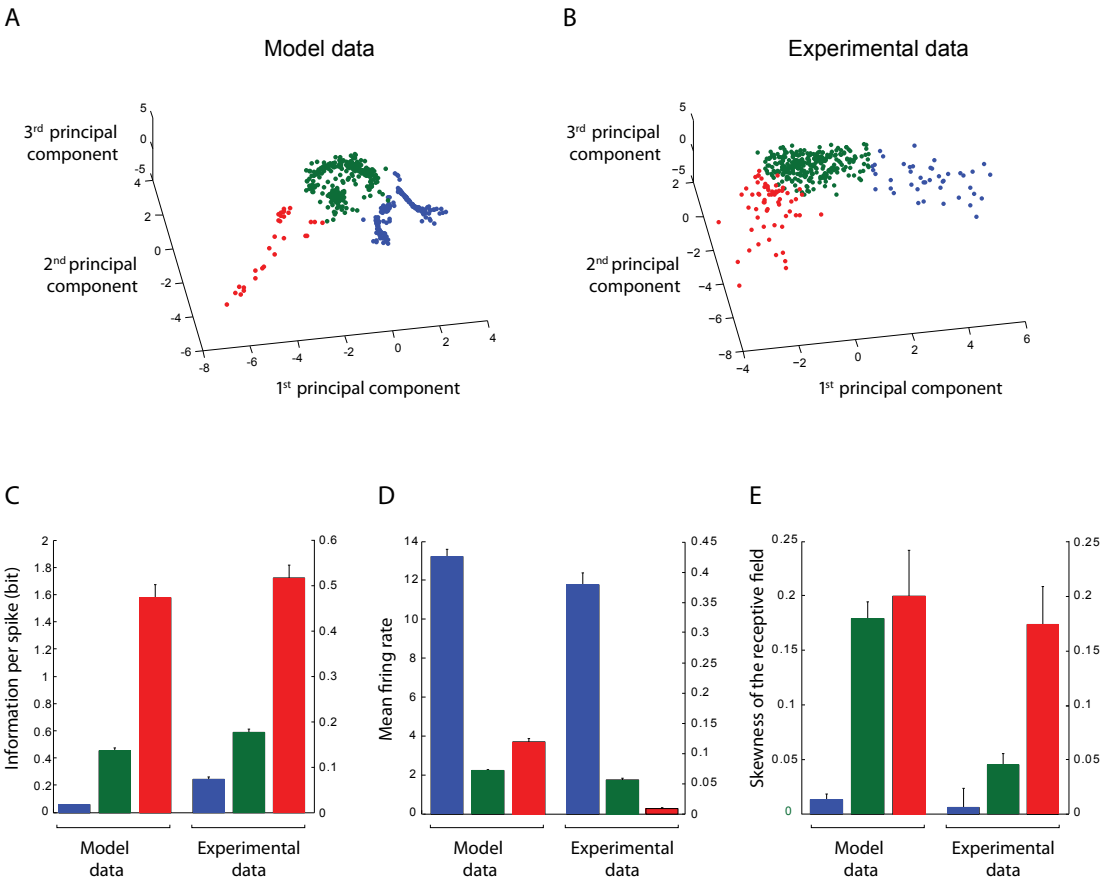

Figure 6.9: *Principal component analysis and unsupervised clustering of simulated and real neuronal activities.* **(A)** Clustering of model activities within the PCA space. The same color scheme (used to discriminate clusters) is applied throughout the entire figure. **(B)** Blind clustering of real PFC recordings represented in the three first principal components space. **(C, D, E)** Mean information per spike, firing rate and skewness for real vs. model subpopulations (i.e. clusters).

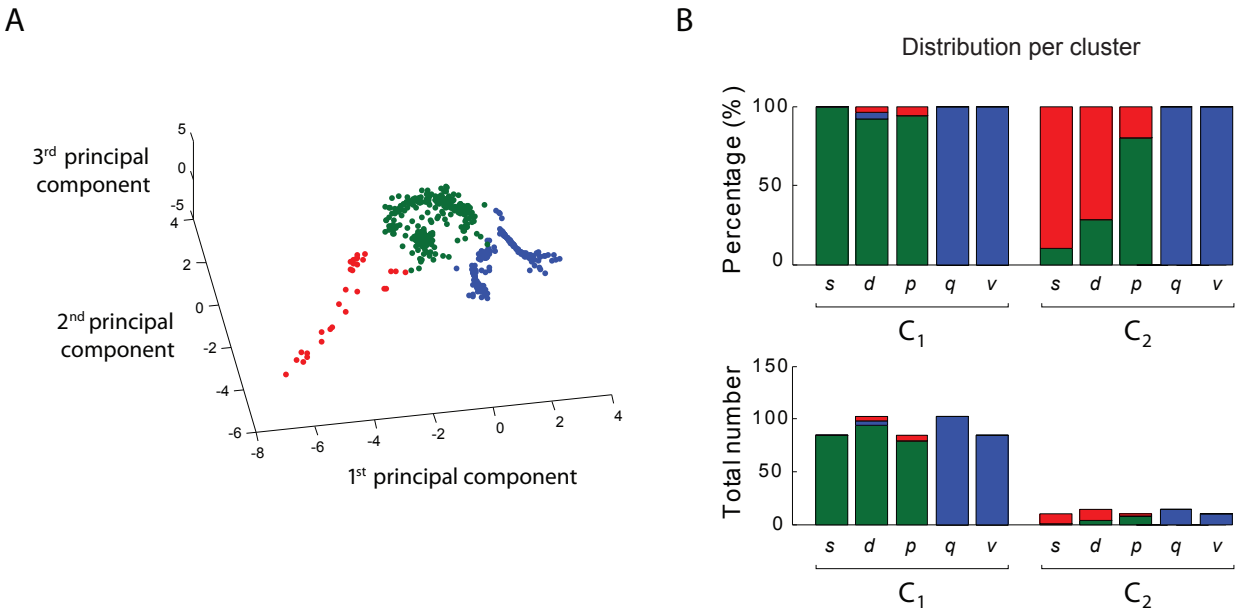

Figure 6.10: *Principal component analysis (PCA) and unsupervised clustering of simulated neuronal activities.* **(A)** Clustering of model activities within the PCA space (first three principal components). **(B)** Distribution of neural populations $s, p, v, d, q \in C_1, C_2$ for each cluster (top: percentages; bottom: absolute counts).

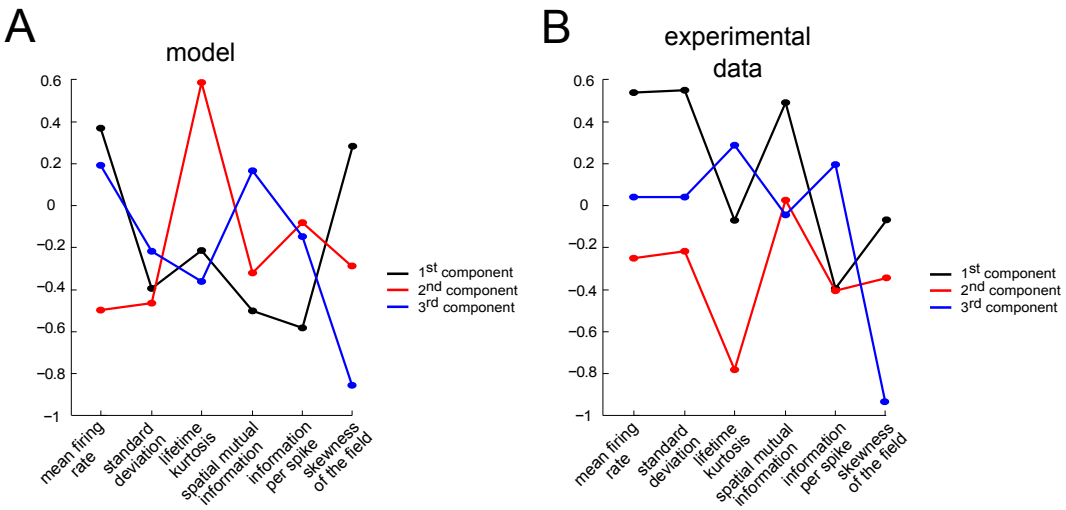

Figure 6.11: *Principal component analysis of simulated (A) and real (B) neuronal activities.* Eigenvalues (top) and structure of the principal components (bottom).

the prefrontal cortex can yield to the encoding of manifold information pertinent to the spatial planning function, including, for example, distance-to-goal correlates. The model also provides a functional framework for interpreting the activity of prefrontal units observed during performance of spatial memory tasks (Watanabe, 1996; Jung et al., 1998; Tremblay and Schultz, 1999; Rainer et al., 1999; Averbeck et al., 2002; Mulder et al., 2003; Hok et al., 2005; Benchenane et al., 2010). In general, our results are consistent with the hypothesis that cognitive control stems from the active maintenance of patterns of activity in the PFC that represent goals and means to achieve them (Miller and Cohen, 2001).

The next chapter provides a short descriptions theoretical models adressing navigation planning in the prefrontal cortex.

Chapter 7

Related works

Computational modeling studies have covered many high level functions related to the PFC, from the gating of information to the working memory, to the mechanisms subserving sustained activation of PFC neurons, to decision making and planning (O'Reilly et al., 2010). Here we focus on models of the neocortex (including the PFC) addressing navigation planning.

7.1 Main models

Topological map learning and path planning have been extensively studied in biomimetic models (see Meyer and Filliat, 2003 for a general review; see also Schmajuk and Voicu, 2006 for theoretical discussions on hierarchical cognitive maps). In particular, several studies took inspiration from the anatomical organization of the cortex and implement planning thanks to an *activation-diffusion* (or *spreading activation*) mechanism which is a neural implementation of a simple breadth-first graph search mechanism (Lei, 1990; Mataric, 1992). Burnod (1988) proposed one of the first models of the cortical column architecture, called "cortical automaton". He also described a "call tree" process that can be seen as a neuromimetic implementation of the activation-diffusion principle. Some subsequent studies employed the cortical automaton concept (Bieszczad, 1994; Frezza-Buet and Alexandre, 1999), while others used either connectionist architectures (Lieblich and Arbib, 1982; Schmajuk and Thieme, 1992; Muller et al., 1996; Franz et al., 1998; Dehaene and Changeux, 1997; Voicu, 2003; Banquet et al., 2005) or Markov decision processes (Fleuret and Brunet, 2000).

7.2 Comparison with Hasselmo's model (2005)

Our approach is similar to that of Hasselmo (2005), who also addressed goal-directed behavior by modeling the PFC columnar structure. Both Hasselmo's and our model architectures employ minicolumns as basic computational units to represent locations and actions, to propagate reward-dependent signals, and mediate decision making. Yet, the two models differ in the encoding principles underlying the learned representations, which generate, consequently, distinct behavioral responses. In contrast to the topological (actually hybrid topological-metrical) maps established by our model, Hasselmo's model builds representations that are closer to goal-directed route-based maps (i.e. two intersecting routes will not necessarily be merged into a common representation; Trullier et al. 1997). Moreover, the connectivity layout of Hasselmo's model permits the encoding of state-response-state chains provided the presence of a reward signal, whereas our model allows unreinforced (i.e. latent) spatial learning to occur (Tolman and Honzik, 1930b; Tolman, 1948; O'Keefe and Nadel, 1978; Gaskin and White, 2007). Within the reinforcement learning framework (Sutton and Barto, 1998), Hasselmo (2005)'s model could be understood in terms of model-free temporal-difference learning, whereas the model presented here would be closer to model-based reinforcement learning principles, proposed to occur in the PFC (Daw et al., 2005). Finally, in contrast to Hasselmo (2005)'s work and as explained henceforth, we focus on the functional relationship between the hippocampus and the PFC in encoding complementary aspects of spatial memory with more emphasis on the time course analysis of neural responses mediating place coding *vs.* decision making.

To test his model, Hasselmo uses a discrete squared maze. The agent's task consists in reaching a goal thanks to its representation of the environment encoded with its minicolumns. Both start and goal locations are fixed. Fig. 7.1 shows the results of both models on 3x3 and 9x9 square maze. Whereas they exhibit almost the same behaviour in the 3x3 maze, the results obtained in the 9x9 maze show that the model of Hasselmo triggers less efficient path than ours and thus reaches the goal a significantly lower number of times. This can be explained by the route-like navigation provided by Hasselmo's model (see Fig. 7.1 for a simple example), which is highly dependent of the exploration performed by the agent.

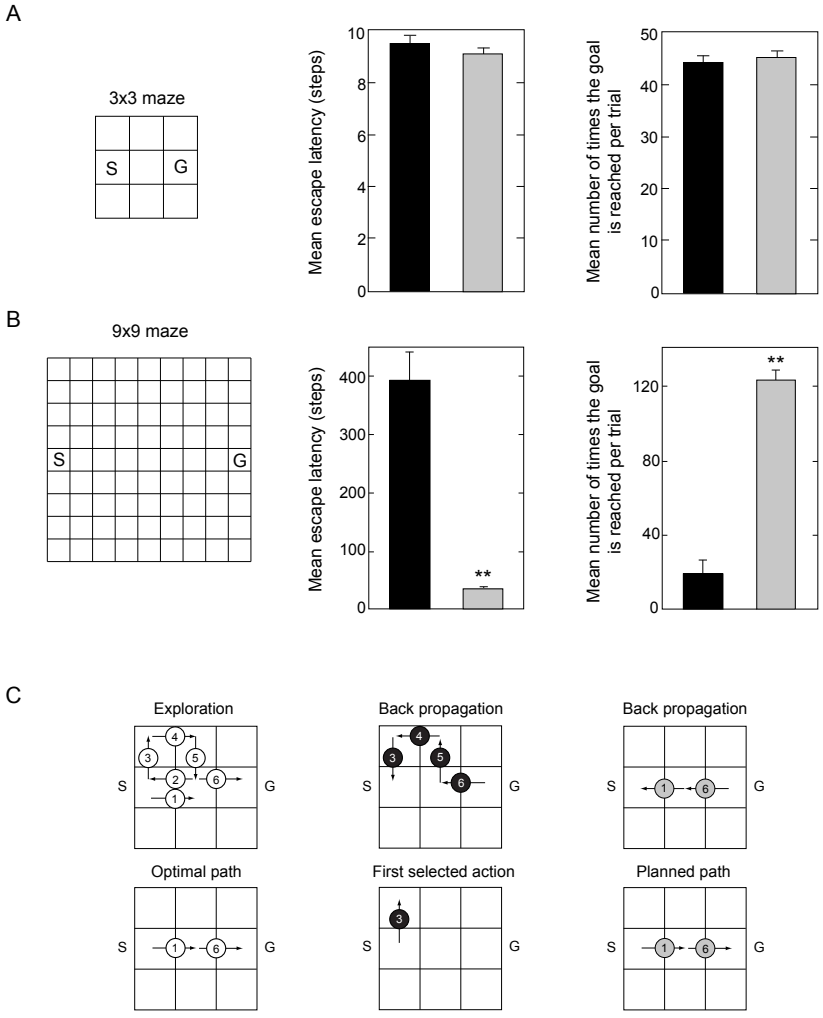

Figure 7.1: *Comparison of behavioural responses of the model by Hasselmo (2005) and our model.* **(A)** Results on a 3x3 square maze (Hasselmo, 2005). S = starting location; G = goal location. Black bars = Hasselmo (2005)'s model. Gray bars = our model. **(B)** Results on a 9x9 square maze. Statistics were computed on n=50 trials, each lasting 2000 time steps. **(C)** A simple example showing the difference between a route-based map (Hasselmo, 2005) vs. a topological map (our model). In Hasselmo's model, the subparts of the route going from S to G are not merged. More precisely, the chains made of transitions 1-2 and 5-6 are not integrated to form the new 1-6 chain. This is only achieved in a topological learning system like ours. As a consequence, the back-propagating signal in Hasselmo's model will trigger the selection of the long route (3-4-5-6), which is suboptimal.

7.3 Conclusion

Several models have been proposed to address spatial planning. Some of them pointed out a role for the hippocampus whereas other models were suggesting a main contribution from the prefrontal cortex. However, to the best of our knowledge, none of these latter models took inspiration from the columnar organization of the PFC to relate neuronal discharges to the behavior. The model of (Hasselmo, 2005) is based on a network of minicolumns, but does not plan sequences of actions as we defined. Thus the model presented in the previous chapters is a new approach to explain planning abilities of rodents, in relation with PFC neuronal activities.

The next chapter will be the final conclusion. It discusses the overall results of the model and summarizes the contributions and possible future developments of this thesis.

Part IV

General discussion & appendices

Chapter 8

General discussion

At the beginning of this dissertation we established two main goals of this thesis work: *(i)* understanding and modeling neural mechanisms underlying biological spatial navigation planning; and *(ii)* inferring links between electrophysiological discharges recorded in the brain and behavior of the model. In this chapter, we discuss the achievements of this work. We also discuss our future direction of research.

8.1 Contributions

We presented a model focusing on navigation planning, mediated by a population of prefrontal cortical columns. Our simulation results demonstrate that the model can reproduce rodent behavior previously attributed to the animals' ability to experience a cognitive "insight" about the structure of the environment (Tolman and Honzik, 1930a), invariantly with respect to the size of the maze. This property relies on the ability of the model to encode cognitive maps with a resolution that fits the structure of the environment (e.g. alleys). Another property of the model is its ability to find shortcuts through unexplored portions of the environment. We also characterized the activities of model neurons and compared them to electrophysiological data from real PFC neurons. Our neural response analysis suggests how the interplay between the model hippocampus and the prefrontal cortex can support the spatial planning function. The model also provides a functional framework for interpreting the activity of prefrontal units observed during performance of spatial memory tasks.

8.2 Main assumptions of the model

Our model is based upon two main assumptions. First, the model relies on the columnar organization of the cortex. The existence of cortical columns is supported by many experimental studies (Mountcastle, 1997; Buxhoeveden and Casanova, 2002), although no clear general function has been proposed to explain their role in cortical processing (Horton and Adams, 2005). In addition, Rakic (2008) stressed that the size, cell composition, synaptic organization, expression of signaling molecules, and function of various types of columns are dramatically different across the cortex, so that the general concept of column should be employed carefully. In our model, we use the term "column" for a local micro-circuit composed by neurons processing common spatial information, and we propose that columnar organization may be a substrate suitable to implement a topological representation of the environment. Second, our planning model relies on an activation diffusion mechanism. At the neural level, this mechanism suggests waves of action potentials through the neocortex. This is not a strong assumption, since several studies have demonstrated such phenomena as propagating waves of activity in the brain (Vogels et al., 2005; Wu et al., 2008). For example, Rubino et al. (2006) suggested that oscillations propagate as waves across the surface of the motor cortex, carrying relevant information during movement preparation and execution.

8.3 Differential roles of PFC and hippocampus in spatial learning

The successful performance of our model in large environments relies on its ability to build multiscale environment representations. This is in line with the proposal by McNamara et al. (1989) who have suggested that humans can solve complex spatial problems by building a hierarchical cognitive map, including multiple representations of the same environment at different spatial scales. Moreover, animals may be able to chunk available information and build hierarchical representations to facilitate learning (Roberts, 1979; Dallal and Meck, 1990; Fountain and Rowan, 1995; Macuda and Roberts, 1995; Meck and Williams, 1997). Recently, multiscale spatial representations have been identified at the neural level.

For example in the entorhinal cortex, Hafting et al. (2005) have shown that grid cells have spatial fields forming a grid of variable resolution. Kjelstrup et al. (2008) have provided neural recording of place cell activities in a large maze, and their results support the same multiscale coding property in the hippocampus. In our model, we suggest that this kind of multiscale representations should also be found in the neocortical areas such as the prefrontal cortex, commonly associated with high-level cognitive processes. The role of the PFC in the learning of hierarchical representations has been proposed before. For example, Botvinick et al. (2009) reviewed how the hierarchical reinforcement learning framework (Sutton et al., 1999) could explain the mechanism by which the PFC aggregates actions into reusable subroutines or skills. The multiscale property is applied there for actions instead of states as in our approach. From a biological point of view, recent studies directly pointed out the role of the PFC for hierarchical representations, with a possible anatomical mapping of the hierarchical levels along the rostro-caudal axis of the PFC (Koechlin et al., 2003).

In spite of a possible common role for the PFC and the hippocampus in multiscale spatial coding, our work suggests different roles of the PFC and the hippocampus in the planning process. Namely, we propose that the hippocampus is more involved in the representation of location (O'Keefe and Nadel, 1978) and, possibly, route learning (Dragoi and Buzsáki, 2006; Rondi-Reig et al., 2006), while the PFC is responsible for topological representations and action selection. From a more general perspective, a route could be seen as an example of navigation from a point to another, or, in non-spatial terms, an episode. In contrast, the more integrated topological representation would be more similar to a set of navigation rules. This hypothesis is in accordance with data showing that the hippocampus would be involved in instance-based episodic memory, whereas the PFC would be linked to rule learning from examples (Doeller et al., 2005, 2006; Winocur et al., 2007).

Our model is consistent with recent studies suggesting a role for the PFC in prospective memory (Goto and Grace, 2008; Schacter et al., 2008). Goto and Grace (2008) showed that, depending on the dopamine receptors activation, PFC either incorporates retrospective information processed by the hippocampus or processes its own information to effect preparation of future actions. This is in accordance with our model which includes hippocampal information to localize

itself in the environment, and then propagates reward signal to generate a goal-directed sequence of action. Moreover, Mushiake et al. (2006) showed that neural activity in the PFC reflects multiple steps of future events in action plans. They suggested that animals may be engaged in planning sequences in a retrograde order (starting from the goal to the first motion), in conjunction with a sequence planning with an anterograde order. At the cognitive level, the activation diffusion planning process provides a capacity of mental simulation of action selection. Schacter et al. (2008) recently reviewed theories on simulation of future events and neural structures associated with this cognitive ability. They showed that the same core network, which plays a role in remembering, is also implied in mental simulation. This network involves prefrontal as well as medial temporal regions including the hippocampus, thought to encode prospective and retrospective memories (Mehta, 2000; Ferbinteanu and Shapiro, 2003).

8.4 From neural activity in the PFC to behavior

The results of the simulation of Tolman and Honzik detour task show that the behavior of the model is consistent with an "insight" demonstrated by rats in this task. The insight, as defined by Tolman and Honzik, is the ability to conceive that two paths have a common section, and so when a passage through the common section is blocked, both of these paths are necessarily blocked and a third, alternative pathway, should be chosen. The realization that a common section exists leads to two conclusions. First, animals do not act exclusively according to stimulus-response associations, but use some kind of mental representation of the environment (Tolman, 1948). For example, in the conditions of the detour task (Figure 5.1A), the rats chose path 3 without actually testing path 2 during probe trials and so they did not have a chance to form the correct stimulus-response associations to solve the task. In order to choose the correct path 3, rats had to mentally replay path 2 and realize that it was blocked, suggesting the existence of a spatial representation. Second, a representation of the environment in terms of *routes* is not sufficient to solve the task. Indeed, if after training animals store separate representations of routes via paths 1-3, then the fact that route 1 is blocked should not lead to the conclusion that route 2 is also blocked. In summary, the results of this experiment suggest the existence of a *topological graph*-like representation in

which common points (nodes) and common sections (edges) are identified. The model presented here proposes a plausible way of how such a representation can be built. In terms of the model, the insight capability in the detour task is mediated by the propagation of the goal signal through the nodes of the spatial graph, in which the common section of paths 1 and 2 is blocked. In addition, studies demonstrating the ability of animals to make shortcuts through unexplored portions of the environment suggest that at least some metrical information is present in mental spatial maps. In our model, this metric information is represented by the angular differences between the paths originating from a common node. We show how this information can be used to make novel shortcuts, in agreement with the results of animal studies (Chapuis et al., 1983; Poucet et al., 1983)

The other important question addressed by the present study is whether the requirements of the proposed model are consistent with the neural activities observed in the PFC. We show that *all* types of neurons that are required by the model, have actually been observed in the PFC. Namely, *(i)* the state-encoding s neurons in the model correspond to spatially selective prefrontal neurons with different receptive field sizes (Figure 6.1D, see also Hok et al., 2005); *(ii)* the distance-to-goal, or value, neurons v correspond to the PFC neurons with constant discharge rate (Figure 6.4B), giving rise to the prediction that neurons with higher (constant) discharge rates can code for locations closed to reward; *(iii)* the prospective-coding p neurons in the model correspond to PFC neurons with the firing rate that increases when the animal moves toward the goal (Figure 6.6B,D, see also Rainer et al., 1999; Averbeck et al., 2002); and, finally, *(iv)* neurons q and d, which together encode state-action values, show activity patterns similar to strategy-switching neurons observed by Rich and Shapiro (2009). Indeed, the authors reported that in their task (i.e. strategy switching in a plus-maze) during the periods before and after reward contingency change, different subsets of PFC neurons were highly active. This is exactly what was observed in our model. For example, neurons q_1 and d_1 that were more active than neurons q_2 and d_2 *before* the contingency change (Figure 6.5B,C, at 4 s) became relatively less active *after* the change (Figure 6.5B,C, at 5 s).

The model provided a vantage point to interpret PFC eletrophysiological data in terms of quantitative clustering of population activity. On the basis of a set of statistical measures, we performed a principal component analysis on both sim-

ulated and real data sets of PFC recordings. This study gave rise to comparative results based on the identification of clusters of characteristic discharge properties. On the basis of this analysis, we proposed that different clusters correspond to different function in terms of their role in spatial localization and planning, reward coding, and prospective memory. In particular, our results suggest that neurons mediating planning in large scale mazes (i.e. belonging to the cortical population C_2 of the model) could be segregated from other simulated units (red cluster in Fig. 6.9). A corresponding cluster was found when analyzing real recordings, corroborating the hypothesis of the presence of neurons with similar discharge properties in the PFC. In addition, we have identified another cluster of real PFC activities which contained both pyramidal cell and interneuron responses ($\sim$60% and $\sim$40%, respectively). This cluster corresponded to goal propagating neurons of the model (blue cluster in Fig. 6.9), leading to the prediction that interneurons may contribute to decision making by participating to the propagation of information relevant to the next decision to be taken. Interestingly, in their study of spatial navigation, Benchenane et al. (2010) showed that the inhibitory action of PFC interneurons onto pyramidal cells is enhanced during periods of high coherence in theta oscillations between hippocampus and PFC occurring at decision points.

8.5 Extensions of the model and future work

The model can be used to investigate other important questions related to *(i)* PFC and its functional specialization subserving cost-benefit decision making, *(ii)* the hippocampo-frontal pathway, such as the timing relationships between neuronal activity in the PFC and the HP theta rhythm or the effect of memory consolidation on the representation encoded within the PFC. We discuss here how the computational framework provided by the model can be exploited to propose some hypotheses that we will test in future studies.

8.5.1 Cost-benefit decision making and prefrontal subdivisions

We have shown in Part II that the prefrontal cortex seems particularly well suited to integrate manifold spatial information so that it could encode multidimensional contextual representations. This would provide more efficient planning capabilities, employing cost-benefit optimization processes to select the best pathway

within the action space. As discussed in Sec. 3.3.3, Rudebeck et al. (2006) used two simple tasks of cost-benefit decision making (Fig. 3.3). They showed that the ability to choose the larger reward in spite of the effort appeared to be anterior-cingulate-dependent, not orbito-frontal-dependent, whereas the ability to choose the large reward in spite of the delay appeared to be OF-dependent, not AC-dependent. Control rats, AC-lesioned rats and OF-lesioned rats were able to choose the best option when no cost was imposed, indicating that non-conflicting decision making may not involve the PFC. This finding provides interesting data on the functional specialization within the PFC. In order to understand the neural bases of cost-benefit decision making, we discuss here a possible extension of the model with a functional subdivision of the PFC and a representation of aversive signals (effort and delay) conflicting with the reward. In the model presented in Chap. 4, decision in single-goal environment was based on the propagation of a distance-to-goal signal. In fact, it is possible to reinterpret this metrical signal. If we introduce a second goal with a smaller amount of reward, modeled by a smaller synaptic strength w_{vm} between the motivation and the second goal column (see Fig. 4.1B), then the propagated signal will not have the same meaning. It will encode both distance and reward amount. Moreover, distance can be seen as an effort (running from a place to another is tiresome) or as a delay (running from a place to another takes time). Based on these ideas, we suggest that the same model architecture can be used to propagate a cost-benefit signal (a *utility* signal) integrating effort, delay and reward size so that the simulated animal can minimize the costs and maximize the reward at the decision point.

How would ACC and OFC take part in cost-benefit decision making according to this proposed model? Instead of encoding a distance-to-goal signal through the lateral weights of our cortical network, we suggest a distributed mechanism with two separate groups of neurons (i.e., ACC and OFC) the role of which will be to integrate reward with effort and reward with delay, respectively (Fig. 8.1A). Tthe ACC population will compute a trade-off between effort and reward, so that effortful actions leading to high rewards will be favored. The goal signal r_R of the right arm, propagating from the goal column in the PFC network, will be compared to the effort e_R needed to get the right reward (i.e. $E(r_R, e_R)$). This effort-to-goal signal $E(r_R, e_R)$ will then be propagated to the column representing the intersection. The same principle will be applied to encode each topological

transition. The OFC population enables the computation of a delay-to-goal signal D in a similar way so that long delays leading to high rewards are favored. At the intersection point, the action leading to the goal with the best effort-reward and delay-reward trade-off will be selected by the PFC network because its associated (q, d) neurons will be highly active.

If we lesion the ACC population during the effort-based decision-making (Rudebeck et al., 2006), the effort-to-goal signal encoded by this population will not be able to propagate anymore (Fig. 8.1B). The PFC network will only receive information from the OFC population. Since OFC activity does not account for the compromise between effort and reward (i.e. $D(r_L, d_L) = D(r_R, d_R)$), it will be impossible to favor the right arm. As a consequence, the simulated animal will tend to select the left arm, chosen by a more reactive memory system avoiding effort. Similar mechanisms would explain the behavioral patterns observed during the delay-based decision-making task. The mechanism presented above requires a quantitative description of the integrative signals E and D so that they encode the best compromise. An important issue is also how these two signals would be combined. Indeed, what would be the behavior of rats in a T-maze where two rewards of the same size are situated at the end of each arms, but with the left arm blocked by a barrier to be climbed and the right arm blocked by doors with a delay? Another interesting question is whether the population of columns encoding the topological representation would be situated in the dorsolateral PFC of primates. What would be the equivalent structure in rats?

8.5.2 Hippocampo-frontal interactions and memory consolidation

Another interesting direction of future work is to study the hippocampo-frontal interactions in more details, and in particular the influence of the hippocampus on PFC activity (see Sec. 3.1.3 and 3.3.4). Our model uses as input simple place cells which do not encode the presence of barrier in the environment, unlike real hippocampal place cells (Rivard et al., 2004; Alvernhe et al., 2010). Indeed, introducing or moving a barrier in an environment involves some remapping effects, such as place fields appearing, disappearing, or following the barrier. Such cells would certainly modify the dynamic of the spatial learning in the model, but would not prevent it from learning topological representations. A question arises from

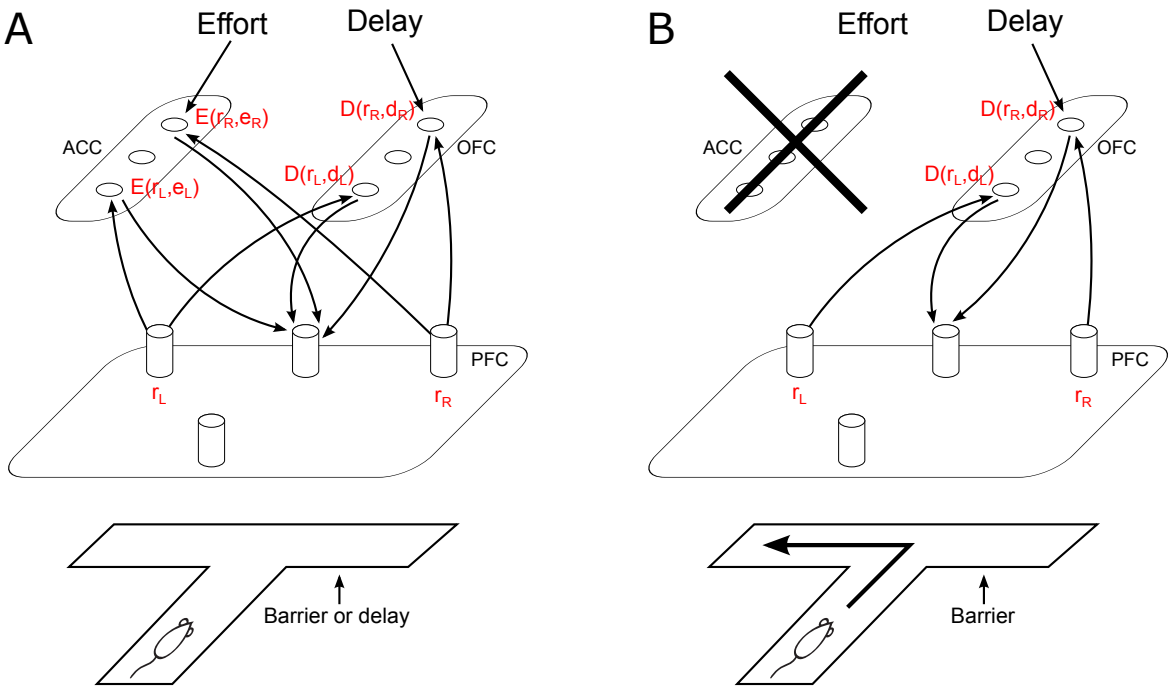

Figure 8.1: *A distributed model encoding effort-to-goal and delay-to-goal information.* **(A)** The topological representation is distributed across three populations. The PFC column network codes for the states and state transitions. The values of these transition is terms of effort-to-goal (E) and delay-to-goal (D) are encoded by the ACC and OFC populations. r_R and r_L represent the reward value. e_R and e_L are the effort to cross the right and left arms, respectively. d_R and d_L are the delays to cross the right and left arms, respectively. **(B)** If the ACC population is lesioned, the back-propagated signal from the left and right goal can not be integrated with effort values anymore. Hence, the PFC network only receives delay-related information, which are not sufficient to favor the right path, leading the simulated rat to choose the left arm.

this issue: how does the PFC deal with remapping within the hippocampus? Does plasticity along the HP-PFC pathway reinforces only stable configurations of the place cell activity? A theoretical study of the learning rule governing the long-term potentiation and long-term depression of w_{sh} synapses should be a useful approach to address this issue.

The discharge of our place cell and prefrontal populations modeled a firing rate function. A suitable improvement of the model would be to generate spikes, or at least a theta rhythm modulating the activity. Introducing a strong temporal component in the model would enable it to exhibit interesting dynamics. First, it would be useful to better understand the phase locking phenomenon between the hippocampus and the prefrontal cortex (see Sec. 3.1.3, Fig. 8.2A). In addition, it would provide the prefrontal columnar population with an alternative planning mechanism: instead of spreading firing rates encoding distance-to-goal information, spikes could be propagated. In this paradigm, the shortest pathway would be encoded by the first spike arrived from the goal column to the column representing the current position. Sequential replay of activity observed in the hippocampus may provide a stronger support for this spiking mechanism than the firing rate propagation. Moreover, Bugmann (1997) suggests that an additional potential advantage of an implementation with spiking neurons is the capability for multi-criteria planning. Whereas the time of arrival of the first spike would encode the shortest pathway, the mean firing rate would represent another information such as costs and benefits, leading to a powerful dual-coding scheme. Finally, spiking discharges by the model prefrontal neurons would be useful to study memory consolidation.

Research studies suggest that neural patterns, reflecting previously acquired information, are replayed during sleep (see Sec. 3.2.2; Peyrache et al., 2009; Benchenane et al., 2010). One possible reason for this is that such replay exchanges information between hippocampus and neocortex, supporting consolidation (see Sec. 3.3.4). In particular, sharp wave-ripple complexes in the hippocampus seem prominent for transferring labile memories from the hippocampus to the neocortex for long-term storage (Girardeau et al., 2009). A key issue for modeling approaches is to understand computational properties of this learning mechanism. In a spiking version of the model, sequential replays in the place cell population would drive replay in the prefrontal population (Fig. 8.2B). This would provide

a way to rehearse previously learned trajectories, leading to a faster learning of the HP-PFC connections (w_{sh}) and the lateral connectivity between columns (w_{qv} and w_{pd}). As expected from the study by Peyrache et al. (2009), neural ensembles of model neurons activated during the navigation would likely be reactivated during sleep. Moreover, blocking this replay mechanism would lead to navigational impairments in comparison with control animals because of the lower number of rehearsals (Girardeau et al., 2009). It is currently under debate when the replay of an experience occurs: do replays favor remote experiences so that they are not forgotten or do they focus on recent experiences so that they are learned faster (e.g. Gupta et al., 2010)? Our modeling approach could be used to interpret available experimental data and to study how and when hippocampal replays should occur to optimize learning.

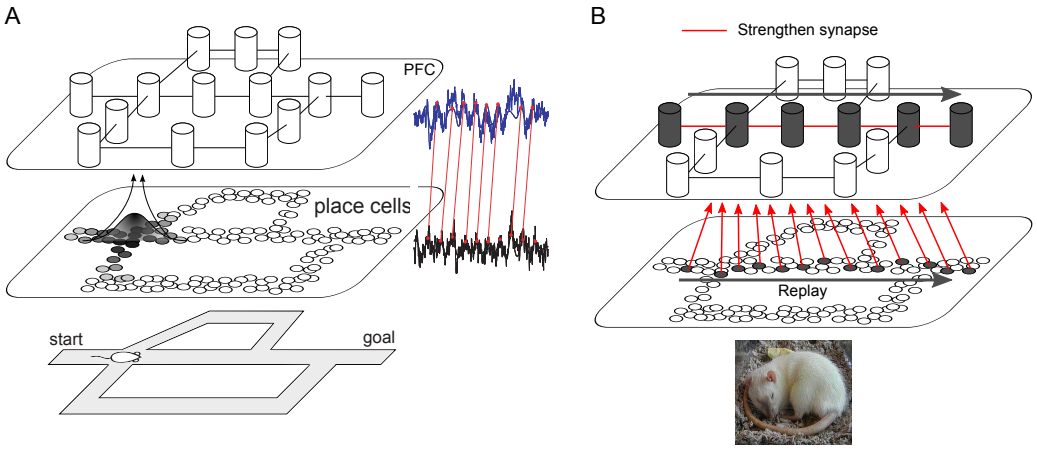

Figure 8.2: *Potential studies of the hippocampo-frontal pathway: phase locking and influence of the sleep.* **(A)** It is suggested that phase coherence in the theta band of prefrontal and hippocampal local field potentials might be an important way for information exchange at specific behavioral periods such as the decision point of a maze (Jones and Wilson, 2005b). A spiking extension of the model should be of value to explore the implications of this phenomenon. Right: local field potential for a place cell population and a prefrontal population (from Jones and Wilson, 2005b). **(B)** During sleep, the simulated population of place cells would reactivate a previous trajectory, leading to a sequential activation of the selected place cells. In turn, this hippocampal activity would excite the prefrontal population, causing a sequential discharge of columns. These sequential co-activations of model HP and PFC would reinforce a set of synapses relevant to the navigation planning.

Appendix A

Additional materials related to the prefrontal cortex

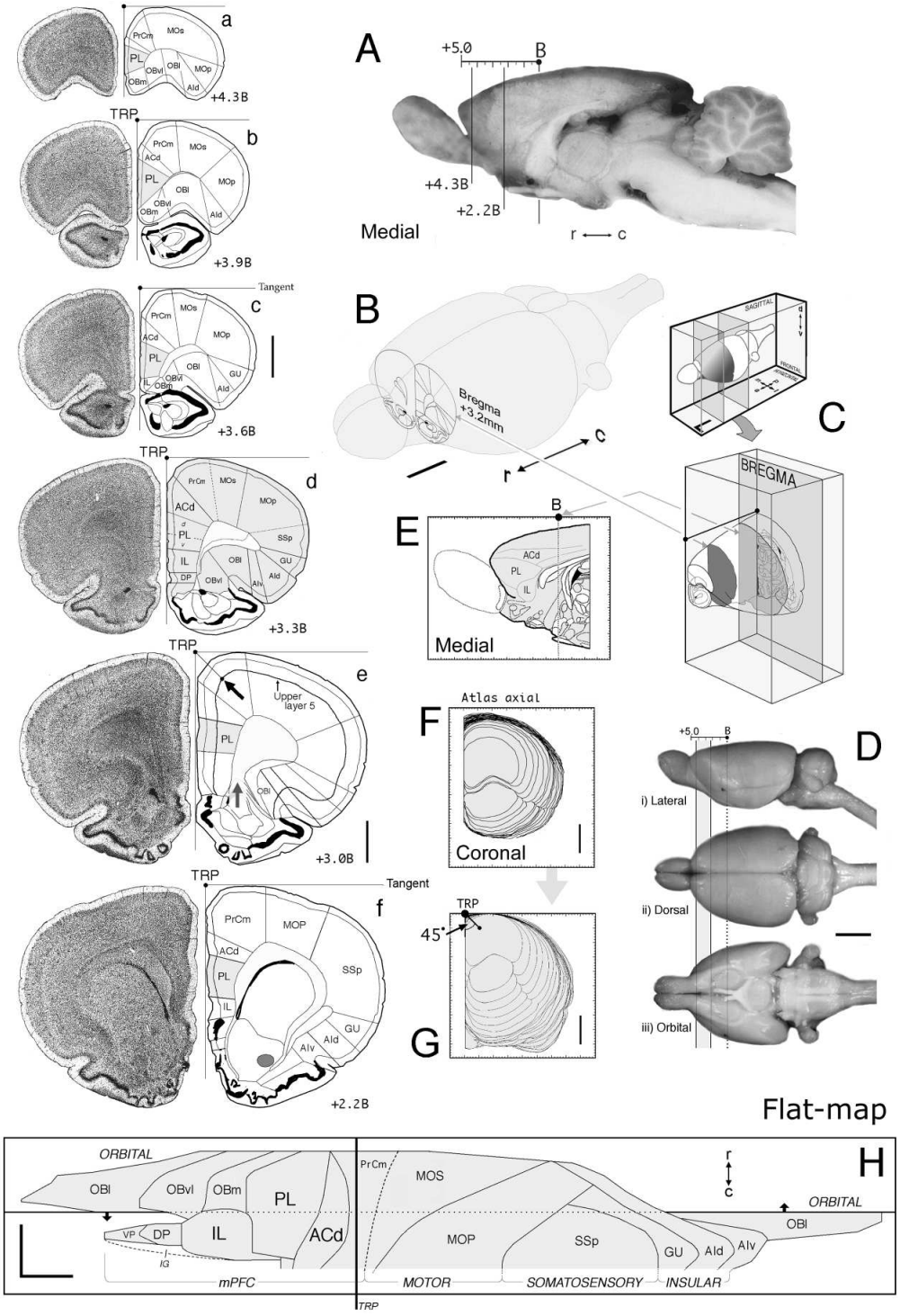

Figure A.1: The PFC, from (Gabbott et al., 2005).

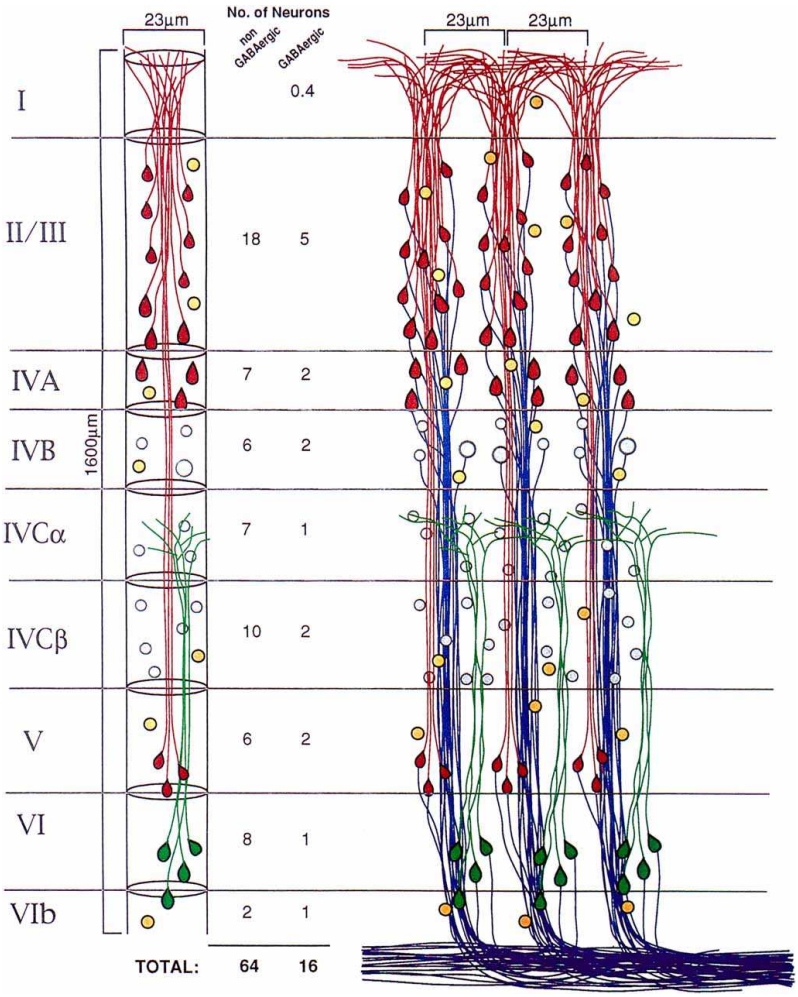

Figure A.2: *Representation of minicolumns of the monkey visual cortex from (Peters and Sethares, 1996).* Diagrams of the arrangements of neurons and their processes within pyramidal cell modules. For the sake of clarity, only 50%of the total number of the neurons actually present is depicted. On the left side is a representation of a pyramidal cell module to show the arrangements of the apical dendrites of pyramidal cells. The pyramidal cells in layers II/III, IVA, and V are shown in red, and the pyramidal cells in layer VI are in green. The neurons of layer IVB and IVC that lack apical dendrites are in grey, while the GABAergic neurons are represented in orange. On the right side is a representation of three pyramidal cell modules to show the arrangements of the apical dendrites and their axons. The axons of the pyramidal cells that aggregate to form the axon bundles are shown in blue.

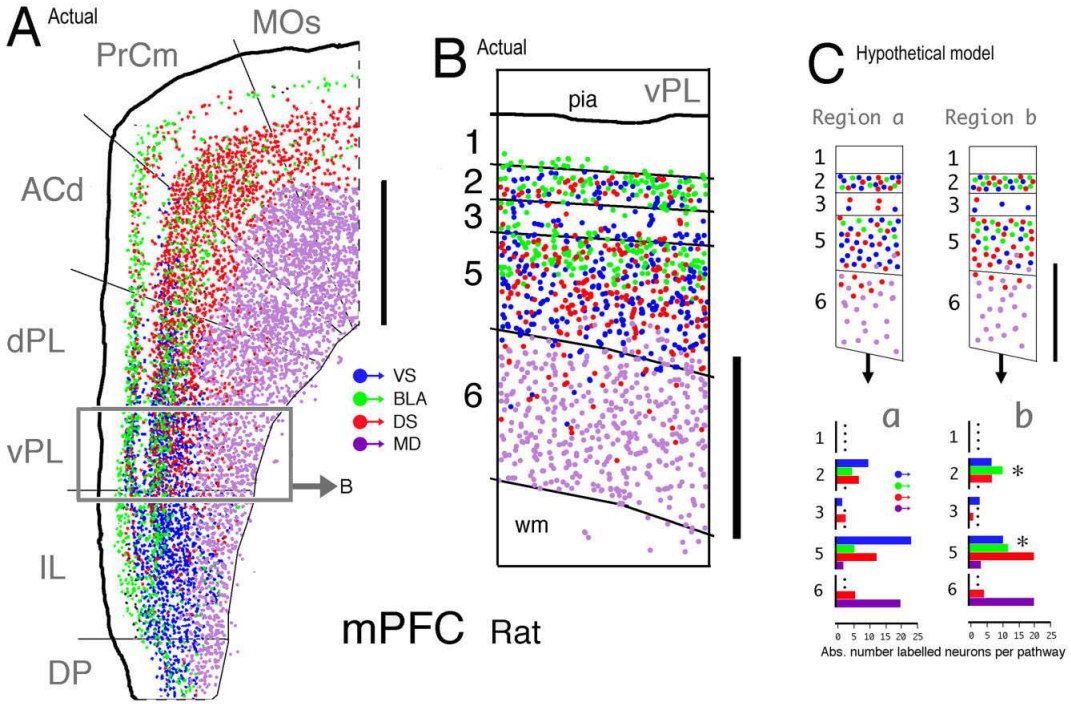

Figure A.3: Efferent projections from the different layers of the PFC, from (Gabbott et al., 2005).

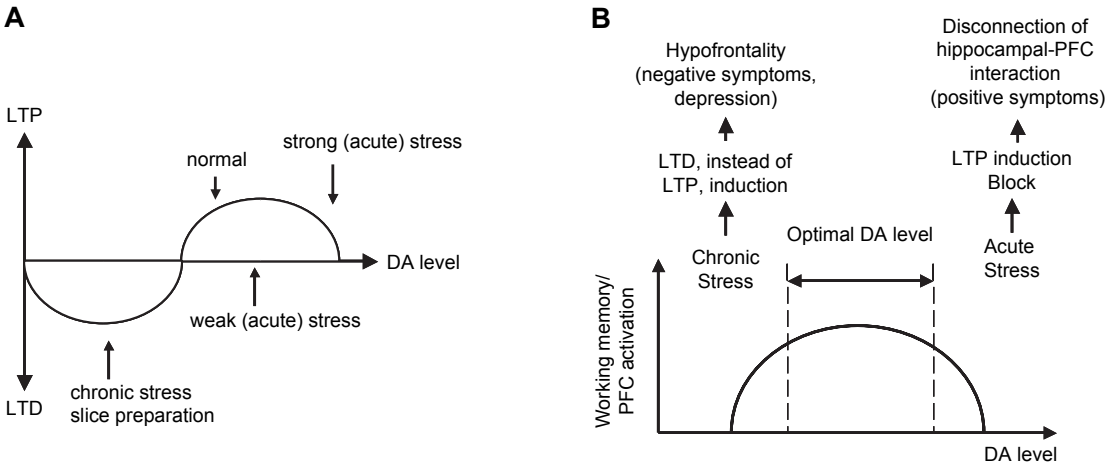

Figure A.4: *Effect of dopamine level on PFC activation and plasticity, from (Goto et al., 2007).* **(A)** In the normal condition at a moderate level of DA tone, long-term potentiation (LTP) is induced with high frequency activation of PFC afferent fibers such as those arising from the hippocampus and participating in memory-guided behavior. A brief exposure to stress would increase DA release in the PFC, and thereby facilitate DA-dependent induction of LTP, whereas if the stress exposure is severe, an excess in DA release could occur, leading to impairment of LTP (e.g. via stimulation of extrasynaptic DA receptors). In contrast, in the case of chronic stress, where a significant decrease in DA tone is produced, PFC networks would preferentially shown LTD. Such a condition is likely to be present in the in vitro slice preparation, in which the DA tone would be expected to be low. **(B)** Acute stress induces excessive DA release, which in turn over-stimulates D1 receptors in the PFC. As a result, information processing mediated by hippocampal-PFC interactions, which depends on LTP, would be disrupted. In contrast, attenuated DA tone, which could be produced by chronic stress exposure, would also interfere with proper information processing in the hippocampal-PFC pathway due to the abnormal induction of LTD. Indeed, this LTD may contribute to suppression of PFC activity (i.e. hypofrontality).

Bibliography

J. Aggleton. *The amygdala: neurobiological aspects of emotion, memory, and mental dysfunction*. Wiley-Liss New York, 1992.

K. Agster, N. Fortin, and H. Eichenbaum. The hippocampus and disambiguation of overlapping sequences. *J. Neurosci*, 22(13):5760–5768, 2002.

J. Ainge, M. Tamosiunaite, F. Woergoetter, and P. Dudchenko. Hippocampal ca1 place cells encode intended destination on a maze with multiple choice points. *J. Neurosci*, 27(36):9769–9779, 2007.

G. Alexander, M. DeLong, and P. Strick. Parallel organization of functionally segregated circuits linking basal ganglia and cortex. *Annu Rev Neurosci*, 9: 357–381, 1986.

A. Alvernhe. *Codage de la topologie de l'espace dans l'hippocampe: approches comportementale et électrophysiologique*. PhD thesis, Université de Provence, Marseille, 2010.

A. Alvernhe, T. Van Cauter, E. Save, and B. Poucet. Different ca1 and ca3 representations of novel routes in a shortcut situation. *J. Neurosci.*, 28(29):7324–7333, 2008.

A. Alvernhe, E. Save, and B. Poucet. Local remapping of place cell firing in the tolman detour task. 2010.

D. Amaral. Emerging principles of intrinsic hippocampal organization. *Curr. Opin. Neurobiol*, 3(2):225–229, 1993.

D. Amaral and M. Witter. The three-dimensional organization of the hippocampal formation: a review of anatomical data. *Neuroscience*, 31(3):571–591, 1989.

D. Amaral, C. Dolorfo, and P. Alvarez-Royo. Organization of ca1 projections to the subiculum: a pha-l analysis in the rat. *Hippocampus*, 1(4):415–435, 1991.

R. Andersen. Encoding of intention and spatial location in the posterior parietal cortex. *Cereb. Cortex*, 5(5):457–469, 1995.

R. Andersen, L. Snyder, D. Bradley, and J. Xing. Multimodal representation of space in the posterior parietal cortex and its use in planning movements. *Annu. Rev. Neurosci*, 20:303–330, 1997.

A. Arleo. *Spatial learning and navigation in neuro-mimetic systems*. PhD thesis, Ecole Polytechnique Fédérale de Lausanne, 2000.

A. Arleo and W. Gerstner. Spatial cognition and neuro-mimetic navigation : a model of hippocampal place cell activity. *Biological Cybernetics*, 83(3):287–299, 2000.

A. Arleo and L. Rondi-Reig. Multimodal sensory integration and concurrent navigation strategies for spatial cognition in real and artificial organisms. *Journal of Integrative Neuroscience*, 6(3):327–366, 2007.

A. Arleo, F. Smeraldi, and W. Gerstner. Cognitive navigation based on nonuniform gabor space sampling, unsupervised growing networks, and reinforcement learning. *IEEE transactions on neural networks*, 15(3):639–651, 2004.

W. Asaad, G. Rainer, and E. Miller. Neural activity in the primate prefrontal cortex during associative learning. *Neuron*, 21(6):1399–1407, 1998.

S. Au-Young, H. Shen, and C. Yang. Medial prefrontal cortical output neurons to the ventral tegmental area (vta) and their responses to burst-patterned stimulation of the vta: neuroanatomical and in vivo electrophysiological analyses. *Synapse*, 34(4):245–255, 1999.

K. Austin, L. White, and M. Shapiro. Short- and long-term effects of experience on hippocampal place fields. In *Society for Neuroscience Abstracts*, page 19:263, 1993.

B. Averbeck and D. Lee. Prefrontal neural correlates of memory for sequences. *J Neurosci*, 27(9):2204–2211, 2007.

B. Averbeck, M. Chafee, D. Crowe, and A. Georgopoulos. Parallel processing of serial movements in prefrontal cortex. *Proc Natl Acad Sci U S A*, 99(20): 13172–13177, 2002.

B. Averbeck, M. Chafee, D. Crowe, and A. Georgopoulos. Neural activity in prefrontal cortex during copying geometrical shapes. i. single cells encode shape, sequence, and metric parameters. *Exp Brain Res*, 150(2):127–141, 2003a.

B. Averbeck, D. Crowe, M. Chafee, and A. Georgopoulos. Neural activity in prefrontal cortex during copying geometrical shapes. ii. decoding shape segments from neural ensembles. *Exp Brain Res*, 150(2):142–153, 2003b.

B. Averbeck, J. Sohn, and D. Lee. Activity in prefrontal cortex during dynamic selection of action sequences. *Nat Neurosci*, 9(2):276–282, 2006.

S. Bacon, A. Headlam, P. Gabbott, and A. Smith. Amygdala input to medial prefrontal cortex (mpfc) in the rat: a light and electron microscope study. *Brain Res*, 720(1-2):211–219, 1996.

E. Baeg, Y. Kim, K. Huh, I. Mook-Jung, H. Kim, and M. Jung. Dynamics of population code for working memory in the prefrontal cortex. *Neuron*, 40(1): 177–188, 2003.

S. Bandyopadhyay and J. Hablitz. Dopaminergic modulation of local network activity in rat prefrontal cortex. *J Neurophysiol*, 97(6):4120–4128, 2007.

D. Bannerman, B. Yee, M. Good, M. Heupel, S. Iversen, and J. Rawlins. Double dissociation of function within the hippocampus: a comparison of dorsal, ventral, and complete hippocampal cytotoxic lesions. *Behav. Neurosci*, 113(6): 1170–1188, 1999.

J. Banquet, P. Gaussier, M. Quoy, A. Revel, and Y. Burnod. A hierarchy of associations in hippocampo-cortical systems: cognitive maps and navigation strategies. *Neural Computation*, 17:1339–1384, 2005.

S. Bao, V. Chan, and M. Merzenich. Cortical remodelling induced by activity of ventral tegmental dopamine neurons. *Nature*, 412(6842):79–83, 2001.

A. Batuev, N. Kursina, and A. Shutov. Unit activity of the medial wall of the frontal cortex during delayed performance in rats. *Behav Brain Res*, 41(2): 95–102, 1990.

K. Benchenane, A. Peyrache, M. Khamassi, P. Tierney, Y. Gioanni, F. Battaglia, and S. Wiener. Coherent theta oscillations and reorganization of spike timing in the hippocampal- prefrontal network upon learning. *Neuron*, 66(6):921–936, 2010.

H. Berendse, Y. Graaf, and H. Groenewegen. Topographical organization and relationship with ventral striatal compartments of prefrontal corticostriatal projections in the rat. *J Comp Neurol*, 316(3):314–347, 1992.

M. Bezzi, I. Samengo, S. Leutgeb, and S. Mizumori. Measuring information spatial densities. *Neural Comput*, 14(2):405–420, 2001.

W. Bialek, F. Rieke, R. de Ruyter van Steveninck, and D. Warland. Reading a neural code. *Science*, 252(5014):1854, 1991.

A. Bieszczad. Neurosolver: a step toward a neuromorphic general problem solver. *Proceedings of the World Congress on Computational Intelligence WCCI94*, 3: 1313–1318, 1994.

M. Botvinick, Y. Niv, and A. Barto. Hierarchically organized behavior and its neural foundations: a reinforcement learning perspective. *Cognition*, 113(3): 262–280, 2009.

M. Bower, D. Euston, and B. McNaughton. Sequential-context-dependent hippocampal activity is not necessary to learn sequences with repeated elements. *J. Neurosci*, 25(6):1313–1323, 2005.

T. Braver. *Mechanisms of cognitive control: a neurocomputational model*. PhD thesis, Carnegie Mellon University, Piitsburgh, PA, 1997.

T. Braver and J. Cohen. Dopamine, cognitive control, and schizophrenia: the gating model. *Prog Brain Res*, 121:327–349, 1999.

T. Braver and J. Cohen. On the control of control: The role of dopamine in regulating prefrontal function and working memory. *Control of cognitive processes: Attention and performance XVIII*, page 713–737, 2000.

T. Braver, J. Cohen, and D. Servan-Schreiber. A computational model of prefrontal cortex function. In *ANIPS*, 1995.

C. Breese, R. Hampson, and S. Deadwyler. Hippocampal place cells: stereotypy and plasticity. *J. Neurosci*, 9(4):1097–1111, 1989.

K. Brodmann. Ergebnisse über die vergleichende histologi. *K Anat Anz Suppl*, 41:157–216, 1895.

E. Brown, L. Frank, D. Tang, M. Quirk, and M. Wilson. A statistical paradigm for neural spike train decoding applied to position prediction from ensemble firing patterns of rat hippocampal place cells. *Journal of Neuroscience*, 18(18):7411, 1998.

J. Brown, D. Bullock, and S. Grossberg. How the basal ganglia use parallel excitatory and inhibitory learning pathways to selectively respond to unexpected rewarding cues. *J Neurosci*, 19(23):10502–10511, 1999.

V. Brown and E. Bowman. Rodent models of prefrontal cortical function. *Trends Neurosci*, 25(7):340–343, 2002.

T. Brozoski, R. Brown, H. Rosvold, and P. Goldman. Cognitive deficit caused by regional depletion of dopamine in prefrontal cortex of rhesus monkey. *Science*, 205(4409):929–932, 1979.

N. Brunel and X. Wang. Effects of neuromodulation in a cortical network model of object working memory dominated by recurrent inhibition. *J Comput Neurosci*, 11(1):63–85, 2001.

G. Bugmann. A connectionist approach to spatial memory and planning. *Basic Concepts in Neural Networks: A survey, In the Series: Perspectives in Neural Networks*, page 109–146, 1997.

F. Burette, T. Jay, and S. Laroche. Synaptic depression of the hippocampal to prefrontal cortex pathway during a spatial working memory task. *Curr. Psychol. Lett*, 1:9–23, 2000.

N. Burgess, K. Jeffery, and J. O'Keefe. Integrating hippocampal and parietal functions: a spatial point of view. In K. Jeffery, N. Burgess, and J. O'Keefe,

editors, *The Hippocampal and Parietal Foundations of Spatial Cognition*, page 3–29. Oxford University Press, 1999.

N. Burgess, E. Maguire, and J. O'Keefe. The human hippocampus and spatial and episodic memory. *Neuron*, 35(4):625–641, 2002.

Y. Burnod. *An adaptative neural network: the cerebral cortex*. Masson, 1988.

Y. Burnod. Organizational levels of the cerebral cortex: an integrated model. *Acta Biotheor*, 39(3-4):351–361, 1991.

B. Burton, V. Hok, E. Save, and B. Poucet. Lesion of the ventral and intermediate hippocampus abolishes anticipatory activity in the medial prefrontal cortex of the rat. *Behav Brain Res*, 199:222–234, 2009.

D. Buxhoeveden and M. Casanova. The minicolumn hypothesis in neuroscience. *Brain*, 125(Pt 5):935–951, 2002.

G. Buzsáki. Hippocampal sharp waves: their origin and significance. *Brain Res*, 398(2):242–252, 1986.

G. Buzsáki. Two-stage model of memory trace formation: a role for "noisy" brain states. *Neuroscience*, 31(3):551–570, 1989.

G. Buzsáki. The hippocampo-neocortical dialogue. *Cereb. Cortex*, 6(2):81–92, 1996.

R. Cardinal. Neural systems implicated in delayed and probabilistic reinforcement. *Neural Netw*, 19(8):1277–1301, 2006.

D. Carr and S. Sesack. Hippocampal afferents to the rat prefrontal cortex: synaptic targets and relation to dopamine terminals. *J Comp Neurol*, 369(1):1–15, 1996.

D. Carr and S. Sesack. Projections from the rat prefrontal cortex to the ventral tegmental area: target specificity in the synaptic associations with mesoaccumbens and mesocortical neurons. *J Neurosci*, 20(10):3864–3873, 2000.

W. Cass and G. Gerhardt. In vivo assessment of dopamine uptake in rat medial prefrontal cortex: comparison with dorsal striatum and nucleus accumbens. *J Neurochem*, 65(1):201–7, 1995.

Q. Chang and P. Gold. Switching memory systems during learning: changes in patterns of brain acetylcholine release in the hippocampus and striatum in rats. *Journal of Neuroscience*, 23(7):3001, 2003.

N. Chapuis, C. Thinus-Blanc, and B. Poucet. Dissociation of mechanisms involved in dogs' oriented displacements. *The Quarterly Journal of Experimental Psychology Section B: Comparative and Physiological Psychology*, 35(3):213, 1983.

T. Cheung and R. Cardinal. Hippocampal lesions facilitate instrumental learning with delayed reinforcement but induce impulsive choice in rats. *BMC Neurosci*, 13:6–36, 2005.

A. Chiba, R. Kesner, and C. Gibson. Memory for temporal order of new and familiar spatial location sequences: role of the medial prefrontal cortex. *Learn Mem*, 4(4):311–317, 1997.

E. Ciaramelli. The role of ventromedial prefrontal cortex in navigation: A case of impaired wayfinding and rehabilitation. *Neuropsychologia*, 46(7):2099–2105, 2008.

H. Clarke, J. Dalley, H. Crofts, T. Robbins, and A. Roberts. Cognitive inflexibility after prefrontal serotonin depletion. *Science*, 304(5672):878–880, 2004.

J. Cohen, T. Braver, and J. Brown. Computational perspectives on dopamine function in prefrontal cortex. *Curr Opin Neurobiol*, 12(2):223–229, 2002.

L. Colgin and E. Moser. Hippocampal theta rhythms follow the beat of their own drum. *Nat. Neurosci*, 12(12):1483–1484, 2009.

F. Condé, E. Maire-Lepoivre, E. Audinat, and F. Crépel. Afferent connections of the medial frontal cortex of the rat. ii. cortical and subcortical afferents. *J Comp Neurol*, 352(4):567–593, 1995.

C. Constantinidis and P. Goldman-Rakic. Correlated discharges among putative pyramidal neurons and interneurons in the primate prefrontal cortex. *J Neurophysiol*, 88(6):3487–3497, 2002.

C. Constantinidis, M. Franowicz, and P. Goldman-Rakic. Coding specificity in cortical microcircuits: a multiple-electrode analysis of primate prefrontal cortex. *J Neurosci*, 21(10):3646–3655, 2001.

C. Constantinidis, G. Williams, and P. Goldman-Rakic. A role for inhibition in shaping the temporal flow of information in prefrontal cortex. *Nat Neurosci*, 5 (2):175–180, 2002.

J. Corwin, M. Fussinger, R. Meyer, V. King, and R. Reep. Bilateral destruction of the ventrolateral orbital cortex produces allocentric but not egocentric spatial deficits in rats. *Behav. Brain Res*, 61(1):79–86, 1994.

A. Cressant, R. Muller, and B. Poucet. Failure of centrally placed objects to control the firing fields of hippocampal place cells. *J. Neurosci*, 17(7):2531–2542, 1997.

J. Csicsvari, J. O'Neill, K. Allen, and T. Senior. Place-selective firing contributes to the reverse-order reactivation of ca1 pyramidal cells during sharp waves in open-field exploration. *Eur. J. Neurosci*, 26(3):704–716, 2007.

N. Dallal and W. Meck. Hierarchical structures: chunking by food type facilitates spatial memory. *J Exp Psychol Anim Behav Process*, 16(1):69–84, 1990.

J. Dalley, R. Cardinal, and T. Robbins. Prefrontal executive and cognitive functions in rodents: neural and neurochemical substrates. *Neurosci Biobehav Rev*, 28(7):771–784, 2004.

T. Davidson, F. Kloosterman, and M. Wilson. Hippocampal replay of extended experience. *Neuron*, 63(4):497–507, 2009.

N. Daw, Y. Niv, and P. Dayan. Uncertainty-based competition between prefrontal and dorsolateral striatal systems for behavioral control. *Nature neuroscience*, 8 (12):1704–1711, 2005.

J. Day, G. Damsma, and H. Fibiger. Cholinergic activity in the rat hippocampus, cortex and striatum correlates with locomotor activity: an in vivo microdialysis study. *Pharmacol Biochem Behav*, 38(4):723–729, 1991.

S. Dayawansa, T. Kobayashi, E. Hori, K. Umeno, T. Tazumi, T. Ono, and H. Nishijo. Conjunctive effects of reward and behavioral episodes on hippocampal place-differential neurons of rats on a mobile treadmill. *Hippocampus*, 16(7):586–595, 2006.

J. De Bruin, F. Sànchez-Santed, R. Heinsbroek, A. Donker, and P. Postmes. A behavioural analysis of rats with damage to the medial prefrontal cortex using the morris water maze: evidence for behavioural flexibility, but not for impaired spatial navigation. *Brain Res*, 652(2):323–333, 1994.

J. De Bruin, W. Swinkels, and J. De Brabander. Response learning of rats in a morris water maze: involvement of the medial prefrontal cortex. *Behav Brain Res*, 85(1):47–55, 1997.

J. DeFelipe, L. Alonso-Nanclares, and J. Arellano. Microstructure of the neocortex: Comparative aspects. *Journal of Neurocytology*, 31(3):299–316, 2002.

E. Dégenètais, A. Thierry, J. Glowinski, and Y. Gioanni. Synaptic influence of hippocampus on pyramidal cells of the rat prefrontal cortex: an in vivo intracellular recording study. *Cereb Cortex*, 13(7):782–792, 2003.

S. Dehaene and J. Changeux. A hierarchical neuronal network for planning behavior. *Proc Natl Acad Sci U S A*, 94(24):13293–13298, 1997.

B. Delatour and P. Gisquet-Verrier. Lesions of the prelimbic-infralimbic cortices in rats do not disrupt response selection processes but induce delay-dependent deficits: evidence for a role in working memory? *Behav Neurosci*, 113(5): 941–955, 1999.

B. Delatour and P. Gisquet-Verrier. Functional role of rat prelimbic-infralimbic cortices in spatial memory: evidence for their involvement in attention and behavioural flexibility. *Behav Brain Res*, 109(1):113–128, 2000.

A. Deutch. Prefrontal cortical dopamine systems and the elaboration of functional corticostriatal circuits: implications for schizophrenia and parkinson's disease. *J Neural Transm Gen Sect*, 91(2-3):197–221, 1993.

M. DeWeese and M. Meister. How to measure the information gained from one symbol. *Network: Computation in Neural Systems*, 10:325–340, 1999.

G. Di Prisco and R. Vertes. Excitatory actions of the ventral midline thalamus (rhomboid/reuniens) on the medial prefrontal cortex in the rat. *Synapse*, 60(1): 45–55, 2006.

K. Diba and G. Buzsáki. Forward and reverse hippocampal place-cell sequences during ripples. *Nat. Neurosci*, 10(10):1241–1242, 2007.

D. Ding, P. Gabbott, and S. Totterdell. Differences in the laminar origin of projections from the medial prefrontal cortex to the nucleus accumbens shell and core regions in the rat. *Brain Res*, 917(1):81–89, 2001.

C. Doeller, B. Opitz, C. Krick, A. Mecklinger, and W. Reith. Prefrontal-hippocampal dynamics involved in learning regularities across episodes. *Cereb. Cortex*, 15(8):1123–1133, 2005.

C. Doeller, B. Opitz, C. Krick, A. Mecklinger, and W. Reith. Differential hippocampal and prefrontal-striatal contributions to instance-based and rule-based learning. *Neuroimage*, 31(4):1802–1816, 2006.

L. Dollé, D. Sheynikhovich, B. Girard, R. Chavarriaga, and A. Guillot. Path planning versus cue responding: a bio-inspired model of switching between navigation strategies. *Biol Cybern*, 103(4):299–317, 2010.

K. Doya. Modulators of decision making. *Nat. Neurosci*, 11(4):410–416, 2008.

G. Dragoi and G. Buzsáki. Temporal encoding of place sequences by hippocampal cell assemblies. *Neuron*, 50(1):145–157, 2006.

J. Dreher, E. Guigon, and Y. Burnod. A model of prefrontal cortex dopaminergic modulation during the delayed alternation task. *Journal of Cognitive Neuroscience*, 14(6):853–865, 2002.

D. Durstewitz. A few important points about dopamine's role in neural network dynamics. *Pharmacopsychiatry*, 39 Suppl 1:S72–S75, 2006.

D. Durstewitz and J. Seamans. The computational role of dopamine d1 receptors in working memory. *Neural Netw*, 15(4-6):561–572, 2002.

D. Durstewitz, M. Kelc, and O. Güntürkün. A neurocomputational theory of the dopaminergic modulation of working memory functions. *J Neurosci*, 19(7): 2807–2822, 1999.

D. Durstewitz, J. Seamans, and T. Sejnowski. Dopamine-mediated stabilization of delay-period activity in a network model of prefrontal cortex. *J Neurophysiol*, 83(3):1733–1750, 2000a.

D. Durstewitz, J. Seamans, and T. Sejnowski. Neurocomputational models of working memory. *Nat Neurosci*, 3 Suppl:1184–1191, 2000b.

J. Eccles. The modular operation of the cerebral neocortex considered as the material basis of mental events. *Neuroscience*, 6(10):1839–1856, 1981.

C. Eden and H. Uylings. Cytoarchitectonic development of the prefrontal cortex in the rat. *The Journal of Comparative Neurology*, 241(3):253–267, 1985.

H. Eichenbaum. The hippocampus and declarative memory: cognitive mechanisms and neural codes. *Behav. Brain Res*, 127(1-2):199–207, 2001.

H. Eichenbaum, C. Stewart, and R. Morris. Hippocampal representation in place learning. *J. Neurosci*, 10(11):3531–3542, 1990.

A. Ekstrom, J. Meltzer, B. McNaughton, and C. Barnes. Nmda receptor antagonism blocks experience-dependent expansion of hippocampal ”place fields”. *Neuron*, 31(4):631–638, 2001.

A. Ekstrom, M. Kahana, J. Caplan, T. Fields, E. Isham, E. Newman, and I. Fried. Cellular networks underlying human spatial navigation. *Nature*, 425(6954): 184–188, 2003.

A. Etienne and K. Jeffery. Path integration in mammals. *Hippocampus*, 14(2): 180–192, 2004.

A. Etienne, R. Maurer, J. Berlie, B. Reverdin, T. Rowe, J. Georgakopoulos, and V. Séguinot. Navigation through vector addition. *Nature*, 396(6707):161–164, 1998.

D. Euston and B. McNaughton. Apparent encoding of sequential context in rat medial prefrontal cortex is accounted for by behavioral variability. *J Neurosci*, 26(51):13143–13155, 2006.

D. Euston, M. Tatsuno, and B. McNaughton. Fast-forward playback of recent memory sequences in prefrontal cortex during sleep. *Science*, 318(5853):1147–1150, 2007.

A. Farovik, L. Dupont, and H. Eichenbaum. Distinct roles for dorsal ca3 and ca1 in memory for sequential nonspatial events. *Learn. Mem*, 17(1):12–17, 2010.

C. Feierstein, M. Quirk, N. Uchida, D. Sosulski, and Z. Mainen. Representation of spatial goals in rat orbitofrontal cortex. *Neuron*, 51(4):495–507, 2006.

A. Fenton and R. Muller. Place cell discharge is extremely variable during individual passes of the rat through the firing field. *Proc. Natl. Acad. Sci. U.S.A*, 95 (6):3182–3187, 1998.

A. Fenton, H. Kao, S. Neymotin, A. Olypher, Y. Vayntrub, W. Lytton, and N. Ludvig. Unmasking the ca1 ensemble place code by exposures to small and large environments: more place cells and multiple, irregularly arranged, and expanded place fields in the larger space. *J. Neurosci*, 28(44):11250–11262, 2008.

J. Ferbinteanu and M. Shapiro. Prospective and retrospective memory coding in the hippocampus. *Neuron*, 40(6):1227–1239, 2003.

F. Ferino, A. Thierry, and J. Glowinski. Anatomical and electrophysiological evidence for a direct projection from ammon's horn to the medial prefrontal cortex in the rat. *Exp Brain Res*, 65(2):421–426, 1987.

A. Ferron, A. Thierry, C. Douarin, and J. Glowinski. Inhibitory influence of the mesocortical dopaminergic system on spontaneous activity or excitatory response induced from the thalamic mediodorsal nucleus in the rat medial prefrontal cortex. *Brain Res*, 302(2):257–265, 1984.

F. Fleuret and E. Brunet. Dea: An architecture for goal planning and classification. *Neural Computation*, 12(9):1987–2008, 2000.

S. Floresco and S. Ghods-Sharifi. Amygdala-prefrontal cortical circuitry regulates effort-based decision making. *Cereb Cortex*, 17(2):251–260, 2007.

S. Floresco, J. Seamans, and A. Phillips. Selective roles for hippocampal, prefrontal cortical, and ventral striatal circuits in radial-arm maze tasks with or without a delay. *J Neurosci*, 17(5):1880–1890, 1997.

N. Fortin, K. Agster, and H. Eichenbaum. Critical role of the hippocampus in memory for sequences of events. *Nat. Neurosci*, 5(5):458–462, 2002.

D. Foster and M. Wilson. Reverse replay of behavioural sequences in hippocampal place cells during the awake state. *Nature*, 440(7084):680–683, 2006.

D. Foster and M. Wilson. Hippocampal theta sequences. *Hippocampus*, 17(11): 1093–1099, 2007.

S. Fountain and J. Rowan. Coding of hierarchical versus linear pattern structure in rats and humans. *J Exp Psychol Anim Behav Process*, 21(3):187–202, 1995.

S. Fox, S. Wolfson, and J. Ranck. Hippocampal theta rhythm and the firing of neurons in walking and urethane anesthetized rats. *Exp Brain Res*, 62(3):495–508, 1986.

L. Frank, E. Brown, and M. Wilson. Trajectory encoding in the hippocampus and entorhinal cortex. *Neuron*, 27(1):169–178, 2000.

P. Frankland and B. Bontempi. The organization of recent and remote memories. *Nat Rev Neurosci*, 6(2):119–130, 2005.

M. Franz, B. Schölkopf, H. Mallot, and H. Bülthoff. Learning view graphs for robot navigation. *Autonomous Robots*, 5(1):111–125, 1998.

T. Freund and V. Meskenaite. gamma-aminobutyric acid-containing basal forebrain neurons innervate inhibitory interneurons in the neocortex. *Proc. Natl. Acad. Sci. U.S.A*, 89(2):738–742, 1992.

H. Frezza-Buet and F. Alexandre. Modeling prefrontal functions for robot navigation. In *IEEE International Joint Conference on Neural Networks*, volume 1, pages 252–257, 1999.

N. Fujii and A. Graybiel. Representation of action sequence boundaries by macaque prefrontal cortical neurons. *Science*, 301(5637):1246–1249, 2003.

J. Fuster. Behavioral electrophysiology of the prefrontal cortex. *Trends in Neurosciences*, 7(11):408–414, 1984.

J. Fuster. Frontal lobes. *Curr. Opin. Neurobiol*, 3(2):160–165, 1993.

J. Fuster. The prefrontal cortex–an update: time is of the essence. *Neuron*, 30(2): 319–333, 2001.

J. Fuster and G. Alexander. Neuron activity related to short-term memory. *Science*, 173(997):652–654, 1971.

P. Gabbott. Radial organisation of neurons and dendrites in human cortical areas 25, 32, and 32'. *Brain Res*, 992(2):298–304, 2003.

P. Gabbott and S. Bacon. Local circuit neurons in the medial prefrontal cortex (areas 24a,b,c, 25 and 32) in the monkey: Ii. quantitative areal and laminar distributions. *J. Comp. Neurol*, 364(4):609–636, 1996a.

P. Gabbott and S. Bacon. The organisation of dendritic bundles in the prelimbic cortex (area 32) of the rat. *Brain Res*, 730(1-2):75–86, 1996b.

P. Gabbott, B. Dickie, R. Vaid, A. Headlam, and S. Bacon. Local-circuit neurones in the medial prefrontal cortex (areas 25, 32 and 24b) in the rat: morphology and quantitative distribution. *J. Comp. Neurol*, 377(4):465–499, 1997.

P. Gabbott, A. Headlam, and S. Busby. Morphological evidence that ca1 hippocampal afferents monosynaptically innervate pv-containing neurons and nadph-diaphorase reactive cells in the medial prefrontal cortex (areas 25/32) of the rat. *Brain Res*, 946(2):314–322, 2002.

P. Gabbott, T. Warner, P. Jays, and S. Bacon. Areal and synaptic interconnectivity of prelimbic (area 32), infralimbic (area 25) and insular cortices in the rat. *Brain Res*, 993(1-2):59–71, 2003.

P. Gabbott, T. Warner, P. Jays, P. Salway, and S. Busby. Prefrontal cortex in the rat: projections to subcortical autonomic, motor, and limbic centers. *J. Comp. Neurol*, 492(2):145–177, 2005.

P. Gabbott, T. Warner, and S. Busby. Amygdala input monosynaptically innervates parvalbumin immunoreactive local circuit neurons in rat medial prefrontal cortex. *Neuroscience*, 139(3):1039–1048, 2006.

M. Gao, C. Liu, S. Yang, G. Jin, B. Bunney, and W. Shi. Functional coupling between the prefrontal cortex and dopamine neurons in the ventral tegmental area. *J Neurosci*, 27(20):5414–5421, 2007.

R. Garcia, R. Vouimba, M. Baudry, and R. Thompson. The amygdala modulates prefrontal cortex activity relative to conditioned fear. *Nature*, 402(6759): 294–296, 1999.

S. Gaskin and N. White. Unreinforced spatial (latent) learning is mediated by a circuit that includes dorsal entorhinal cortex and fimbria fornix. *Hippocampus*, 17(7):586–594, 2007.

C. Gemmell and S. O'Mara. Medial prefrontal cortex lesions cause deficits in a variable-goal location task but not in object exploration. *Behav. Neurosci*, 113 (3):465–474, 1999.

C. Gemmell, M. Anderson, and S. O'Mara. Deep layer prefrontal cortex unit discharge in a cue-controlled open-field environment in the freely-moving rat. *Behav Brain Res*, 133(1):1–10, 2002.

A. Georgopoulos, J. Kalaska, and R. Caminiti. On the relations between the direction of two-dimensional arm movements and cell discharge in primate motor cortex. *Journal of Neuroscience*, 2:1527–1537, 1982.

C. Gerfen. The neostriatal mosaic: striatal patch-matrix organization is related to cortical lamination. *Science*, 246(4928):385–388, 1989.

P. Gilbert, R. Kesner, and I. Lee. Dissociating hippocampal subregions: double dissociation between dentate gyrus and ca1. *Hippocampus*, 11(6):626–636, 2001.

G. Girardeau, K. Benchenane, S. Wiener, G. Buzsaki, and M. Zugaro. Selective suppression of hippocampal ripples impairs spatial memory. *Nat Neurosci*, 12 (10):1222–1223, 2009.

P. Gisquet-Verrier and B. Delatour. The role of the rat prelimbic/infralimbic cortex in working memory: not involved in the short-term maintenance but in monitoring and processing functions. *Neuroscience*, 141(2):585–596, 2006.

A. Gold and R. Kesner. The role of the ca3 subregion of the dorsal hippocampus in spatial pattern completion in the rat. *Hippocampus*, 15(6):808–814, 2005.

P. Goldman-Rakic. Circuitry of primate prefrontal cortex and regulation of behavior by representational memory. *Handbook of physiology*, 5(pt I):373–417, 1987.

P. Goldman-Rakic, L. Selemon, and M. Schwartz. Dual pathways connecting the dorsolateral prefrontal cortex with the hippocampal formation and parahippocampal cortex in the rhesus monkey. *Neuroscience*, 12(3):719–743, 1984.

G. Goodhill and M. Carreira-Perpinan. Cortical columns. In L. Nadel, editor, *The Encyclopedia of Cognitive Science*, volume 1, page 845–851. Macmillan, 2002.

N. Gorelova, J. Seamans, and C. Yang. Mechanisms of dopamine activation of fast-spiking interneurons that exert inhibition in rat prefrontal cortex. *J Neurophysiol*, 88(6):3150–3166, 2002.

Y. Goto and A. Grace. Dopaminergic modulation of limbic and cortical drive of nucleus accumbens in goal-directed behavior. *Nat Neurosci*, 8(6):805–812, 2005.

Y. Goto and A. Grace. Dopamine modulation of hippocampal-prefrontal cortical interaction drives memory-guided behavior. *Cereb. Cortex*, 18(6):1407–1414, 2008.

Y. Goto, S. Otani, and A. Grace. The yin and yang of dopamine release: a new perspective. *Neuropharmacology*, 53(5):583–587, 2007.

S. Granon and B. Poucet. Medial prefrontal lesions in the rat and spatial navigation: evidence for impaired planning. *Behav Neurosci*, 109(3):474–484, 1995.

S. Granon and B. Poucet. Involvement of the rat prefrontal cortex in cognitive functions: a central role for the prelimbic area. *Psychology*, 28(2):229–237, 2000.

S. Granon, E. Save, M. Buhot, and B. Poucet. Effortful information processing in a spontaneous spatial situation by rats with medial prefrontal lesions. *Behav. Brain Res*, 78(2):147–154, 1996.

J. Green and A. Arduini. Hippocampal electrical activity in arousal. *J. Neurophysiol*, 17(6):533–557, 1954.

A. Gupta, M. van der Meer, D. Touretzky, and A. Redish. Hippocampal replay is not a simple function of experience. *Neuron*, 65(5):695–705, 2010.

H. Gurden, J. Tassin, and T. Jay. Integrity of the mesocortical dopaminergic system is necessary for complete expression of in vivo hippocampal-prefrontal cortex long-term potentiation. *Neuroscience*, 94(4):1019–1027, 1999.

H. Gurden, M. Takita, and T. Jay. Essential role of d1 but not d2 receptors in the nmda receptor-dependent long-term potentiation at hippocampal-prefrontal cortex synapses in vivo. *J Neurosci*, 20(22):RC106, 2000.

S. Haber. The primate basal ganglia: parallel and integrative networks. *J Chem Neuroanat*, 26(4):317–330, 2003.

T. Hafting, M. Fyhn, S. Molden, M. Moser, and E. Moser. Microstructure of a spatial map in the entorhinal cortex. *Nature*, 436(7052):801–806, 2005.

D. Hannesson, G. Vacca, J. Howland, and A. Phillips. Medial prefrontal cortex is involved in spatial temporal order memory but not spatial recognition memory in tests relying on spontaneous exploration in rats. *Behav. Brain Res*, 153(1): 273–285, 2004.

M. Hasselmo. A model of prefrontal cortical mechanisms for goal-directed behavior. *J Cogn Neurosci*, 17(7):1115–1129, 2005.

M. Hasselmo and J. Bower. Acetylcholine and memory. *Trends Neurosci*, 16(6): 218–222, 1993.

C. Heidbreder and H. Groenewegen. The medial prefrontal cortex in the rat: evidence for a dorso-ventral distinction based upon functional and anatomical characteristics. *Neurosci Biobehav Rev*, 27(6):555–579, 2003.

E. Henriksen, M. Moser, and E. Moser. Megaspace recording from hippocampal place cells and entorhinal grid cells. In *Society for Neuroscience Abstracts*, page 101.10/FF52, 2009.

B. Hock and M. Bunsey. Differential effects of dorsal and ventral hippocampal lesions. *J. Neurosci*, 18(17):7027–7032, 1998.

V. Hok. *Bases neurales des comportements orientés vers un but : Étude des corrélats de l'activité unitaire préfrontale et hippocampique dans une tâche de navigation*. PhD thesis, Université Toulouse III – Paul Sabatier, Toulouse, 2007.

V. Hok, E. Save, P. Lenck-Santini, and B. Poucet. Coding for spatial goals in the prelimbic/infralimbic area of the rat frontal cortex. *Proceedings of the National Academy of Sciences*, 102(12):4602–4607, 2005.

V. Hok, P. Lenck-Santini, S. Roux, E. Save, R. Muller, and B. Poucet. Goal-related activity in hippocampal place cells. *J Neurosci*, 27(3):472–482, 2007.

P. Holland and M. Gallagher. Amygdala-frontal interactions and reward expectancy. *Curr Opin Neurobiol*, 14(2):148–55, 2004.

S. Hollup, K. Kjelstrup, J. Hoff, M. Moser, and E. Moser. Impaired recognition of the goal location during spatial navigation in rats with hippocampal lesions. *J. Neurosci*, 21(12):4505–4513, 2001a.

S. Hollup, S. Molden, J. Donnett, M. Moser, and E. Moser. Accumulation of hippocampal place fields at the goal location in an annular watermaze task. *J. Neurosci*, 21(5):1635–1644, 2001b.

C. Hölscher, W. Jacob, and H. Mallot. Reward modulates neuronal activity in the hippocampus of the rat. *Behav. Brain Res*, 142(1-2):181–191, 2003.

J. Horton and D. Adams. The cortical column: a structure without a function. *Philos Trans R Soc Lond B Biol Sci*, 360(1456):837–862, 2005.

E. Hoshi, K. Shima, and J. Tanji. Neuronal activity in the primate prefrontal cortex in the process of motor selection based on two behavioral rules. *J Neurophysiol*, 83(4):2355–2373, 2000.

D. Hubel and T. Wiesel. Functional architecture of macaque monkey visual cortex. *Proceedings of the Royal Society of London. Series B. Biological Sciences*, 198 (1130):1, 1977.

P. Huerta, L. Sun, M. Wilson, and S. Tonegawa. Formation of temporal memory requires nmda receptors within ca1 pyramidal neurons. *Neuron*, 25(2):473–480, 2000.

J. Huxter, T. Senior, K. Allen, and J. Csicsvari. Theta phase-specific codes for two-dimensional position, trajectory and heading in the hippocampus. *Nat Neurosci*, 11(5):587–594, 2008.

J. Hyman, E. Zilli, A. Paley, and M. Hasselmo. Medial prefrontal cortex cells show dynamic modulation with the hippocampal theta rhythm dependent on behavior. *Hippocampus*, 15(6):739–749, 2005.

R. Insausti, M. Herrero, and M. Witter. Entorhinal cortex of the rat: cytoarchitectonic subdivisions and the origin and distribution of cortical efferents. *Hippocampus*, 7(2):146–183, 1997.

A. Ishikawa and S. Nakamura. Convergence and interaction of hippocampal and amygdalar projections within the prefrontal cortex in the rat. *J Neurosci*, 23 (31):9987–9995, 2003.

A. Ishikawa and S. Nakamura. Ventral hippocampal neurons project axons simultaneously to the medial prefrontal cortex and amygdala in the rat. *J Neurophysiol*, 96(4):2134–2138, 2006.

M. Ito. Historical review of the significance of the cerebellum and the role of purkinje cells in motor learning. *Annals of the New York Academy of Sciences*, 978:273–288, 2002.

Y. Izaki, M. Nomura, and T. Akema. Evoked prefrontal gamma oscillation by hippocampal train stimulation in anesthetized rats. *Neurosci Lett*, 343(1):53–56, 2003.

T. Jay and M. Witter. Distribution of hippocampal ca1 and subicular efferents in the prefrontal cortex of the rat studied by means of anterograde transport of phaseolus vulgaris-leucoagglutinin. *J Comp Neurol*, 313(4):574–586, 1991.

T. Jay, J. Glowinski, and A. Thierry. Selectivity of the hippocampal projection to the prelimbic area of the prefrontal cortex in the rat. *Brain Res*, 505(2): 337–340, 1989.

T. Jay, A. Thierry, L. Wiklund, and J. Glowinski. Excitatory amino acid pathway from the hippocampus to the prefrontal cortex. contribution of ampa receptors in hippocampo-prefrontal cortex transmission. *Eur J Neurosci*, 4(12): 1285–1295, 1992.

T. Jay, F. Burette, and S. Laroche. Nmda receptor-dependent long-term potentiation in the hippocampal afferent fibre system to the prefrontal cortex in the rat. *Eur J Neurosci*, 7(2):247–250, 1995a.

T. Jay, J. Glowinski, and A. Thierry. Inhibition of hippocampoprefrontal cortex excitatory responses by the mesocortical da system. *Neuroreport*, 6(14): 1845–1848, 1995b.

T. Jay, F. Burette, and S. Laroche. Plasticity of the hippocampal-prefrontal cortex synapses. *J Physiol Paris*, 90(5-6):361–366, 1996.

T. Jay, C. Rocher, M. Hotte, L. Naudon, H. Gurden, and M. Spedding. Plasticity at hippocampal to prefrontal cortex synapses is impaired by loss of dopamine and stress: importance for psychiatric diseases. *Neurotox Res*, 6(3):233–244, 2004.

O. Jensen and J. Lisman. Hippocampal ca3 region predicts memory sequences: accounting for the phase precession of place cells. *Learning & Memory*, 3(2-3): 279–287, 1996.

O. Jensen and J. Lisman. Position reconstruction from an ensemble of hippocampal place cells: contribution of theta phase coding. *J. Neurophysiol*, 83(5): 2602–2609, 2000.

A. Johnson and A. Redish. Neural ensembles in ca3 transiently encode paths forward of the animal at a decision point. *J. Neurosci*, 27(45):12176–12189, 2007.

M. Jones and M. Wilson. Phase precession of medial prefrontal cortical activity relative to the hippocampal theta rhythm. *Hippocampus*, 15(7):867–873, 2005a.

M. Jones and M. Wilson. Theta rhythms coordinate hippocampal-prefrontal interactions in a spatial memory task. *PLoS Biol*, 3(12):e402, 2005b.

M. Jouvet. Biogenic amines and the states of sleep. *Science*, 163(862):32–41, 1969.

M. Jung, S. Wiener, and B. McNaughton. Comparison of spatial firing characteristics of units in dorsal and ventral hippocampus of the rat. *J Neurosci*, 14(12): 7347–7356, 1994.

M. Jung, Y. Qin, B. McNaughton, and C. Barnes. Firing characteristics of deep layer neurons in prefrontal cortex in rats performing spatial working memory tasks. *Cereb Cortex*, 8(5):437–450, 1998.

M. Jung, Y. Qin, D. Lee, and I. Mook-Jung. Relationship among discharges of neighboring neurons in the rat prefrontal cortex during spatial working memory tasks. *J Neurosci*, 20(16):6166–6172, 2000.

W. Kargo, B. Szatmary, and D. Nitz. Adaptation of prefrontal cortical firing patterns and their fidelity to changes in action-reward contingencies. *J. Neurosci.*, 27(13):3548–3559, 2007.

M. Karlsson and L. Frank. Awake replay of remote experiences in the hippocampus. *Nature Neuroscience*, 12(7):913–918, 2009.

Y. Kawaguchi and Y. Kubota. Gabaergic cell subtypes and their synaptic connections in rat frontal cortex. *Cereb Cortex*, 7(6):476–486, 1997.

H. Kawashima, Y. Izaki, A. Grace, and M. Takita. Cooperativity between hippocampal-prefrontal short-term plasticity through associative long-term potentiation. *Brain Res*, 1109(1):37–44, 2006.

R. Kesner. Retrospective and prospective coding of information: role of the medial prefrontal cortex. *Exp Brain Res*, 74(1):163–167, 1989.

R. Kesner and T. Holbrook. Dissociation of item and order spatial memory in rats following medial prefrontal cortex lesions. *Neuropsychologia*, 25(4):653–664, 1987.

R. Kesner, G. Farnsworth, and B. DiMattia. Double dissociation of egocentric and allocentric space following medial prefrontal and parietal cortex lesions in the rat. *Behav Neurosci*, 103(5):956–961, 1989.

R. Kesner, P. Gilbert, and L. Barua. The role of the hippocampus in memory for the temporal order of a sequence of odors. *Behav. Neurosci*, 116(2):286–290, 2002.

M. Khamassi. *Complementary roles of the rat prefrontal cortex and striatum in reward-based learning and shifting navigation strategies: Electrophysiological and computational studies, application to simulated autonomous robotics.* PhD thesis, Université Pierre et Marie Curie, Paris, 2007.

V. King and J. Corwin. Spatial deficits and hemispheric asymmetries in the rat following unilateral and bilateral lesions of posterior parietal or medial agranular cortex. *Behav. Brain Res*, 50(1-2):53–68, 1992.

Z. Kisvárday, D. Kim, U. Eysel, and T. Bonhoeffer. Relationship between lateral inhibitory connections and the topography of the orientation map in cat visual cortex. *Eur J Neurosci*, 6(10):1619–1632, 1994.

H. Kita and S. Kitai. Amygdaloid projections to the frontal cortex and the striatum in the rat. *J. Comp. Neurol*, 298(1):40–49, 1990.

K. Kjelstrup, T. Solstad, V. Brun, T. Hafting, S. Leutgeb, M. Witter, E. Moser, and M. Moser. Finite scale of spatial representation in the hippocampus. *Science*, 321(5885):140–143, 2008.

J. Knierim. Neural representations of location outside the hippocampus. *Learn. Mem*, 13(4):405–415, 2006.

J. Knierim, H. Kudrimoti, and B. McNaughton. Place cells, head direction cells, and the learning of landmark stability. *J. Neurosci*, 15(3 Pt 1):1648–1659, 1995.

E. Koechlin, C. Ody, and F. Kouneiher. The architecture of cognitive control in the human prefrontal cortex. *Science*, 302(5648):1181–1185, 2003.

P. König, A. Engel, and W. Singer. Integrator or coincidence detector? the role of the cortical neuron revisited. *Trends Neurosci*, 19(4):130–137, 1996.

J. Krettek and J. Price. Projections from the amygdaloid complex to the cerebral cortex and thalamus in the rat and cat. *J. Comp. Neurol*, 172(4):687–722, 1977.

S. Kröner, L. Krimer, D. Lewis, and G. Barrionuevo. Dopamine increases inhibition in the monkey dorsolateral prefrontal cortex through cell type-specific modulation of interneurons. *Cereb Cortex*, 17(5):1020–1032, 2007.

J. Kubie and A. Fenton. Heading-vector navigation based on head-direction cells and path integration. *Hippocampus*, 19(5):456–479, 2009.

R. Kyd and D. Bilkey. Prefrontal cortex lesions modify the spatial properties of hippocampal place cells. *Cereb. Cortex*, 13(5):444–451, 2003.

R. Kyd and D. Bilkey. Hippocampal place cells show increased sensitivity to changes in the local environment following prefrontal cortex lesions. *Cereb. Cortex*, 15(6):720–731, 2005.

C. Lapish, S. Kroener, D. Durstewitz, A. Lavin, and J. Seamans. The ability of the mesocortical dopamine system to operate in distinct temporal modes. *Psychopharmacology (Berl)*, 191(3):609–625, 2007.

S. Laroche, T. Jay, and A. Thierry. Long-term potentiation in the prefrontal cortex following stimulation of the hippocampal ca1/subicular region. *Neurosci Lett*, 114(2):184–190, 1990.

S. Laroche, S. Davis, and T. Jay. Plasticity at hippocampal to prefrontal cortex synapses: dual roles in working memory and consolidation. *Hippocampus*, 10 (4):438–446, 2000.

K. Lashley. The problem of serial order in behavior. In L. Jeffress, editor, *Cerebral Mechanisms in Behavior*, pages 112–136. Wiley, New York, 1951.

D. Law-Tho, J. Desce, and F. Crepel. Dopamine favours the emergence of long-term depression versus long-term potentiation in slices of rat prefrontal cortex. *Neurosci Lett*, 188(2):125–128, 1995.

A. Lee and M. Wilson. Memory of sequential experience in the hippocampus during slow wave sleep. *Neuron*, 36(6):1183–1194, 2002.

I. Lee and R. Kesner. Differential roles of dorsal hippocampal subregions in spatial working memory with short versus intermediate delay. *Behav. Neurosci*, 117(5):1044–1053, 2003.

I. Lee, G. Rao, and J. Knierim. A double dissociation between hippocampal subfields: differential time course of ca3 and ca1 place cells for processing changed environments. *Neuron*, 42(5):803–815, 2004.

I. Lee, T. Jerman, and R. Kesner. Disruption of delayed memory for a sequence of spatial locations following ca1- or ca3-lesions of the dorsal hippocampus. *Neurobiol Learn Mem*, 84(2):138–147, 2005.

I. Lee, A. Griffin, E. Zilli, H. Eichenbaum, and M. Hasselmo. Gradual translocation of spatial correlates of neuronal firing in the hippocampus toward prospective reward locations. *Neuron*, 51(5):639–650, 2006.

G. Lei. A neuron model with fluid properties for solving labyrinthian puzzle. *Biological Cybernetics*, 64(1):61–67, 1990.

P. Lenck-Santini, E. Save, and B. Poucet. Evidence for a relationship between place-cell spatial firing and spatial memory performance. *Hippocampus*, 11(4): 377–390, 2001a.

P. Lenck-Santini, E. Save, and B. Poucet. Place-cell firing does not depend on the direction of turn in a y-maze alternation task. *Eur. J. Neurosci*, 13(5):1055–1058, 2001b.

P. Lenck-Santini, B. Rivard, R. Muller, and B. Poucet. Study of ca1 place cell activity and exploratory behavior following spatial and nonspatial changes in the environment. *Hippocampus*, 15(3):356–369, 2005.

D. Lewis, D. Melchitzky, and G. Burgos. Specificity in the functional architecture of primate prefrontal cortex. *J. Neurocytol*, 31(3-5):265–276, 2002.

I. Lieblich and M. Arbib. Multiple representations of space underlying behavior. *Behavioral and Brain Sciences*, 5(04):627–640, 1982.

J. Lisman and A. Redish. Prediction, sequences and the hippocampus. *Philosophical Transactions of the Royal Society B: Biological Sciences*, 364(1521): 1193–1201, 2009.

R. Lorente de No. Cerebral cortex: architecture, intracortical connections, motor projections. *Physiology of the nervous system*, page 291–340, 1938.

K. Louie and M. Wilson. Temporally structured replay of awake hippocampal ensemble activity during rapid eye movement sleep. *Neuron*, 29(1):145–156, 2001.

T. Macuda and W. Roberts. Further evidence for hierarchical chunking in rat spatial memory. *J Exp Psychol Anim Behav Process*, 21(1):20–32, 1995.

H. Mallot and K. Basten. Embodied spatial cognition: Biological and artificial systems. *Image and Vision Computing*, 27(11):1658–1670, 2009.

H. Markram. The blue brain project. *Nat Rev Neurosci*, 7(2):153–160, 2006.

H. Markram, M. Toledo-Rodriguez, Y. Wang, A. Gupta, G. Silberberg, and C. Wu. Interneurons of the neocortical inhibitory system. *Nat Rev Neurosci*, 5(10): 793–807, 2004.

E. Markus, Y. Qin, B. Leonard, W. Skaggs, B. McNaughton, and C. Barnes. Interactions between location and task affect the spatial and directional firing of hippocampal neurons. *J. Neurosci*, 15(11):7079–7094, 1995.

D. Marr. Simple memory: a theory for archicortex. *Philos. Trans. R. Soc. Lond., B, Biol. Sci*, 262(841):23–81, 1971.

M. Mataric. Integration of representation into goal-driven behavior-based robots. *IEEE transactions on robotics and automation*, 8(3):304–312, 1992.

Y. Matsuda, A. Marzo, and S. Otani. The presence of background dopamine signal converts long-term synaptic depression to potentiation in rat prefrontal cortex. *J Neurosci*, 26(18):4803–4810, 2006.

A. Maurer and B. McNaughton. Network and intrinsic cellular mechanisms underlying theta phase precession of hippocampal neurons. *Trends in Neurosciences*, 30(7):325–333, 2007.

A. Maurer, S. Vanrhoads, G. Sutherland, P. Lipa, and B. McNaughton. Self-motion and the origin of differential spatial scaling along the septo-temporal axis of the hippocampus. *Hippocampus*, 15(7):841–852, 2005.

J. McClelland, B. McNaughton, and R. O'Reilly. Why there are complementary learning systems in the hippocampus and neocortex: Insights from the successes and failures of connectionist models of learning and memory. *Psychological Review*, 102(3):419–457, 1995.

A. Mcdonald. Organization of amygdaloid projections to the prefrontal cortex and associated striatum in the rat. *Neuroscience*, 44(1):1–14, 1991.

A. McDonald and F. Mascagni. Projections of the lateral entorhinal cortex to the amygdala: a phaseolus vulgaris leucoagglutinin study in the rat. *Neuroscience*, 77(2):445–459, 1997.

A. Mcdonald, F. Mascagni, and L. Guo. Projections of the medial and lateral prefrontal cortices to the amygdala: a phaseolus vulgaris leucoagglutinin study in the rat. *Neuroscience*, 71(1):55–75, 1996.

J. McGaughy, R. Ross, and H. Eichenbaum. Noradrenergic, but not cholinergic, deafferentation of prefrontal cortex impairs attentional set-shifting. *Neuroscience*, 153(1):63–71, 2008.

A. McGregor, A. Hayward, J. Pearce, and M. Good. Hippocampal lesions disrupt navigation based on the shape of the environment. *Behav Neurosci*, 118(5): 1011–1021, 2004.

T. McNamara, J. Hardy, and S. Hirtle. Subjective hierarchies in spatial memory. *J Exp Psychol Learn Mem Cogn*, 15(2):211–227, 1989.

B. McNaughton, F. Battaglia, O. Jensen, E. Moser, and M. Moser. Path integration and the neural basis of the 'cognitive map'. *Nat Rev Neurosci*, 7(8):663–678, 2006.

W. Meck and C. Williams. Perinatal choline supplementation increases the threshold for chunking in spatial memory. *Neuroreport*, 8(14):3053–3059, 1997.

M. Mehta. Experience-dependent asymmetric shape of hippocampal receptive fields. *Neuron*, 25(3):707–715, 2000.

M. Mehta, C. Barnes, and B. McNaughton. Experience-dependent, asymmetric expansion of hippocampal place fields. *Proc Natl Acad Sci USA*, 94(16): 8918–8921, 1997.

J. Meyer and D. Filliat. Map-based navigation in mobile robots - ii. a review of map-learning and path-planing strategies. *Journal of Cognitive Systems Research*, 4(4):283–317, 2003.

E. Miller and J. Cohen. An integrative theory of prefrontal function. *Annual Review of Neuroscience*, 24(1):167–202, 2001.

K. Miyazaki, K. Miyazaki, and G. Matsumoto. Different representation of forthcoming reward in nucleus accumbens and medial prefrontal cortex. *Neuroreport*, 15(4):721–726, 2004.

J. Mogensen and S. Holm. The prefrontal cortex and variants of sequential behaviour indications of functional differentiation between subdivisions of the rat's prefrontal cortex. *Behav. Brain Res*, 63(1):89–100, 1994.

C. Molter, N. Sato, and Y. Yamaguchi. Reactivation of behavioral activity during sharp waves: a computational model for two stage hippocampal dynamics. *Hippocampus*, 17(3):201–209, 2007.

P. Montague, P. Dayan, and T. Sejnowski. A framework for mesencephalic dopamine systems based on predictive hebbian learning. *J Neurosci*, 16(5): 1936–1947, 1996.

R. Morris, P. Garrud, J. Rawlins, and J. O'Keefe. Place navigation impaired in rats with hippocampal lesions. *Nature*, 297(5868):681–683, 1982.

R. Morris, F. Schenk, F. Tweedie, and L. Jarrard. Ibotenate lesions of hippocampus and/or subiculum: Dissociating components of allocentric spatial learning. *Eur. J. Neurosci*, 2(12):1016–1028, 1990.

M. Moscovitch, L. Nadel, G. Winocur, A. Gilboa, and R. Rosenbaum. The cognitive neuroscience of remote episodic, semantic and spatial memory. *Curr. Opin. Neurobiol*, 16(2):179–190, 2006.

E. Moser, M. Moser, and P. Andersen. Spatial learning impairment parallels the magnitude of dorsal hippocampal lesions, but is hardly present following ventral lesions. *J. Neurosci*, 13(9):3916–3925, 1993.

V. Mountcastle. Modality and topographic properties of single neurons of cat's somatic sensory cortex. *J. Neurophysiol*, 20(4):408–434, 1957.

V. Mountcastle. The columnar organization of the neocortex. *Brain*, 120 (Pt 4): 701–722, 1997.

V. Mountcastle. Introduction. computation in cortical columns. *Cereb. Cortex*, 13 (1):2–4, 2003.

A. Mulder, M. Arts, and F. Lopes da Silva. Short- and long-term plasticity of the hippocampus to nucleus accumbens and prefrontal cortex pathways in the rat, in vivo. *Eur. J. Neurosci*, 9(8):1603–1611, 1997.

A. Mulder, R. Nordquist, O. Orgüt, and C. Pennartz. Learning-related changes in response patterns of prefrontal neurons during instrumental conditioning. *Behav. Brain Res*, 146(1-2):77–88, 2003.

R. Muller and J. Kubie. The effects of changes in the environment on the spatial firing of hippocampal complex-spike cells. *J. Neurosci*, 7(7):1951–1968, 1987.

R. Muller, J. Kubie, and J. Ranck. Spatial firing patterns of hippocampal complex-spike cells in a fixed environment. *J. Neurosci*, 7(7):1935–1950, 1987.

R. Muller, J. Kubie, E. Bostock, J. Taube, and G. Quirk. Spatial firing correlates of neurons in the hippocampal formation of freely moving rats. In J. Paillard, editor, *Brain and Space*, page 296–333. Oxford University Press, New York, 1991.

R. Muller, E. Bostock, J. Taube, and J. Kubie. On the directional firing properties of hippocampal place cells. *J. Neurosci.*, 14(12):7235–7251, 1994.

R. Muller, M. Stead, and J. Pach. The hippocampus as a cognitive graph. *J. Gen. Physiol*, 107(6):663–694, 1996.

R. Muller, B. Poucet, and B. Rivard. Sensory determinants of hippocampal place cell firing fields. In *The neural basis of navigation: evidence from single cell recording*, pages 1–22. P.E. Sharp, norwell, ma: kluwer academic edition, 2001.

S. Murase, J. Grenhoff, G. Chouvet, F. Gonon, and T. Svensson. Prefrontal cortex regulates burst firing and transmitter release in rat mesolimbic dopamine neurons studied in vivo. *Neurosci Lett*, 157(1):53–56, 1993.

B. Murphy, A. Arnsten, P. Goldman-Rakic, and R. Roth. Increased dopamine turnover in the prefrontal cortex impairs spatial working memory performance in rats and monkeys. *Proc Natl Acad Sci U S A*, 93(3):1325–1329, 1996.

H. Mushiake, N. Saito, K. Sakamoto, Y. Itoyama, and J. Tanji. Activity in the lateral prefrontal cortex reflects multiple steps of future events in action plans. *Neuron*, 50(4):631–641, 2006.

L. Nadel and M. Moscovitch. The hippocampal complex and long-term memory revisited. *Trends Cogn. Sci. (Regul. Ed.)*, 5(6):228–230, 2001.

K. Nakazawa, L. Sun, M. Quirk, L. Rondi-Reig, M. Wilson, and S. Tonegawa. Hippocampal ca3 nmda receptors are crucial for memory acquisition of one-time experience. *Neuron*, 38(2):305–315, 2003.

W. Nauta. The problem of the frontal lobe: a reinterpretation. *J Psychiatr Res*, 8 (3):167–187, 1971.

D. Nitz. Tracking route progression in the posterior parietal cortex. *Neuron*, 49 (5):747–756, 2006.

S. Ohashi, M. Matsumoto, H. Otani, K. Mori, H. Togashi, K. Ueno, A. Kaku, and M. Yoshioka. Changes in synaptic plasticity in the rat hippocampo-medial prefrontal cortex pathway induced by repeated treatments with fluvoxamine. *Brain Res*, 949(1-2):131–138, 2002.

J. O'Keefe and N. Burgess. Geometric determinants of the place fields of hippocampal neurons. *Nature*, 381(6581):425–428, 1996.

J. O'Keefe and D. Conway. Hippocampal place units in the freely moving rat: why they fire where they fire. *Exp Brain Res*, 31(4):573–590, 1978.

J. O'Keefe and J. Dostrovsky. The hippocampus as a spatial map. preliminary evidence from unit activity in the freely-moving rat. *Brain Research*, 34(1): 171–175, 1971.

J. O'Keefe and L. Nadel. *The hippocampus as a cognitive map*. Oxford University Press., 1978.

J. O'Keefe and M. Recce. Phase relationship between hippocampal place units and the eeg theta rhythm. *Hippocampus*, 3(3):317–330, 1993.

J. O'Neill, T. Senior, and J. Csicsvari. Place-selective firing of ca1 pyramidal cells during sharp wave/ripple network patterns in exploratory behavior. *Neuron*, 49 (1):143–155, 2006.

J. O'Neill, T. Senior, K. Allen, J. Huxter, and J. Csicsvari. Reactivation of experience-dependent cell assembly patterns in the hippocampus. *Nat. Neurosci*, 11(2):209–215, 2008.

D. Öngür and J. Price. The organization of networks within the orbital and medial prefrontal cortex of rats, monkeys and humans. *Cerebral Cortex*, 10(3): 206–219, 2000.

R. O'Reilly, D. Noelle, T. Braver, and J. Cohen. Prefrontal cortex and dynamic categorization tasks: representational organization and neuromodulatory control. *Cereb Cortex*, 12(3):246–257, 2002.

R. O'Reilly, S. Herd, and W. Pauli. Computational models of cognitive control. *Current Opinion in Neurobiology*, 20(2):257–261, 2010.

S. Otani. Prefrontal cortex function, quasi-physiological stimuli, and synaptic plasticity. *J Physiol Paris*, 97(4-6):423–430, 2003.

S. Otani, O. Blond, J. Desce, and F. Crépel. Dopamine facilitates long-term depression of glutamatergic transmission in rat prefrontal cortex. *Neuroscience*, 85(3):669–676, 1998.

C. Padoa-Schioppa and J. Assad. Neurons in the orbitofrontal cortex encode economic value. *Nature*, 441(7090):223–226, 2006.

S. Panzeri and A. Treves. Analytical estimates of limited sampling biases in different information measures. *Netw Comput Neur Syst*, 7:87–107, 1996.

E. Pastalkova, V. Itskov, A. Amarasingham, and G. Buzsaki. Internally generated cell assembly sequences in the rat hippocampus. *Science*, 321(5894):1322–1327, 2008.

G. Paxinos and C. Watson. *The Rat Brain In Stereotaxic Coordinates*. Academic Press, Boston, 1998.

C. Pennartz, H. Groenewegen, and F. Lopes da Silva. The nucleus accumbens as a complex of functionally distinct neuronal ensembles: an integration of behavioural, electrophysiological and anatomical data. *Prog Neurobiol*, 42: 719–761, 1994.

A. Peters. Examining neocortical circuits: Some background and facts. *Journal of Neurocytology*, 31:183–193, 2002.

A. Peters and D. Kara. The neuronal composition of area 17 of rat visual cortex. iv. the organization of pyramidal cells. *J. Comp. Neurol*, 260(4):573–590, 1987.

A. Peters and C. Sethares. Myelinated axons and the pyramidal cell modules in monkey primary visual cortex. *J. Comp. Neurol*, 365(2):232–255, 1996.

M. Petrides and B. Milner. Deficits on subject-ordered tasks after frontal- and temporal-lobe lesions in man. *Neuropsychologia*, 20(3):249–262, 1982.

A. Peyrache, M. Khamassi, K. Benchenane, S. Wiener, and F. Battaglia. Replay of rule-learning related neural patterns in the prefrontal cortex during sleep. *Nat. Neurosci*, 12(7):919–926, 2009.

A. Phillips, S. Ahn, and S. Floresco. Magnitude of dopamine release in medial prefrontal cortex predicts accuracy of memory on a delayed response task. *J Neurosci*, 24(2):547–553, 2004.

S. Pirot, R. Godbout, J. Mantz, J. Tassin, J. Glowinski, and A. Thierry. Inhibitory effects of ventral tegmental area stimulation on the activity of prefrontal cortical neurons: evidence for the involvement of both dopaminergic and gabaergic components. *Neuroscience*, 49(4):857–865, 1992.

S. Pirot, J. Glowinski, and A. Thierry. Mediodorsal thalamic evoked responses in the rat prefrontal cortex: influence of the mesocortical da system. *Neuroreport*, 7(8):1437–1441, 1996.

W. Pohl. Dissociation of spatial discrimination deficits following frontal and parietal lesions in monkeys. *J Comp Physiol Psychol*, 82(2):227–239, 1973.

B. Poucet. Spatial cognitive maps in animals: new hypotheses on their structure and neural mechanisms. *Psychol Rev*, 100(2):163–182, 1993.

B. Poucet. Searching for spatial unit firing in the prelimbic area of the rat medial prefrontal cortex. *Behav Brain Res*, 84(1-2):151–159, 1997.

B. Poucet and S. Benhamou. The neuropsychology of spatial cognition in the rat. *Crit Rev Neurobiol*, 11(2-3):101–120, 1997.

B. Poucet and T. Herrmann. Septum and medial frontal cortex contribution to spatial problem-solving. *Behav. Brain Res*, 37(3):269–280, 1990.

B. Poucet, C. Thinus-Blanc, and N. Chapuis. Route planning in cats, in relation to the visibility of the goal. *Animal Behaviour*, 31(2):594–599, 1983.

B. Poucet, C. Thinus-Blanc, and R. Muller. Place cells in the ventral hippocampus of rats. *Neuroreport*, 5(16):2045–2048, 1994.

B. Poucet, P. Lenck-Santini, V. Hok, E. Save, J. Banquet, P. Gaussier, and R. Muller. Spatial navigation and hippocampal place cell firing: the problem of goal encoding. *Reviews in Neuroscience*, 15(2):89–107, 2004.

F. Pouille and M. Scanziani. Enforcement of temporal fidelity in pyramidal cells by somatic feed-forward inhibition. *Science*, 293(5532):1159–1163, 2001.

N. Povysheva, G. Gonzalez-Burgos, A. Zaitsev, S. Kröner, G. Barrionuevo, D. Lewis, and L. Krimer. Properties of excitatory synaptic responses in fast-spiking interneurons and pyramidal cells from monkey and rat prefrontal cortex. *Cereb Cortex*, 16(4):541–552, 2006.

W. Pratt and S. Mizumori. Neurons in rat medial prefrontal cortex show anticipatory rate changes to predictable differential rewards in a spatial memory task. *Behav Brain Res*, 123(2):165–183, 2001.

T. Preuss. Do rats have prefrontal cortex. *The Rose-Woolsey-Akert program reconsidered. J Cogn Neurosci*, 7:1–24, 1995.

E. Procyk, Y. Tanaka, and J. Joseph. Anterior cingulate activity during routine and non-routine sequential behaviors in macaques. *Nat Neurosci*, 3(5):502–508, 2000.

G. Quirk, R. Muller, and J. Kubie. The firing of hippocampal place cells in the dark depends on the rat's recent experience. *J. Neurosci*, 10(6):2008–2017, 1990.

M. Raghanti, M. Spocter, C. Butti, P. Hof, and C. Sherwood. A comparative perspective on minicolumns and inhibitory gabaergic interneurons in the neocortex. *Front Neuroanat*, 4, 2010.

M. Ragozzino and R. Kesner. The effects of muscarinic cholinergic receptor blockade in the rat anterior cingulate and prelimbic/infralimbic cortices on spatial working memory. *Neurobiol Learn Mem*, 69(3):241–257, 1998.

M. Ragozzino, S. Detrick, and R. Kesner. Involvement of the prelimbic-infralimbic areas of the rodent prefontal cortex in behavioral flexibility for place and response learning. *The Journal of Neuroscience*, 19(11):4585–4594, 1999.

G. Rainer, S. Rao, and E. Miller. Prospective coding for objects in primate prefrontal cortex. *J Neurosci*, 19(13):5493–5505, 1999.

P. Rakic. Specification of cerebral cortical areas. *Science*, 241(4862):170–176, 1988.

P. Rakic. Evolving concepts of cortical radial and areal specification. *Prog. Brain Res*, 136:265–280, 2002.

P. Rakic. Confusing cortical columns. *Proceedings of the National Academy of Sciences*, 105(34):12099–12100, 2008.

S. Rao, G. Williams, and P. Goldman-Rakic. Isodirectional tuning of adjacent interneurons and pyramidal cells during working memory: evidence for microcolumnar organization in pfc. *J Neurophysiol*, 81(4):1903–1916, 1999.

S. Rao, G. Williams, and P. Goldman-Rakic. Destruction and creation of spatial tuning by disinhibition: Gaba(a) blockade of prefrontal cortical neurons engaged by working memory. *J Neurosci*, 20(1):485–494, 2000.

P. Redgrave and K. Gurney. The short-latency dopamine signal: a role in discovering novel actions? *Nat Rev Neurosci*, 7(12):967–975, 2006.

P. Redgrave, T. Prescott, and K. Gurney. The basal ganglia: a vertebrate solution to the selection problem? *Neuroscience*, 89(4):1009–1023, 1999.

R. Reep, J. Corwin, and V. King. Neuronal connections of orbital cortex in rats: topography of cortical and thalamic afferents. *Exp Brain Res*, 111(2):215–232, 1996.

E. Rich and M. Shapiro. Rat prefrontal cortical neurons selectively code strategy switches. *J. Neurosci.*, 29(22):7208–7219, 2009.

M. Riesenhuber and T. Poggio. Hierarchical models of object recognition in cortex. *Nat. Neurosci*, 2(11):1019–1025, 1999.

B. Rivard, Y. Li, P. Lenck-Santini, B. Poucet, and R. Muller. Representation of objects in space by two classes of hippocampal pyramidal cells. *J. Gen. Physiol*, 124(1):9–25, 2004.

W. Roberts. Spatial memory in the rat on a hierarchical maze. *Learning and Motivation*, 10:117–140, 1979.

K. Rockland and N. Ichinohe. Some thoughts on cortical minicolumns. *Experimental Brain Research*, 158(3):265–277, 2004.

M. Roesch, A. Taylor, and G. Schoenbaum. Encoding of time-discounted rewards in orbitofrontal cortex is independent of value representation. *Neuron*, 51(4): 509–520, 2006.

E. Rolls. A model of the operation of the hippocampus and entorhinal cortex in memory. *International Journal of Neural Systems*, 6:51–70, 1995.

L. Rondi-Reig, M. Libbey, H. Eichenbaum, and S. Tonegawa. Ca1-specific n-methyl-d-aspartate receptor knockout mice are deficient in solving a nonspatial transverse patterning task. *Proc. Natl. Acad. Sci. U.S.A*, 98(6):3543–3548, 2001.

L. Rondi-Reig, G. Petit, C. Tobin, S. Tonegawa, J. Mariani, and A. Berthoz. Impaired sequential egocentric and allocentric memories in forebrain-specific-nmda receptor knock-out mice during a new task dissociating strategies of navigation. *J. Neurosci*, 26(15):4071–4081, 2006.

Z. Rossetti and S. Carboni. Noradrenaline and dopamine elevations in the rat prefrontal cortex in spatial working memory. *J Neurosci*, 25(9):2322–2329, 2005.

D. Rubino, K. Robbins, and N. Hatsopoulos. Propagating waves mediate information transfer in the motor cortex. *Nat Neurosci*, 9(12):1549–1557, 2006.

P. Rudebeck, M. Walton, A. Smyth, D. Bannerman, and M. Rushworth. Separate neural pathways process different decision costs. *Nat Neurosci*, 9(9): 1161–1168, 2006.

M. Rushworth. Intention, choice, and the medial frontal cortex. *Annals of the New York Academy of Sciences*, 1124(The Year in Cognitive Neuroscience 2008): 181–207, 2008.

M. Rushworth, T. Behrens, P. Rudebeck, and M. Walton. Contrasting roles for cingulate and orbitofrontal cortex in decisions and social behaviour. *Trends in Cognitive Sciences*, 11(4):168–176, 2007.

N. Saito, H. Mushiake, K. Sakamoto, Y. Itoyama, and J. Tanji. Representation of immediate and final behavioral goals in the monkey prefrontal cortex during an instructed delay period. *Cerebral Cortex*, 15(10):1535 –1546, 2005.

M. Sarter and J. Bruno. Cognitive functions of cortical acetylcholine: toward a unifying hypothesis. *Brain Res Brain Res Rev*, 23(1-2):28–46, 1997.

D. Schacter, D. Addis, and R. Buckner. Episodic simulation of future events: concepts, data, and applications. *Ann. N. Y. Acad. Sci*, 1124:39–60, 2008.

N. Schmajuk and A. Thieme. Purposive behavior and cognitive mapping: a neural network model. *Biol Cybern*, 67(2):165–174, 1992.

N. Schmajuk and H. Voicu. Exploration and navigation using hierarchical cognitive maps. In *Animal Spatial Cognition: Comparative, Neural, and Computational Approaches*. M.F. Brown and R.G. Cook, 2006.

W. Schultz. Predictive reward signal of dopamine neurons. *Journal of Neurophysiology*, 80(1):1–27, 1998.

W. Schultz. Getting formal with dopamine and reward. *Neuron*, 36(2):241–263, 2002.

W. Schultz. Multiple dopamine functions at different time courses. *Annu. Rev. Neurosci*, 30:259–288, 2007.

W. Schultz, P. Dayan, and P. Montague. A neural substrate of prediction and reward. *Science*, 275(14), 1997.

J. Seamans and C. Yang. The principal features and mechanisms of dopamine modulation in the prefrontal cortex. *Prog Neurobiol*, 74(1):1–58, 2004.

J. Seamans, S. Floresco, and A. Phillips. Functional differences between the prelimbic and anterior cingulate regions of the rat prefrontal cortex. *Behav. Neurosci*, 109(6):1063–1073, 1995.

J. Seamans, S. Floresco, and A. Phillips. D1 receptor modulation of hippocampal-prefrontal cortical circuits integrating spatial memory with executive functions in the rat. *J Neurosci*, 18(4):1613–1621, 1998.

J. Seamans, D. Durstewitz, B. Christie, C. Stevens, and T. Sejnowski. Dopamine d1/d5 receptor modulation of excitatory synaptic inputs to layer v prefrontal cortex neurons. *Proc Natl Acad Sci U S A*, 98(1):301–306, 2001.

J. Semmes, S. Weinstein, L. Ghent, and H. Teuber. correlates of impaired orientation in personal and extrapersonal space. *Brain*, 86:747–772, 1963.

D. Servan-Schreiber, H. Printz, and J. Cohen. A network model of catecholamine effects: gain, signal-to-noise ratio, and behavior. *Science*, 249(4971):892–895, 1990.

S. Sesack, A. Deutch, R. Roth, and B. Bunney. Topographical organization of the efferent projections of the medial prefrontal cortex in the rat: An anterograde tract-tracing study with phaseolus vulgaris leucoagglutinin. *The Journal of Comparative Neurology*, 290(2):213–242, 1989.

S. Sesack, C. Snyder, and D. Lewis. Axon terminals immunolabeled for dopamine or tyrosine hydroxylase synapse on gaba-immunoreactive dendrites in rat and monkey cortex. *J. Comp. Neurol*, 363(2):264–280, 1995.

M. Shadlen and W. Newsome. The variable discharge of cortical neurons: implications for connectivity, computation, and information coding. *J Neurosci*, 18 (10):3870–3896, 1998.

T. Shallice and P. Burgess. Deficits in strategy application following frontal lobe damage in man. *Brain*, 114(2):727–741, 1991.

C. Shannon. A mathematical theory of communication. *The Bell System Technical Journal*, 27:379–423, 623–656, 1948.

M. Shapiro and J. Ferbinteanu. Relative spike timing in pairs of hippocampal neurons distinguishes the beginning and end of journeys. *Proc. Natl. Acad. Sci. U.S.A*, 103(11):4287–4292, 2006.

P. Sharp and C. Green. Spatial correlates of firing patterns of single cells in the subiculum of the freely moving rat. *J. Neurosci*, 14(4):2339–2356, 1994.

P. Sharp, J. Kubie, and R. Muller. Firing properties of hippocampal neurons in a visually symmetrical environment: contributions of multiple sensory cues and mnemonic processes. *J. Neurosci*, 10(9):3093–3105, 1990.

P. Sharp, H. Blair, D. Etkin, and D. Tzanetos. Influences of vestibular and visual motion information on the spatial firing patterns of hippocampal place cells. *J. Neurosci*, 15(1 Pt 1):173–189, 1995.

D. Sheynikhovich, R. Chavarriaga, T. Strösslin, A. Arleo, and W. Gerstner. Is there a geometric module for spatial orientation? insights from a rodent navigation model. *Psychol Rev*, 116(3):540–566, 2009.

K. Shima, M. Isoda, H. Mushiake, and J. Tanji. Categorization of behavioural sequences in the prefrontal cortex. *Nature*, 445:315–318, 2007.

A. Siapas, E. Lubenov, and M. Wilson. Prefrontal phase locking to hippocampal theta oscillations. *Neuron*, 46(1):141–151, 2005.

G. Silberberg and H. Markram. Disynaptic inhibition between neocortical pyramidal cells mediated by martinotti cells. *Neuron*, 53(5):735–746, 2007.

A. Singer and L. Frank. Rewarded outcomes enhance reactivation of experience in the hippocampus. *Neuron*, 64(6):910–921, 2009.

W. Skaggs and B. McNaughton. Replay of neuronal firing sequences in rat hippocampus during sleep following spatial experience. *Science*, 271(5257):1870–1873, 1996.

W. Skaggs, B. McNaughton, K. Gothard, and E. Markus. An information-theoretic approach to deciphering the hippocampal code. In *Advances in neural information processing systems*, page 1030–1030, 1993.

W. Skaggs, B. McNaughton, M. Wilson, and C. Barnes. Theta phase precession in hippocampal neuronal populations and the compression of temporal sequences. *Hippocampus*, 6(2):149–172, 1996.

U. Slawińska and S. Kasicki. The frequency of rat's hippocampal theta rhythm is related to the speed of locomotion. *Brain Res*, 796(1-2):327–331, 1998.

D. Smith and S. Mizumori. Learning-related development of context-specific neuronal responses to places and events: the hippocampal role in context processing. *J. Neurosci*, 26(12):3154–3163, 2006.

D. Somers, S. Nelson, and M. Sur. An emergent model of orientation selectivity in cat visual cortical simple cells. *J Neurosci*, 15(8):5448–5465, 1995.

A. Speakman and J. O'Keefe. Hippocampal complex spike cells do not change their place fields if the goal is moved within a cue controlled environment. *Eur. J. Neurosci*, 2(6):544–555, 1990.

H. Spiers. Keeping the goal in mind: Prefrontal contributions to spatial navigation. *Neuropsychologia*, 46(7):2106–2108, 2008.

H. Spiers and E. Maguire. Thoughts, behaviour, and brain dynamics during navigation in the real world. *NeuroImage*, 31(4):1826–1840, 2006.

H. Spiers and E. Maguire. A navigational guidance system in the human brain. *Hippocampus*, 17(8):618–626, 2007a.

H. Spiers and E. Maguire. The neuroscience of remote spatial memory: a tale of two cities. *Neuroscience*, 149(1):7–27, 2007b.

L. Squire, B. Knowlton, and G. Musen. The structure and organization of memory. *Annu. Rev. Psychol.*, 44(1):453–495, 1993.

R. Steele and R. Morris. Delay-dependent impairment of a matching-to-place task with chronic and intrahippocampal infusion of the nmda-antagonist d-ap 5. *Hippocampus*, 9(2):118–136, 1999.

D. Stephens and J. Krebs. *Foraging theory*. Princeton University Press, 1986.

R. Suri and W. Schultz. A neural network model with dopamine-like reinforcement signal that learns a spatial delayed response task. *Neuroscience*, 91(3): 871–890, 1999.

R. Sutherland and A. Rodriguez. The role of the fornix/fimbria and some related subcortical structures in place learning and memory. *Behav. Brain Res*, 32(3): 265–277, 1989.

R. Sutherland, I. Whishaw, and B. Kolb. A behavioural analysis of spatial localization following electrolytic, kainate- or colchicine-induced damage to the hippocampal formation in the rat. *Behav. Brain Res*, 7(2):133–153, 1983.

R. Sutton and A. Barto. *Reinforcement learning: an introduction*. Bradford Book, 1998.

R. Sutton, D. Precup, and S. Singh. Between mdps and semi-mdps: A framework for temporal abstraction in reinforcement learning. *Artificial intelligence*, 112 (1):181–211, 1999.

L. Swanson. A direct projection from ammon's horn to prefrontal cortex in the rat. *Brain Res*, 217(1):150–154, 1981.

L. Swanson and W. Cowan. An autoradiographic study of the organization of the efferent connections of the hippocampal formation in the rat. *J. Comp. Neurol*, 172(1):49–84, 1977.

J. Szentágothai. The 'module-concept' in cerebral cortex architecture. *Brain Res*, 95(2-3):475–496, 1975.

E. Tabuchi, A. Mulder, and S. Wiener. Reward value invariant place responses and reward site associated activity in hippocampal neurons of behaving rats. *Hippocampus*, 13(1):117–132, 2003.

K. Takeda and S. Funahashi. Prefrontal task-related activity representing visual cue location or saccade direction in spatial working memory tasks. *J. Neurophysiol*, 87(1):567–588, 2002.

S. Tanaka. Dopaminergic control of working memory and its relevance to schizophrenia: a circuit dynamics perspective. *Neuroscience*, 139(1):153–171, 2006.

J. Tanji and E. Hoshi. Behavioral planning in the prefrontal cortex. *Curr Opin Neurobiol*, 11(2):164–170, 2001.

A. Thierry, G. Blanc, A. Sobel, L. Stinus, and J. Golwinski. Dopaminergic terminals in the rat cortex. *Science*, 182(4111):499–501, 1973.

A. Thierry, Y. Gioanni, E. Degenetais, and J. Glowinski. Hippocampo-prefrontal cortex pathway: anatomical and electrophysiological characteristics. *Hippocampus*, 10(4):411–419, 2000.

L. Thompson and P. Best. Place cells and silent cells in the hippocampus of freely-behaving rats. *J. Neurosci*, 9(7):2382–2390, 1989.

A. Thomson and A. Bannister. Interlaminar connections in the neocortex. *Cerebral Cortex*, 13(1):5–14, 2003.

A. Thomson and J. Deuchars. Synaptic interactions in neocortical local circuits: dual intracellular recordings in vitro. *Cereb Cortex*, 7(6):510–522, 1997.

P. Tierney, E. Dégenètais, A. Thierry, J. Glowinski, and Y. Gioanni. Influence of the hippocampus on interneurons of the rat prefrontal cortex. *Eur J Neurosci*, 20(2):514–524, 2004.

P. Tierney, A. Thierry, J. Glowinski, J. Deniau, and Y. Gioanni. Dopamine modulates temporal dynamics of feedforward inhibition in rat prefrontal cortex in vivo. *Cereb. Cortex*, 18(10):2251–2262, 2008.

E. Tolman. Cognitive maps in rats and men. *The Psychological Review*, 55(4): 189–208, 1948.

E. Tolman and C. Honzik. ”insight” in rats. *University of California Publication in Psychology*, 4(14):215–232, 1930a.

E. Tolman and C. Honzik. Introduction and removal of reward and maze learning in rats. *University of California Publications in Psychology*, 4:257–275, 1930b.

L. Tremblay and W. Schultz. Relative reward preference in primate orbitofrontal cortex. *Nature*, 398(6729):704–708, 1999.

M. Trivedi and G. Coover. Lesions of the ventral hippocampus, but not the dorsal hippocampus, impair conditioned fear expression and inhibitory avoidance on the elevated t-maze. *Neurobiol Learn Mem*, 81(3):172–184, 2004.

O. Trullier, S. Wiener, A. Berthoz, and J. Meyer. Biologically based artificial navigation systems: review and prospects. *Prog. Neurobiol*, 51(5):483–544, 1997.

O. Trullier, R. Shibata, A. Mulder, and S. Wiener. Hippocampal neuronal position selectivity remains fixed to room cues only in rats alternating between place navigation and beacon approach tasks. *Eur. J. Neurosci*, 11(12):4381–4388, 1999.

K. Tseng and P. O'Donnell. Dopamine-glutamate interactions controlling prefrontal cortical pyramidal cell excitability involve multiple signaling mechanisms. *J Neurosci*, 24(22):5131–5139, 2004.

K. Tseng and P. O'Donnell. D2 dopamine receptors recruit a gaba component for their attenuation of excitatory synaptic transmission in the adult rat prefrontal cortex. *Synapse*, 61(10):843–850, 2007.

M. Tsodyks, W. Skaggs, T. Sejnowski, and B. McNaughton. Population dynamics and theta rhythm phase precession of hippocampal place cell firing : A spiking neuron model. *Hippocampus*, 1996.

T. Tsujimoto, H. Shimazu, and Y. Isomura. Direct recording of theta oscillations in primate prefrontal and anterior cingulate cortices. *J Neurophysiol*, 95(5): 2987–3000, 2006.

H. Uylings, H. Groenewegen, and B. Kolb. Do rats have a prefrontal cortex? *Behav Brain Res*, 146(1-2):3–17, 2003.

O. Valenti and A. Grace. Entorhinal cortex inhibits medial prefrontal cortex and modulates the activity states of electrophysiologically characterized pyramidal neurons in vivo. *Cereb. Cortex*, 19(3):658–674, 2009.

C. Vanderwolf. Hippocampal electrical activity and voluntary movement in the rat. *Electroencephalogr Clin Neurophysiol*, 26(4):407–418, 1969.

F. Varela, J. Lachaux, E. Rodriguez, and J. Martinerie. The brainweb: phase synchronization and large-scale integration. *Nat. Rev. Neurosci*, 2(4):229–239, 2001.

R. Vertes. Interactions among the medial prefrontal cortex, hippocampus and midline thalamus in emotional and cognitive processing in the rat. *Neuroscience*, 142(1):1–20, 2006.

R. Vertes, W. Hoover, A. Do Valle, A. Sherman, and J. Rodriguez. Efferent projections of reuniens and rhomboid nuclei of the thalamus in the rat. *J Comp Neurol*, 499(5):768–796, 2006.

R. Vertes, W. Hoover, K. Szigeti-Buck, and C. Leranth. Nucleus reuniens of the midline thalamus: link between the medial prefrontal cortex and the hippocampus. *Brain Res Bull*, 71(6):601–609, 2007.

R. Verwer, R. Meijer, H. Uum, and M. Witter. Collateral projections from the rat hippocampal formation to the lateral and medial prefrontal cortex. *Hippocampus*, 7(4):397–402, 1997.

T. Vogels, K. Rajan, and L. Abbott. Neural network dynamics. *Annu. Rev. Neurosci*, 28:357–376, 2005.

B. Vogt and M. Gabriel. *Neurobiology of cingulate cortex and limbic thalamus: A comprehensive handbook*. Birkhauser, 1993.

H. Voicu. Hierarchical cognitive maps. *Neural Netw*, 16(5-6):569–576, 2003.

P. Voorn, L. Vanderschuren, H. Groenewegen, T. Robbins, and C. Pennartz. Putting a spin on the dorsal-ventral divide of the striatum. *Trends in Neurosciences*, 27(8):468–474, 2004.

J. Wallis. Orbitofrontal cortex and its contribution to decision-making. *Annu Rev Neurosci*, 30:31–56, 2007.

M. Walton, D. Bannerman, and M. Rushworth. The role of rat medial frontal cortex in effort-based decision making. *J. Neurosci.*, 22(24):10996–11003, 2002.

M. Walton, D. Bannerman, K. Alterescu, and M. Rushworth. Functional specialization within medial frontal cortex of the anterior cingulate for evaluating effort-related decisions. *J Neurosci*, 23(16):6475–6479, 2003.

Y. Wang and P. Goldman-Rakic. D2 receptor regulation of synaptic burst firing in prefrontal cortical pyramidal neurons. *Proc Natl Acad Sci U S A*, 101(14): 5093–5098, 2004.

M. Watanabe. Reward expectancy in primate prefrontal neurons. *Nature*, 382 (6592):629–632, 1996.

M. Weel and M. Witter. Projections from the nucleus reuniens thalami to the entorhinal cortex, hippocampal field ca1, and the subiculum in the rat arise from different populations of neurons. *J Comp Neurol*, 364(4):637–650, 1996.

M. Weel and M. Witter. Nucleus reuniens thalami innervates gamma aminobutyric acid positive cells in hippocampal field ca1 of the rat. *Neurosci Lett*, 278(3): 145–148, 2000.

I. Whishaw. Hippocampal electroencephalographic activity in the mongolian gerbil during natural behaviours and wheel running and in the rat during wheel running and conditioned immobility. *Can J Psychol*, 26(3):219–239, 1972.

I. Whishaw and L. Jarrard. Similarities vs. differences in place learning and circadian activity in rats after fimbria-fornix section or ibotenate removal of hippocampal cells. *Hippocampus*, 5(6):595–604, 1995.

N. White and R. McDonald. Multiple parallel memory systems in the brain of the rat. *Neurobiology of Learning and Memory*, 77:125–184, 2002.

S. Wiener and J. Taube. *Head Direction Cells and the Neural Mechansims of Spatial Orientation*. MIT Press, 2005.

G. Williams and P. Goldman-Rakic. Modulation of memory fields by dopamine d1 receptors in prefrontal cortex. *Nature*, 376(6541):572–575, 1995.

B. Willmore and D. Tolhurst. Characterizing the sparseness of neural codes. *Netw Comput Neur Syst*, 12(3):255–270, 2001.

M. Wilson and B. McNaughton. Dynamics of the hippocampal ensemble code for space. *Science*, 261:1055–1058, 1993.

M. Wilson and B. McNaughton. Reactivation of hippocampal ensemble memories during sleep. *Science*, 265(5172):676–679, 1994.

G. Winocur, M. Moscovitch, and M. Sekeres. Memory consolidation or transformation: context manipulation and hippocampal representations of memory. *Nat Neurosci*, 10(5):555–557, 2007.

G. Winocur, M. Moscovitch, and B. Bontempi. Memory formation and long-term retention in humans and animals: Convergence towards a transformation account of hippocampal-neocortical interactions. *Neuropsychologia*, 48(8):2339–2356, 2010a.

G. Winocur, M. Moscovitch, R. Rosenbaum, and M. Sekeres. An investigation of the effects of hippocampal lesions in rats on pre- and postoperatively acquired spatial memory in a complex environment. *Hippocampus*, 2010b.

M. Witter. Organization of the entorhinal-hippocampal system: a review of current anatomical data. *Hippocampus*, 3 Spec No:33–44, 1993.

E. Wood, P. Dudchenko, R. Robitsek, and H. Eichenbaum. Hippocampal neurons encode information about different types of memory episodes occurring in the same location. *Neuron*, 27(3):623–633, 2000.

F. Wörgötter and C. Koch. A detailed model of the primary visual pathway in the cat: comparison of afferent excitatory and intracortical inhibitory connection schemes for orientation selectivity. *J Neurosci*, 11(7):1959–1979, 1991.

J. Wu, Xiaoying Huang, and Chuan Zhang. Propagating waves of activity in the neocortex: what they are, what they do. *Neuroscientist*, 14(5):487–502, 2008.

C. Yang and J. Seamans. Dopamine d1 receptor actions in layers v-vi rat prefrontal cortex neurons in vitro: modulation of dendritic-somatic signal integration. *J Neurosci*, 16(5):1922–1935, 1996.

C. Yang, J. Seamans, and N. Gorelova. Developing a neuronal model for the pathophysiology of schizophrenia based on the nature of electrophysiological actions of dopamine in the prefrontal cortex. *Neuropsychopharmacology*, 21 (2):161–194, 1999.

A. Yu and P. Dayan. Uncertainty, neuromodulation, and attention. *Neuron*, 46: 681–692, 2005.

A. Yu, M. Giese, and T. Poggio. Biophysiologically plausible implementations of the maximum operation. *Neural Comput*, 14(12):2857–2881, 2002.

J. Zahrt, J. Taylor, R. Mathew, and A. Arnsten. Supranormal stimulation of d1 dopamine receptors in the rodent prefrontal cortex impairs spatial working memory performance. *J Neurosci*, 17(21):8528–8535, 1997.

D. Zhang and E. Bertram. Midline thalamic region: widespread excitatory input to the entorhinal cortex and amygdala. *J Neurosci*, 22(8):3277–3284, 2002.

P. Zheng, X. Zhang, B. Bunney, and W. Shi. Opposite modulation of cortical n-methyl-d-aspartate receptor-mediated responses by low and high concentrations of dopamine. *Neuroscience*, 91(2):527–535, 1999.

E. Zohary, M. Shadlen, and W. Newsome. Correlated neuronal discharge rate and its implication for psychophysical performance. *Nature*, 370:140–143, 1994.